Instytut Chemii Bioorganicznej

Polskiej Akademii Nauk

Krótkie niekodujące RNA (tRF i sdRNA) asocjujące z rybosomami w *Saccharomyces cerevisiae* – geneza i funkcje regulatorowe w zróżnicowanych warunkach środowiskowych

---

Anna Maria Mleczko

Praca doktorska wykonana w Zespole Transkryptomiki Funkcjonalnej

Promotor: dr hab. Kamilla Bąkowska-Żywicka, prof. ICHB PAN

Poznań 2020

Pragnę złożyć najserdeczniejsze podziękowania

Mojemu Promotorowi,
dr hab. Kamilli Bąkowskiej-Żywickiej, prof. ICHB PAN
za wzbudzenie we mnie miłości do Nauki,
za opiekę nad moim rozwojem,
za całą przekazaną wiedzę i wiele cennych rad
oraz za życzliwość, wsparcie i wszystkie dobre słowa, które niejednokrotnie pomogły mi gdy zwątpiłam w siebie.

dr. Piotrowi Machtelowi
za nieocenioną przyjaźń, twórcze rozmowy, cenne wskazówki, ogromną pomoc w przygotowywaniu tej pracy i wsparcie podczas trudów całego doktoratu.

prof. dr hab. Tomaszowi Twardowskiemu i prof. dr hab. Piotrowi Kozłowskiemu
za wszystkie rady i wskazówki.

mgr Katarzynie Solce, mgr Annie Wasilewskiej,
mgr. Mateuszowi Walkowiakowi i lic. Agacie Sobisiak
za pomoc w badaniach, dzięki czemu mogłam z powodzeniem skończyć tę rozprawę.

dr Paulinie Żydowicz – Machtel, mgr inż. Klementynie Marciniak,
mgr. inż. Piotrowi Pietrasowi, inż. Julianowi Zacharjaszowi
za niezliczone, ciekawe rozmowy, za przyjaźń i wsparcie oraz wszelką pomoc.

dr Agacie Tyczewskiej, dr Joannie Gracz-Bernaciak i mgr. inż. Jakubowi Kuczyńskiemu
za przemiłą atmosferę w pracy i nieocenioną pomoc.

Kolegom i Koleżankom z Zakładu Neuroonkologii Molekularnej oraz
z Zakładu Genetyki Molekularnej, zwłaszcza mgr Katarzynie Chojnackiej
za miłą współpracę i wszelką pomoc.

Rafałowi
za ogromne wsparcie przez te wszystkie lata i za to, że nigdy we mnie nie zwątpił i dodawał sił, gdy mi ich brakło.

Moim Kochanym Rodzicom, Bratu, Babciom, oraz całej Rodzinie i Przyjaciołom
za ogromne wsparcie oraz dzielne kibicowanie do samego końca.

Dziękuję

Pracę tę dedykuję moim Rodzicom, Agnieszce i Krzysztofowi,
którzy nieustannie we mnie wierzyli i wspierali moje zamiłowanie do Nauki.

Niniejsza rozprawa doktorska składa się z następujących części:

SPIS PUBLIKACJI WCHODZĄCYCH W SKŁAD ROZPRAWY DOKTORSKIEJ

1. Bąkowska-Żywicka K, **Mleczko AM**, Kasprzyk M, Machtel P, Żywicki M, Twardowski T
   The widespread occurrence of tRNA-derived fragments in Saccharomyces cerevisiae
   FEBS Open Bio, 2016, 6(12):1186-1200 **(IF$_{2016}$= 2.143)**

2. **Mleczko AM,** Celichowski P, Bąkowska-Żywicka K
   Transfer RNA-derived fragments target and regulate ribosome-associated aminoacyl-transfer RNA synthetases
   Biochimica et Biophysica Acta – Gene Regulatory Mechanisms, 2018, 1861(7): 647-656 **(IF$_{2018}$= 4.599)**

3. **Mleczko AM**, Bąkowska – Żywicka K
   When small RNAs become smaller: emerging functions of snoRNAs and their derivatives
   Acta Biochimica Polonica, 2016, 63(4):601-607 **(IF$_{2016}$=1.159)**

4. Walkowiak M*, **Mleczko AM***, Bąkowska-Żywicka K
   Evaluation of methods for detection of low-abundant snoRNA-derived small RNAs in Saccharomyces cerevisiae
   BioTechnologia, 2016, 97(1):19-26 *Autorzy mieli taki sam wkład w przygotowanie publikacji

5. **Mleczko AM***, Machtel P*, Walkowiak M, Wasilewska A, Pietras PJ, Bąkowska-Żywicka K
   Levels of sdRNAs in cytoplasm and their association with ribosomes are dependent upon stress conditions but independent from snoRNA expression
   Scientific Reports, 2019, 9 (1) **(IF$_{2018}$=4.011)** *Autorzy mieli taki sam wkład w przygotowanie publikacji

Spis innych publikacji, niewchodzących w skład rozprawy doktorskiej

1. Gebetsberger J, Wyss L, **Mleczko AM**, Reuther J, Polacek N
   A tRNA-derived fragment competes with mRNA for ribosome binding and regulates translation during stress
   RNA Biology, 2017, 14(10):1364-1373 **(IF_{2017}=5.216)**

2. Nowicki G, Walkowiak-Nowicka K, Zameleduch-Barylska A, **Mleczko A**, Frąckowiak P, Nowaczyk N, Kozdrowska E, Barylski J
   Complete genome sequences of two novel autographiviruses infecting a bacterium from the Pseudomonas fluorescens group
   Archives of Virology, 2017, 162(9):2907-2911 (**IF_{2017}=2.160**)

3. **Mleczko AM,** Celichowski P, Bąkowska-Żywicka K
   Ex-translational function of tRNAs and their fragments in cancer
   Acta Biochimica Polonica, 2014, 61(2):211-216 **(IF_{2014}=1.153)**

4. Kasprzyk M, **Mleczko AM,** Celichowski P, Bąkowska-Żywicka K
   Przetwarzanie RNA — niezwykły mechanizm powstawania nowych klas niekodujących RNA z funkcjonalnych RNA
   Postępy Biochemii, 2014, 60(3):295-304

STRESZCZENIE

Rozwój technik z zastosowaniem głębokiego sekwencjonowania i wysokowydajnych analiz doprowadził do odkrycia szerokiej gamy cząsteczek RNA, które nie kodują białek (ncRNA). Cząsteczki te mogą pełnić kluczowe role w procesach regulacji ekspresji genów na wielu etapach życia komórki. W ostatnich latach pojawiły się doniesienia, że komórkowe ncRNA mogą w określonych warunkach stać się prekursorami krótszych RNA. Ten stosunkowo nowy temat jest obecnie obiektem intensywnych badań, których wyniki wykazały istnienie wielu nieznanych dotąd mechanizmów regulujących istotne funkcje komórek, jak odpowiedź na stres, metabolizm czy cykl komórkowy. W 2012 roku odkryto istnienie nowej ścieżki regulacji procesu biosyntezy białka poprzez bezpośrednią asocjację krótkich RNA z rybosomami u drożdży piekarskich *Saccharomyces cerevisiae*. Te krótkie RNA asocjujące z rybosomem nazwano rancRNAs (*ang. ribosome-associated noncoding RNAs*). Pośród rancRNA wykryto wiele nowych klas krótkich RNA, które powstają podczas warunków stresowych poprzez cięcie dobrze znanych niekodujących RNA takich jak snoRNA, rRNA, mRNA czy tRNA.

Celem badań podjętych w niniejszej pracy było pogłębienie wiedzy na temat rancRNA, ze szczególnym uwzględnieniem dwóch klas rancRNA: tRF (*ang. tRNA-derived fragments*) oraz sdRNA (*ang. snoRNA-derived RNAs*). W rozprawie zbadano zależne od stresu cięcie tRNA oraz snoRNA do krótszych RNA, analizę ich asocjacji z rybosomami oraz potencjalną funkcję u drożdży *S. cerevisiae*.

W pierwszym etapie pracy skupiono się na krótkich RNA powstających z tRNA. Najpierw zbadano zależne od stresu cięcie tRNA do tRF. Wyniki pokazały, że pula tRF pozostaje niezmienna, niezależnie od warunków środowiskowych, w których hodowano drożdże *S. cerevisiae*. Kolejnym krokiem było zbadanie funkcji wybranych tRF. Wykazano, że sześć tRF obniża poziom globalnej biosyntezy białka na etapie aminoacylacji tRNA poprzez bezpośrednią asocjację z rybosomem oraz syntetazami aminoacylo-tRNA.

Następnie zbadano cięcie oraz lokalizację subkomórkową snoRNA i sdRNA. Udowodniono, że zarówno sdRNA, jak i ich prekursory, snoRNA, są obecne w cytoplazmie, a ich ilość jest zależna od warunków stresowych. Co więcej, wykazano, że zarówno snoRNA jak i sdRNA asocjują z aktywnymi translacyjnie rybosomami wpływając na proces biosyntezy białka *in vitro* i *in vivo*.

Wyniki prezentowane w niniejszej rozprawie doktorskiej zostały opublikowane w czterech recenzowanych artykułach eksperymentalnych. Zagadnienia dotyczące cięcia snoRNA do sdRNA oraz ich funkcji zgromadzone w wyniku przeglądu dostępnej literatury zostały podsumowane w pracy przeglądowej, która również wchodzi w skład niniejszej rozprawy doktorskiej.

ABSTRACT

Development of deep sequencing and high-throughput techniques has led to the discovery of a wide range of non-coding RNA molecules (ncRNAs). These molecules play key roles during regulation of gene expression and they shape cellular life. In recent years it has been shown that under certain conditions non-coding RNAs may become precursors of shorter RNAs. This relatively new topic is currently the object of intense research. The existence of many unknown mechanisms that regulate important functions of cells, such as stress response, metabolism or cell cycle has recently been shown. Lately, the existence of a new protein biosynthesis regulation pathway was discovered. It has been shown that translation may be regulated by direct association of short RNAs with ribosomes in baker′s yeast *Saccharomyces cerevisiae*. Short RNAs which associate with the ribosome are named ribosome-associated noncoding RNAs (rancRNAs). Among rancRNAs, many new classes of short RNAs have been detected. These RNAs arise during stress conditions by processing of a well-known non-coding RNAs such as snoRNA, rRNA, mRNA or tRNA.

The aim of this study was to extend the knowledge about rancRNAs, with particular emphasis on two classes of rancRNAs: tRFs (tRNA-derived fragments) and sdRNAs (snoRNA-derived RNAs). I have examined stress-dependent processing of tRNAs and snoRNAs to shorter RNAs, performed analysis of their association with ribosomes and studied the potential function of tRFs and sdRNAs in yeast *S. cerevisiae*.

At initial steps of work, I have focused on short RNAs derived from tRNAs. I have examined stress-dependent cleavage of tRNAs to tRFs. The results showed that global tRF pool remains unchanged, regardless of the environmental conditions in which yeast *S. cerevisiae* was grown. The next step was to examine the functions of selected tRFs. I have shown that six ranc-tRFs are capable of decreasing the level of global protein biosynthesis at the tRNA aminoacylation level. tRFs achieve this by direct association with the ribosome and aminoacyl-tRNA synthetases.

Subsequently, the cleavage and subcellular localization of snoRNAs and sdRNAs were examined. I have found that both sdRNAs and their precursors, snoRNAs, are present in the cytoplasm and their abundance depends on stress conditions. Moreover, I showed that both snoRNAs and sdRNAs associate with translationally active ribosomes and thus sdRNAs may regulate protein biosynthesis *in vitro*.

The results presented in this doctoral dissertation have been published in four peer-reviewed experimental articles. Issues regarding processing of snoRNAs to sdRNAs and their functions are described and summarized in the review, which is also part of this doctoral dissertation.

OPIS WYNIKÓW PRACY DOKTORSKIEJ

Wprowadzenie

Rys historyczny

W połowie lat 50. XX wieku przyszły laureat Nagrody Nobla, George Palade zwrócił swą uwagę na nieznane jeszcze wtedy komponenty cytoplazmy [1]. Po dogłębnej analizie cząsteczek pod mikroskopem elektronowym Palade zauważył, że struktury te nie tylko występują w formie swobodnie pływającej w cytoplazmie, ale są również związane z retikulum endoplazmatycznym. Komponentami tymi okazały się rybosomy, określane wówczas jako „cząsteczki mikrosomalne". Jak zauważyli uczeni, „cząsteczki mikrosomalne" zbudowane były zarówno z RNA, jak i białek i znajdowały się w miejscach biosyntezy białek w komórce [2]. Kilka lat później, podczas sympozjum Towarzystwa Biofizycznego w 1958 roku zaproponowano nową, adekwatną nazwę: rybosom. W ten oto sposób świat nauki odkrył rybosomy, niezwykłe maszyny molekularne spełniające jedną z najważniejszych funkcji w życiu komórek-biosyntezę białka.

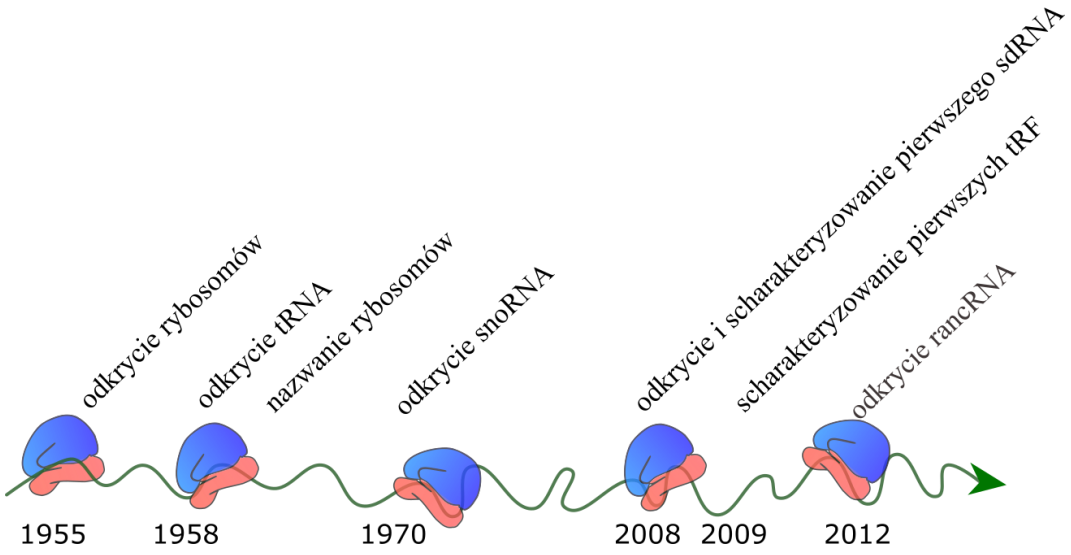

Rysunek 1. Rys historyczny odkryć związanych z rybosomami, tRNA oraz snoRNA [1-7].

Okres ten obfitował także w inne przełomowe odkrycia. Paul C. Zamecnik i Mahlon Hoagland odkryli kolejną cząsteczkę niezbędną do syntezy białek: transportujące RNA (tRNA) [3]. Było to istotne odkrycie również dlatego, że tRNA było pierwszym kiedykolwiek odkrytym RNA niekodującym białek. Dopiero pod koniec lat 60. XX wieku odkryto inne niekodujące RNA, będące przedmiotem niniejszej rozprawy doktorskiej, małe jąderkowe RNA (snoRNA) [4]. Sam termin „snoRNA" został wprowadzony dopiero w latach 80., ponad

dekadę po ich odkryciu [8]. Wszystkie te kamienie milowe na kartach historii odkryć biologii molekularnej (Rysunek 1) sprawiły, że wielu uczonych jeszcze do niedawna sądziło, iż w pełni zrozumieliśmy proces biosyntezy białka, czy też w pełni poznaliśmy funkcje tRNA i snoRNA. Dlatego też, kiedy w latach 70. zaobserwowano po raz pierwszy fragmenty tRNA, sądzono, że są to pozbawione jakiejkolwiek funkcji produkty degradacji RNA [9-11]. Dopiero po wielu latach, w pierwszej dekadzie XXI wieku odkryto, że zarówno krótkie RNA powstające ze snoRNA (sdRNAs, *ang. snoRNA-derived RNAs*) jak i tRNA (tRFs, *ang. tRNA fragments*) mogą posiadać funkcję i kształtować życie komórkowe. W 2008 roku po raz pierwszy zdefiniowano możliwą funkcję sdRNA [6]. Odkryto, że ludzki fragment snoRNA o nazwie ACA45 jest, podobnie jak miRNA, cięty przez enzym Dicer, wiąże się z białkami Ago oraz może być zaangażowany w post-transkrypcyjne wyciszanie genów. Rok później odkryto, że krótkie RNA powstające z tRNA nie są produktami degradacji, lecz także sprawują pewne funkcje w organizmach żywych [5]. Fragment tRNA o nazwie tRF-1001 ulega nadekspresji w wielu liniach komórek rakowych, a jego wyciszenie powoduje znaczne obniżenie proliferacji komórek. Ponadto odkryto, że fragment ten asocjuje z białkami Ago, co może wskazywać, że jego działanie jest podobne do działania miRNA [12]. W 2012 roku u drożdży piekarskich *Saccharomyces cerevisiae* odkryto istnienie krótkich RNA asocjujących z rybosomami, czyli rancRNA (*ang. ribosome-associated noncoding RNAs*) [7], co zasugerowało istnienie nowej ścieżki regulacji biosyntezy białka poprzez bezpośrednią asocjację RNA z rybosomami. Wśród licznych klas drożdżowych rancRNA znalazły się zarówno tRF jak i sdRNA.

Krótkie RNA powstające z tRNA

Od czasu odkrycia krótkich RNA powstających z tRNA ich nazewnictwo było bardzo niespójne. Pojawiały się takie nazwy jak połówki tRNA (*ang. tRNA halves*), fragmenty RNA pochodzące z tRNA (tRFs, *ang. tRNA fragments*) [5], krótkie RNA indukowane stresem (tiRNAs, *ang. tRNA-derived stress-induced RNAs*) [13], krótkie RNA pochodzące z tRNA (tsRNAs, *ang. tRNA-derived small RNAs*) [12] lub RNA z raka pęcherza moczowego (ubcRNAs, *ang. urinary bladder carcinoma RNAs*) [14]. Niespójne nazewnictwo prowadziło do licznych nieporozumień. Dlatego też, w 2011 roku zaproponowano nową nomenklaturę opartą na wielkości fragmentu tRNA i części cząsteczki tRNA, z której pochodzi [15]. Zgodnie z nią, fragmenty tRNA można podzielić na dwie główne klasy: 3′ i 5′ połówki tRNA oraz 3′ i 5′ fragmenty tRNA (tRF) (Rysunek 2).

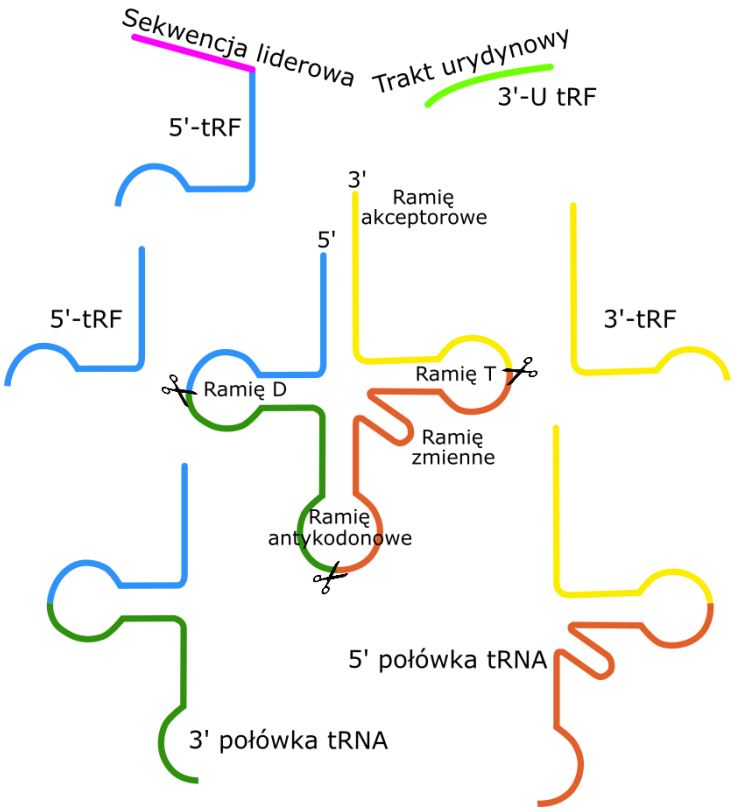

Rysunek 2. Uproszczona drugorzędowa struktura tRNA oraz fragmentów, które z niej powstają.

Dowiedziono, że zarówno połówki jak i fragmenty tRNA powstają często podczas warunków stresowych dla organizmu [13,16-27]. U orzęska *Tetrahymena thermophila* powstają np. w wyniku działania głodu aminokwasowego [16], u *Arabidopsis thaliana* podczas głodu fosforanowego i stresu oksydacyjnego [19], u *Giardia lamblia* podczas tworzenia cyst [20], u *Escherichia coli* podczas infekcji fagiem T [21], u ludzi podczas stresu oksydacyjnego, UV, hiperosmotycznego, szoku cieplnego, hipotermii, hipoksji czy też podczas rozwoju choroby nowotworowej [5,12,13,22-26,28], a u drożdży *S. cerevisiae* podczas wielu warunków stresowych, jak np. stres oksydacyjny, stres niskiego lub wysokiego pH, stres osmotyczny oraz podczas warunków optymalnych wzrostu, co zostało opisane dokładnie w publikacji wchodzącej w skład niniejszej rozprawy doktorskiej [27].

Połówki tRNA mają długość ~30-35 nt i powstają poprzez cięcie w pętli antykodonowej. U wyższych eukariontów enzymem odpowiedzialnym za cięcie jest angiogenina, należąca do rodziny RNaz A [13]. U drożdży cząsteczki tRNA cięte są na połówki przez Rny1p należącą do rodziny rybonukleaz T2 [29]. tRF mają długość około 20 nt są przetwarzane z końca 5′ lub 3′ dojrzałych tRNA (5′-tRF i 3′-tRF) lub niedojrzałych tRNA (pre-tRNA) [30-32]. Fragmenty powstałe z końca 3′ pre-tRNA nazywane są 3′-UtRF i powstają podczas przetwarzania pre-tRNA przez RNazę Z lub jej homolog, endonukleazę ELAC2 [5,33,34]. Mechanizmy powstawania tRF nie są jeszcze

całkowicie poznane, nie odkryto też jeszcze wszystkich enzymów odpowiedzialnych za ten proces. Odkryto jednak, że rybonukleaza Dicer może brać udział w powstawaniu tRF, pomimo, że tRNA nie spełnia klasycznych kryteriów strukturalnych substratu dla Dicer [24,35-37].

Do tej pory poznano różnorodne funkcje i mechanizmy działania tRF oraz połówek tRNA. Najlepiej poznanym mechanizmem działania krótkich RNA powstających z tRNA jest odkrycie, że mogą one działać podobnie do siRNA lub miRNA [12,26,37-40]. Co istotne, fragmenty tRNA mogą wpływać na biogenezę rybosomów [41], mogą także regulować odpowiedź immunologiczną [42]. Przypuszcza się, że krótkie RNA powstające z tRNA mogą działać jako czynnik epigenetyczny. Odkryto, że połówki tRNA są najbardziej rozpowszechnionymi krótkimi RNA w nasieniu myszy [43]. Połówki tRNA jak i tRF z plemników, dostarczone podczas zapłodnienia, mogą zmienić transkryptom zarodków we wczesnym stadium rozwoju [44,45].Wszystkie te odkrycia pokazują, że klasa tych cząsteczek charakteryzuje się niezwykłymi możliwościami regulatorowymi.

Krótkie RNA powstające ze snoRNA

snoRNA mogą być przetwarzane do krótszych, funkcjonalnych fragmentów i podobnie jak w przypadku tRF, niektóre sdRNA mogą powstawać poprzez ciecie enzymem Dicer [6,46,47]. Wiadomo, że snoRNA z rodziny H/ACA są cięte do fragmentów o długości 17-19 nt, natomiast te z rodziny C/D do fragmentów dłuższych niż 27 nt [48]. Krótkie RNA powstające ze snoRNA mogą być wycinane zarówno z końców jak i ze środka snoRNA, tak jak ma to miejsce u drożdży *S. cerevisiae* (Rysunek 3)[7].

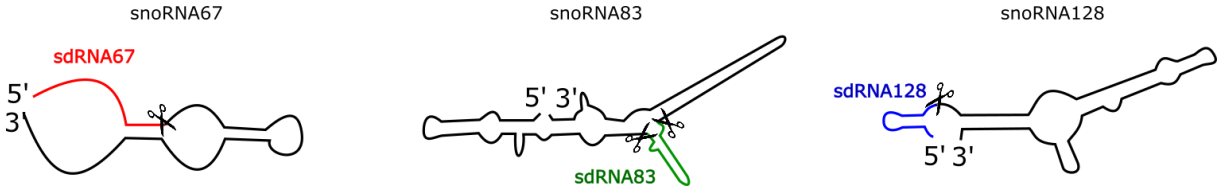

Rysunek 3. Uproszczona struktura drugorzędowa badanych w niniejszej rozprawie doktorskiej drożdżowych snoRNA oraz fragmentów, które z nich pochodzą (zaznaczone kolorami).

Tak jak w przypadku tRF, najlepiej poznaną funkcją sdRNA jest ich działanie na ścieżce podobnej do miRNA [6,46,47,49]. Fragmenty snoRNA mogą również brać udział w regulacji alternatywnego składania [50]. Zagadnienie niekanonicznych funkcji snoRNA jak i powstających z nich sdRNA zostało szczegółowo opisane w pracy przeglądowej pt.: *„When small RNAs become smaller: emerging functions of snoRNA and their derivatives”* wchodzącej w skład rozprawy doktorskiej.

Krótkie RNA asocjujące z rybosomem (rancRNA)

Krótkie RNA mogą asocjować bezpośrednio z rybosomami (Rysunek 34) i w konsekwencji wpływać na proces biosyntezy białka [7]. Wśród rancRNA wykryto krótkie RNA będące produktami przetwarzania: tRNA, rRNA, mRNA i snoRNA. Krótki, 18-nukleotydowy rancRNA (rancRNA_18) powstający z mRNA genu *TRM10* kodującego metylotransferazę tRNA oddziałuje z rybosomami 80S drożdży *S. cerevisiae* hodowanych w optymalnych warunkach wzrostu [51]. Jednak pod wpływem stresu hiperosmotycznego asocjuje z aktywnymi translacyjnie polisomami i obniża poziom translacji. Kolejnego odkrycia dokonano w komórkach *E. coli*, gdzie wykazano przetwarzanie dojrzałego 16S rRNA do fragmentu o długości około 80 nt [52]. Fragment 16S rRNA powstaje tylko podczas fazy stacjonarnej i łączy się z małą podjednostką rybosomalną 30S. Rybosomy, do których przyłączony jest fragment, wykazują wyraźnie zmniejszoną aktywność translacyjną.

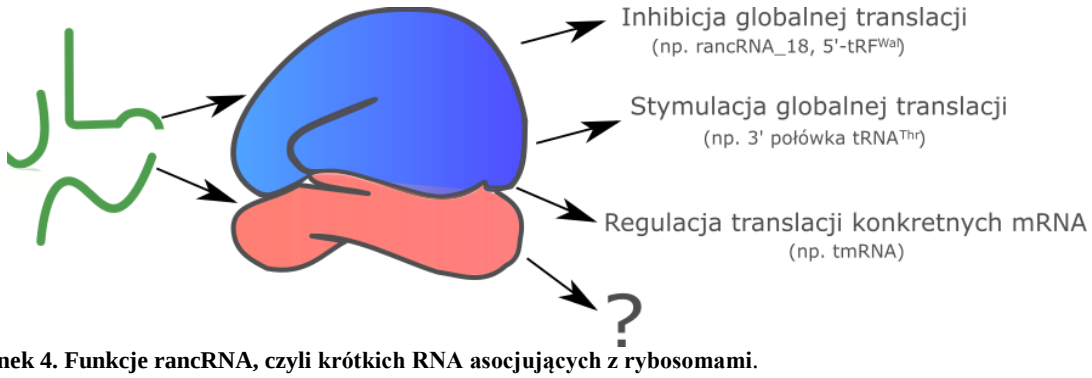

Rysunek 4. Funkcje rancRNA, czyli krótkich RNA asocjujących z rybosomami.

U *Haloferax volcanii* 5′-tRF pochodzący z $tRNA^{Wal}$ powstaje podczas stresu wysokiego pH i wiąże się do małej podjednostki rybosomu [53,54]. W konsekwencji mRNA zostaje wyparty z kompleksu inicjacyjnego, co powoduje globalne zmniejszenie translacji *in vivo* i *in vitro*. Wykazano też, że fragmenty tRNA mogą mieć stymulujący wpływ na syntezę białka [55]. Podczas stresu głodu u świdrowca *Trypanosoma brucei* najliczniej wytwarzanym krótkim RNA powstającym z tRNA jest 3′ połówka $tRNA^{Thr}$. Kiedy komórki się regenerują po ustaniu warunków głodu, połówka $tRNA^{Thr}$ wiąże się z rybosomami oraz z aktywnymi translacyjnie polisomami i stymuluje translację, ułatwiając ładowanie mRNA do rybosomu. Celowe wyciszenie endogennych połówek $tRNA^{Thr}$ łagodzi ten efekt zarówno *in vivo*, jak i *in vitro*. Wśród rancRNA są też takie RNA, które regulują translację konkretnych mRNA. Jako przykład można potraktować występujący u bakterii tmRNA (*ang. transfer messenger RNA*), który strukturalnie i funkcjonalnie przypomina tRNA oraz mRNA. Koniec 5′ tego RNA jest cięty przez RNazę P, RNA ten ma też modyfikacje typowe dla tRNA, ulega aminoacylacji alaniną i wiąże się do czynnika translacyjnego EF-Tu

i razem z nim oraz GTP łączy się z rybosomem [56-59]. tmRNA działa także jako mRNA: w jego środkowej części kodowany jest krótki peptyd [60]. Dzięki cechom tRNA, tmRNA wchodzi do rybosomu w miejsce A wiązania tRNA, po czym następuje synteza krótkiego peptydu kodowanego w środkowej części tmRNA. Umożliwia to zarówno recykling zatrzymanych na mRNA rybosomów, jak i znakowanie niepoprawnie powstałego białka w celu degradacji [61]. Nasza grupa badawcza skupia się na krótkich RNA powstających z tRNA i snoRNA u drożdży *S. cerevisiae*. tRF i sdRNA asocjują z rybosomem i pełnią rolę regulacyjną podczas translacji. Szczegółowe wyniki badań nad funkcją tRF i sdRNA u drożdży *S. cerevisiae* zostały opisane w publikacjach wchodzących w skład niniejszej rozprawy doktorskiej.

Spektrum działania rancRNA na translację jest bardzo różne. Cząsteczki te asocjują zarówno z małą, dużą podjednostką rybosomu jak i z aktywnymi translacyjnie polisomami, tym samym mogąc zarówno hamować jak i wspomagać syntezę białka. Wszystkie doniesienia naukowe na temat rancRNA wskazują na to, że nie są one pasywnymi autostopowiczami maszynerii translacyjnej czy też produktami degradacji, lecz są nowo poznawaną klasą rybo-regulatorów biosyntezy białek, być może tworzących wyspecjalizowane rybosomy.

Cel i uzasadnienie podjętej tematyki pracy

Celem badań podjętych w ramach niniejszej rozprawy doktorskiej było pogłębienie wiedzy na temat krótkich RNA asocjujących z rybosomami u drożdży *Saccharomyces cerevisiae*. Najważniejszym aspektem pracy było poznanie genezy i funkcji krótkich RNA powstających z tRNA i snoRNA w zróżnicowanych warunkach środowiskowych.

Kiedy poznano mechanizmy działania pierwszych odkrytych tRF i sdRNA, uwaga badaczy skupiona była na funkcjonowaniu tych cząsteczek na ścieżce podobnej do miRNA [5,6]. Wiele późniejszych badań nad tymi krótkimi RNA w istocie wykazało, że mogą działać podobnie do miRNA i być cięte przez te same enzymy. Kiedy zatem w 2012 roku zaobserwowano, że w puli krótkich RNA asocjujących z rybosomem (rancRNA) u drożdży *S. cerevisiae* znajdują się tRF oraz sdRNA [7], zadano sobie pytanie, w jaki sposób cząsteczki te mogą działać w organizmie pozbawionym ścieżki miRNA? Jak do tej pory, z kilkoma wyjątkami, nie wyjaśniono funkcji tych krótkich RNA na ścieżce niezależnej od miRNA.

Nadal nie wiadomo, co leży u podstaw przetwarzania znanych niekodujących RNA do krótszych, stabilnych cząsteczek, stąd punktem wyjścia w moim doktoracie było przeanalizowanie warunków powstawania tRF w organizmie modelowym *S. cerevisiae*. Aby odkryć funkcję tRF, najpierw należało zbadać ich biogenezę podczas zmiennych warunków środowiskowych. Jak zostało wspomniane we wstępie, powstawanie tRF i połówek tRNA może być indukowane, gdy komórka jest narażona na warunki stresowe. Aby odpowiedzieć na pytanie w jakich warunkach z tRNA powstają tRF u drożdży, przeanalizowałam przetwarzanie czterdziestu drożdżowych izoform tRNA w 12 warunkach środowiskowych za pomocą techniki hybrydyzacji typu northern **(Publikacja 1)**. W badaniu tym zdecydowałam się na wykorzystanie właśnie tej techniki, gdyż inne, nowoczesne metody badań RNA, takie jak sekwencjonowanie, stwarzają pewne problemy. Podczas przygotowania bibliotek cDNA do sekwencjonowania, modyfikacje tRNA mogą wpływać na działanie odwrotnej transkryptazy i prowadzić do fałszywego wykrywania fragmentów tRNA, które nie są w istocie tRF. W niniejszej pracy określiłam również wpływ czterech różnych metod izolacji RNA na ilość oraz jakość uzyskiwanych fragmentów tRNA, udowadniając, że ten początkowy etap badań ma kluczowe znaczenie dla dalszych wyników. Potrzeba porównania różnych metod izolacji RNA wynikała z faktu, że różne metody oczyszczania RNA mogą znacznie wpłynąć na skład i ilość krótkich RNA w uzyskanej

próbie [62]. Dotychczas przeprowadzano optymalizację warunków izolacji miRNA [63,64], natomiast nie było badań optymalizujących izolację innych krótkich RNA.

W kolejnym etapie badań skupiłam się na sprawdzeniu funkcji wybranych krótkich RNA powstających z tRNA. Wiadomo, że te krótkie RNA bezpośrednio asocjują z rybosomem, zatem moim celem było sprawdzenie możliwych funkcji tRF podczas biosyntezy białka. Prawie wszystkie poprzednie badania funkcjonalne nad tRF koncentrowały się na krótkich RNA powstających z 5′ końca tRNA. Co więcej, niemalże wszystkie funkcjonalnie scharakteryzowane 3′-tRF działały na ścieżce miRNA. W związku z powyższym, kolejnym zadaniem było funkcjonalne scharakteryzowanie pięciu krótkich RNA pochodzących z 3′ końca tRNA (oraz jednego pochodzącego z końca 5′) w *S. cerevisiae*, organizmie, który nie posiada mechanizmów regulacji ekspresji genów zależnych od miRNA **(Publikacja 2).**

Moją pracę nad krótkimi RNA powstającymi ze snoRNA rozpoczęłam od przeglądu literatury poruszającej tę tematykę. sdRNA to nowa klasa niekodujących RNA i w mojej opinii, wiedza na ten temat nie była dostatecznie usystematyzowania. W związku z tym rozpoczęłam pracę nad artykułem przeglądowym poruszającym ten temat, co zaowocowało publikacją opisującą niekanoniczne funkcje snoRNA i ich pochodnych **(Publikacja 3)**.

Następnie skupiłam się na przeanalizowaniu powstawania, lokalizacji subkomórkowej oraz funkcji krótkich RNA powstających ze snoRNA. Podobnie jak w przypadku krótkich RNA powstających z tRNA, początkowym etapem badań była analiza warunków powstawania sdRNA. Z poprzednich doniesień naukowych wiadomo, że w komórkach drożdży ilość sdRNA jest znacznie mniejsza niż ilość tRF [7]. Ze względu na niski poziom tych krótkich RNA w komórkach, konwencjonalne techniki detekcji RNA takie jak hybrydyzacja typu northern czy mikromacierze mogą być niewystarczające, aby je wykryć [65,66]. W ramach wstępu do dalszych badań przeprowadziliśmy szereg eksperymentów mających na celu możliwie najlepsze zoptymalizowanie techniki hybrydyzacji typu northern **(Publikacja 4)**. W związku z tym, że technika ta w istocie okazała się niedostatecznie czuła do wykrycia sdRNA, zdecydowałam się na zastosowanie techniki odwrotnej transkrypcji z użyciem specyficznych starterów o strukturze spinki (SL-RT PCR, *ang. stem-loop reverse transcription PCR*), następnie stosując PCR pulsacyjny. Metody te zostały jednak wcześniej zoptymalizowane pod kątem wykrywania miRNA [67,68], natomiast nigdy nie były używane do wykrycia innych krótkich RNA. Moim celem było zatem zoptymalizowanie wyżej wymienionych metod do wykrywania występujących w niewielkich ilościach sdRNA**.**

Obecnie powszechnie przyjmuje się, że snoRNA nie są zlokalizowane wyłącznie w jądrze komórkowym, ale też w cytoplazmie, gdzie ich ilość może ulegać dynamicznym zmianom pod wpływem zmiennych warunków, w jakich żyje komórka [69,70]. Dysponując odpowiednimi narzędziami do detekcji sdRNA, podobnie jak w przypadku tRF, przeanalizowałam wpływ 12 warunków środowiskowych na ilość oraz lokalizację sdRNA i snoRNA (rybosom/cytoplazma). Do tej pory nie istniały żadne badania, które miałyby na celu odkrycie ilości i lokalizacji tychże RNA w komórkach poddawanym różnym stresom środowiskowym. W związku z tym podjęłam się analizy lokalizacji subkomórkowej zarówno pełnej długości snoRNA jak i krótkich RNA pochodzących ze snoRNA **(Publikacja 5).** Biorąc pod uwagę fakt, że snoRNA oraz ich pochodne mogą znajdować poza jądrem komórkowym i asocjują z rybosomami, można podejrzewać, że w cytoplazmie sterują one odpowiedzią na stres środowiskowy. Pomimo niewielkich ilości sdRNA u drożdży, nie można wykluczyć ich potencjału regulatorowego wpływającego na biosyntezę białka. Wykazano, że nawet stosunkowo niewielka ilość (w porównaniu do ~ 200 000 rybosomów/komórkę) rancRNA o nazwie rancRNA_18 (~ 27 000 cząsteczek/komórkę) jest wystarczająca, aby wpłynąć na translację [51]. Wiadomo też, że sdRNA asocjują z rybosomami *S. cerevisiae*. W związku z tymi doniesieniami postanowiłam również sprawdzić, czy drożdżowe sdRNA mogą wpłynąć na proces biosyntezy białka u *S. cerevisiae* i innych organizmów.

Metody

W publikacjach wchodzących w skład niniejszej rozprawy doktorskiej wykorzystano następujące metody:

Szczep drożdży i warunki hodowli

W badaniach użyto drożdży *Saccharomyces cerevisiae*, szczep BY4741. Drożdże hodowano w optymalnym medium YPD w temperaturze 30°C. Zastosowano 11 warunków stresowych: ciepła, zimna, wysokiego zasolenia, światła UV, anaerobowy, wysokiego pH, niskiego pH, głodu aminokwasowego, głodu cukrowego, hipoosmotyczny i hiperosmotyczny. Indukcja stresów została zweryfikowana metodą RT-qPCR poprzez sprawdzenie poziomów ekspresji genów regulowanych stresem środowiskowym: *HSP12*, *GPD1*, *PDR12* i *EXO1*.

Krótkie RNA powstające z tRNA i snoRNA

tRF i sdRNA do eksperymentów funkcjonalnych wybrano na podstawie ilości odczytów w bibliotece rancRNA [7]. Zbadano sześć tRF: 3′-tRF^{His} (GTG), 3′-tRF^{Ser} (AGA), 3′-tRF^{Gly} (GCC), 3′-tRF^{Leu} (TAA), 3′-tRF^{Thr} (TGT), 5′-tRF^{His} (GTG), trzy snoRNA (snR67, snR83 i snR128) oraz powstające z nich trzy sdRNA (sdR67, sdR83 i sdR128).

Izolacja RNA

Izolacja RNA przeprowadzana była pięcioma metodami, zależnie od dalszych eksperymentów:

1) z użyciem zestawu *MicroRNA isolation kit* firmy A&A Biotechnology. Metoda ta oparta jest na ekstrakcji RNA fenolem/chloroformem a oczyszczanie wymaga użycia kolumienek krzemionkowych.

2) z użyciem zestawu *MasterPureTM Yeast Purification* firmy Epicentre. Izolacja RNA odbywa się przez trawienie komórek proteinazą K, po którym następuje szybki proces odsalania w celu usunięcia zanieczyszczeń. RNA wytrącano różną ilością izopropanolu, aby uzyskać nisko- i wysokocząsteczkowe RNA.

3) z użyciem 90% fenolu. Jest to metoda izolacji niskocząsteczkowych RNA, tzw. izolacja „bulk tRNA” z komórek drożdży opracowana przez Monier i wsp. [71]. Metoda opiera się na izolacji RNA poprzez łagodne traktowanie komórek 90% fenolem.

Po tym etapie, RNA traktowano chlorkiem litu, aby usunąć rybosomalne RNA, następnie RNA wytrącano etanolem.

4) z użyciem buforu LET [29]. RNA izolowane tą metodą wymaga etapu izolacji fenol/chloroform, a następnie wytrącane jest etanolem.

5) z użyciem odczynnika *TRIzol* (Ambion) według protokołu producenta.

Jakość wyizolowanego RNA sprawdzana była na spektrofotometrze NanoDrop ND-1000 oraz Bioanalyzer 2100 przy użyciu zestawu *Agilent Small RNA kit* i *RNA Nano 6000* (Agilent Technologies).

Do dalszej analizy metodą SL-RT-PCR, RNA wyizolowane metodą TRIzol rozdzielono w 10% żelu poliakrylamidowym (PAA), po czym odpowiedniej długości RNA eluowano z żelu.

Hybrydyzacja typu northern

RNA rozdzielono na 12% denaturującym żelu PAA i przenoszono na dodatnio naładowaną membranę nitrocelulozową z zastosowaniem transferu półsuchego. Kwasy nukleinowe utrwalano na membranie przy użyciu światła UV. Fragmenty tRNA i snoRNA wykrywano za pomocą antysensowych sond DNA lub LNA znakowanych na końcu 5′ fosforem [^{32}P]. Temperatury hybrydyzacji różniły się zależnie od użytej sondy. Do wizualizacji wyników użyto ekranów odwzorowujących (GE Healthcare) i analizatora fluorescencyjnego Fujifilm FLA-5100.

Pulsacyjna odwrotna transkrypcja z użyciem starterów o strukturze spinki połączona z PCR (SL-RT-PCR)

Pulsacyjną odwrotną transkrypcję sdRNA i snoRNA przeprowadzono przy użyciu zestawu *SuperScriptIII* (Invitrogen). Do odwrotnej transkrypcji snoRNA zastosowano standardowe startery zaprojektowane przy użyciu narzędzia Primmer3Plus. Do odwrotnej transkrypcji sdRNA zastosowano startery o strukturze spinki. Reakcje RT zostały wykonane w sposób multipleksowy. Produkty odwrotnej transkrypcji poddano reakcji PCR.

Emulsyjny PCR (ddPCR, ang. droplet digital PCR)

Liczba kopii sdRNA i snoRNA została określona przy użyciu systemu QX100 ™ Droplet Digital ™ PCR (Bio-Rad, Pleasanton, CA). Do przeprowadzenia reakcji zastosowano dedykowaną dla tej metody i dostępną komercyjnie mieszaninę reakcyjną *2x QX200 ™ ddPCR ™ EvaGreen Supermix*.

Profilowanie polisomów

Profilowanie polisomów przeprowadzono według protokołu Pospisek i wsp., [72] z niewielkimi modyfikacjami. Na 15 min przed zbiorem, do hodowli drożdży *S. cerevisiae* dodano antybiotyk cykloheksymid. Następnie z drożdży uzyskano oczyszczone lizaty, które nakładano na liniowy gradient sacharozy 8-40%. Gradienty wirowano w rotorze Beckman SW40 Ti 39000 rpm/min Gradienty sacharozy analizowano za pomocą monitorowania absorbancji w świetle A254 za pomocą detektora UV.

Izolacja rybosomów i frakcji post-rybosomalnej

Rybosomy drożdży izolowano zgodnie z wcześniejszym opisem, z niewielkimi modyfikacjami [73]. Po uzyskaniu czystego lizatu komórkowego, rybosomy (P100) pozyskano przez wirowanie przy 41800 rpm/min w rotorze Beckman 70.1 Ti. Następnie zebrano część supernatantu, zamrożono i oznaczono, jako frakcja S100. Osad rybosomów, czyli frakcję P100, rozpuszczono w odpowiednim buforze i przechowywano do dalszych eksperymentów w -80°C. Czystość frakcji P100 i S100 była sprawdzona za pomocą Agilent Bioanalyzer 2100 z wykorzystaniem zestawu *RNA Nano 6000*.

Testy asocjacji in vitro

Niekowalencyjne wiązanie tRF z rybosomami 80S oraz podjednostkami 60S i 40S zmierzono stosując test przeprowadzony zgodnie z opisem w [74]. W skrócie, 80S, 60S i 40S inkubowano z syntetycznym RNA znakowanym na końcu 5′ fosforem [^{32}P]. Po inkubacji, reakcje przesączono przez membranę nitrocelulozową, a następnie poziom radioaktywności monitorowano za pomocą ekranów odwzorowujących (GE Healthcare) i analizatora fluorescencyjnego Fujifilm FLA-5100. Podjednostki 60S i 40S izolowano według protokołu [75].

Testy translacji in vivo i in vitro

Wpływ tRF i sdRNA na translację *in vivo* sprawdzono za pomocą znakowania metabolicznego. Do sferoplastów drożdżowych wprowadzono metodą elektroporacji odpowiednią ilość syntetycznych tRF lub sdRNA. Jako kontrolę zastosowano cykloheksymid. Po elektroporacji próbki inkubowano przez godzinę w pożywce YPD w środowisku izoosmotycznym w obecności znakowanej radioaktywnie metioniny [^{35}S]. Następnie, białka wytrącono kwasem trichlorooctowym i filtrowano na filtrach z włókna szklanego. Ilość wyznakowanego białka oznaczano za pomocą licznika scyntylacyjnego.

Translację *in vitro* w bezkomórkowym systemie drożdżowym przeprowadzano według protokołów [76,77] z niewielkimi modyfikacjami. W skrócie, z drożdży uzyskano oczyszczony i aktywny translacyjnie ekstrakt. Do ekstraktu dodawano: koktajl translacyjny, znakowaną radioaktywnie metioninę [^{35}S] oraz syntetyczne krótkie RNA powstające z tRNA lub snoRNA. Wyniki analizowano za pomocą licznika scyntylacyjnego (ilość wyznakowanego białka związanego z filtrem) lub rozdziału elektroforetycznego białek.

Translację matryc poli(U) przeprowadzano według protokołu [74]. W reakcjach użyto rybosomów izolowanych z drożdży, matrycy poli(U), czynników białkowych wyizolowanych z drożdży (frakcja S100), deacylowanych tRNA drożdży, znakowanej radioaktywnie fenyloalaniny [^{3}H] oraz badanych, syntetycznych krótkich RNA. Po inkubacji białka wytrącono za pomocą kwasu trichlorooctowego, filtrowano na filtrze z włókna szklanego i oceniono ilość wyznakowanego białka w próbie za pomocą licznika scyntylacyjnego.

Reakcje translacji *in vitro* w innych niż drożdże organizmach przeprowadzono przy użyciu dostępnych komercyjnie zestawów do translacji w kiełkach pszenicy (Promega), retikulocytach króliczych (Promega) i komórkach ludzkich HeLa (Pierce) zgodnie z instrukcjami producentów.

Testy aminoacylacji tRNA

Badania nad aminoacylacją wszystkich tRNA drożdżowych przeprowadzano przy użyciu wyizolowanych z drożdży tRNA oraz wyznakowanych radioaktywnie wodorem [^{3}H] aminokwasów (His, Ser, Gly, Leu, i Thr) lub mieszaniny aminokwasów wyznakowanych [^{14}C]. Do mieszaniny reakcyjnej dodawano bufor do aminoacylacji oraz czynniki białkowe wyizolowane z drożdży (frakcja S100). Aby zmierzyć aktywność aminoacylacyjną cząsteczek asocjujących ze składowymi rybosomu, zamiast frakcji S100 do mieszaniny reakcyjnej dodawano odpowiednie składowe rybosomu. Po inkubacji produkty reakcji wytrącano kwasem trichlorooctowym i przesączano przez filtry z włókna szklanego. Efektywność aminoacylacji mierzono następnie na liczniku scyntylacyjnym.

Wpływ tRF na aminoacylację *in vivo* oceniono poprzez elektroporację sferoplastów syntetycznymi tRF. Następnie ze sferoplastów izolowano RNA, które rozpuszczono w buforze o pH 5,0. Jako kontrolę porcję RNA poddano deacylowaniu. Następnie deacylowane RNA oraz RNA wyizolowane ze sferoplastów rozdzielono w kwaśnym denaturującym 6,5% żelu PAA (jak opisano w [78]). Następnie wykonano hybrydyzację typu northern z sondą komplementarną do tRNA^{His} (GTG).

Technika opóźnienia migracji cząsteczek w żelu poliakrylamidowym (EMSA, ang. electrophoretic mobility shift assay)

Najpierw inkubowano syntetyczne, wyznakowane [^{32}P] tRF w odpowiednim buforze razem z oczyszczonymi syntetazami aminoacylo-tRNA lub z rozpuszczalnymi czynnikami białkowymi (S100) lub z rybosomami (P100). Następnie, produkty reakcji rozdzielono w 8% niedenaturujących żelach PAA a kompleksy cząsteczek w żelu uwidoczniono za pomocą ekranów odwzorowujących (GE Healthcare) i analizatora fluorescencyjnego Fujifilm FLA-5100.

Testy sprawdzające wiązanie syntetaz aminoacylo-tRNA do rybosomów

Testy wiązania i sedymentacji przeprowadzono jak opisano wcześniej w [79]. Syntetazy aminoacylo-tRNA i oczyszczone rybosomy inkubowano, a następnie wirowano. Zebrany osad rozdzielono w żelu PAA i wykonano transfer białek na membranę poliwinylową w celu przeprowadzenia analizy metodą western z przeciwciałami anti-GST lub anti-RPL5 (kontrola). Po przepłukaniu membran inkubowano je w obecności króliczego przeciwciała skoniugowanego z alkaliczną fosfatazą. Membrany ponownie przepłukano i rozwinięto kolorymetrycznie w systemie alkalicznej fosfatazy.

Testy statystyczne

Analiza statystyczna była bardzo istotnym elementem wszystkich etapów prowadzonych badań. Do analizy i interpretacji otrzymanych wyników stosowano: obliczanie odchylenia standardowego, t-test, test ANOVA, test HSD Tukeya, stosowano też statystyczne metody analizy danych R.

Skrótowy opis publikacji wchodzących w skład rozprawy doktorskiej

1. **Bąkowska-Żywicka K, Mleczko AM, Kasprzyk M, Machtel P, Żywicki M, Twardowski T**
   The widespread occurrence of tRNA-derived fragments in Saccharomyces cerevisiae
   FEBS Open Bio, 2016, 6(12):1186-1200

W pierwszej pracy opublikowanej podczas mojego doktoratu wspólnie z zespołem skupiliśmy się na globalnej analizie występowania krótkich RNA powstających z tRNA w *S. cerevisiae*. Na pierwszym etapie badań postanowiliśmy porównać wydajność izolacji krótkich RNA powstających z tRNA między czterema różnymi metodami izolacji RNA. Oprócz metody izolacji całkowitego RNA z użyciem buforu LET, która była wcześniej używana przez inną grupę do badań nad tRF w drożdżach [29], postanowiliśmy zweryfikować skuteczność trzech innych metod izolacji niskocząsteczkowych RNA: zestawu *MicroRNA isolation kit*, zestawu *MasterPureTM Yeast Purification kit* oraz powszechnie stosowanej metody do izolacji tRNA, tzw. izolacji „bulk tRNA". Po analizie wszystkich metod, wykazaliśmy, że najwięcej RNA zostało wyizolowane metodą LET. Jednak najwięcej niskocząsteczkowych RNA, które były w centrum naszego zainteresowania zostało wyizolowane metodą „bulk tRNA". W dalszych badaniach sprawdziliśmy, która z analizowanych metod wykazuje największy odsetek izolowanych tRF. Wyniki analizy metodą typu northern potwierdziły jednoznacznie, że metodą najlepszą do analizy tRF jest metoda „bulk tRNA". Głównym celem niniejszej publikacji było globalne przeanalizowanie powstawania tRF w zmiennych warunkach wzrostu. Drożdże hodowaliśmy w 12 różnych warunkach środowiskowych, aby następnie zbadać powstawanie 5′- oraz 3′-tRF z wszystkich izoform drożdżowych tRNA. Używając wcześniej zoptymalizowanego protokołu izolacji RNA i hybrydyzacji typu northern, oszacowaliśmy ilość osiemdziesięciu tRF na podstawie uzyskiwanego sygnału dla tRF w stosunku do tRNA. Najczęściej przetwarzane izoformy tRNA to: $tRNA^{Ala}$ (TGC), $tRNA^{Arg}$ (CCT), $tRNA^{Asn}$ (GTT), $tRNA^{Asp}$ (GTC), $tRNA^{Gly}$ (CCC), $tRNA^{Gly}$ (GCC), $tRNA^{Met}$ (CAT), $tRNA^{Lys}$ (CTT), $tRNA^{Leu}$ (TAA) i $tRNA^{Thr}$ (CGT). W trzech z tych przypadków ($tRNA^{Gly}$, $tRNA^{Lys}$ i $tRNA^{Thr}$), zaobserwowaliśmy, że cięcie tRF pochodzących z końców 5′ i 3′ tRNA zależy od izoformy danego tRNA. Większość tRNA przetwarzana była do tRF z wydajnością 2-20%. tRF występujące w największej ilości wykazywały preferencyjną akumulację pod wpływem takich warunków jak wysokie zasolenie, niskie pH, a także w warunkach głodu aminokwasowego i cukrowego. Nie zaobserwowaliśmy też żadnego tRF, który powstawałby w stosunkowo dużej ilości

w warunkach wysokiego pH. Wykazaliśmy, że poszczególne tRNA mają różną podatność na cięcie, najczęściej ciętym (sumując wszystkie warunki hodowli) z obu końców tRNA jest $tRNA^{Thr}$(CGT). Analizując wszystkie wyniki badań wskaźnikiem *Z-score,* zauważyliśmy, że podczas stresu UV, stresu beztlenowego, głodu aminokwasowego i głodu cukru oraz podczas stresów hipo- i hiperosmotycznych większość tRF kumulowała się istotnie powyżej średniej, natomiast w warunkach optymalnych, wysokiego stężenia soli, niskiego i wysokiego pH oraz zimna i ciepła przetwarzanie tRNA do tRF było niższe niż średnia. Warto zwrócić uwagę, że chociaż ilość poszczególnych tRF różni się w zależności od warunków wzrostu, to uśredniony poziom przetwarzania wszystkich tRNA w *S. cerevisiae* nie wykazuje istotnych różnic. W naszych danych po raz pierwszy zaobserwowaliśmy, że we wszystkich testowanych warunkach wzrostu, pule tRF pochodzące zarówno z 3′ końca jak i 5′ końca są niemalże równe.

Podsumowując, nasza analiza pozwoliła wyłonić optymalną metodę izolacji krótkich RNA powstających z tRNA. Udowodniliśmy, że wybór techniki izolacji RNA ma istotne znaczenie dla późniejszych wyników. Po raz pierwszy wykazaliśmy, że pula tRF nie zmienia się pod wpływem warunków stresowych. Zmianom podlega natomiast kompozycja poszczególnych tRF. Odmiennie od poprzednich doniesień [80], wykazaliśmy także, że pula 3′-tRF jest niemalże taka sama jak pula 5′-tRF.

Dysponując wiedzą na temat powstawania tRF, w kolejnym etapie prac mogliśmy przejść do analiz funkcjonalnych krótkich RNA powstających z tRNA.

2. **Mleczko AM, Celichowski P, Bąkowska-Żywicka K**
   Transfer RNA-derived fragments target and regulate ribosome-associated aminoacyl-transfer RNA synthetases
   Biochimica et Biophysica Acta - Gene Regulatory Mechanisms, 2018, 1861(7): 647-656

Brak wyjaśnienia w jaki sposób mogą funkcjonować krótkie RNA powstające z tRNA w drożdżach, organizmie pozbawionym ścieżki miRNA skłonił mnie, dr. Piotra Celichowskiego i prof. Kamillę Bąkowską-Żywicką do zgłębienia tego tematu. Z poprzednich badań wiedzieliśmy, że tRF asocjują bezpośrednio z rybosomami *S. cerevisiae* [7]. Na początku pracy nad funkcją tRF postanowiliśmy dokładniej przyjrzeć się miejscu asocjacji wybranych tRF (3′-tRF^{His} (GTG), 3′-tRF^{Ser} (AGA), 3′-tRF^{Gly} (GCC), 3′-tRF^{Leu} (TAA), 3′-tRF^{Thr} (TGT), 5′-tRF^{His} (GTG)) do rybosomu. W tym celu wykonaliśmy analizę hybrydyzacji typu northern poprzedzoną profilowaniem polisomowym. Odkryliśmy, że najwięcej tRF znajduje się we frakcji niezwiązanej z rybosomem, natomiast

najwięcej tRF związanych z rybosomami znajduje się we frakcji z małą podjednostką 40S. Preferencyjne wiązanie tRF do małej podjednostki rybosomalnej potwierdziliśmy eksperymentem *in vitro,* gdzie badaliśmy wiązanie syntetycznych tRF do 80S, 60S i 40S. Aby sprawdzić potencjalny wpływ tRF na biosyntezę białka, przeprowadziliśmy szereg eksperymentów analizujących translację *in vitro* i *in vivo*. Najpierw testowaliśmy włączanie metioniny [^{35}S] w nowosyntetyzowane białka w obecności tRF przy użyciu techniki znakowania metabolicznego. Wszystkie badane tRF obniżały translację *in vivo* o około 80%. Efektywność inhibicji biosyntezy białka była porównywalna do efektywności antybiotyku cykloheksymidu, wiążącego się z rybosomami. Następnie wykonaliśmy translacje *in vitro* w drożdżowym systemie bezkomórkowym. Wyniki tego eksperymentu potwierdziły, że tRF wpływają na proces biosyntezy białka obniżając go. Ponieważ zarówno tRNA jak i rybosomy są zakonserwowane ewolucyjnie, sprawdziliśmy czy drożdżowe tRF wpływają na translacje w innych organizmach. tRF obniżały znacząco translację *in vitro* w kiełkach pszenicy, natomiast w retikulocytach króliczych i komórkach ludzkich w minimalnym stopniu. W kolejnym kroku postanowiliśmy zbadać, na jaki etap translacji mają wpływ tRF. W wyniku testów sprawdzających wpływ tRF na aminoacylację odkryliśmy, że te krótkie RNA wpływają już na ten wczesny, przygotowawczy etap biosyntezy białka. Zaobserwowaliśmy, że najsilniejszy wpływ tRF na aminoacylację był obserwowany wtedy, gdy tRF i tRNA były w stosunku molowym 1:1 (obniżanie aminoacylacji wynosiło 72-83%). Sprawdziliśmy także, czy jeden z wybranych tRF wpływa na aminoacylację *in vivo*. Wykazaliśmy, że aminoacylacja *in vivo* została obniżona przez 5′-tRF^{His} (GTG) o około 50%. Aby uzyskać lepszy wgląd w mechanizm działania tRF na aminoacylację tRNA, przeprowadziliśmy serię eksperymentów mających na celu zidentyfikować potencjalnych partnerów interakcji dla tRF. W związku z faktem, że tRF obniżają aminoacylację tRNA, planowaliśmy zweryfikować, czy tworzą one kompleksy rybonukleoproteinowe z czynnikami wymaganymi do aminoacylacji. W wyniku testów EMSA nie tyko potwierdziliśmy fakt, że tRF asocjują z rybosomami (P100), ale odkryliśmy też, że cząsteczki te asocjują z nieznanym komponentem frakcji S100. Co więcej, kompleksy te migrują z tą samą prędkością w żelu natywnym. Kolejne eksperymenty EMSA wykazały, że wszystkie badane tRF asocjują z syntetazami aminoacylo-tRNA (His-RS, Ser-RS, Gly-RS, Leu-RS, Thr-RS). Wykryliśmy zatem, że: a) drożdżowe tRF asocjują z rybosomami, b) drożdżowe tRF asocjują z syntetazami aminoacylo-tRNA, c) kompleksy tRF/S100 i tRF/P100 migrują z tą samą prędkością w natywnym żelu PAA. Biorąc pod uwagę nasze wyniki oraz fakt, iż syntetazy aminoacylo-tRNA tworzą kompleksy z rybosomami w niektórych organizmach [79,81], postanowiliśmy sprawdzić, czy badane przez nas

syntetazy również mogą tworzyć kompleksy z drożdżowymi rybosomami. Analiza techniką hybrydyzacji typu western, poprzedzona testem wiązania syntetaz aminoacylo-tRNA do rybosomu udowodniła, że w istocie, drożdżowe syntetazy wiążą się z rybosomami. Wyniki te zostały następnie potwierdzone przez sprawdzenie potencjału aminoacylacyjnego polisomów i poszczególnych składowych rybosomu (80S, 60S, 40S). Zaobserwowaliśmy, że polisomy, 40S oraz monosomy 80S w istocie posiadają aktywność enzymatyczną aminoacylowania tRNA, co z kolei zapewniło dalsze wsparcie naszej tezy o powiązaniu między drożdżowymi syntetazami aminoacylo-tRNA i rybosomami.

Podsumowując, udowodniliśmy, że wybrane tRF asocjują z małą podjednostką rybosomu oraz syntetazami aminoacylo-tRNA, prawdopodobnie tworząc kompleks syntetaza-tRF-rybosom. Poprzez tworzenie kompleksu, zostaje obniżona aminoacylacja tRNA i jednocześnie globalna biosynteza białka. Nasze wyniki mogą również sugerować istnienie nowego, nieznanego jeszcze kompleksu multisytetazowego w *S. cerevisiae*.

W kolejnych pracach nad moją rozprawą doktorską skupiłam się na analizie powstawania i funkcji krótkich RNA powstających ze snoRNA.

3. **Mleczko AM, Bąkowska-Żywicka K**
   When small RNAs become smaller: emerging functions of snoRNAs and their derivatives
   Acta Biochimica Polonica, 2016, 63(4):601-607

Moją pracę nad krótkimi RNA powstającymi ze snoRNA rozpoczęłam od przeglądu literatury poruszającej szeroko pojętą tematykę niekanonicznych funkcji snoRNA oraz powstających z nich sdRNA. snoRNA, czyli małe jąderkowe RNA, znajdują się głównie w jąderku, gdzie biorą udział w chemicznej modyfikacji nukleotydów innych RNA. Oprócz swojej głównej funkcji snoRNA może brać udział w regulacji reakcji organizmu na stres czy rozwoju niektórych chorób lub zaburzeń, takich jak nowotwory i zespół Pradera-Williego. Moją szczególną uwagę zwróciły zagadnienia dotyczące cięcia snoRNA do krótszych, funkcjonalnych RNA. sdRNA mogą pełnić w organizmach różne role, m.in. regulować ekspresję genów na ścieżce miRNA czy brać udział w alternatywnym składaniu mRNA. W niniejszej pracy przeglądowej przedstawiłam współczesny stan wiedzy na temat funkcji snoRNA i sdRNA.

4. Walkowiak M*, Mleczko AM*, Bąkowska-Żywicka K

Evaluation of methods for detection of low-abundant snoRNA-derived small RNAs in Saccharomyces cerevisiae

BioTechnologia, 2016, 97(1):19-26 ***Autorzy mieli taki sam wkład w przygotowanie publikacji**

Do tej pory wykrycie sdRNA było możliwe podczas sekwencjonowania, jednak ich niewielka liczebność utrudniała wykrywanie tych cząsteczek metodami biochemicznymi. W niniejszej pracy wraz z mgr. Mateuszem Walkowiakiem oraz prof. Kamillą Bąkowską-Żywicką opracowaliśmy i zoptymalizowaliśmy metodę eksperymentalną do wykrywania krótkich RNA powstających ze snoRNA. W początkowym etapie badań postanowiliśmy wykryć komórkowe sdRNA za pomocą hybrydyzacji typu northern, tak jak robiliśmy to w przypadku tRF. Aby zwiększyć prawdopodobieństwo wykrycia nielicznych sdRNA tą techniką, stosowaliśmy szereg różnych metod izolacji RNA oraz sondy DNA i LNA. Niestety procedura ta okazała się niewystarczająco czuła, aby wykryć cząsteczki występujące w komórkach w tak niewielkich ilościach. Postanowiliśmy zatem skupić się na metodach opartych na amplifikacji. Wybraliśmy technikę odwrotnej transkrypcji opartą na starterach o kształcie spinki (SL-RT), która z powiedzeniem stosowana jest do wykrywania miRNA [67]. Izolowane z komórek całkowite RNA zawiera stosunkowo duże ilości snoRNA o tej samej sekwencji, co powstające z nich sdRNA. By zbadać zdolność testów SL-RT-PCR w do wykrycia wyłącznie sdRNA, reakcje zostały przeprowadzone z puli niskocząsteczkowego RNA (10-60 nt), która z całkowitego RNA została eluowana z żelu. Żeby ocenić czułość techniki, reakcje przeprowadzono w obecności różnej ilości RNA (10-200 ng) oraz różnej ilości cykli amplifikacji PCR (25-31). Po rozdzieleniu produktów reakcji PCR w żelu PAA, obserwowaliśmy wyraźne sygnały sdRNA. 5′-sdR128 widoczne było już od 50 ng RNA w reakcji i po 25 cyklach PCR, 3′-sdR128 od 100 ng RNA po 25 cyklach, 5′-sdR67 ze 100 ng RNA po 29 cyklach. Przy takiej ilości cykli w reakcji kontrolnej nie obserwowaliśmy niespecyficznych produktów reakcji, natomiast amplifikacja powyżej 31 cykli spowodowała pojawienie się niespecyficznego produktu dla starterów 5′-sdR128.

Nasze wyniki sugerują, że SL-RT-PCR zapewnia czułość wystarczającą do wykrycia sdRNA w puli niskocząsteczkowych RNA.

W kolejnym kroku postanowiliśmy dogłębnie przyjrzeć się powstawaniu sdRNA u drożdży oraz skupić się na scharakteryzowaniu ich potencjalnej funkcji.

5. Mleczko AM*, Machtel P*, Walkowiak M, Wasilewska A, Pietras PJ, Bąkowska-Żywicka K

Levels of sdRNAs in cytoplasm and their association with ribosomes are dependent upon stress conditions but independent from snoRNA expression

Scientific Reports, 2019 (IF$_{2018}$=4.011) ***Autorzy mieli taki sam wkład w przygotowanie publikacji**

W ostatnim etapie prac nad moją rozprawą doktorską postanowiliśmy przyjrzeć się bliżej powstawaniu, lokalizacji oraz funkcji wybranych snoRNA (snR67, snR83 i snR128) oraz powstających z nich sdRNA (sdR67, sdR83 i sdR128). W celu zbadania ilości oraz subkomórkowej lokalizacji tych cząsteczek w *S. cerevisiae*, zastosowaliśmy metodę opartą na amplifikacji, gdzie do odwrotnej transkrypcji użyliśmy zoptymalizowanych starterów o strukturze spinki. Aby umożliwić bezwzględną kwantyfikację RNA, po odwrotnej transkrypcji zastosowaliśmy PCR emulsyjny (*ang. digital droplet,* ddPCR). Nasza kompleksowa analiza liczebności i lokalizacji sdRNA i snoRNA została przeprowadzona w 12 różnych warunkach wzrostu drożdży oraz w trzech różnych frakcjach: S30-zawierającej komórkowe, całkowite RNA, P100-zawierającej rybosomalne RNA, S100-zawierającej RNA niezwiązane z rybosomem. Technika ddPCR pozwala na określenie bezwzględnej (absolutnej) ilości kwasów nukleinowych w badanej próbie. Jako odniesienie w eksperymentach ddPCR zastosowano dodanie syntetycznego krótkiego RNA do całkowitego RNA. Bezwzględne ilości referencyjnego RNA w różnych próbach cDNA rozkładały się równomiernie, w związku z tym wywnioskowaliśmy, że możliwe różnice w stężeniach snoRNA lub sdRNA w określonych warunkach stresu wynikają z różnić w ich liczebności. Wyniki wykazały, że wszystkie snoRNA znajdowały się w komórkach drożdży (frakcja S30) w ilości najmniejszej w stresie niskiego pH. Co więcej, wszystkie badane snoRNA są przetwarzane do sdRNA. sdR67 był obserwowany w najmniejszej ilości we wszystkich warunkach hodowlanych. sdRNA występującym w największej ilości było sdR128, którego najwyższe stężenia obserwowano w stresach ciepła, światła UV oraz stresu hipoosmotycznego. Następnie sprawdziliśmy możliwe korelacje pomiędzy ilością sdRNA a snoRNA w różnych warunkach środowiskowych. W stresie niskiego pH dla snR67, wysokiego zasolenia dla snR83 i stresie cieplnym dla snR128 ilości snoRNA były znacznie mniejsze niż sdRNA. Poza tymi trzema przypadkami, w większości warunków stresowych poziomy snoRNA nie korelowały z ilością sdRNA. Ta obserwacja sugeruje, że w określonych warunkach wzrostu drożdży akumulacja sdRNA nie jest bezpośrednio zależna od ilości poszczególnych snoRNA. Sugeruje to możliwą zależną od stresu regulację cięcia snoRNA do sdRNA. Co więcej, zaobserwowaliśmy, że zarówno sdRNA jak i snoRNA znajdują się we frakcji RNA izolowanej z rybosomów (frakcja P100). Nasze wyniki wykazały,

że RNA te mogą asocjować z rybosomami *S. cerevisiae* w sposób zależny od stresu, a snoRNA asocjują z rybosomami w ilościach znacznie większych niż sdRNA. Wykazaliśmy, że stres cieplny i stres wysokiego pH wywoływały znaczny wzrost ilości snoRNA asocjujących rybosomami. Wśród badanych sdRNA, sdR67 było najmniej licznie związane z rybosomami w porównaniu do sdR83 i sdR128. sdR83 najliczniejsze było w stresie wysokiego pH, a sdR128 w stresie hipo- i hiperosmotycznym. Porównanie ilości sdRNA i snoRNA związanych z rybosomem wyjawiło, że w przypadku stresu wysokiego pH zarówno sdR83 jak i snR83 były wyjątkowo liczne. Poza tym przypadkiem, nie zaobserwowano żadnych korelacji miedzy ilością snoRNA a sdRNA. Taka obserwacja sugeruje, że wiązanie tych cząsteczek do rybosomów w stresie jest niezależne od siebie. Zarówno snoRNA jak i sdRNA są obecne we frakcji post-rybosomalnej (frakcja S100), a ich stężenie zależy od warunków stresowych. We frakcji S100, stężenia snoRNA są znacznie wyższe niż stężenia sdRNA, podobnie jak w pozostałych badanych frakcjach. W tym przypadku, badane snoRNA były najmniej liczne w stresie głodu cukrowego oraz wzrostu beztlenowego. Okazało się też, że w tej frakcji sdR67 występuje najmniej licznie spośród wszystkich badanych sdRNA.

Potwierdzenie faktu, że sdRNA asocjują z rybosomami skłoniło nas do rozpoczęcia prac nad funkcją sdRNA w biosyntezie białka. W tym celu wykonaliśmy eksperymenty sprawdzające translację *in vitro* i *in vivo*. Dodanie do mieszaniny reakcyjnej sdRNA zmniejszało translację *in vitro* do 40-75%. Najwyższy efekt hamujący biosyntezę białka zaobserwowano po dodaniu sdR128, którego nawet niewielkie stężenia (0,7 μM) zauważalnie zmniejszyły syntezę białka *in vitro*. Aby sprawdzić wpływ sdRNA na translację w bardziej fizjologicznych warunkach, wykonaliśmy znakowanie metaboliczne w drożdżowych sferoplastach. Badanie to potwierdziło, że sdRNA hamują proces biosyntezy białka *in vivo* na poziomie porównywalnym do cykloheksymidu. Co więcej, wykazaliśmy, że wszystkie badane przez nas sdRNA hamują translację *in vitro* w kiełkach pszenicy, a samo sdR67 dodatkowo hamuje translację w retikulocytach króliczych. Obserwacje te sugerują, że mechanizm regulacji translacji przez sdRNA może być ewolucyjnie zakonserwowany.

Podsumowując, ujawniliśmy, że snoRNA i sdRNA w *S. cerevisiae* są obecne w cytoplazmie, gdzie wiążą się z rybosomami. Akumulacja snoRNA i sdRNA we frakcjach cytoplazmatycznych i rybosomalnych jest silnie zależna od warunków stresowych, w których żyją drożdże. Co więcej, sdRNA wpływają na biosyntezę białek *in vivo* i *in vitro*. Po raz pierwszy wykazaliśmy, że poziomy snoRNA i sdRNA w cytoplazmie i ich możliwa asocjacja z rybosomami są od siebie niezależne.

Inne publikacje, niewchodzące w skład niniejszej rozprawy doktorskiej

Jestem współautorką pracy eksperymentalnej [54], będącej wynikiem projektu związanego z tematyką krótkich RNA asocjujących rybosomami, która nie stanowiła głównego wątku moich badań. Praca ta wykonywana była na archeonie *Haloferax volcanii*. Odmienna budowa aparatu translacyjnego w porównaniu do drożdży oraz inne mechanizmy działania tRF w tym organizmie spowodowały, że zdecydowałam nie włączać niniejszej publikacji do mojej pracy doktorskiej. Projekt ten wykonywałam będąc na stażu pod opieką prof. Norberta Polacka na Uniwersytecie w Bern w Szwajcarii. Praca ta udowadnia, że fragment pochodzący z tRNA walinowego (5′-tRF^{Wal}), jest wytwarzany w warunkach stresowych w halofilnym archeonie *H. volcanii* i jest zdolny do wiązania się z małą podjednostką rybosomalną. Wiązanie 5′-tRF^{Wal} do rybosomu powoduje globalne obniżenie translacji *in vivo* i *in vitro*.

Jestem też współautorką publikacji eksperymentalnej o tematyce niezwiązanej z rozprawą doktorską [82]. Praca o tematyce wirusologicznej opisuje nowego członka podrodziny *Autographivirinae,* faga Pseudomonas KNP. Praca ta powstała podczas realizowania grantu studenckiego przyznanego Sekcji Wirusologii i Biotechnologii Molekularnej Koła Naukowego Przyrodników UAM.

Ponadto jestem współautorką dwóch prac przeglądowych pozostających w tematyce krótkich RNA asocjujących z rybosomami [83,84], które zostały opublikowane przed rozpoczęciem studiów doktorskich, dlatego nie wchodzą one w skład rozprawy doktorskiej.

Wykaz skrótów

ddPCR – PCR emulsyjny *(ang. droplet-digital PCR)*

EMSA – technika opóźnienia migracji cząsteczek w żelu poliakrylamidowym *(ang. electrophoretic mobility shift assay)*

PAA – żel poliakrylamidowy *(ang. polyacrylamide gel electrophoresis)*

rancRNA – krótkie RNA zasocjowane z rybosomami *(ang. ribosome-associated noncoding RNAs)*

sdRNA – krótkie RNA powstające ze snoRNA *(ang. snoRNA-derived RNAs)*

SL-RT – odwrotna transkrypcja z użyciem starterów o strukturze spinki *(ang. stem-loop reverse transcription)*

tiRNA – krótkie RNA indukowane stresem *(ang. tRNA-derived stress-induced RNAs)*

tmRNA – bakteryjne RNA, które strukturalnie i funkcjonalnie przypomina tRNA oraz mRNA (*ang. transfer messenger RNA*)

tRF – krótkie RNA powstające z tRNA *(ang. tRNA-derived fragments)*

tsRNA – krótkie RNA pochodzące z tRNA *(ang. tRNA-derived small RNAs)*

ubcRNA – RNA z raka pęcherza moczowego *(ang. urinary bladder carcinoma RNAs)*

Bibliografia

1. Palade GE (1955) A small particulate component of the cytoplasm. J Biophys Biochem Cytol 1: 59-68.
2. Littlefield JW, Keller EB, Gross J, Zamecnik PC (1955) Studies on cytoplasmic ribonucleoprotein particles from the liver of the rat. J Biol Chem 217: 111-123.
3. Hoagland MB, Stephenson ML, Scott JF, Hecht LI, Zamecnik PC (1958) A soluble ribonucleic acid intermediate in protein synthesis. J Biol Chem 231: 241-257.
4. Weinberg RA, Penman S (1968) Small molecular weight monodisperse nuclear RNA. J Mol Biol 38: 289-304.
5. Lee YS, Shibata Y, Malhotra A, Dutta A (2009) A novel class of small RNAs: tRNA-derived RNA fragments (tRFs). Genes Dev 23: 2639-2649.
6. Ender C, Krek A, Friedlander MR, Beitzinger M, Weinmann L, et al. (2008) A human snoRNA with microRNA-like functions. Mol Cell 32: 519-528.
7. Zywicki M, Bakowska-Zywicka K, Polacek N (2012) Revealing stable processing products from ribosome-associated small RNAs by deep-sequencing data analysis. Nucleic Acids Res 40: 4013-4024.
8. Busch H, Reddy R, Rothblum L, Choi YC (1982) SnRNAs, SnRNPs, and RNA processing. Annu Rev Biochem 51: 617-654.
9. Borek E, Baliga BS, Gehrke CW, Kuo CW, Belman S, et al. (1977) High turnover rate of transfer RNA in tumor tissue. Cancer Res 37: 3362-3366.
10. Speer J, Gehrke CW, Kuo KC, Waalkes TP, Borek E (1979) tRNA breakdown products as markers for cancer. Cancer 44: 2120-2123.
11. Waalkes TP, Gehrke CW, Tormey DC, Zumwalt RW, Hueser JN, et al. (1975) Urinary excretion of polyamines by patients with advanced malignancy. Cancer Chemother Rep 59: 1103-1116.
12. Haussecker D, Huang Y, Lau A, Parameswaran P, Fire AZ, et al. (2010) Human tRNA-derived small RNAs in the global regulation of RNA silencing. RNA 16: 673-695.
13. Yamasaki S, Ivanov P, Hu GF, Anderson P (2009) Angiogenin cleaves tRNA and promotes stress-induced translational repression. J Cell Biol 185: 35-42.
14. Zhao H, Bojanowski K, Ingber DE, Panigrahy D, Pepper MS, et al. (1999) New role for tRNA and its fragment purified from human urinary bladder carcinoma conditioned medium: inhibition of endothelial cell growth. J Cell Biochem 76: 109-117.
15. Sobala A, Hutvagner G (2011) Transfer RNA-derived fragments: origins, processing, and functions. Wiley Interdiscip Rev RNA 2: 853-862.
16. Lee SR, Collins K (2005) Starvation-induced cleavage of the tRNA anticodon loop in Tetrahymena thermophila. J Biol Chem 280: 42744-42749.
17. Couvillion MT, Sachidanandam R, Collins K (2010) A growth-essential Tetrahymena Piwi protein carries tRNA fragment cargo. Genes Dev 24: 2742-2747.
18. Andersen KL, Collins K (2012) Several RNase T2 enzymes function in induced tRNA and rRNA turnover in the ciliate Tetrahymena. Mol Biol Cell 23: 36-44.
19. Loss-Morais G, Waterhouse PM, Margis R (2013) Description of plant tRNA-derived RNA fragments (tRFs) associated with argonaute and identification of their putative targets. Biol Direct 8: 6.
20. Li Y, Luo J, Zhou H, Liao JY, Ma LM, et al. (2008) Stress-induced tRNA-derived RNAs: a novel class of small RNAs in the primitive eukaryote Giardia lamblia. Nucleic Acids Res 36: 6048-6055.
21. Yudelevich A (1971) Specific cleavage of an Escherichia coli leucine transfer RNA following bacteriophage T4 infection. J Mol Biol 60: 21-29.
22. Emara MM, Ivanov P, Hickman T, Dawra N, Tisdale S, et al. (2010) Angiogenin-induced tRNA-derived stress-induced RNAs promote stress-induced stress granule assembly. J Biol Chem 285: 10959-10968.

23. Ivanov P, Emara MM, Villen J, Gygi SP, Anderson P (2011) Angiogenin-induced tRNA fragments inhibit translation initiation. Mol Cell 43: 613-623.
24. Cole C, Sobala A, Lu C, Thatcher SR, Bowman A, et al. (2009) Filtering of deep sequencing data reveals the existence of abundant Dicer-dependent small RNAs derived from tRNAs. RNA 15: 2147-2160.
25. Burroughs AM, Ando Y, de Hoon MJ, Tomaru Y, Suzuki H, et al. (2011) Deep-sequencing of human Argonaute-associated small RNAs provides insight into miRNA sorting and reveals Argonaute association with RNA fragments of diverse origin. RNA Biol 8: 158-177.
26. Sobala A, Hutvagner G (2013) Small RNAs derived from the 5' end of tRNA can inhibit protein translation in human cells. RNA Biol 10: 553-563.
27. Bakowska-Zywicka K, Mleczko AM, Kasprzyk M, Machtel P, Zywicki M, et al. (2016) The widespread occurrence of tRNA-derived fragments in Saccharomyces cerevisiae. FEBS Open Bio 6: 1186-1200.
28. Kawaji H, Nakamura M, Takahashi Y, Sandelin A, Katayama S, et al. (2008) Hidden layers of human small RNAs. BMC Genomics 9: 157.
29. Thompson DM, Parker R (2009) The RNase Rny1p cleaves tRNAs and promotes cell death during oxidative stress in Saccharomyces cerevisiae. J Cell Biol 185: 43-50.
30. Kumar P, Mudunuri SB, Anaya J, Dutta A (2015) tRFdb: a database for transfer RNA fragments. Nucleic Acids Res 43: D141-145.
31. Li Z, Ender C, Meister G, Moore PS, Chang Y, et al. (2012) Extensive terminal and asymmetric processing of small RNAs from rRNAs, snoRNAs, snRNAs, and tRNAs. Nucleic Acids Res 40: 6787-6799.
32. Maraia RJ, Lamichhane TN (2011) 3' processing of eukaryotic precursor tRNAs. Wiley Interdiscip Rev RNA 2: 362-375.
33. Wang Q, Lee I, Ren J, Ajay SS, Lee YS, et al. (2013) Identification and functional characterization of tRNA-derived RNA fragments (tRFs) in respiratory syncytial virus infection. Mol Ther 21: 368-379.
34. Liao JY, Ma LM, Guo YH, Zhang YC, Zhou H, et al. (2010) Deep sequencing of human nuclear and cytoplasmic small RNAs reveals an unexpectedly complex subcellular distribution of miRNAs and tRNA 3' trailers. PLoS One 5: e10563.
35. Babiarz JE, Ruby JG, Wang Y, Bartel DP, Blelloch R (2008) Mouse ES cells express endogenous shRNAs, siRNAs, and other Microprocessor-independent, Dicer-dependent small RNAs. Genes Dev 22: 2773-2785.
36. Calabrese JM, Seila AC, Yeo GW, Sharp PA (2007) RNA sequence analysis defines Dicer's role in mouse embryonic stem cells. Proc Natl Acad Sci U S A 104: 18097-18102.
37. Maute RL, Schneider C, Sumazin P, Holmes A, Califano A, et al. (2013) tRNA-derived microRNA modulates proliferation and the DNA damage response and is down-regulated in B cell lymphoma. Proc Natl Acad Sci U S A 110: 1404-1409.
38. Kawamura Y, Saito K, Kin T, Ono Y, Asai K, et al. (2008) Drosophila endogenous small RNAs bind to Argonaute 2 in somatic cells. Nature 453: 793-797.
39. Lau NC, Seto AG, Kim J, Kuramochi-Miyagawa S, Nakano T, et al. (2006) Characterization of the piRNA complex from rat testes. Science 313: 363-367.
40. Shao Y, Sun Q, Liu X, Wang P, Wu R, et al. (2017) tRF-Leu-CAG promotes cell proliferation and cell cycle in non-small cell lung cancer. Chem Biol Drug Des 90: 730-738.
41. Couvillion MT, Bounova G, Purdom E, Speed TP, Collins K (2012) A Tetrahymena Piwi bound to mature tRNA 3' fragments activates the exonuclease Xrn2 for RNA processing in the nucleus. Mol Cell 48: 509-520.

42. Wang Z, Xiang L, Shao J, Yuan Z (2006) The 3' CCACCA sequence of tRNAAla(UGC) is the motif that is important in inducing Th1-like immune response, and this motif can be recognized by Toll-like receptor 3. Clin Vaccine Immunol 13: 733-739.
43. Peng H, Shi J, Zhang Y, Zhang H, Liao S, et al. (2012) A novel class of tRNA-derived small RNAs extremely enriched in mature mouse sperm. Cell Res 22: 1609-1612.
44. Chen Q, Yan M, Cao Z, Li X, Zhang Y, et al. (2016) Sperm tsRNAs contribute to intergenerational inheritance of an acquired metabolic disorder. Science 351: 397-400.
45. Sharma U, Conine CC, Shea JM, Boskovic A, Derr AG, et al. (2016) Biogenesis and function of tRNA fragments during sperm maturation and fertilization in mammals. Science 351: 391-396.
46. Saraiya AA, Wang CC (2008) snoRNA, a novel precursor of microRNA in Giardia lamblia. PLoS Pathog 4: e1000224.
47. Taft RJ, Glazov EA, Lassmann T, Hayashizaki Y, Carninci P, et al. (2009) Small RNAs derived from snoRNAs. RNA 15: 1233-1240.
48. Falaleeva M, Stamm S (2013) Processing of snoRNAs as a new source of regulatory non-coding RNAs: snoRNA fragments form a new class of functional RNAs. Bioessays 35: 46-54.
49. Brameier M, Herwig A, Reinhardt R, Walter L, Gruber J (2011) Human box C/D snoRNAs with miRNA like functions: expanding the range of regulatory RNAs. Nucleic Acids Res 39: 675-686.
50. Kishore S, Khanna A, Zhang Z, Hui J, Balwierz PJ, et al. (2010) The snoRNA MBII-52 (SNORD 115) is processed into smaller RNAs and regulates alternative splicing. Hum Mol Genet 19: 1153-1164.
51. Pircher A, Bakowska-Zywicka K, Schneider L, Zywicki M, Polacek N (2014) An mRNA-derived noncoding RNA targets and regulates the ribosome. Mol Cell 54: 147-155.
52. Luidalepp H, Berger S, Joss O, Tenson T, Polacek N (2016) Ribosome Shut-Down by 16S rRNA Fragmentation in Stationary-Phase Escherichia coli. J Mol Biol 428: 2237-2247.
53. Gebetsberger J, Zywicki M, Kunzi A, Polacek N (2012) tRNA-derived fragments target the ribosome and function as regulatory non-coding RNA in Haloferax volcanii. Archaea 2012: 260909.
54. Gebetsberger J, Wyss L, Mleczko AM, Reuther J, Polacek N (2017) A tRNA-derived fragment competes with mRNA for ribosome binding and regulates translation during stress. RNA Biol 14: 1364-1373.
55. Fricker R, Brogli R, Luidalepp H, Wyss L, Fasnacht M, et al. (2019) A tRNA half modulates translation as stress response in Trypanosoma brucei. Nat Commun 10: 118.
56. Felden B, Himeno H, Muto A, McCutcheon JP, Atkins JF, et al. (1997) Probing the structure of the Escherichia coli 10Sa RNA (tmRNA). RNA 3: 89-103.
57. Komine Y, Kitabatake M, Yokogawa T, Nishikawa K, Inokuchi H (1994) A tRNA-like structure is present in 10Sa RNA, a small stable RNA from Escherichia coli. Proc Natl Acad Sci U S A 91: 9223-9227.
58. Ushida C, Himeno H, Watanabe T, Muto A (1994) tRNA-like structures in 10Sa RNAs of Mycoplasma capricolum and Bacillus subtilis. Nucleic Acids Res 22: 3392-3396.
59. Rudinger-Thirion J, Giege R, Felden B (1999) Aminoacylated tmRNA from Escherichia coli interacts with prokaryotic elongation factor Tu. RNA 5: 989-992.
60. Tu GF, Reid GE, Zhang JG, Moritz RL, Simpson RJ (1995) C-terminal extension of truncated recombinant proteins in Escherichia coli with a 10Sa RNA decapeptide. J Biol Chem 270: 9322-9326.
61. Himeno H, Kurita D, Muto A (2014) tmRNA-mediated trans-translation as the major ribosome rescue system in a bacterial cell. Front Genet 5: 66.

62. Kim YK, Yeo J, Kim B, Ha M, Kim VN (2012) Short structured RNAs with low GC content are selectively lost during extraction from a small number of cells. Mol Cell 46: 893-895.
63. Monleau M, Bonnel S, Gostan T, Blanchard D, Courgnaud V, et al. (2014) Comparison of different extraction techniques to profile microRNAs from human sera and peripheral blood mononuclear cells. BMC Genomics 15: 395.
64. Podolska A, Kaczkowski B, Litman T, Fredholm M, Cirera S (2011) How the RNA isolation method can affect microRNA microarray results. Acta Biochim Pol 58: 535-540.
65. Lim LP, Glasner ME, Yekta S, Burge CB, Bartel DP (2003) Vertebrate microRNA genes. Science 299: 1540.
66. Krichevsky AM, King KS, Donahue CP, Khrapko K, Kosik KS (2003) A microRNA array reveals extensive regulation of microRNAs during brain development. RNA 9: 1274-1281.
67. Chen C, Ridzon DA, Broomer AJ, Zhou Z, Lee DH, et al. (2005) Real-time quantification of microRNAs by stem-loop RT-PCR. Nucleic Acids Res 33: e179.
68. Tang F, Hajkova P, Barton SC, Lao K, Surani MA (2006) MicroRNA expression profiling of single whole embryonic stem cells. Nucleic Acids Res 34: e9.
69. Holley CL, Li MW, Scruggs BS, Matkovich SJ, Ory DS, et al. (2015) Cytosolic accumulation of small nucleolar RNAs (snoRNAs) is dynamically regulated by NADPH oxidase. J Biol Chem 290: 11741-11748.
70. Chen MS, Goswami PC, Laszlo A (2002) Differential accumulation of U14 snoRNA and hsc70 mRNA in Chinese hamster cells after exposure to various stress conditions. Cell Stress Chaperones 7: 65-72.
71. Monier R, Stephenson ML, Zamecnik PC (1960) The preparation and some properties of a low molecular weight ribonucleic acid from baker's yeast. Biochim Biophys Acta 43: 1-8.
72. Pospisek M, Valasek L (2013) Polysome profile analysis--yeast. Methods Enzymol 530: 173-181.
73. Velichutina IV, Dresios J, Hong JY, Li C, Mankin A, et al. (2000) Mutations in helix 27 of the yeast Saccharomyces cerevisiae 18S rRNA affect the function of the decoding center of the ribosome. RNA 6: 1174-1184.
74. Bakowska-Zywicka K, Kasprzyk M, Twardowski T (2016) tRNA-derived short RNAs bind to Saccharomyces cerevisiae ribosomes in a stress-dependent manner and inhibit protein synthesis in vitro. FEMS Yeast Res 16.
75. Acker MG, Kolitz SE, Mitchell SF, Nanda JS, Lorsch JR (2007) Reconstitution of yeast translation initiation. Methods Enzymol 430: 111-145.
76. Hofbauer R, Fessl F, Hamilton B, Ruis H (1982) Preparation of a mRNA-dependent cell-free translation system from whole cells of Saccharomyces cerevisiae. Eur J Biochem 122: 199-203.
77. Wu C, Sachs MS (2014) Preparation of a Saccharomyces cerevisiae cell-free extract for in vitro translation. Methods Enzymol 539: 17-28.
78. Janssen BD, Diner EJ, Hayes CS (2012) Analysis of aminoacyl- and peptidyl-tRNAs by gel electrophoresis. Methods Mol Biol 905: 291-309.
79. Godinic-Mikulcic V, Jaric J, Greber BJ, Franke V, Hodnik V, et al. (2014) Archaeal aminoacyl-tRNA synthetases interact with the ribosome to recycle tRNAs. Nucleic Acids Res 42: 5191-5201.
80. Kumar P, Anaya J, Mudunuri SB, Dutta A (2014) Meta-analysis of tRNA derived RNA fragments reveals that they are evolutionarily conserved and associate with AGO proteins to recognize specific RNA targets. BMC Biol 12: 78.

81. David A, Netzer N, Strader MB, Das SR, Chen CY, et al. (2011) RNA binding targets aminoacyl-tRNA synthetases to translating ribosomes. J Biol Chem 286: 20688-20700.
82. Nowicki G, Walkowiak-Nowicka K, Zemleduch-Barylska A, Mleczko A, Frackowiak P, et al. (2017) Complete genome sequences of two novel autographiviruses infecting a bacterium from the Pseudomonas fluorescens group. Arch Virol 162: 2907-2911.
83. Mleczko AM, Celichowski P, Bakowska-Zywicka K (2014) Ex-translational function of tRNAs and their fragments in cancer. Acta Biochim Pol 61: 211-216.
84. Kasprzyk M, Mleczko AM, Celichowski P, Bakowska-Zywickal K (2014) [RNA processing - unusual mechanism of generation of novel classes of noncoding RNAs from functional RNAs]. Postepy Biochem 60: 295-304.

DOROBEK NAUKOWY

Publikacje

1) **Mleczko AM***, Machtel P*, Walkowiak M, Wasilewska A, Pietras PJ, Bąkowska-Żywicka K., Levels of sdRNAs in cytoplasm and their association with ribosomes are dependent upon stress conditions but independent from snoRNA expression, *Scientific Reports*. 2019: 9(1):18397 *Autorzy mieli taki sam wkład w przygotowanie publikacji (IF_{2018}=4.011)

2) **Mleczko AM**, Celichowski P, Bąkowska-Żywicka K., Transfer RNA-derived fragments target and regulate ribosome-associated aminoacyl-transfer RNA synthetases, *Biochimica et Biophysica Acta –Gene Regulatory Mechanisms.* 2018: 1861(7): 647-656 (IF_{2018}= 4.599)

3) Nowicki G, Walkowiak-Nowicka K, Zemleduch-Barylska A, **Mleczko A**, Frąckowiak P, Nowaczyk N, Kozdrowska E, Barylski J., Complete genome sequences of two novel autographiviruses infecting a bacterium from the *Pseudomonas fluorescens* group, *Archives of Virology*. 2017: 162(9):2907-2911 (IF_{2017}=2.160)

4) Gebetsberger J, Wyss L, **Mleczko AM**, Reuther J, Polacek N., A tRNA-derived fragment competes with mRNA for ribosome binding and regulates translation during stress, *RNA Biology*. 2017: 14(10):1364-1373 (IF_{2017}=5.216)

5) Bąkowska-Żywicka K, **Mleczko AM**, Kasprzyk M, Machtel P, Żywicki M, Twardowski T., The widespread occurrence of tRNA-derived fragments in *Saccharomyces cerevisiae, FEBS Open Bio.* 2016:6(12):1186-1200 (IF_{2016}= 2.143)

6) **Mleczko AM**, Bąkowska – Żywicka K., When small RNAs become smaller: emerging functions of snoRNAs and their derivatives, *Acta Biochimica Polonica.* 2016:63(4):601-607 (IF_{2016}=1.159)

7) Walkowiak M*, **Mleczko AM***, Bąkowska – Żywicka K., Evaluation of methods for detection of low-abundant snoRNA-derived small RNAs in *Saccharomyces cerevisiae*, *Biotechnologia.* 2016:1(97):19-26 *Autorzy mieli taki sam wkład w przygotowanie publikacji

8) Kasprzyk M**, Mleczko AM**, Celichowski P, Bąkowska-Żywicka K., Przetwarzanie RNA — niezwykły mechanizm powstawania nowych klas niekodujących RNA z funkcjonalnych RNA, *Postępy Biochemii.* 2014:60(3):295-304

9) **Mleczko AM,** Celichowski P, Bąkowska-Żywicka K., Ex – translational function of tRNAs and their fragments in cancer, *Acta Biochimica Polonica.* 2014:61(2):211-6 (IF_{2014}=1.153)

Projekty badawcze

1. Grant dla Młodych Naukowców ICHB PAN 2017

Opracowanie nowej metody identyfikacji oddziaływań krótkich RNA z rybosomami *in vivo*.

Kierownik projektu

2. Grant dla Młodych Naukowców ICHB PAN 2016

Badanie wpływu stresu abiotycznego na aktywność translacyjną drożdży *Saccharomyces cerevisiae*.

Kierownik projektu

3. NCN OPUS 14, UMO-2017/27/B/NZ1/01416

Zmiany w składzie białek rybosomalnych i w oddziałujących z rybosomami krótkich niekodujących RNA w *Saccharomyces cerevisiae* w odpowiedzi na stres środowiskowy.

Wykonawca projektu

4. NCN SONATA 7, UMO-2014/13/D/NZ1/00061

W poszukiwaniu mechanizmów regulacji ekspresji genów niezależnych od RNAi – krótkie, niekodujące RNA powstające ze snoRNA

Wykonawca projektu

5. FNP POMOST, POMOST/2011-4/1

W poszukiwaniu nieznanej funkcji niekodujących RNA powstających z cząsteczek tRNA w *Saccharomyces cerevisiae*.

Wykonawca projektu

Konferencje naukowe

Postery

1. 11 – 16.06.2019, Kraków, Polska, 24th Annual Meeting of the RNA Society (RNA 2019)

Dealing with pressure: Levels of snoRNA -derived fragments in cytoplasm and their association with ribosomes are dependent upon stress conditions but independent from snoRNA expression.
Mleczko A. M., Machtel P., Walkowiak M., Wasilewska A., Bąkowska – Żywicka K.

2. 23 – 27. 09. 2018, Strasbourg, Francja, The 27th tRNA Conference (tRNA2018)

Transfer RNA-derived fragments target and regulate ribosome-associated aminoacyl-transfer RNA synthetases.
Mleczko A. M., Celichowski P., Bąkowska – Żywicka K.

3. 4 -12.07.2018, Praga, Czechy, 18th FEBS Young Scientists′ Forum, The 43rd FEBS Congress

Transfer RNA-derived fragments target and regulate ribosome-associated aminoacyl-transfer RNA synthetases.
Mleczko A. M., Celichowski P., Bąkowska – Żywicka K.

4. 18-19.09. 2017, Poznań, Polska, RNAtion, Computational and Experimental RNA Biology Conference for Young Scientists

A new method for identification of rancRNA/ribosome complexes *in vivo*.
Mleczko A.M., Sobisiak A., Chodań M., Bąkowska – Żywicka K.

5. 30.05– 3.06. 2017, Praga, Czechy, The 22nd annual meeting of the RNA society

The widespread occurrence of tRNA-derived fragments in *Saccharomyces cerevisiae.*
Bąkowska-Żywicka K., **Mleczko A.M.**, Kasprzyk M., Żywicki M., Twardowski T.

6. 26 – 28.05.2017, Warszawa, Polska, III Intercollegiate Biotechnology Symposium

Kolejna tajemnica RNA odkryta! Czyli kilka słów o sdRNA – krótkich, niekodujących RNA powstających ze snoRNA.
Mleczko A.M., Bąkowska – Żywicka K.

7. 13-16.10.2016, Wrocław, Polska, 2nd Congress BIO2016 ”Expanding beyond the limits

When ribosomes get stressed – how the environment influences yeast translational activity and association between small non coding RNAs and the ribosome
Mleczko A.M., Bąkowska – Żywicka K.

8. 6-12.10.2015 Levico Terme, Włochy, 27° International conference on yeast genetics and molecular biology

How does yeast regulate translation? SnoRNA processing in *S. cerevisiae*
Mleczko A.M., Twardowski T., Bąkowska-Żywicka K.

9. 2-3.07.2015, Warszawa, Polska, EMBO Young Scientists Forum

Another tRNA mystery revealed in *Saccharomyces cerevisiae*
Mleczko A.M., Kasprzyk M., Twardowski T., Bąkowska-Żywicka K.

10. 15.06.2015, Poznań, Polska, 9th Central and Eastern European Proteomic Conference

rancRNAs as novel group of stress – related protein biosynthesis regulators
Mleczko A.M., Twardowski T., Bąkowska-Żywicka K.

Wystąpienia ustne

1. 8.04.2017, Poznań, Polska, Biosfera, Spotkania Młodych z Nauką

Tajemnice krótkich RNA, czyli kilka słów o sdRNA –krótkich, niekodujących RNA powstających ze snoRNA" **– I miejsce za najlepszą prezentację**
Mleczko A.M., Bąkowska – Żywicka K.

2. 22-24.04.2016, Warszawa, Polska, Międzyuczelniane Sympozjum Biotechnologiczne "Symbioza"

snoRNA – niezwykła cząsteczka z milionem tajemnic – czyli małe, niekodujące RNA powstające ze snoRNA
Mleczko A.M., Bąkowska – Żywicka K.

3. 12-13.-3.2016, Lublin, Polska, VIII Interdyscyplinarna Konferencja Naukowa TYGIEL

Życie po życiu – czyli kilka słów o przetwarzaniu snoRNA do krótkich RNA
Mleczko A.M., Bąkowska – Żywicka K.

Organizacja konferencji

2019 Organizacja konferencji „**The 19th FEBS Young Scientists′ Forum**" (YSF) w Krakowie, poprzedzającej The 44th FEBS Congress.

Stypendia

2016/2017 Stypendium dla najlepszych doktorantów, ICHB, PAN
2017/2018 Stypendium dla najlepszych doktorantów, ICHB, PAN
2018/2019 Stypendium dla najlepszych doktorantów, ICHB, PAN

Wskaźnik Hirscha według bazy Web of Science 4

PUBLIKACJE WCHODZĄCE W SKŁAD ROZPRAWY DOKTORSKIEJ

1

Bąkowska-Żywicka K, **Mleczko AM**, Kasprzyk M, Machtel P, Żywicki M, Twardowski T

The widespread occurrence of tRNA-derived fragments in Saccharomyces cerevisiae

FEBS Open Bio, 2016, 6(12):1186-1200

FEBS openbio

FEBS PRESS
science publishing by scientists

The widespread occurrence of tRNA-derived fragments in *Saccharomyces cerevisiae*

Kamilla Bąkowska-Żywicka[1], Anna M. Mleczko[1], Marta Kasprzyk[1], Piotr Machtel[1], Marek Żywicki[2] and Tomasz Twardowski[1]

1 Institute of Bioorganic Chemistry Polish Academy of Sciences, Poznan, Poland
2 Department of Computational Biology, Institute of Molecular Biology and Biotechnology, Faculty of Biology A. Mickiewicz University in Poznan, Poland

Keywords
northern blot hybridization; *Saccharomyces cerevisiae*; small RNAs; tRNA; tRNA-derived fragments

Correspondence
K. Bąkowska-Żywicka, Institute of Bioorganic Chemistry Polish Academy of Sciences, Noskowskiego 12/14, 61-704 Poznan, Poland
Fax: +48/6185280532
Tel: +48/618528503
E-mail: bakowska@ibch.poznan.pl

(Received 1 April 2016, revised 19 July 2016, accepted 13 September 2016)

doi:10.1002/2211-5463.12127

Short RNAs derived from the cleavage of tRNA molecules are observed in most organisms. Their occurrence seems to be induced by stress conditions, but still little is known about their biogenesis and functions. We find that the recovery of tRNA fragments depends on the RNA isolation method. Using an optimized RNA extraction protocol and northern blot hybridization technique, we show that the tRNA-derived fragments in yeast are widespread in 12 different growth conditions. We did not observe significant stress-dependent changes in the amounts of tRNA fragments pool. Instead, we show the differential processing of almost all individual tRNAs. We also provide evidence that 3′-part-derived tRNA fragments are as abundant as the 5′- one in *Saccharomyces cerevisiae*. The resulting set of *S. cerevisiae* tRNA fragments provides a robust basis for further experimental studies on biological functions of tRFs.

Transfer RNA are molecules mostly recognized from their role during protein synthesis. However, a growing number of other, ex-translational functions have recently been described. The most spectacular examples come from bacterial cells and include induction of the stringent control, regulation of transcription of some operons, and control of replication of ColE1-type plasmids by uncharged tRNA [1]. In yeast and mammals, in response to starvation conditions, tRNA induces phosphorylation of eukaryotic initiation factor 2 through binding to the Gcn2 kinase which modulates the transcription of amino acid biosynthesis genes and reduces total protein biosynthesis [2,3]. Moreover, during stress response, tRNA transcription is reduced, and a retrograde transport of tRNA into the nucleus is observed [4]. Also aminoacylated tRNA has been shown in recent studies to serve as substrates in biochemical processes other than translation, such as cell wall formation, tagging of proteins for degradation, aminoacylation of phospholipids in the cell membrane, and antibiotic biosynthesis [5].

Recently, using high throughput sequencing, sensitive northern blot assays or computational analysis, a novel ex-translational role of tRNA has been revealed. In response to various stress conditions, cleavage of cytosolic tRNA into stable shorter molecules has been observed, giving rise to tRNA halves (when the cleavage occurs in the anticodon loop) and tRFs (other breakage points in tRNA) (for a review, see [6] and references therein). To date, the function of tRNA-

Abbreviations
eIF, eukaryotic initiation factor; EXO1, exonuclease 1; GPD1, glycerol-3-phosphate dehydrogenase 1; gtRNAdb, genomic tRNA database; HSP12, heat-shock protein 12; LMW RNA, low molecular weight RNA; PDR12, plasma membrane ATP-binding cassette (ABC) transporter; T_H, hybridization temperature; T_m, melting temperature; tRF, tRNA-derived fragment.

derived fragments has been studied in many organisms and it appeared that those molecules represent a wide functional repertoire. tRNA halves seem to act as global translation regulators by displacing eIF4G/eIF4A from uncapped to capped RNA in human cell lines [7]. Shorter tRFs can bind directly to 30S ribosomal subunits and inhibit translation in *Archaea* [8]. tRNA fragments have also been identified in pools of small RNA copurified with Argonaute and Piwi complexes [9,10] or being processed by Dicer [9,11], suggesting that they could function in a way similar to siRNAs or miRNAs. Although regulation of gene expression by miRNAs is conserved in diverse eukaryotic species, including budding yeast *Saccharomyces castellii* and *Candida albicans* [12], it has been lost in *Saccharomyces cerevisiae*. Thus, this organism provides an optimal system for studying the Dicer/Argonaute-independent mechanisms of tRNA-derived fragments' biogenesis and function.

It has been shown that tRNA fragments are present in small amounts even in unstressed cells, but they are highly induced when cell is exposed to stress conditions, like heat shock, low temperature, amino acid, or phosphate starvation, oxidative stress, high pH, and during development ([6] and references therein). In this aspect, the best studied are tRNA halves which are generated by specific ribonucleases that are secreted from the stressed cells. These are Rny1p in yeast [13] and angiogenin in mammalian cells [14].

In 2014, the computational meta-analysis of more than 50 short RNA libraries revealed that fragments derived from tRNA are present in all domains of life (bacteria to humans) [15]. However, during estimation of their length and abundance with the use of deep-sequencing methods, two important issues have to be addressed. First, during the cDNA library preparation, tRNA modifications can affect reverse transcriptase and therefore lead to detection of spurious truncated tRNA fragments. Since tRNA molecules are extremely abundant in cells, such truncated cDNAs could be observed in cDNA libraries. Second, cDNA libraries in the mentioned study were originally developed for detection of miRNAs, thus usually only RNA of a length less than 30 nucleotides were included (36 nucleotide of sequencing read minus significant 3′ adaptor overlap ensuring the full-length small RNA has been sequenced). Therefore, the amounts of the tRNA fragments longer than 30 nucleotides, including tRNA halves, could be currently underestimated. On the other hand, the employment of other experimental approaches is hampered by relatively low concentration of tRNA fragments in the cells, as has been reported in previous studies [13,16]. It has been shown, however, that different purification methods may significantly affect the composition of RNA species in the isolated RNA fractions [17]. Several studies have tackled this point, focusing on methods for miRNA extraction [18–20]. The influence of RNA isolation on recovery of tRNA-derived fragments which differ from miRNAs in GC content and structural features has not yet been studied.

Considering all of the above, we decided to perform the comprehensive analysis of tRNA fragment abundance in yeast *S. cerevisiae* under 12 different growth conditions. In order to measure the abundance of highly modified tRNA-derived fragments, we have employed the northern blotting method, which is independent from the reverse transcription. In our study, we have also verified the influence of four different RNA isolation methods on tRNA fragments' recovery, revealing that this initial step is of major impact on observed fragments' quantities.

Results

RNA isolation method severely influences the detection of tRNA-derived fragments

At the very first step, we decided to compare the efficiency of recovery of tRNA fragments between four different methods of RNA isolation. In addition to well proven total RNA isolation method LET, which was used previously for studies on tRNA fragments in *S. cerevisiae* [13], we decided to verify the efficiency of three additional protocols resulting in enrichment of low molecular weight (LMW) RNA in the sample: standard MicroRNA kit, MasterPure kit with isopropanol enrichment step and the method widely used for isolation of bulk tRNA. The basic outline of these four methods is presented in Fig. 1.

In terms of total RNA quantity, as measured by a Nanodrop, the LET method resulted in highest yield of RNA (1.5–6-fold higher). Among the methods for LMW RNA isolation, the median RNA yield obtained with the bulk tRNA isolation method was about 2.4-fold higher than that obtained with MasterPure and about 1.7 higher than with MicroRNA kit. Measurement of absorbance ratio at 260 nm and 280 nm (A260/280) showed that no significant differences were observed in term of RNA purity. The variation in RNA quantities obtained from different stress conditions was in all methods about twofold.

More significant differences between the tested methods were observed in recovery of short RNA fraction, which contain the tRNA-derived fragments

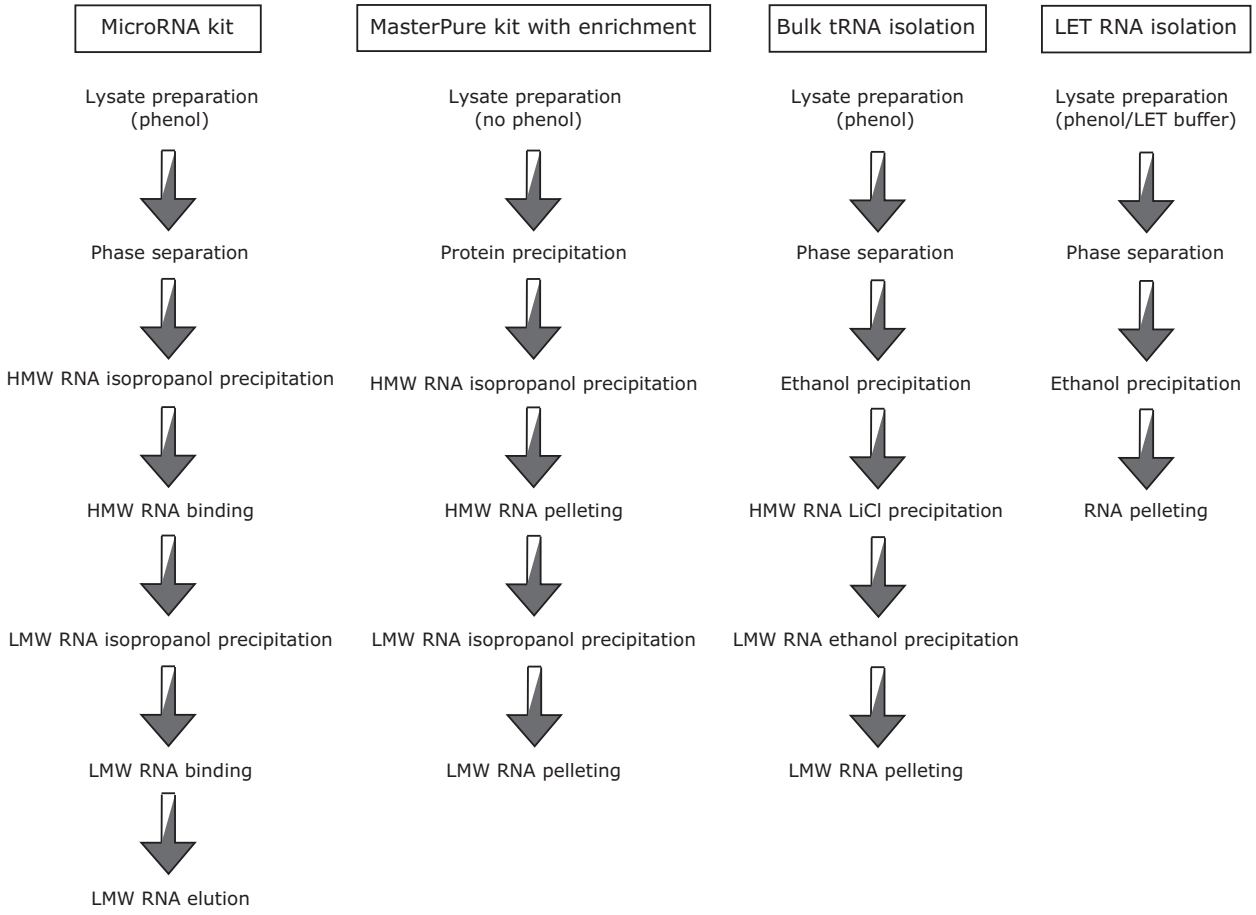

Fig. 1. Schematic illustration of different RNA isolation methods used in this study.

(14–40 nt, Fig. 2A). For those measurements, we have used the most reliable method available (Bioanalyzer 2100; Agilent Technologies, Santa Clara, CA, USA), which, however, excluded the LET-isolated RNA pool from this comparison, due to the RNA size composition of the sample. In RNA pool isolated with MasterPure kit (Epicentre, Madison, WI, USA), similar to the total RNA quantity, the ratio of short versus LMW RNA was the lowest (median among growth conditions of 3%). In contrast, the content of short RNA obtained with MicroRNA kit (A&A Biotechnology, Gdynia, Poland) and bulk tRNA extraction methods was threefold higher with median of 9%. Interestingly, the full-length tRNA content was similar in all isolation methods with a median amount of 50%. Overall, taking into consideration the quantity of LMW RNA as well as short RNA content, the bulk RNA isolation method resulted in 9.1-fold higher median yields of short (14–40 nucleotides) RNA compared to the two other methods for LMW RNA isolation.

In order to provide a reliable comparison of RNA derived from all four different isolation procedures and to address the LET isolation method missing in Bioanalyzer analysis, we have additionally checked the quality of RNA (Fig. 2B). After loading 5 μg of the total LET RNA or 2.5 μg of low molecular weight RNA (derived from MicroRNA kit isolation, MasterPure kit isolation or bulk tRNA isolation) on 12% polyacrylamide gels and SYBR® Safe staining, we clearly observed good separation of distinct RNA, including bulk tRNA, 5S rRNA, and a portion of small RNA. RNA isolated with the LET method were additionally enriched with the high molecular weight RNA, as expected.

In order to verify whether short RNA content in the sample is correlated with the recovery of tRNA-derived fragments, we have performed northern blot experiments using the probe specific for the 5′ part of tRNA-Ala(AGC) and for the 3′ part of tRNA-Asn (GTT). As expected from our previous observations, also in tRNA fragments' recovery, the bulk tRNA

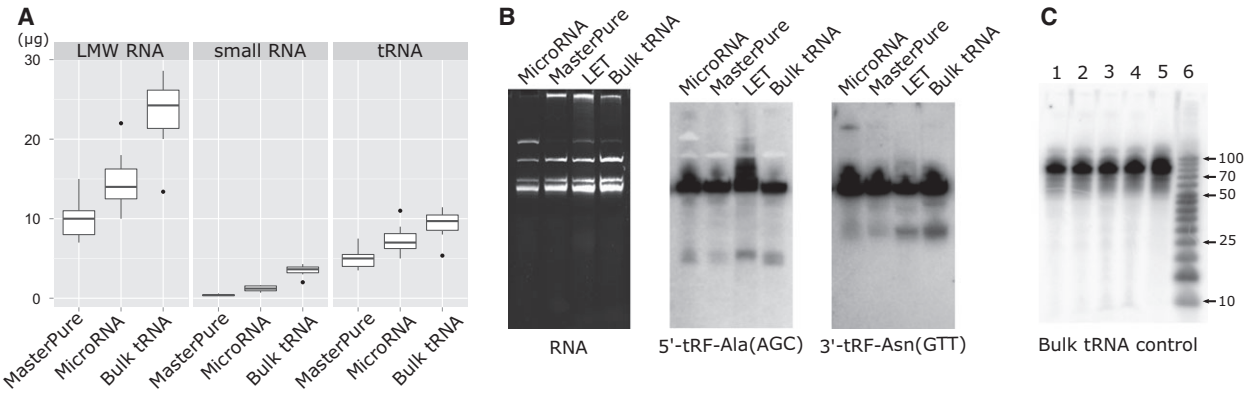

Fig. 2. Comparison of LMW RNA extraction methods. (A) Box plot diagram showing the distributions of the absolute RNA amounts [µg] obtained from 3×10^7 *S. cerevisiae* cells grown in 12 different conditions. Three different isolation methods, MasterPure, Micro RNA, and bulk tRNA are compared. Panels are representing the amounts of low molecular weight RNA (LMW, < 200 nt), small RNA (14–40 nt), and tRNA obtained with every method. The quantities were measured by Bioanalyzer 2100 using Small RNA kit. Central lines represent the medians, boxes indicate the range from 25th to 75th percentile, whiskers extend 1.5 times the above interquartile range, outliers are represented as dots. $n = 12$ sample points for all panels. (B) PAGE result showing RNA samples obtained by the employment of four different isolation procedures: Micro RNA, MasterPure, LET and bulk tRNA, and Northern blot hybridization result. Detection of 5′-tRF-Ala (AGC) and 3′-tRNA-Asn(GTT) is shown. All membranes were exposed for 16 h. Differential recovery of tRF can be observed. (C) Visualization of exogenous cellular tRNA pool (1) added at the following steps of the bulk tRNA isolation procedure: 2) directly to the cell pellet; 3) to the unbuffered phenol before shaking; 4) to the aqueous phase after phenol extraction and 5) during removal of ribosomal RNAs with LiCl. 6—size marker.

isolation method was very efficient. The MicroRNA kit and MasterPure methods failed to provide amounts of tRNA fragments above the clear detection threshold. The LET isolation method, which was previously used in yeast tRNA-derived fragments research [13,16] resulted in a visible detection of tRNA fragments. However, when we compared the intensity of bands corresponding to the tRF in relation to the tRNA intensity, the bulk tRNA isolation method clearly outperformed the LET isolation method (tRF signals were ~ five times more intense). The above observations indicate that compared RNA isolation methods differ not only in the amounts of short RNA but also in the composition of the short RNA fractions.

The surprisingly high performance of bulk tRNA isolation method in recovery of tRNA-derived fragments from every growth condition raises a concern about the method reliability. It could be possible that by release or activation of cellular nucleases during the isolation procedure, tRNA could be subjected to non-physiological degradation. In order to verify this scenario, we have spiked-in the previously isolated and radiolabeled full-length yeast tRNA at various steps of the bulk tRNA isolation procedure. The gel electrophoresis and autoradiography of isolated RNA did not reveal any degradation of spiked-in tRNA, thus confirming the cellular origin of high amounts of observed tRNA-derived fragments (Fig. 2C).

Based on above results for further investigation of tRNA-derived fragments in yeast, we have used the bulk tRNA isolation method.

All tested tRNA isoforms are processed into tRNA fragments

To determine the extent of tRNA isoforms that are the source of stable tRNA fragments, we performed northern blot hybridization experiments using LMW RNA pools (up to ~ 200 nucleotides) isolated with bulk tRNA method. Due to the significant changes in cell metabolism, we have used yeast cells subjected to 12 different environmental conditions: heat shock, high salinity, UV irradiation, anaerobic and optimal growth, high or low pH conditions, amino acid depletion, sugar starvation, and hypo- and hyper-osmotic conditions [13,16,21–23]. We have grown *S. cerevisiae* in optimal conditions overnight. The stress was applied for 15 min as it has been shown that rapid transcriptome changes occur most efficiently 15–20 min after stress initiation [22,23]. We have controlled the status of the cell stress by analyzing the expression of four selected well-known stress-regulated genes: HSP12, GPD1, PDR12, and EXO1. These genes were selected to cover all stress conditions used in this study. Full description of selected genes as well as their expression changes are summarized in Table 1. Our quantitative real-time PCR

Table 1. Genes used in this study as markers for stress conditions.

Gene name	Gene description	Expression change	
		Literature	This study
HSP12 (heat-shock protein 12)	Plasma membrane protein involved in maintaining organization during multiple stress conditions	Upregulation during: heat shock, oxidative stress, osmostress, stationary phase, glucose depletion, oleate, alcohol [22,23,27–31]	Significant upregulation during: heat shock (10-fold), osmostress (high salt—50-fold, and hyper-osmotic conditions—50-fold) Significant downregulation during cold shock (fivefold) and anaerobic growth (40-fold)
GPD1 (NAD-dependent glycerol-3-phosphate dehydrogenase)	Key enzyme of glycerol synthesis	Upregulation during: osmostress [22,23,28,32]	Significant upregulation during: osmostress: high salt (50-fold) and hyper-osmotic conditions (10-fold)
PDR12 (plasma membrane ATP-binding cassette ABC transporter)	Required for weak organic acid resistance	Upregulation during: low pH [22,23,33]	Significant upregulation during low pH (1000-fold)
EXO1 (5′-3′ exonuclease and flap-endonuclease)	Involved in recombination and double-strand break repair, UV-sensitive	Upregulation during: UV [34]	The highest upregulation during UV stress (eightfold), also during anaerobic growth (sevenfold) and under high pH (sixfold)

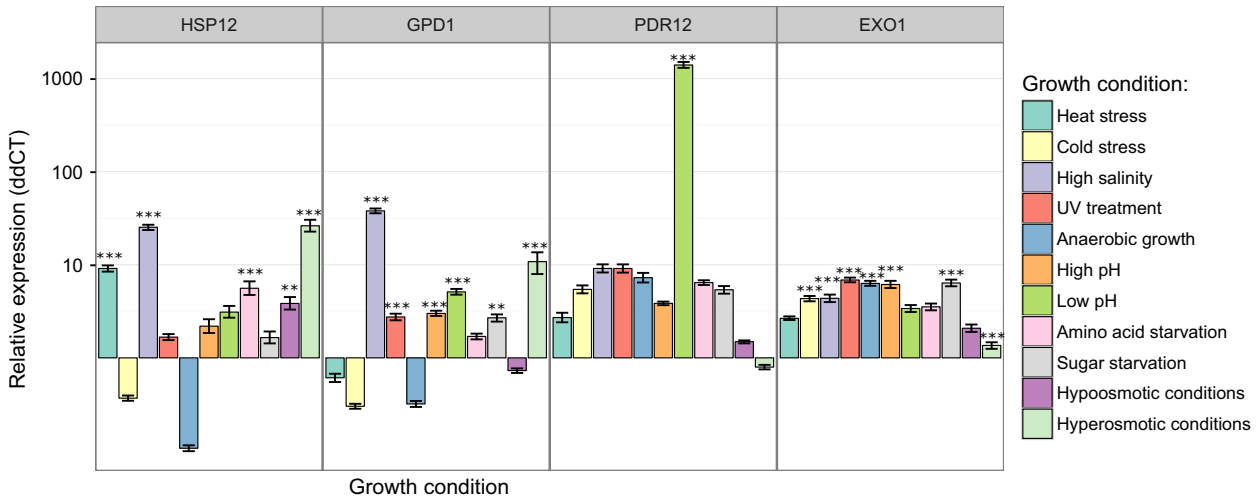

Fig. 3. Status of a cell stress analyzed by quantitative real-time PCR method. The expression change of four stress-regulated yeast genes (HSP12, GPD1, PDR12, and EXO1) is shown. Expression changes are presented in $\log_{10}$ scale as the expression relative to the optimal growth conditions (ΔΔCT values). Significance was designated as ** $P < 0.01$, and *** $P < 0.001$.

analysis showed that the HSP12, GPD1, PDR12, and EXO1 gene expression changes under particular stresses when compared to the optimal growth conditions as expected, thus confirming the induction of the stress response in yeast cells (Fig. 3 and Table 1).

Although there are 41 unique mature tRNA species encoded by 275 tRNA genes in yeast (according to gtRNAdb), by careful selection of target regions, we were able to design the isoform-specific probes that are able to detect 40 isoform variants. Due to the experimental setup, we were not able to examine the individual processing of tRNA-Ser(TGA) and tRNA-Ser (CGA), since the hybridization probes were identical. Therefore, both isoforms were investigated as a pool. However, we were able to design 80 specific antisense DNA probes complementary either to the 5′ or 3′ part of 40 yeast tRNA isoforms (Table S1). For some of the probes, the differences between the optimal hybridization temperature (T_H) for the 3′-part- and 5′-part-derived tRNA fragment of the same tRNA isoform reached 10–12 °C. Therefore, in order to provide a reliable comparison between different northern blot results, we have examined the possibility of differential efficiency of hybridization of antisense DNA probes to the full-length tRNA, depending on the hybridization temperatures influencing tRNA secondary structure

melting. We have selected two tRNA species for which the optimal northern blot hybridization temperature calculated by us varied most between the 5′-part- and 3′-part-derived tRNA fragments. These were: tRNA-Arg(TCT) (T_H for the 5′ probe: 55 °C; T_H for the 3′ probe: 45 °C) and tRNA-Asp(GTC) (T_H for the 5′ probe: 42 °C; T_H for the 3′ probe: 55 °C). We performed the northern blot hybridization assays aiming at detection of the above tRNA at four different temperatures and compared the results with the optimal T_H (Fig. 4A). We have quantified the signal intensities of full-length tRNA (hybridized at different temperatures) and normalized it to the signals of a loading control, U6 snRNA (hybridized at a constant temperature). In all cases, the intensity of a band corresponding to the full-length tRNA did not change in optimal and nonoptimal temperatures. The values of normalized signal intensities were in a range from 112 073 to 113 472 for tRNA-Arg(TCT) with a mean value of 112 845 (SD = 718) and from 125 008 to 125 845 for tRNA-Asp(GTC) with a mean value of 125 479 (SD = 351). These results indicate that (a) different temperatures of hybridization used in this study for 5′-part- and 3′-part-derived fragments of the same tRNA do not change the hybridization efficiency to the full-length tRNA and (b) observed differences in tRFs abundance and processing efficiency are indeed related to their different levels. As a result, we were able to observe different patterns of tRF levels among the growth conditions for closely related probes, for example, 5′ parts and 3′ parts of three isoforms of tRNA-Thr (Fig. 4B). However, despite the efforts to ensure the probe specificity, we do not know to what extent the probes used are complementary to the processed tRNA fragments. Thus, the probes might possibly hybridize with different efficiencies and we cannot exclude the possibility of minor cross-hybridization.

Using the optimized RNA isolation protocol, we were able to detect fragments derived from all the 40 tested tRNA isoforms (Fig. S1). We estimated the abundance of the fragments as a percentage of the fragment's band intensity divided by the sum of fragment and full-length tRNA band intensity (after background subtraction). In order to provide a robust quantification, the autoradiograms, revealed by quantification software to exhibit full saturation of the quantified bands, were re-exposed. Within every group of tRNA isoforms specific for same amino acid, we

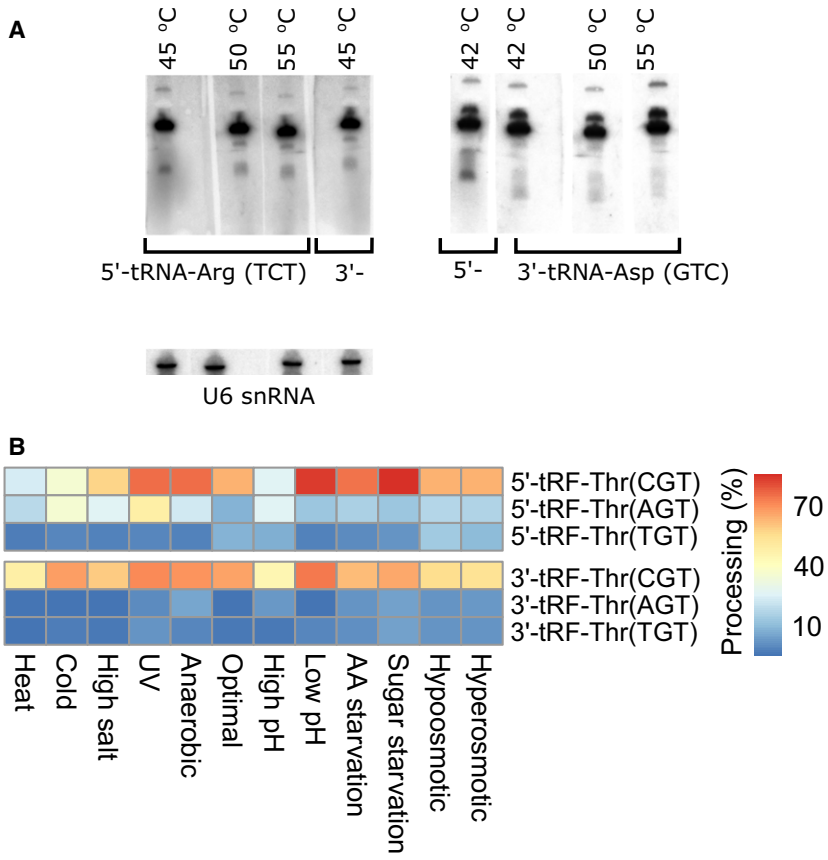

Fig. 4. Verification of the possibility to distinguish the differential processing of tRNA isoforms. (A) Northern blot hybridization result. Detection of 5′- and 3′-tRNA-Arg (TCT) and 5′- and 3′- tRNA-Asp (GTC) at different hybridization temperatures. U6 snRNA served as a loading control. (B) Differential processing of 3′ and 5′ parts of individual threonine tRNA isoforms. Absolute processing efficiency, calculated as the percentage of tRNA-derived fragment signal compared to overall (fragment + tRNA) signal, is encoded in a color scale.

have observed that at least one of the 5′ or 3′-derived fragments was present in much higher amounts than others. The most preferentially processed tRNA isoforms include: tRNA-Ala(TGC), tRNA-Arg(CCT), tRNA-Asn(GTT), tRNA-Asp(GTC), tRNA-Gly(CCC), tRNA-Gly(GCC), tRNA-Met(CAT), tRNA-Lys(CTT), tRNA-Leu(TAA), and tRNA-Thr(CGT). Interestingly, in three of these cases (tRNA-Gly, tRNA-Lys and tRNA-Thr), we observed isoform-dependent accumulation of both, 5′- and 3′-part-derived fragments.

The composition but not total amount of the tRNA-derived fragments' pool depends on the growth condition

In order to verify whether the processing of tRNA to shorter fragments is stress-dependent, we have compared the cleavage efficiencies among 12 tested environmental conditions of *S. cerevisiae* growth. Surprisingly, we did not observe any significant differences in global efficiency of tRNA processing, neither between individual stress conditions nor in comparison to optimal growth conditions (Fig. 5). Most of the tRNA were processed with 2–20% efficiency, with the median value for each condition varying between 2–4%. However, highly abundant tRNA-derived fragments showed preferential accumulation under high salt and low pH conditions as well as under amino acids or sugar starvation. We did not observe any highly abundant tRNA fragments under high pH conditions and just two fragments in heat stress. Next, we have investigated the changes in accumulation of individual tRNA-derived fragments among different yeast growth conditions. The first observation was that both the median and the dynamic range of tRNA processing efficiency significantly differ between individual tRNA fragments (Fig. 6A). The lowest observed processing efficiency was 0.1% for 3′-tRNA-Ser(CGA) and the highest was 85.4% for 3′-tRNA-Asn(GTT). We have noticed that tRNA fragments which are present in high amounts are usually differentially accumulated between individual growth conditions in terms of absolute tRNA processing efficiency. However, based on the analysis of normalized changes in tRNA processing efficiency (calculation of *Z*-scores which represent the deviation from mean processing of a given tRNA among growth conditions), we have concluded that in fact all tRNA fragments reveal similar degree of accumulation variability (Fig. 6B). Our data suggest that there are only minor differences in global tRNA cleavage efficiency between optimal and stress conditions. However, clustering of the tRNA processing profiles revealed two distinct groups of yeast growth conditions which were characterized with slightly different relative tRNA processing patterns. Under UV irradiation, anaerobic, AA starvation, sugar starvation, hypoosmotic, and hyperosmotic growth conditions, most of the tRNA fragments were accumulating more efficiently than the average, whereas in optimal, high salt, low pH, high pH, and cold and heat conditions, the relative processing seemed to be lower than the average. Those differences are only visible when analyzing the *Z*-score-transformed data, but not when comparing the absolute processing efficiencies (Fig. 6B versus Fig. 5). Looking at the individual tRNA fragments, we were able to observe significant differences in stress-dependent cleavage. Interestingly, most of the tRNA fragments could be grouped into clusters of similar accumulation patterns. Those observations

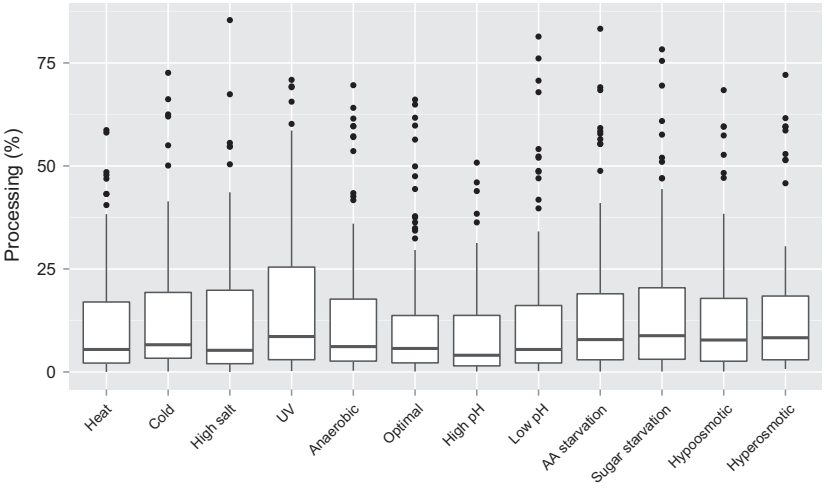

Fig. 5. Distribution of tRNA processing efficiency in 12 growth conditions. Box plot representing distributions of the processing efficiencies of tRNAs in individual stress conditions. Central lines represent the medians, boxes indicate the range from 25th to 75th percentile, whiskers extend 1.5 times the above interquartile range, outliers are represented as dots. $n = 96$ sample points for all conditions.

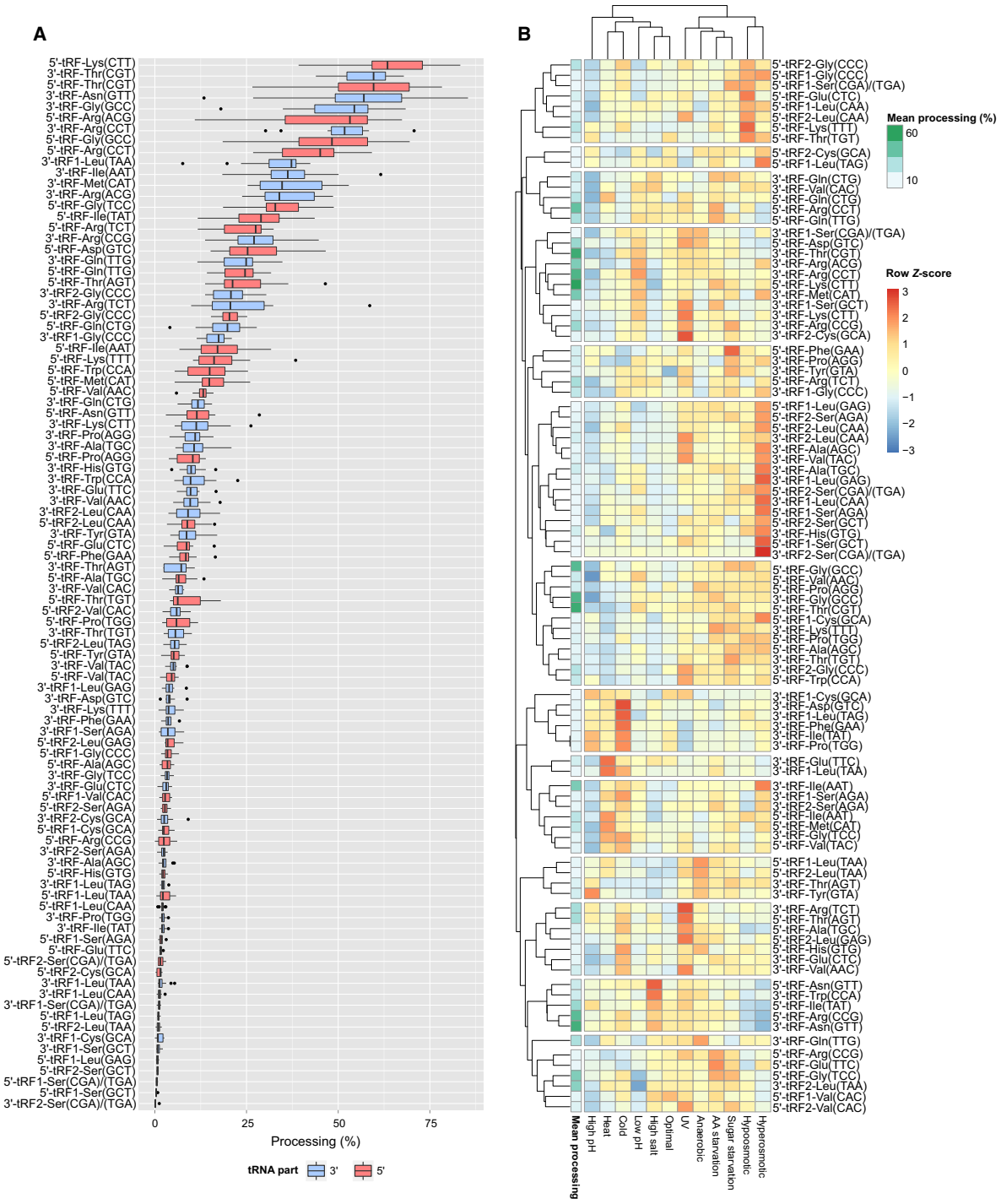

Fig. 6. Differential processing of tRNAs. (A) Box plot representing the distributions of processing efficiencies of individual tRNA-derived fragments among 12 different yeast growth conditions. Fragments are ordered by mean processing efficiency. tRNA fragments derived from 3′ part of tRNAs are marked with blue, and those derived from 5′ part with red. 2 tRFs, derived from the same part of particular tRNA are marked as follows: tRF1—longer tRF, tRF2—shorter tRF. Central lines represent the medians, boxes indicate the range from 25th to 75th percentile, whiskers extend 1.5 times the above interquartile range, outliers are represented as dots. $n = 12$ sample points for all tRNA fragments. (B) Clustered heat map representing the variations in tRNA processing efficiencies among 12 yeast growth conditions. The color scale encodes for the normalized *Z*-scores calculated within the rows of the matrix, representing deviation of processing of a given tRNA fragment in a given condition from the mean processing of a given tRNA. In the first column, in a green scale, the mean processing efficiency of tRNAs has been presented.

suggest that in general, tRNA processing in *S. cerevisiae* is not stress-induced, but the composition of the tRNA-derived fragments' pool differs with changes in growth conditions.

To investigate this hypothesis in more detail, we have analyzed the correlation between the absolute accumulation of all tRNA-derived fragments and individual growth conditions (Fig. 7). In most of the comparisons, the Pearson correlation was in the range 0.86–0.94 (median: 0.9), suggesting that in most of the growth condition comparisons, tRNA reveal similar processing level. It was especially striking in the case

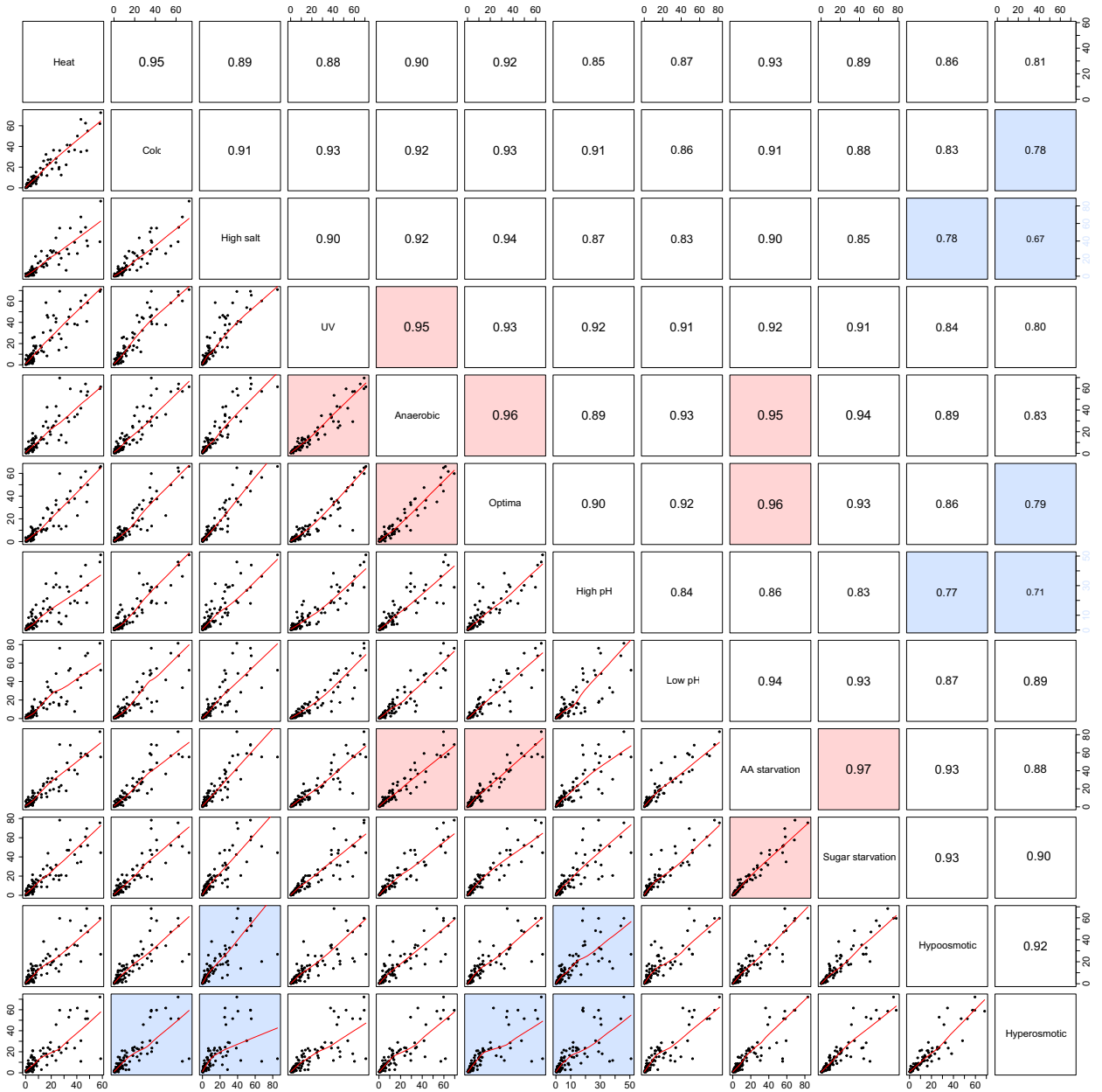

Fig. 7. Cross-comparison of the tRNA processing efficiencies. Scatter plot matrix containing the series of 1 : 1 comparisons of tRNA processing efficiencies between individual growth conditions. The lower triangle of the matrix represents the scatter plots of tRNA-derived signals from compared growth conditions together with the loess fit (the red line). The upper triangle of the matrix represents the Pearson correlation of the tRNA processing between given growth conditions. Fields highlighted in red represent the conditions with highest correlation (lowest variation) of the tRNA processing, fields highlighted in blue represent the lowest correlation (highest variation). $n = 96$ for every comparison.

of comparisons to the optimal growth conditions (median 0.93). On the other hand, the largest changes in tRF levels were observed for hyperosmotic stress: 0.81 median correlation with other growth conditions, with the lowest values for comparison with high salt conditions (0.67), high pH (0.71), cold stress (0.78), or with optimal growth conditions (0.79).

3′-part-derived tRNA fragments are as abundant as the 5′- ones

We have compared the abundance of fragments derived either from 5′ or from 3′ part of tRNA molecules. In a previous report, based on the analysis of 50 different small RNA-seq libraries, it was shown that 5′-tRFs were present in higher abundance than 3′-tRFs in mouse, *Drosophila* and *Schizosaccharomyces pombe* [15]. In our data, we have observed that in all tested growth conditions, both 5′-derived as well as 3′-derived tRNA fragments' pools were almost equally abundant (Fig. 8). However, we observed individual differences in the levels of fragments derived either from 5′-part or 3′-part of the same tRNA. We found 10 most prominent examples where the abundance differences between parts of the same tRNA reached almost 50% (Fig. 6A). These were: tRNA-Arg(CCG), tRNA-Asn (GTT), tRNA-Asp(GTC), tRNA-Gly(TCC), tRNA-Gly(CCC), tRNA-Ile(TAT), tRNA-Leu(TAA), tRNA-Lys(CTT), tRNA-Lys(TTT), and tRNA-Thr(AGT). In six of these tRNA species, fragment derived from the 5′-part was more stable.

Discussion

Previous studies by Thompson *et al.* [13] demonstrated that *S. cerevisiae* contains small RNA populations consisting primarily of tRNA halves and rRNA fragments. In our recent studies, by the employment of high throughput sequencing, we have found similar tRNA-derived RNA to interact with yeast ribosomes [21]. In this study, we have performed an independent cross-comparison of three extraction procedures for

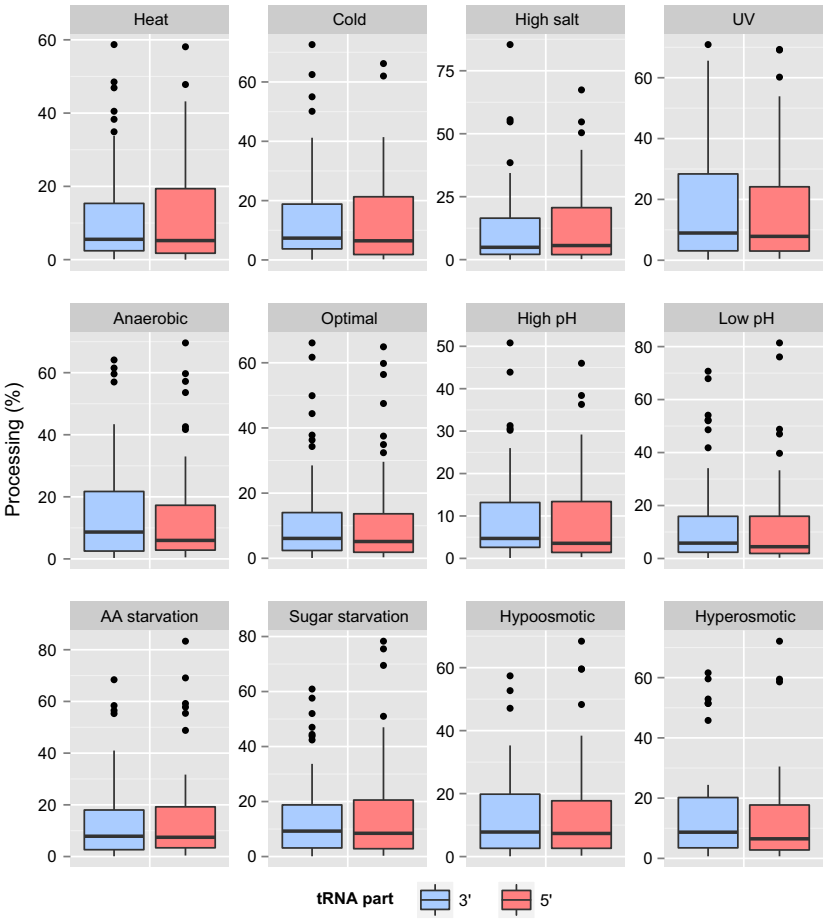

Fig. 8. Comparison of 3′- and 5′-derived tRNA fragments processing. Box plot representing the distribution of processing efficiencies of 3′- and 5′-derived tRNA fragments in 12 yeast growth conditions. Central lines represent the medians, boxes indicate the range from 25th to 75th percentile, whiskers extend 1.5 times the above interquartile range, outliers are represented as dots. $n = 46$ for 3′ and 50 for 5′ fragments for all panels.

low molecular weight (LMW) RNA isolation form *S. cerevisiae* samples using MicroRNA kit, MasterPure kit with isopropanol enrichment and bulk tRNA isolation method. We have compared their efficiency in recovery of tRNA-derived fragments with the total RNA isolation method which was previously successfully used to detect several tRNA fragments in yeast under oxidative stress, methionine starvation, nitrogen starvation, heat shock, and entry into the stationary phase [13,16]. All four methods evaluated in this study are widely applied for RNA isolation, but employ different biochemical principles. The first method, MicroRNA kit from A&A Biotechnology, employs phenol/chloroform extraction with a column-based enrichment of RNA molecules of size below 200 nucleotides. Although in our experiments, this pool contained 6–10% of short RNA (14–40 nucleotides), we were unable to detect any clear northern blot signals corresponding to the tested tRNA fragments, while full-length tRNA were highly abundant. We have obtained similar results for MasterPure kit with isopropanol enrichment of LMW RNA. Although this method was characterized with the lowest short RNA/LMW RNA ratio of ~ 2–4%, we were able to detect minor amounts of tRNA-derived fragments with northern blot. The third method of LMW RNA isolation, the bulk tRNA protocol [23], gave superior results in both short RNA/LMW RNA ratio of 8–14% as well as tRNA-derived fragments' detection with northern blots (up to over fourfold more intensive signal for tRNA fragment than for full-length tRNA). We compared the efficiency of all three LMW RNA isolation methods with LET protocol for total RNA extraction which previously gave positive results when detecting tRNA fragments in several stress-derived RNA pools [13,16]. However, the intensity of the tRNA fragment-specific northern blot signals obtained with LET method was comparable to those obtained with the MasterPure kit and clearly weaker than with the bulk tRNA isolation method.

It was surprising for us to observe the lack of correlation between the amounts of short RNA isolated with individual methods and the ability to detect tRNA-derived fragments. This suggests that there are some specific interactions of tRNA-derived fragments which might influence the efficiency of their extraction. One possibility that has already been shown is that some small RNA species can bind to larger RNA molecules, and therefore may comigrate with high molecular weight RNA. This results in loss of small RNA and may introduce sample–to-sample variation in the composition and abundance of small RNA species. This phenomenon, named as the carrier effect of cellular RNA, has already been observed by Podolska *et al.* [20] in the miRVana-isolated RNA samples tested for the presence of miRNA and further proved by Kim *et al.* [17]. Another possible explanation could be that the presence of additional compounds (associated proteins and/or nucleic acids) can affect the efficiency of the tRNA fragments' extraction. These compounds could further be lost during the RNA purification procedure. However, their presence in the initial steps of the purification could severely influence the composition of the purified RNA. This issue has already been postulated by Monleau *et al.* [18] Since we were able to gain the best results with the method that was optimized for isolation of bulk tRNA, we speculate that the mechanism of tRNA-derived fragments loss during the isolation procedure is related to specific characteristics of tRNA molecules, including sequence, structure or high molecular interaction partners.

It was postulated by several research groups that the cleavage of tRNA is a stress-related phenomenon. This dependence was especially well described in higher eukaryotes for tRNA halves derived by angiogenin activity [7] and tRNA fragments processed from pre-tRNA transcripts [9]. Site-specific tRNA cleavage in *S. cerevisiae* was only observed in a limited subset of stress conditions, for example, during oxidative stress or heat shock [13,16]. The same studies in *S. cerevisiae* revealed that tRNA cleavage was not detected in yeast cells undergoing amino acid or glucose starvation and UV irradiation [16]. The failure of these stress stimuli to increase tRNA fragment levels in *S. cerevisiae* suggested that the cleavage is neither a general mechanism of stress response nor a general effect of a decrease in translation rates. It has been also reported that in unstressed *S. cerevisiae* cells, only low levels a of tRNA cleavage may be detected [16]. However, our data presented in this manuscript suggest that the tRNA cleavage is a general phenomenon in yeast cell, occurring independently of the growth conditions.

Due to experimental design, we were unable to estimate the exact size of the observed tRNA-derived fragments or assign whether fragments were generated from mature tRNA or pre-tRNA. Thus, the data presented here reflect rather general overview of tRNA processing in *S. cerevisiae*. As previously suggested by several research groups (for review see [6] and references therein), we have experimentally verified that the cleavage is not limited to specific tRNA, although the relative efficiency of cleavage can differ. Moreover, we did not observe significant differences in the accumulation of total tRNA fragments pool depending on stress condition nor increase in the relation to the optimal

conditions. However, our data strongly suggest that the tRNA cleavage is regulated in a stress-dependent manner by specific selection of tRNA species which serve as substrates for a defined processing. We believe that such widespread processing of tRNA was not observed before in *S. cerevisiae* due to two major reasons, employment of the nonoptimal RNA isolation method and/or using the high throughput sequencing data for tRNA fragments profiling, which are hampered by not well characterized dependence of reverse transcription on numerous tRNA base modifications. Previous reports showed that the 5′-tRFs are present in higher levels than 3′-tRFs in mouse, *Drosophila* and yeast *S. pombe* [15]. However, we observed that the total pools of 5′-derived as well as 3′-derived tRNA fragments are almost equally abundant, independently of *S. cerevisiae* growth conditions.

In most cases reported until now, full-length tRNA levels do not decline significantly when the tRNA processing is observed and tRNA fragments' levels are consistently lower than those of full-length tRNA [14,16]. This suggests that only a small portion of tRNA could be targeted as a substrate for cleavage. This is in contrast to the complete depletion of tRNA targeted by colicins [24]. This is also in contrast to our data, which show that in the case of highly and very highly abundant tRNA-derived fragments, the signal on northern blot membrane that corresponds to the fragment is stronger than the signal of full-length tRNA.

Methods

Strain and growth conditions

Saccharomyces cerevisiae strain BY4741 (MATα; his3Δ 1; leu2Δ 0; met15Δ 0; ura3Δ 0) was grown in synthetic optimal YPD yeast medium supplemented with 2% carbon source at 30 °C.

Cells were grown in 12 different growth conditions as described [13,21,22]. Briefly, stress treatments were performed as follows: cells were grown to mid-log phase (optical density at 600 nm 0.7), the stress was applied for 15 min, the cells were harvested by centrifugation and stored at −20 °C. The temperature shifts to 37 °C (heat shock) or to 15 °C (cold shock) were carried out by the addition of an equal volume of YPD prewarmed to 50 °C or chilled to 4 °C, respectively. The heat-shocked cultures were continued to grow for 15 min at 37 °C, and cold-shocked at 15 °C. The cultures were either supplemented with 1 M NaCl (high salt conditions), with 0.1 M Tris–HCl pH 8.3, resulting in a final pH of 7.9 (high pH conditions) or with 1 M citric acid (low pH conditions of pH 4.0). UV exposure was performed in a Stratalinker (Stratagene, La Jolla, CA, USA). Cells were grown to mid-log phase, then moved into Petri plates and exposed to 120 $J \cdot m^{-2}$ UV. Yeast were returned to a flask and continued to growth for further 15 min. To induce hyperosmotic shock, the cultures were supplemented with 1 M sorbitol. For hypoosmotic conditions, the cells were grown to mid-log phase in YPD supplemented with 1 M sorbitol, then collected by centrifugation, and resuspended in YPD without sorbitol. For amino acid and sugar starvation stresses, the cells were collected by centrifugation at mid-log phase, washed in starvation medium and further grown in medium lacking amino acids or sugar, respectively. In parallel, anaerobic and normal growth of *S. cerevisiae* was performed.

RNA isolation

LMW RNA (up to ~ 200 nt) were isolated from *S. cerevisiae* according to three different protocols: (a) MicroRNA isolation kit (A&A Biotechnology) following the manufacturers' protocol, (b) MasterPure™ Yeast Purification kit (Epicentre) combined with the enrichment of low molecular weight RNA with isopropanol and (c) bulk tRNA isolation method as previously described [25]. Additionally, total RNA was prepared as described in Thompson *et al.* [13]. The same biological material derived from a single yeast culture was subjected to all three isolation procedures.

MicroRNA isolation kit requires a phenol/chloroform extraction step and purification is based on silica matrix columns. 3×10^7 cells from mid-log culture were pelleted and treated with 800 μL of Fenozol. The lysed cells were incubated at 50 °C for 5 min. 200 μL of chloroform was added and left at the room temperature for 3 min. The probes were centrifuged for 10 min at 10 000 ***g*** and nucleic acids within the resulting supernatant were precipitated with 1/3 volume of isopropanol. This mixture was filtered through the silica columns by centrifugation for 1 min at 10 000 ***g***. High molecular weight (HMW) RNA remained bound to the columns. Low molecular weight (LMW) RNA from the flow through were precipitated with 2/3 volume of isopropanol and filtered through the silica columns by centrifugation for 1 min at 10 000 ***g***. LMW RNA were recovered from the columns with 50 μL of DEPC-treated water.

MasterPure™ Yeast Purification kit utilizes a simplified method for sample deproteinization: digestion of cell lysates with Proteinase K followed by a rapid desalting process to remove contaminating macromolecules [26]. This method does not require a phenol/chloroform extraction step nor column-based purifications. In this study, MasterPure kit procedure was combined with a differential isopropanol precipitation of low- and high molecular weight RNA; 3×10^7 cells from mid-log culture were pelleted and 300 μL of Extraction Reagent RNA containing the Proteinase K (50 μg) was added for RNA extraction and

incubated at 70 °C for 15 min. The samples were then placed on ice for 5 min and 175 μL of MPC Protein Precipitation Reagent was added to the lysed sample. Cell debris were pelleted by centrifugation for 10 min at 4 °C at 10 000 ***g***. HMW RNA was precipitated with the use of 1/3 volume of the isopropanol and then discarded. LMW RNA, which remained in the supernatant were precipitated with the use of 1 volume of isopropanol.

Bulk (unfractionated) tRNA from *S. cerevisiae* were prepared as previously described [25]. 3×10^7 cells from mid-log culture were pelleted and washed twice with a solution of 50 mM Na acetate pH 6.5, 10 mM $MgCl_2$, and 0.1 mM EDTA. The cell pellet was immediately resuspended in 10 volumes of the same buffer (410 μL). An equal volume of unbuffered phenol 90% (equilibrated with water, Sigma) was added and mildly shook at room temperature for 15 min. Under such mild phenol treatment, mainly the 'soluble' RNA (essentially tRNA, 5S-RNA and small cellular RNA) are released from the unbroken cells [23]. The mix was then centrifuged for 20 min at 16 000 ***g*** and nucleic acids from the recovered aqueous phase were ethanol precipitated. The nucleic acid pellet was dissolved in 200 μL of 50 mM Na acetate, pH 6.5, 10 mM $MgCl_2$, and 150 mM NaCl to which 12 M LiCl was added to reach 2 M final concentration in order to remove eventual contamination of ribosomal RNA resulting from the small fraction of cells that broke during phenol extraction (as signaled by the small amount of denatured proteins floating at the interphase of phenol:water). Following an incubation time of 1 h on ice, the insoluble ribosomal RNA was eliminated by centrifugation. Bulk 'soluble' RNA from supernatant (mainly tRNA, 5S RNA and small cellular RNA, as verified by electrophoresis) was recovered by ethanol precipitation.

Total RNA was prepared as previously described [13]. 3×10^7 cells from mid-log culture were pelleted and resuspended in 150 μL of LET (25 mM Tris/HCl pH 8, 100 mM LiCl, 20 mM EDTA) and 150 μL of phenol equilibrated with LET. The tubes were then vortexed for 5 min with acid-washed glass beads, after which 250 μL of phenol/chloroform equilibrated with LET and 250 μL of DEPC-treated water were added. The aqueous phase was extracted with phenol/chloroform, chloroform extracted and ethanol precipitated.

RNA quantity and quality

The RNA concentration and quality were first assessed using the NanoDrop ND-1000 spectrophotometer (NanoDrop Products, Wilmington, DE, USA). The sample purity was estimated by measuring the ratio of spectrophotometric absorbance (260 nm/280 nm). For a pure RNA sample, this ratio should be comprised between 1.8 and 2. LWM RNA were further analyzed with the Bioanalyzer 2100 using Agilent Small RNA kit (Agilent Technologies).

Quantitative reverse transcriptase PCR (qRT-PCR) assay

The induction of stresses was verified by quantification of the expression levels of stress-regulated genes: HSP12, GPD1, PDR12, and EXO1. Description of the genes is presented in Table 1. We have used 5S rRNA gene (RDN5) as a reference with constant expression. Reverse transcription reactions were carried out using a Superscript reverse transcriptase II (SS RT II) system (Invitrogen, Thermo Fisher Scientific, Waltham, MA, USA). Primers were used at a final concentration of 100 μM. Sequences of the primers are as follows: HSP12 Fwd 5′-TCTTCCAAGGTGTCCAC GAC-3′; HSP12 Rev 5′-TCGTTCAACTTGGACTTGGC -3′; GPD1 Fwd 5′-GGTTGGAAACATGTGGCTCT-3′; GPD1 Rev 5′-GGCAGGTTCTTCATTGGGTA-3′; PD R12 Fwd 5′-GTCGTTGAATCTGGTGAAATG-3′; PD R12 Rev 5′-AGACATCATTTCGCTTTGGTC-3′; EXO1 Fwd 5′-TGGTGATGCCATTCCAGTTA-3′; EXO1 Rev 5′-AACGGAGCCACTATGTACCG-3′; RDN5 Fwd 5′-AGA TTGCAGCACCTGAGTTT3′; RDN5 Rev 5′-GGTTGCG GCCATATCTACCA-3′. Quantitative PCRs (25 μL) were performed on aliquots of a reverse transcription reaction using Eva green system (Solis Biodyne, Tartu, Estonia). Datasets were collected on an Agilent real-time PCR system and analyzed using MAXPRO version 3.1 software (Honeywell, Louisville, KY, USA). The cycling conditions were as follows: 3 min at 95 °C, followed by 40 cycles consisting of 45 s at 94 °C, 30 s at 57 °C, and 20 s at 72 °C. Fluorescence signal data were collected during the 72 °C phase of each cycle. Melt curves from 56 °C to 95 °C (in 0.5 °C increments, measuring fluorescence at each temperature) were collected for all samples following the last cycle and showed the presence of only one product in each reaction. The standard curves were used to derive the copy number of each transcript in each RNA sample, which was determined in triplicate. Statistical analysis was performed using GraphPad Prism v5.01. Data were collected as triplicate from at least three independent experiments. The results were expressed as mean ± standard deviation (SD). Differences between the means of treatments were evaluated using one-way analysis of variance (ANOVA) followed by Tukey's test.

Specificity of the bulk tRNA isolation method

Cellular tRNA pool from *S. cerevisiae* was prepared with phenol/chloroform extraction method, purified with polyacrylamide gel electrophoresis and 5-[^{32}P]-end-labeled as previously described [21]. 20 000 cpm of the tRNA pool was added during the following steps of the bulk tRNA isolation procedure: (a) directly to the cell pellet; (b) to the unbuffered phenol before shaking; (c) to the aqueous phase after phenol extraction and (d) during removal of ribosomal RNA with LiCl. In each case bulk tRNA procedure

was completed according to the protocol. The resulting RNA was recovered by ethanol precipitation and separated with the use of polyacrylamide gel electrophoresis. The gels were exposed on the phosphor – storage intensity screen (Fujifilm, Tokyo, Japan) overnight. Screens were scanned with Fujifilm Fluorescent Image Analyzer FLA – 5100 and analyzed quantitatively with the densitometric program MULTI GAUGE IMAGE ANALYZER (Fujifilm).

Northern blot analysis

Twenty-five micrograms of LMW RNA or 50 μg of total RNA were separated on 12% denaturing polyacrylamide gels and electro transferred to the positively charged Amersham Hybond N^+ membrane using a semidry blotter (BioRad) for 45 min with 0.8 mA·cm^{-2} of the membrane. Nucleic acids were UV-cross-linked to the membranes, which were then used immediately for northern blot hybridization or stored at room temperature. tRNA fragments were detected with antisense 5-[^{32}P]-end-labeled DNA probes as previously described [21]. DNA oligonucleotide probes were synthesized by Genomed. The sequences as well as the hybridization temperature are presented in Table S1. Hybridization was carried out overnight in 30 mL of a buffer (178 mM Na_2HPO_4, 882 mM NaH_2PO4, 7% SDS) at specific hybridization temperature ($T_H = T_m$ – 10–15 °C) with gentle rotation. Two-step washing was performed after hybridization at T_H with rapid rotation: for 2 min in a washing solution I (2× SSC, 0.1% SDS) and for 1 min in a washing solution II (0.1× SSC, 0.1% SDS). The membranes were exposed on the phosphor – storage intensity screen (Fujifilm) overnight. Screens were scanned with Fujifilm Fluorescent Image Analyzer FLA – 5100 and analyzed quantitatively with the densitometric program MULTI GAUGE IMAGE ANALYZER.

The membranes were reused for up to five times for blotting with different probes. For that reason, the detachment of radioactive probes was performed. Membranes were placed in hybridization tubes and the buffer was added (0.2× SSC, 0.5% SDS). The procedure was performed for 30 min at 85 °C with rapid rotation.

Hybridizations of every DNA probe were repeated at least twice, but in most cases, three times to different membranes, which were derived from biological replicates. Since the measurements of repetitions were highly consistent (median of relative standard deviation of quantifications = 0.158%), we decided to use the mean values for subsequent analysis. Statistical analysis of the results has been performed using R statistical environment.

Acknowledgements

This work was supported by the Foundation for Polish Science [POMOST/2011-4/1 to KBŻ] and National Science Centre, Poland [2014/13/D/NZ1/00061 to KBŻ]. The work was also supported by the Polish Ministry of Science and Higher Education, under the KNOW program.

Author contributions

KBŻ planned experiments. KBŻ, AMM, MK and PM performed experiments. KBŻ, MŻ and TT analyzed data. KBŻ and MŻ wrote the paper.

References

1 Węgrzyn G and Węgrzyn A (2008) Is tRNA only a translation factor or also a regulator of other processes? *J Appl Genet* **49**, 115–122.
2 Dong J, Qiu H, Garcia-Barrio M, Anderson J and Hinnebusch AG (2000) Uncharged tRNA activates GCN2 by displacing the protein kinase moiety from a bipartite tRNA-binding domain. *Mol Cell* **6**, 269–279.
3 Hao S, Sharp JW, Ross-Inta CM, McDaniel BJ, Anthony TG, Wek RC, Cavener DR, McGrath BC, Rudell JB, Koehnle TJ *et al.* (2005) Uncharged tRNA and sensing of amino acid deficiency in mammalian piriform cortex. *Science* **307**, 1776–1778.
4 Hopper AK and Shaheen HH (2008) A decade of surprises for tRNA nuclear-cytoplasmic dynamics. *Trends Cell Biol* **18**, 98–104.
5 Raina M and Ibba M (2014) tRNAs as regulators of biological processes. *Front Genet* **11**, 5–171.
6 Gebetsberger J and Polacek N (2013) Slicing tRNAs to boost functional ncRNA diversity. *RNA Biol* **10**, 1798–17806.
7 Ivanov P, Emara MM, Villen J, Gygi SP and Anderson P (2011) Angiogenin-induced tRNA fragments inhibit translation initiation. *Mol Cell* **43**, 613–623.
8 Gebetsberger J, Zywicki M, Künzi A and Polacek N (2012) tRNA-derived fragments target the ribosome and function as regulatory non-coding RNA in *Haloferax volcanii*. *Archaea* **2012**, 260909.
9 Haussecker D, Huang Y, Lau A, Parameswaran P, Fire AZ and Kay MA (2010) Human tRNA-derived small RNAs in the global regulation of RNA silencing. *RNA* **16**, 673–695.
10 Loss-Morais G, Waterhouse PM and Margis R (2013) Description of plant tRNA-derived RNA fragments (tRFs) associated with argonaute and identification of their putative targets. *Biol Direct* **8**, 6.
11 Li Z, Ender C, Meister G, Moore PS, Chang Y and John B (2012) Extensive terminal and asymmetric processing of small RNAs from rRNAs, snoRNAs, snRNAs, and tRNAs. *Nucleic Acids Res* **40**, 6787–6799.
12 Drinnenberg IA, Weinberg DE, Xie KT, Mower JP, Wolfe KH, Fink GR and Bartel DP (2009) RNAi in budding yeast. *Science* **326**, 544–550.

13 Thompson DM and Parker R (2009) The RNase Rny1p cleaves tRNAs and promotes cell death during oxidative stress in *Saccharomyces cerevisiae*. *J Cell Biol* **185**, 43–50.
14 Yamasaki S, Ivanov P, Hu GF and Anderson P (2009) Angiogenin cleaves tRNA and promotes stress-induced translational repression. *J Cell Biol* **185**, 35–42.
15 Kumar P, Anaya J, Mudunuri SB and Dutta A (2014) Meta-analysis of tRNA derived RNA fragments reveals that they are evolutionarily conserved and associate with AGO proteins to recognize specific RNA targets. *BMC Biol* **1**, 12–78.
16 Thompson DM, Lu C, Green PJ and Parker R (2008) tRNA cleavage is a conserved response to oxidative stress in eukaryotes. *RNA* **14**, 2095–2103.
17 Kim YK, Yeo J, Kim B, Ha M and Kim VN (2012) Short structured RNAs with low GC content are selectively lost during extraction from a small number of cells. *Mol Cell* **46**, 893–895.
18 Monleau M, Bonnel S, Gostan T, Blanchard D, Courgnaud V and Lecellier CH (2014) Comparison of different extraction techniques to profile microRNAs from human sera and peripheral blood mononuclear cells. *BMC Genom* **15**, 395.
19 Li Y and Kowdley KV (2012) Method for microRNA isolation from clinical serum samples. *Anal Biochem* **431**, 69–75.
20 Podolska A, Kaczkowski B, Litman T, Fredholm M and Cirera S (2011) How the RNA isolation method can affect microRNA microarray results. *Acta Biochim Pol* **58**, 535–540.
21 Zywicki M, Bakowska-Zywicka K and Polacek N (2012) Revealing stable processing products from ribosome-associated small RNAs by deep-sequencing data analysis. *Nucleic Acids Res* **40**, 4013–4024.
22 Causton HC, Ren B, Koh SS, Harbison CT, Kanin E, Jennings EG, Lee TI, True HL, Lander ES and Young RA (2001) Remodeling of yeast genome expression in response to environmental changes. *Mol Biol Cell* **12**, 323–337.
23 Gasch AP, Spellman PT, Kao CM, Carmel-Harel O, Eisen MB, Storz G, Botstein D and Brown PO (2000) Genomic expression programs in the response of yeast cells to environmental changes. *Mol Biol Cell* **11**, 4241–4257.
24 Masaki H and Ogawa T (2002) The modes of action of colicins E5 and D, and related cytotoxic tRNases. *Biochimie* **84**, 433–438.
25 Monier R, Stephenson ML and Zamenick PC (1960) The preparation and some properties of a low molecular weight ribonucleic acid from baker's yeast. *Biochim Biophys Acta* **9**, 1–8.
26 Miller SA, Dykes DD and Polesky HF (1988) A simple salting out procedure for extracting DNA from human nucleated cells. *Nucleic Acids Res* **16**, 1215.
27 Praekelt UM and Meacock PA (1990) HSP12, a new small heat shock gene of *Saccharomyces cerevisiae*: analysis of structure, regulation and function. *Mol Gen Genet* **223**, 97–106.
28 Hirayama T, Maeda T, Saito H and Shinozaki K (1995) Cloning and characterization of seven cDNAs for hyperosmolarity-responsive (HOR) genes of *Saccharomyces cerevisiae*. *Mol Gen Genet* **249**, 127–138.
29 Siderius M, Rots E and Mager WH (1997) High-osmolarity signalling in *Saccharomyces cerevisiae* is modulated in a carbon-source-dependent fashion. *Microbiology* **143**, 3241–3250.
30 Sales K, Brandt W, Rumbak E and Lindsey G (2000) The LEA-like protein HSP 12 in *Saccharomyces cerevisiae* has a plasma membrane location and protects membranes against desiccation and ethanol-induced stress. *Biochim Biophys Acta* **1463**, 267–278.
31 Stone RL, Matarese V, Magee BB, Magee PT and Bernlohr DA (1990) Cloning, sequencing and chromosomal assignment of a gene from *Saccharomyces cerevisiae* which is negatively regulated by glucose and positively by lipids. *Gene* **96**, 171–176.
32 Albertyn J, Hohmann S, Thevelein JM and Prior BA (1994) GPD1, which encodes glycerol-3-phosphate dehydrogenase, is essential for growth under osmotic stress in *Saccharomyces cerevisiae*, and its expression is regulated by the high-osmolarity glycerol response pathway. *Mol Cell Biol* **14**, 4135–4144.
33 Piper P, Mahé Y, Thompson S, Pandjaitan R, Holyoak C, Egner R, Mühlbauer M, Coote P and Kuchler K (1998) The pdr12 ABC transporter is required for the development of weak organic acid resistance in yeast. *EMBO J* **17**, 4257–4265.
34 Qiu J, Guan MX, Bailis AM and Shen B (1998) *Saccharomyces cerevisiae* exonuclease-1 plays a role in UV resistance that is distinct from nucleotide excision repair. *Nucleic Acids Res* **26**, 3077–3083.

Supporting information

Additional Supporting Information may be found online in the supporting information tab for this article:

Table S1. Sequences of antisense DNA probes used in this study. Hybridization temperature is indicated (T_H).

Fig. S1. tRNA-derived fragments in *Saccharomyces cerevisiae*.

Supporting material

The widespread occurrence of tRNA-derived fragments in *Saccharomyces cerevisiae*

Kamilla Bąkowska-Żywicka[1*], Anna M. Mleczko[1], Marta Kasprzyk[1], Piotr Machtel[1], Marek Żywicki[2], and Tomasz Twardowski[1]

[1]Institute of Bioorganic Chemistry Polish Academy of Sciences, Noskowskiego 12/14, 61-704 Poznan, Poland

[2] Department of Computational Biology, Institute of Molecular Biology and Biotechnology, Faculty of Biology A. Mickiewicz University in Poznan, Umultowska 89, 61-614 Poznan, Poland

* To whom correspondence should be addressed. Tel: +48/618528503; Fax: +48/6185280532; Email: bakowska@ibch.poznan.pl

Table S1. Sequences of antisense DNA probes used in this study. Hybridization temperature is indicated (T_H).

tRNA isotype	5'-probe sequence	T_H	3'-probe sequence	T_H
$tRNA^{Ala}$ (AGC)	AGGGAGCGCGCTACCGACTACGCCACACGCCC	55ºC	TTGGACGAGTCCGGAATCGAACCGGAGACC	55ºC
$tRNA^{Ala}$ (TGC)	GGGAAGCGCGCTACCAACTGCGCCATGTGCCC	45ºC	TTGGACGCAACCGGAATCGAACCGATGACC	45ºC
$tRNA^{Arg}$ (ACG)	TGACCATTGGGCCACGAGGA	45ºC	CCCCGCCAGGACTCGAACCTGGAATC	55ºC
$tRNA^{Arg}$ (CCG)	GAATGCATGCTAACCATTGCACTAGAGGAGC	50ºC	TCCTCCCGGGACTCGAACCCGGATC	55ºC
$tRNA^{Arg}$ (CCT)	GGGAGACGCGTTACCATTACGCCAACGGAAC	55ºC	TCCGTACGGGACTCGAACCCGCAGT	50ºC
$tRNA^{Arg}$ (TCT)	GTCAGACGCGTTGCCATTACGCCACGCGAGC	55ºC	CGATGGGGGTCGAACCCATAATCTT	45ºC
$tRNA^{Asn}$ (GTT)	GCACGCCTTAACCAACTTGGCCATGGAGTC	50ºC	CGACCCCAGTGAGGGTTGAACTCACGATCTTGCGAT	45ºC
$tRNA^{Asp}$ (GTC)	GCGCCCATTCTGACCATTAAAC	42ºC	GGCTCCGCGACGGGGAATTGAACCCCG	55ºC
$tRNA^{Cys}$ (GCA)	GCGCTACCACTGCGCCATACGAGC	50ºC	CGCACTCAGGATCGAACTAAGGACC	50ºC
$tRNA^{Gln}$ (CTG)	CCGAAAGTGATAACCACTACACTATAGGAC	50ºC	TCCCACCCGGATTCGAACTGGGG	50ºC
$tRNA^{Gln}$ (TTG)	CCGAAAGTGATAACCACTACACTATAAAAC	42ºC	TCTTACCCGGATTCGAACCGGGG	42ºC
$tRNA^{Glu}$ (CTC)	CGTGATGTGATAGCCGTTACACTACATCGG	50ºC	GGCTCCGAAGCGGGGAGTCGAACCCCGG	55ºC
$tRNA^{Glu}$ (TTC)	CGTGATGTGATAGCCGTTACACTATATCGG	50ºC	GGCTCCGCTACGGGGAGTCGAACCCCGG	55ºC
$tRNA^{Gly}$ (CCC)	AACCACTGAACCACTTTCGC	42ºC	GAAGCCGGGAATCGAAC	42ºC
$tRNA^{Gly}$ (GCC)	TACCACTAAACCACTTGCGC	42ºC	CAAGCCCGGAATCGAAC	42ºC
$tRNA^{Gly}$ (TCC)	AACCACTACACTAACCGCCC	42ºC	GAGCGGTACGAGAATCGAAC	42ºC
$tRNA^{His}$ (GTG)	TGTGTACTAACCACTATACTAAGATGG	45ºC	AGAATCGAACCAGGGTTTCA	60ºC
$tRNA^{Ile}$ (AAT)	GCCTTAACCAACTGGGCCAAGAGACC	50ºC	TGGTCTCTAGCGGGATCG	42ºC
$tRNA^{Ile}$ (TAT)	CGAAGCTCTAACCACTGAGCTACACGAGC	50ºC	ATTGAACCCACGACGGTCGCGT	45ºC
$tRNA^{Leu}$ (CAA)	TGAATCAGGCGCCTTAGACCGCTCGGCC	55ºC	GGTTGCTAAGAGATTCGAACTCTTGCATCT	50ºC
$tRNA^{Leu}$ (GAG)	TCGACCTGACGCCTTAGACCACTCGGCC	55ºC	GATACCCGCGGGGTTTGAACCCGCGCCTCC	55ºC
$tRNA^{Leu}$ (TAA)	TAAGTCTGCCGCCTTAGACCACTCGGCC	55ºC	GAAGGATGCGAGGTTCGAACTCGCGCGGAC	42ºC
$tRNA^{Leu}$ (TAG)	TAAATCTGACGCCTTAAACCACTCGGCC	50ºC	GAGAGCTAAGGGATTCGAACCCTTGCATCC	50ºC
$tRNA^{Lys}$ (CTT)	CGCGCTACCGATTGCGCCAACAAGGC	55ºC	GGCTCGAACCCCTAACCTT	42ºC
$tRNA^{Lys}$ (TTT)	GCCGAACGCTCTACCAACTGAGC	45ºC	CTCCTCATAGGGGGCTCGAACCCC	50ºC
$tRNA^{Met}$ (CAT)	CTGACGCTCTTCCTACTGAGCTACTGAAGC	50ºC	TGCTCCAGGGGAGGTTCGAACTCTCGACCTTCAG	55ºC
$tRNA^{Phe}$ (GAA)	CTCTCCCAACTGAGCTAAATCCG	45ºC	TGCGAATTCTGTGGATCGAACACAGGACC	50ºC
$tRNA^{Pro}$ (AGG)	CGAGAATCATACCTCTAGACCACACGCCC	50ºC	CGAGCCGGGACTCGAACCCGGG	55ºC
$tRNA^{Pro}$ (TGG)	CGAGAATCATACCACTAGACCACACGCCC	50ºC	CGAGCTGGGAATTGAACCCAGG	45ºC
$tRNA^{Ser}$ (AGA)	CGCCTTAACCACTCGGCCAAGTTGCC	50ºC	ACAACTGCAGGACTCGAACC	42ºC
$tRNA^{Ser}$ (CGA)	CGCCTTAACCACTCGGCCATAGTGCC	50ºC	CGACACCAGCAGGATTTGAACCAGCG	50ºC
$tRNA^{Ser}$ (GCT)	CGCCTTAACCACTCGGCCACTGGGAC	55ºC	CGTCACAGACAGGATTCGAACCTGCG	50ºC
$tRNA^{Thr}$ (AGT)	GCCTTACCAACTTGGCCATA	42ºC	TTGAACCGATGATCTCCACA	42ºC
$tRNA^{Thr}$ (CGT)	AGTGCGATGCCTTACCACTTGGCC	45ºC	CTGTGGGAATTGAACCCACGATCCCCGC	55ºC
$tRNA^{Thr}$ (TGT)	ACAAGTGCAACGCTCTACCA	42ºC	GAATTGAACTAACGACCTTTGC	42ºC
$tRNA^{Trp}$ (CCA)	GCTCTACCATTGAGCCACCGCTTC	50ºC	TGAAACGGACAGGAATTGAACC	42ºC
$tRNA^{Tyr}$ (GTA)	GCGCCTTAAACCAACTTGGCTACCGAGAG	50ºC	TCTCCCGGGGGCGAGTCG	45ºC
$tRNA^{Val}$ (AAC)	GCCATAACCGACTAGACCACGAAAC	50ºC	ATTTCGCCCAGGAACGAACTGGGGACG	42ºC
$tRNA^{Val}$ (CAC)	CGTGATAGCCGCTACACTATTGGAAC	50ºC	GTTCCAACCGAGGATCGAACTCGGGACC	50ºC
$tRNA^{Val}$ (TAC)	CTTGAACCACTGGACCATTGGACC	50ºC	GATCCAACCGAGGTTCGAACTCGGGATC	50ºC

Figure S1. tRNA-derived fragments in *Saccharomyces cerevisiae*.

Detection of 3'- and 5'-derived tRNA fragments visualized by northern blot hybridization assays. Numbers correspond to the RNA samples derived from *S. cerevisiae* grown under the following conditions: 1- heat stress, 2 – cold stress, 3 – high salinity, 4 – UV treatment, 5 – anaerobic growth, 6 – optimal conditions, 7 – high pH, 8 – low pH, 9 – amino acid starvation, 10 – sugar starvation, 11- hypoosmotic conditions, 12 – hyperosmotic conditions.

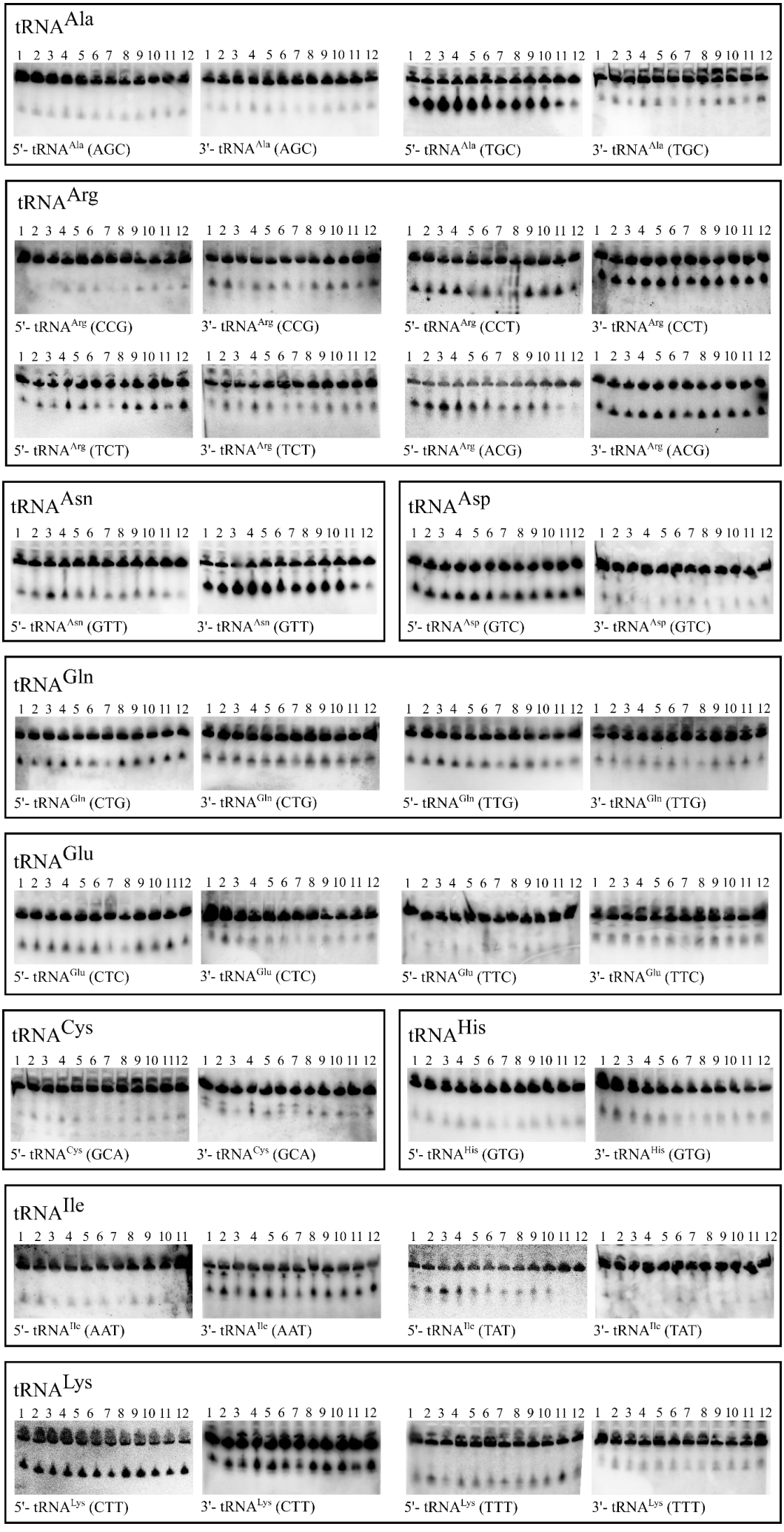
tRNA^Ala
1 2 3 4 5 6 7 8 9 10 11 12
5'- tRNA^Ala (AGC)
3'- tRNA^Ala (AGC)
5'- tRNA^Ala (TGC)
3'- tRNA^Ala (TGC)
tRNA^Arg
5'- tRNA^Arg (CCG)
3'- tRNA^Arg (CCG)
5'- tRNA^Arg (CCT)
3'- tRNA^Arg (CCT)
5'- tRNA^Arg (TCT)
3'- tRNA^Arg (TCT)
5'- tRNA^Arg (ACG)
3'- tRNA^Arg (ACG)
tRNA^Asn
5'- tRNA^Asn (GTT)
3'- tRNA^Asn (GTT)
tRNA^Asp
5'- tRNA^Asp (GTC)
3'- tRNA^Asp (GTC)
tRNA^Gln
5'- tRNA^Gln (CTG)
3'- tRNA^Gln (CTG)
5'- tRNA^Gln (TTG)
3'- tRNA^Gln (TTG)
tRNA^Glu
5'- tRNA^Glu (CTC)
3'- tRNA^Glu (CTC)
5'- tRNA^Glu (TTC)
3'- tRNA^Glu (TTC)
tRNA^Cys
5'- tRNA^Cys (GCA)
3'- tRNA^Cys (GCA)
tRNA^His
5'- tRNA^His (GTG)
3'- tRNA^His (GTG)
tRNA^Ile
5'- tRNA^Ile (AAT)
3'- tRNA^Ile (AAT)
5'- tRNA^Ile (TAT)
3'- tRNA^Ile (TAT)
tRNA^Lys
5'- tRNA^Lys (CTT)
3'- tRNA^Lys (CTT)
5'- tRNA^Lys (TTT)
3'- tRNA^Lys (TTT)

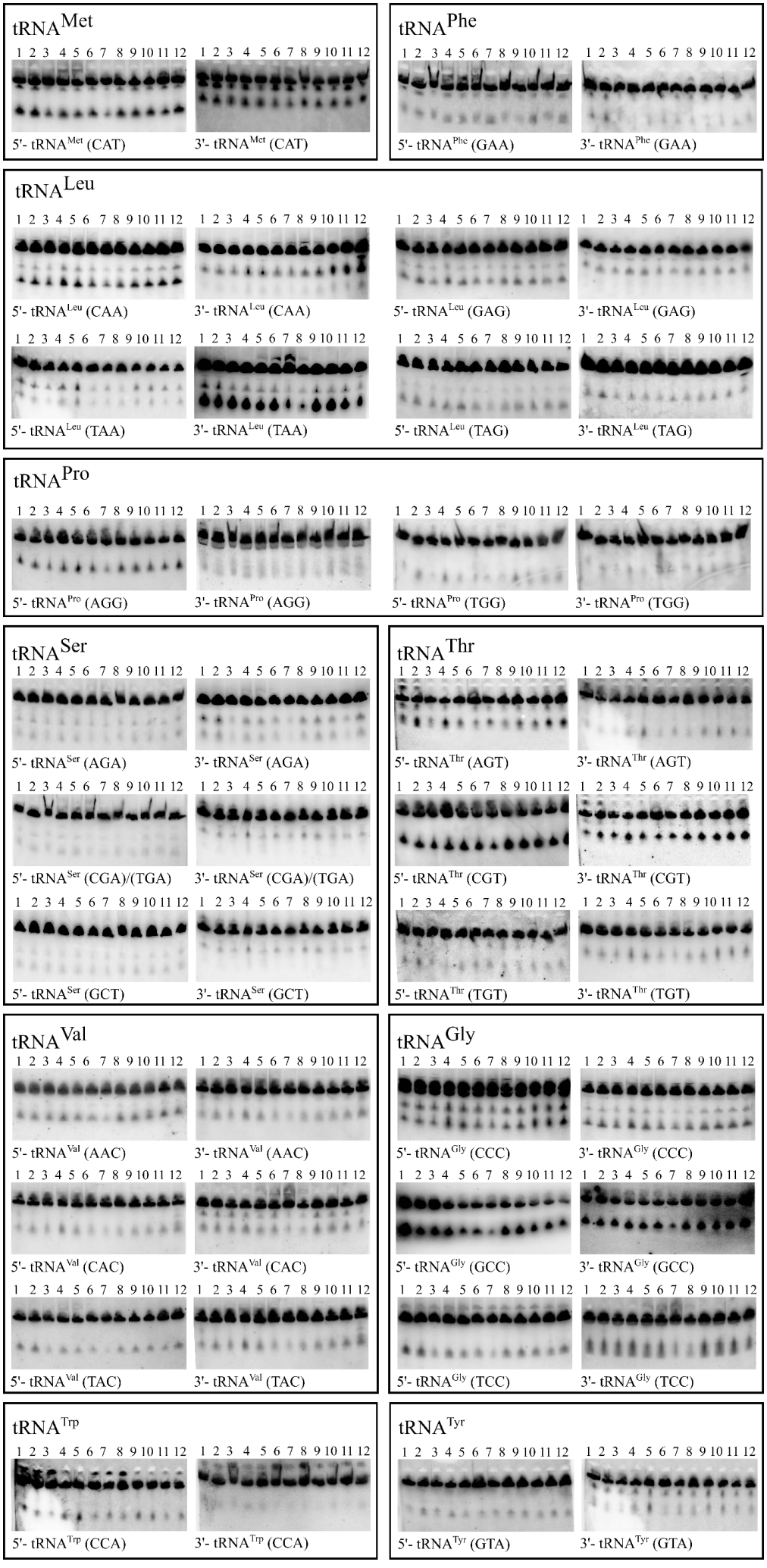
tRNA Met
1 2 3 4 5 6 7 8 9 10 11 12
5'- tRNA Met (CAT)
3'- tRNA Met (CAT)
tRNA Phe
5'- tRNA Phe (GAA)
3'- tRNA Phe (GAA)
tRNA Leu
5'- tRNA Leu (CAA)
3'- tRNA Leu (CAA)
5'- tRNA Leu (GAG)
3'- tRNA Leu (GAG)
5'- tRNA Leu (TAA)
3'- tRNA Leu (TAA)
5'- tRNA Leu (TAG)
3'- tRNA Leu (TAG)
tRNA Pro
5'- tRNA Pro (AGG)
3'- tRNA Pro (AGG)
5'- tRNA Pro (TGG)
3'- tRNA Pro (TGG)
tRNA Ser
5'- tRNA Ser (AGA)
3'- tRNA Ser (AGA)
5'- tRNA Ser (CGA)/(TGA)
3'- tRNA Ser (CGA)/(TGA)
5'- tRNA Ser (GCT)
3'- tRNA Ser (GCT)
tRNA Thr
5'- tRNA Thr (AGT)
3'- tRNA Thr (AGT)
5'- tRNA Thr (CGT)
3'- tRNA Thr (CGT)
5'- tRNA Thr (TGT)
3'- tRNA Thr (TGT)
tRNA Val
5'- tRNA Val (AAC)
3'- tRNA Val (AAC)
5'- tRNA Val (CAC)
3'- tRNA Val (CAC)
5'- tRNA Val (TAC)
3'- tRNA Val (TAC)
tRNA Gly
5'- tRNA Gly (CCC)
3'- tRNA Gly (CCC)
5'- tRNA Gly (GCC)
3'- tRNA Gly (GCC)
5'- tRNA Gly (TCC)
3'- tRNA Gly (TCC)
tRNA Trp
5'- tRNA Trp (CCA)
3'- tRNA Trp (CCA)
tRNA Tyr
5'- tRNA Tyr (GTA)
3'- tRNA Tyr (GTA)

2

Mleczko AM, Celichowski P, Bąkowska-Żywicka K

Transfer RNA-derived fragments target and regulate ribosome-associated aminoacyl-transfer RNA synthetases

Biochimica et Biophysica Acta – Gene Regulatory Mechanisms, 2018, 1861(7): 647-656

BBA - Gene Regulatory Mechanisms 1861 (2018) 647–656

Contents lists available at ScienceDirect

BBA - Gene Regulatory Mechanisms

journal homepage: www.elsevier.com/locate/bbagrm

Transfer RNA-derived fragments target and regulate ribosome-associated aminoacyl-transfer RNA synthetases

Anna M. Mleczko, Piotr Celichowski[1], Kamilla Bąkowska-Żywicka*

Institute of Bioorganic Chemistry Polish Academy of Sciences, Noskowskiego St. 12/14, 61-704 Poznan, Poland

ARTICLE INFO

Keywords:
tRNA-derived fragments
Ribosome-associated ncRNA
Regulation of translation
Ribosome
Aminoacyl-tRNA synthetase

ABSTRACT

Ribosome-associated noncoding (ranc) RNAs are a novel class of short regulatory RNAs with functions and origins that have not been well studied. In this present study, we functionally characterized the molecular activity of *Saccharomyces cerevisiae* transfer RNA (tRNA)-derived fragments (tRFs) during protein biosynthesis. Our results indicate ribosome-associated tRFs derived from both 5′ (ranc-5′-tRFs) and 3′-part of tRNAs (ranc-3′-tRFs) have regulatory roles during translation. We demonstrated five 3′-tRFs and one 5′-tRF associate with a small ribosomal subunit and aminoacyl-tRNA synthetases (aa-RSs) in yeast. Furthermore, we discovered that four yeast aa-RSs interact directly with yeast ribosomes. tRFs interactions with ribosome-associated aa-RSs correlate with impaired efficiency of tRNA aminoacylation.

1. Introduction

Ribosomes are unique cellular machines responsible for synthesizing proteins in all living organisms. Because proper functioning of ribosomes is crucial, cells have methods of precisely regulating translation. Proteomic studies on *Saccharomyces cerevisiae* ribosomes identified 77 ribosome-associated proteins, where these direct interactions with ribosomes may modulate their activity. Cells lacking some of these proteins have defects in the rate and fidelity of protein synthesis, as well as ribosome biogenesis [1]. Conversely, DNA and RNA oligonucleotides complementary to selected ribosomal RNA (rRNA) sequences modulate protein biosynthesis at different stages of translation, which is reviewed in [2, 3]. Recently, multiple short and long ribosome-associated noncoding RNAs (rancRNAs) have been identified in organisms in all 3 domains of life, which is reviewed in [4]. Several rancRNAs and the mechanism of action of their regulation of protein biosynthesis have already been characterized. This includes mRNA-derived rancRNA_18 in *S. cerevisiae* [5], 16S rRNA-derived fragment in *Escherichia coli* [6], and tRNA-derived fragments (tRFs) in archaeon *Haloferax volcanii* [7, 8] and *S. cerevisiae* [9]. These tRFs, as well as a distinct class of tRNA-derived noncoding RNAs (ncRNAs), designated tRNA halves, have been especially well recognized recently due to their widespread presence in multiple organisms. Furthermore, tRFs and tRNA halves have expression patterns, abundances, subcellular localizations, and biological roles that are distinct from their parental tRNA molecules, as reviewed in [10–15]. To date, tRNA-derived small RNAs have been reported to be involved in regulation of translation, viral infections, and carcinogenesis. In several organisms, tRFs regulate gene-expression using microRNA (miRNA)-like pathways through interactions with Argonaute proteins [16–18]. It is now generally accepted that miRNAs are generated from pre-existing tRNAs [16–18]. Moreover, it is believed that, due to frequent misannotation when cross-mapping tRFs and tRNA-derived miRNAs during deep sequencing data analysis, an accurate frequency of tRNA-derived miRNAs has yet to be determined.

Although many studies have shown that tRNA is processed into shorter, stable forms in a broad range of species, the molecular functions of non-miRNA-like tRFs remain largely unexplored with only a few exceptions. In breast cancer cells, tRFs act on a post-transcriptional level, where they decrease the stability of multiple oncogenic transcripts by displacing their 3' UTRs from the RNA-binding protein YBX1 [19]. Sex hormone-dependent tRNA-derived RNAs enhance breast and prostate cancer cell proliferation [20]. Recently, two studies characterized the epigenetic functions of tRNA-derived small RNAs in mouse sperm. Chen et al. observed that injection of sperm tRFs obtained from high-fat diet males into normal zygotes caused metabolic disorders in the offspring and altered expression of metabolic pathway genes in early embryos and islets [21]. In addition, Sharma et al. linked tRFs to the regulation of endogenous MERVL retroelements active in preimplantation embryos [22].

Strikingly, tRFs have been shown to be regulators of protein biosynthesis from even the first tRF studies. One possible mechanism of tRF-dependent regulation of translation was observed in U2OS cells,

* Corresponding author.
E-mail address: bakowska@ibch.poznan.pl (K. Bąkowska-Żywicka).
[1] Present address: Department of Histology and Embryology, Poznan University of Medical Sciences, Poznan, Poland.

https://doi.org/10.1016/j.bbagrm.2018.06.001
Received 3 November 2017; Received in revised form 2 June 2018; Accepted 2 June 2018
Available online 06 June 2018

where selected angiogenin-induced 5′-tRNA halves inhibit translation at the initiation step by displacing the cap-binding complex eIF4F from capped mRNAs [23]. Translationally active tRFs assemble unique G-quadruplex structures required for inhibition of translation [24]. In addition, tRFs derived from the 5′ end of tRNAs inhibit protein translation without requiring complementary target sites in the corresponding mRNAs [25]. In *Haloferax volcanii*, the 5′- derived Val-tRF, produced extensively under alkaline stress, binds to the small ribosomal subunit *in vitro* and *in vivo* [7] and affects translation by competing with mRNA within the small ribosomal subunit [8]. Interestingly, Keam et al. reported in 2017 that 5′-tRFs interact with the mammalian multi-synthetase complex, which increases the efficiency of ribosomal protein biosynthesis [26]. The authors suggested that such stimulation of translation is potentially caused by inactivation or suppression of transcriptional precursors followed by degradation and transcriptional reactivation. Together, these results implicate the involvement of 5′-tRFs in newly discovered mechanisms of gene expression regulation at a translational level; however, the molecular details of this mechanism are still elusive.

Almost all functional studies of tRFs have focused on 5′-part tRNA-derived RNAs. Moreover, nearly all functionally characterized 3′-tRFs associate with components of RNA interference machinery and/or exert miRNA-like functions. We have therefore we aimed to functionally characterize 3′-tRNA-derived small RNAs in the model organism *Saccharomyces cerevisiae*, a species which lacks miRNA machinery. Our recent studies in *S. cerevisiae* have shown that processing of tRNA molecules is widespread in a number of growth conditions (27) and that both tRF binding to ribosomes and subsequent inhibition of translation are stress-dependent [9]. Here, we provide evidence that five 3′-tRFs and one 5′-tRF in yeast target small ribosomal subunits and aminoacyl-tRNA synthetases. Moreover, we discovered direct interactions between yeast ribosomes and several aminoacyl-tRNA synthetases (aa-RSs). Consequently, tRF binding to ribosome-associated aa-RSs results in inhibition of *in vitro* translation by affecting tRNA aminoacylation.

2. Materials and methods

2.1. Fragments derived from tRNAs

Based on our previous screens for ribosome-associated ncRNAs, tRFs were chosen for further study [28]. The 6 tRFs we focused on had robust read coverages of over 40 reads in the rancRNA library. Of these tRFs, 5 were derived from the 3′-part of the corresponding tRNAs and one was from the 5′-part. RNA oligonucleotides were chemically synthetized. Sequences of the oligonucleotides are as follows: 3′-tRF-His (GTG), 5′-GAUGAAACCCUGGUUCGAUUCUAGGAGAUG-3′; 3′-tRF-Ser (AGA), 5′-GGUUCGAGUCCUGCAGUUGU-3′; 3′-tRF-Gly (GCC), 5′-CAUCGUUGGGCCCCCGGUUCGAUUCCGGGCUUGCGCA-3′; 3′-tRF-Leu (TAA), 5′-UUGUCCGCGCGAGUUCGAACCUCGCAUCCUUCA-3′; 3′-tRF-Thr (TGT), 5′-GCAAAGGUCGUUAGUUCAUUUCUGACAGGUGGCA-3′; 5′-tRF-His (GTG), 5′-GCCAUCUUAGUAUAGUGGUUAGUACACAU-3′. A control oligomer, scrambled 3′-tRF-Thr (TGT) has been designed to reflect the mean nucleotide composition of all tested tRFs: scr-3′-tRF-Thr (TGT), 5′-AUAGGCCAUAAGGAGUCUCGGUACGUCUUGUAUG-3′. Predicted secondary structure of tested tRFs is presented in Supplementary Fig. 1.

2.2. Strains and growth conditions

A *Saccharomyces cerevisiae* wild-type strain BY4741 (MATα; his3Δ 1; leu2Δ0; met15Δ0; ura3Δ0) was grown in YPD medium at 30 °C. MATα BY4741 strains overexpressing aa-RS obtained from the ThermoScientific Yeast GST Fusion Collection were grown on synthetic complete medium supplemented with 2% galactose.

2.3. Polysome profiling

Polysome profiling was performed as described in [29] with slight modifications. First, 300 ml of *S. cerevisiae* cell culture was grown to mid-exponential phase (OD_{600} of 0.8). Next, 500 μg/ml cycloheximide (f.c.) was added to the culture 15 min before harvest. Cell debris was precipitated by centrifuging at 11300 × *g* for 2 min at 4 °C. Lysates were clarified by centrifuging at 11300 × *g* for 10 min at 4 °C. Approximately 30 A_{260} units of cell lysate (1 ml) were loaded onto a linear 8–40% sucrose gradient. The gradients were centrifuged in a Beckman SW40 Ti rotor at 39000 rpm for 2.5 h at 4 °C. Sucrose gradients were analyzed by continuously monitoring absorbance at A_{254} with a UV detector.

2.4. Northern blot analysis

RNA pools isolated from fractions obtained as described from polysome profiling were separated on 12% denaturing polyacrylamide gels and electrotransferred as previously described [27]. The following DNA oligonucleotides were used as antisense probes: 5′-TGTGTACTAACCACTATACTAAGATGG-3′ for 5′-tRF-His (GTG); 5′-AGAATCGAACCAGGGTTTCA-3′ for 3′-tRF-His (GTG); 5′-ACAACTGCAGGACTCGAACC-3′ for 3′-tRF-Ser (AGA); 5′-CAAGCCCGGAATCGAAC-3′ for 3′-tRF-Gly (GCC); 5′-GAAGGATGCGAGGTTCGAACTCGCGCGGAC-3′ for 3′-tRF-Leu (TAA); 5′-GAATTGAACTAACGACCTTTGC-3′ for 3′-tRF-Thr (TGT). For each probe, northern blot hybridizations were performed in duplicate using different membranes and standard error (SE) has been calculated.

2.5. Ribosome and post-ribosomal supernatant isolation

Yeast ribosomes were prepared as described previously [30] with modifications. Cell debris was precipitated by centrifuging at 27000 × g for 15 min at 4 °C. Lysates were clarified by centrifuging at 30000 × g for 20 min at 4 °C. Ribosomes were then pelleted from the lysates by centrifuging at 100000 × g for 2 h at 4 °C (P100). The top two-thirds of the post-ribosomal supernatant were collected and frozen, and designated as the S100 fraction. The purity of P100 and S100 fraction was verified with Agilent Bioanalyzer 2100 with the use of RNA Nano 6000 kit.

2.6. Isolation of ribosomal subunits

Yeast ribosomal subunits were prepared as described in [31] with modifications. An equal volume of glass beads (400 μm in diameter) was added to the cells and cells were broken by vortexing in 8 pulses of 30 s with 1 min cooling on ice between pulses. Cell debris was precipitated by centrifuging at 11300 x g for 2 min at 4 °C. Lysates were clarified by centrifuging at 11300 × g for 10 min at 4 °C. In order to chelate metal ions necessary for subunit interactions, approximately 30 A_{260} units of cell lysate (1 ml) were mixed with EDTA to a final concentration of 50 mM. Afterwards, lysates were loaded onto linear 5–20% sucrose gradients, which were centrifuged in a Beckman SW40 rotor at 39000 rpm for 2.5 h at 4 °C. Sucrose gradients were analyzed by continuously monitoring absorbance at A_{254} with a UV detector.

2.7. In vitro association assays

Non-covalent binding of tRFs to *S. cerevisiae* 80S ribosomes and ribosomal 60S and 40S subunits was measured using an “association assay” performed as described in [9]. Association measurements were performed in triplicate and standard error (SE) has been calculated. The values reported were corrected against control samples lacking ribosomes, which were typically 1 to 3% of the total counts of when a probe was applied.

2.8. Metabolic labeling

Yeast spheroplasts were prepared from a 50 ml culture grown to an OD_{600} of 0.8 by adding 350 U of zymolyase (Zymo Research) and incubating at 30 °C for 25–30 min as previously described [5]. Spheroplasts (115 µl) were combined with 10 pmol synthetic tRFs and electroporated (1500 V, 25 µF, and 200 Ω) using a BioRad Micro Pulser. For a control, translation was inhibited by adding 7.5 µg/µl cycloheximide to the spheroplasts. Subsequent to electroporation, 1 ml YPD supplemented with 1 M sorbitol was added to the spheroplasts and the reaction was transferred into a 1.5 ml Eppendorf tube. Next, 450 µl of the sample was incubated at 30 °C for 15 min before adding 1 µl ^{35}S-methionine (1000 Ci/mmol, 10 mCi/ml) and incubating for an additional 1 h. Labeled proteins were precipitated by adding 1 ml 20% (f.c.) trichloroacetic acid and incubating at 95 °C for 20 min. This solution was then filtered through a glass-fiber filter and quantified by liquid scintillation counting. Metabolic labeling measurements were performed at least in triplicate and standard error (SE) has been calculated. *p*-value has been calculated using *t*-test.

2.9. In vitro translation

S. cerevisiae cell-free extracts were prepared as previously described in [32] with modifications. To prepare *S. cerevisiae* S30 extract, 1.5 l of yeast culture was grown to a final OD_{600} of 1.5 at 30 °C in YPD medium. Cells were lysed by adding glass beads (400 µm in diameter) and performing ten-1 min cycles of handshaking (approximately 2 Hz over 50 cm hand patch). To remove the glass beads, the lysates were centrifuged at 4000 ×*g* for 1 min at 4 °C, transferred to a fresh tube, and centrifuged at 30000 ×*g* for 7 min at 4 °C. The resulting S30 supernatant was purified on a G-50 Sephadex column, aliquoted, and snap-frozen in liquid nitrogen.

For *in vitro* translation assays, 2.5 µl creatine phosphokinase (10 mg/ml, Roche), 7.5 µl $CaCl_2$ (20 mM), 25 µl 10× translation cocktail (100 mM HEPES/KOH [pH 7.5], 10 mM $MgAc_2$, 760 mM KCl, 4 mM GTP, 10 mM ATP, and 19 amino acids at 500 µM, where methionine was excluded), 5 µl creatine phosphate (0.6 M, Roche), and 2.5 µl $MgAc_2$ (100 mM) were mixed with 150 µl S30 and 16 µl ^{35}S-methionine (1000 Ci/mmol and 10 mCi/ml, respectively). The resulting translation mix was split into 12 µl aliquots, sterile H_2O, synthetic RNA (10–250 pmol), or cycloheximide (7.5 µg/µl) was added to reach a final volume of 15 µl, and the mixtures were incubated at 23 °C for 30 min. The labeled proteins were precipitated by adding 1 ml 20% TCA and incubating at 95 °C for 20 min. The labeled proteins were then filtered through a glass-fiber filter and quantified by liquid scintillation counting. All measurements were performed at least in triplicate and standard error (SE) has been calculated. *p*-value has been calculated using *t*-test.

In vitro translation reactions were performed in wheat germ (Promega), rabbit reticulocyte (Promega), and human (Pierce Human *In Vitro* Protein Expression Kit, Fisher Scientific) systems according to the manufacturers' instructions. The reactions were incubated for 90 min. at 25 °C (wheat germ extract) or at 30 °C (rabbit reticulocyte and human systems). In all cases, an uncapped *in vitro*-transcribed luciferase mRNA containing a 30-base poly(A) tail was used as a template. ^{35}S-labeled proteins were resolved using SDS-PAGE and visualized on a storage phosphor intensity screen (Fujifilm) overnight. Screens were scanned using a Fujifilm Fluorescent Image Analyzer FLA-5100. All reactions were performed in triplicate and standard error (SE) has been calculated.

2.10. Assays assessing tRNA aminoacylation

Aminoacylation of bulk tRNAs was performed using 40 pmol of *S. cerevisiae* bulk tRNAs isolated as previously described in [27] and 0.3 nmol of [^{3}H]-labeled amino acids (His, Ser, Gly, Leu, and Thr) or a [^{14}C]-L-amino acid mixture in aminoacylation buffer (100 mM Tris/HCl pH 7.5, 20 mM $MgCl_2$, 10 mM KCl, 2 mM β-mercaptoethanol, and 10 mM ATP) with 100 mg of soluble protein factors (post-ribosomal supernatant, S100). To measure aminoacylation activity associated with ribosomal particles, 60 pmol of polysomes, monosomes, or large or small subunits were used instead of S100 with all components of standard bulk tRNA aminoacylation assay. All reactions were incubated at 37 °C for 20 min. The products were precipitated in 7% trichloroacetic acid and immobilized on Whatmann glass fiber GF/C, and then aminoacylation efficiency was determined by scintillation counting. All reactions were performed in triplicate and standard error (SE) has been calculated. *p*-value has been calculated using *t*-test.

Aminoacylation activity of cellular tRNAs *in vivo* was assessed using yeast spheroplasts electroporated with 50–250 pmol synthetic tRFs. RNA from spheroplasts was isolated with TRI Reagent® (MRC), following the manufacturer's instructions. RNA pellets were dissolved in buffer containing 10 mM NaOAc (pH 5.0) and 1 mM EDTA. A portion of RNA was subjected to deacylation with 100 mM Tris/HCl pH 8.9 for 60 min at 37 °C. 30 µg of deacylated RNA or RNA derived from spheroplasts subjected to tRF electroporation were resolved on an acid-urea 6.5%-polyacrylamide gel (as described in [33]) for 24 h in the cold room, followed by northern blot hybridization with a radiolabeled oligonucleotide probe specific for tRNA-His (GTG). Northern blot hybridizations were performed in duplicate using different membranes.

2.11. Electrophoretic mobility shift assays (EMSAs)

First, 5′-[^{32}P]-end-labeled synthetic tRFs (5–500 pmol) were incubated with 0.1 mg of purified aa-RS or 100 mg of soluble protein factors in aminoacylation buffer for 20 min at 37 °C. Next, band shifts were resolved on 8% nondenaturating polyacrylamide gels and visualized on a storage phosphor intensity screen (Fujifilm) overnight. Screens were scanned using a Fujifilm Fluorescent Image Analyzer FLA-5100.

2.12. Aa-RS expression and purification

Yeast GST fusion strains (ThermoScientific): HST1/YPR033C (His-RS), SES1/YDR023W (Ser-RS), GRS1/YBR121C (Gly-RS), CDC60/YPL160W (Leu-RS), THS1/YIL078W (Thr-RS), were used for overexpression studies. Protein overexpression was induced with galactose overnight in 3 l of synthetic complete medium. After cell lysis and centrifugation, proteins were affinity purified from supernatants using Protino® Glutathione Agarose 4B (Macherey-Nagel) according to manufacturer's protocol. The purity of the overexpressed proteins was verified by denaturating sodium dodecyl sulfate polyacrylamide gel electrophoresis (SDS-PAGE).

2.13. Pelleting assays

Sedimentation binding assays were performed as previously described in [34]. Briefly, different concentrations of aa-RSs and ribosomes that had been purified through a 40% (w/v) sucrose cushion were incubated as in [33] and then centrifuged for 3 or 5 h in a TLA-55 rotor (Beckmann) to pellet ribosome-bound proteins. For the negative controls, ribosomes were replaced with an equal volume of buffer.

2.14. Western blot analysis

Whole cell extracts were fractionated by SDS-PAGE and transferred to polyvinylidene difluoride membranes using a transfer apparatus according to the manufacturer's protocols (Bio-Rad). After incubating overnight with 1–2.5% bovine serum albumin in phosphate buffered saline with Tween 20 (PBST) at 4 °C, the membranes were washed once with PBST and incubated with anti-GST or anti-RPL5 antibody (1:10000) at 25 °C for 1 h. Membranes were washed once for 15 min

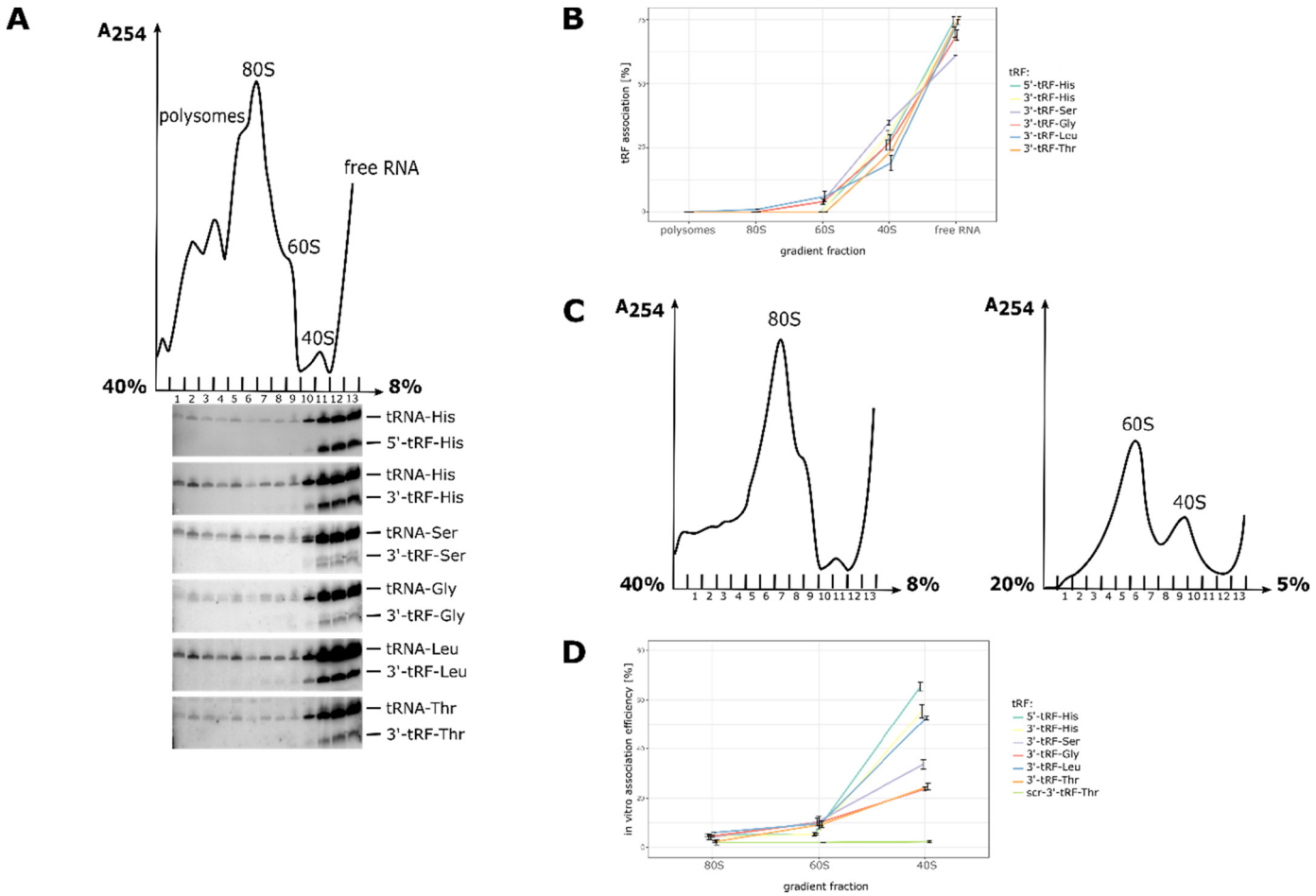

Fig. 1. Ribosome-associated Saccharomyces cerevisiae tRFs primarily co-migrate with small ribosomal subunits.
(A) A representative polysome gradient of S. cerevisiae and northern blot hybridization results. There were 13 fractions per gradient, where fractions 1–6 contained polysomes, 7–8 contained 80S, 9 contained 60S subunits, 10 contained 40S subunits, and 11–13 contained free RNAs, collected and used for northern blot analyses. Full-length tRNA and tRNA-derived fragments are indicated.
(B) Quantification of the results of northern blot analysis. *In vivo* association between tRF/ribosomal particles presented as a percentage of the band intensity of the fragment in a particular ribosomal fraction divided by the sum of the total fragment band intensity in all fractions. The mean and SE of two experiments are shown.
(C) Representative ribosomal gradients of *S. cerevisiae*. There were 13 fractions per each gradient, where in 8–40% gradient fractions 6–7 contained monosomes and in 5–20% gradient, fractions 4–6 contained 60S subunits and 9–10 contained 40S subunits. Collected fractions were used for *in vitro* association assays.
(D) *In vitro* association assay results. Efficiency of *in vitro* association between tRF/ribosomal particles shown as a percentage of input tRF used for the association reaction. The mean and SE of three experiments are shown.

and three additional times for 5 min each, and then incubated with a 1:50000 dilution of alkaline phosphatase-conjugated anti-rabbit antibody for 1 h. Blots were washed with PBST and developed with the colorimetric alkaline phosphatase system using soluble 5-bromo-4-chloro-3-indolyl phosphate and nitroblue tetrazolium as substrates.

3. Results

3.1. S. cerevisiae tRFs co-sediment with small ribosomal subunits

To gain insight into tRF ribosomal binding sites in the yeast model species *S. cerevisiae,* we performed increasingly detailed experimental validations of tRF and ribosome interactions using polysome gradient analyses and *in vitro* association assays.

To test tRF interactions with ribosomal particles *in vivo*, we employed polysome gradient analyses followed by northern blot hybridization. *S. cerevisiae* cell lysates were passed through a linear sucrose gradient to separate the polysomal fraction from 80S ribosomes, ribosomal subunits, and free RNAs. RNA isolated from each fraction was analyzed by northern blot using radiolabeled antisense probes targeting yeast tRFs (Fig. 1). We found 57–86% of yeast tRFs in the light fractions of the gradient (that is ribosome-free fraction), depending on the tRF. Ribosome-associated tRFs primarily co-migrated with the 40S subunit (Fig. 1A, B). Specifically, 32% of detected 5′-tRF-His migrated with 40S subunits. The other tRFs were found in the 40S fraction in the following amounts: 29% of 3′-tRF-His, 17% of 3′-tRF-Ser, 11% of 3′-tRF-Gly, 22% of 3′-tRF-Leu, and 12% of 3′-tRF-Thr. We observed that 6% of detected 3′-tRF-Ser, 20% of 3′-tRF-Gly, and 16% of 3′-tRF-Leu migrated with the large 60S subunits. Furthermore, 5% of 3′-tRF-Gly and 4% of 3′-tRF-Leu appeared to associate with 80S monosomes. Only for 3′-tRF-Leu were interactions observed with polysomes, where as little as 1% of total 3′-tRF-Leu detected in all fractions.

For *in vitro* association assays, we used 80S monosomes and large 60S and small 40S ribosomal subunits purified using sucrose gradients. We used a 1:1 M ratio of yeast tRFs to ribosomal particles in the optimized amount determined in our previous studies [9]. *In vitro* association data demonstrated that yeast tRFs indeed associate with 40S subunits, while 60S particles and whole ribosomes appeared to not be targeted (Fig. 1D).

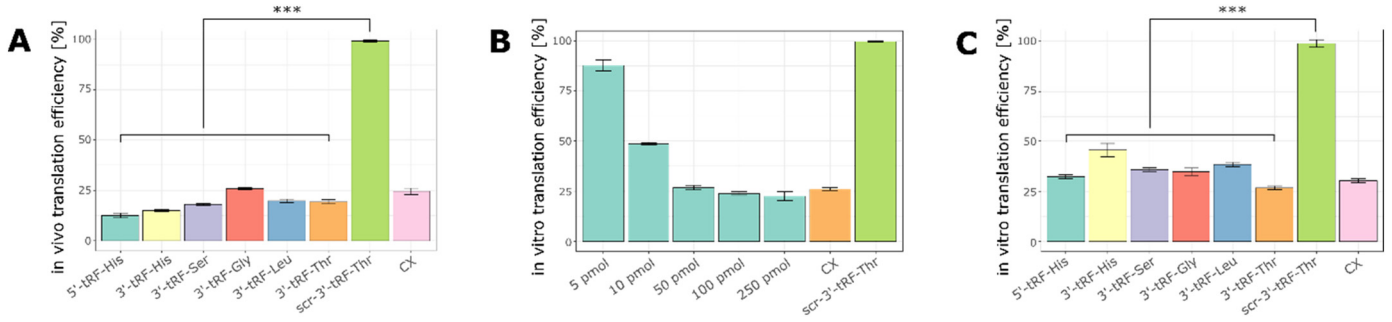

Fig. 2. *S. cerevisiae* tRNA-derived fragment inhibition of protein biosynthesis.
Cycloheximide (CX) served as a control translational inhibitor. The mean and SE of at three experiments are shown.
(A) Incorporation of ^{35}S-methionine into the translatome of yeast spheroplasts is presented as *in vivo* translation efficiency [%]. The efficiency of metabolic labelling in the absence of tRFs was set at 100% and spheroplasts harboring the synthetic tRFs or a scrambled 3′-tRF-Thr were compared to this value. *** p-value < 0.005. (B) Dose-dependent cell-free *in vitro* inhibition of translation by 3′-tRF-Thr and (C) the influence of *S. cerevisiae* tRFs on *in vitro* translation. The efficiency of cell-free *in vitro* translation is shown [%]. Sample in the absence of any tRFs served as a positive translation control and was set to 100%. *** p-value < 0.005.

3.2. The inhibitory potential of S. cerevisiae tRFs is evolutionally conserved

To study the role of ribosome-associated 3′-tRFs and 5′-tRF-His in a physiological context, we performed metabolic-labeling experiments using yeast spheroplasts [35]. We measured ^{35}S-Met incorporation into newly synthetized proteins in the presence and absence of tRFs, where the amount of tRFs used was previously optimized in [9]. Repeatedly, all tested tRFs decreased translational efficiency *in vivo* (Fig. 2A). Inhibition efficiency was in a range similar to the well-known ribosome-targeting antibiotic cycloheximide. By contrast, a 44-mer composed of a scrambled 3′-tRF-Thr sequence did not inhibit protein synthesis.

To corroborate these findings, *in vitro* translation reactions were performed using *S. cerevisiae* cell-free extracts. Interestingly, even small concentrations of 3′-tRF-Thr, specifically 0.6 μM (equivalent to 5 pmol tRF per reaction), observably reduced *in vitro* protein synthesis (Fig. 2B). Conversely, the addition of the highest tested dose of the scrambled tRF used as the negative control, 17.5 μM (equivalent to 250 pmol tRF per reaction), did not have any influence on translation efficiency. Inhibition of translation by 3′-tRF-Thr was dose-dependent with a half maximal inhibitory concentration (IC_{50}) of 2.2 μM. At this concentration, remaining tRFs observably influenced cell-free *in vitro* translation efficiency (Fig. 2C).

Because both tRNAs and ribosomes are universally conserved translational machinery components, we tested if tRF-mediated repression of translation is functionally conserved in other eukaryotic species as well. To test this possibility, we examined three cell-free *in vitro* translation systems using wheat germ extracts, rabbit reticulocyte lysates, and HeLa cell lysates (Fig. 3). *In vitro* translation reactions were performed either in the absence (no tRF) or in the presence of synthetic tRFs. The addition of *S. cerevisiae* tRFs reproducibly inhibited *in vitro* protein biosynthesis in the wheat germ system (Fig. 3A). The tRF tested that exhibited the highest inhibition in this system was 3′-tRF-Thr, which had an IC_{50} for inhibition of protein biosynthesis of 3.0 μM. IC_{50} values for other yeast tRFs in the wheat germ system were 3.9 μM for 3′-tRF-His, 4.2 μM for 3′-tRF-Ser, 20.2 μM for 3′-tRF-Gly, and 4.8 μM for 3′-tRF-Leu. *In vitro* translation was only mildly inhibited by yeast tRFs in the rabbit reticulocyte (Fig. 3B) and human systems (Fig. 3C). These data suggest that *S. cerevisiae* tRFs might potentially inhibit some translation systems in selected eukaryotes.

3.3. S. cerevisiae tRFs inhibit in vitro translation by interfering with tRNA aminoacylation

To investigate the influence of tRFs on protein biosynthesis in-depth, we first focused our attention on the earliest step of proper translation, tRNA aminoacylation. We isolated bulk *S. cerevisiae* tRNAs and tested tRNA aminoacylation in an *in vitro* charging assay with increasing amounts of 6 different tRFs. We performed a series of experiments and tested the aminoacylation of the tRNA from which a particular yeast tRF was derived (*e.g.*, we tested the influence of 3′-tRF-Ser on tRNA aminoacylation with [^{3}H]-Ser or 3′-tRF-Leu on tRNA aminoacylation with [^{3}H]-Leu). Our results clearly show that all tested *S. cerevisiae* tRFs affect aminoacylation of the corresponding full-length tRNA in a dose-dependent manner (Fig. 4A). A slight inhibition was observed when as little as 4 pmol of a particular tRF per 40 pmol of tRNA was used for aminoacylation, where an 8–30% decrease in aminoacylation was observed. The strongest shutdown of aminoacylation was observed when a 1:1 M ratio of a particular tRF to bulk tRNAs was used, where a reduction in aminoacylation efficiency ranged from 72 to 83% for all tested tRFs. Increasing the tRF/tRNA molar ratio above 1:1 did not significantly change the inhibitory effect of the tRFs, as there was a 75–88% decrease in efficiency of aminoacylation when a 5:1 M ratio of tRF:tRNA was used. Importantly, scr-3′-tRF-Thr, which served as a control, did not affect the efficiency of aminoacylation of any tested tRNA, even when the highest dose of this oligonucleotide was used. Moreover, a similar decrease in tRNA-His aminoacylation efficiency was observed when 3′-tRF-His or 5′-tRF-His were introduced.

To test if a tRF affects only aminoacylation of a corresponding tRNA or if this is a more general phenomenon, we used a [^{14}C]-L-amino acid mixture to charge bulk tRNAs isolated from *S. cerevisiae* in the presence of yeast tRFs. Therefore, we were able to measure the global aminoacylation efficiency of all tRNAs present in the bulk tRNA fraction. We used a 1:1 M ratio of tRF/tRNA. All tested *S. cerevisiae* tRFs affected global efficiency of aminoacylation of different types of tRNAs (Fig. 4B). However, this inhibition was to a smaller extent than aminoacylation of the corresponding tRNA as inhibition of global aminoacylation ranged from 35 to 63%.

In the next step, we have verified if yeast tRFs do influence the aminoacylation efficiency of cellular tRNAs *in vivo*. We have introduced yeast tRFs *via* electroporation into fresh spheroplasts, extracted total RNA and resolved it on 6.5% acid-urea gel followed by northern blot analysis. Therefore, we were able to observe differences in migration of deacylated tRNAs (tRNA-His) *versus* aminoacylated tRNAs (His-tRNA-His). We have noticed that introduction of 50 pmol tRFs clearly reduced aminoacylation of cellular tRNA-His *in vivo* by ~50%. Increasing amount of tRFs to 100 pmol or 250 pmol did not significantly change the aminoacylation efficiency, which oscillated around 60% and 55%, respectively (Fig. 4C).

3.4. S. cerevisiae tRFs form ribonucleoprotein complexes

To gain more insight into the mechanism of yeast tRF inhibition of tRNA aminoacylation, we set up a series of experiments aiming to identify the interaction partners for tRFs. In Eukaryotes, most, if not all,

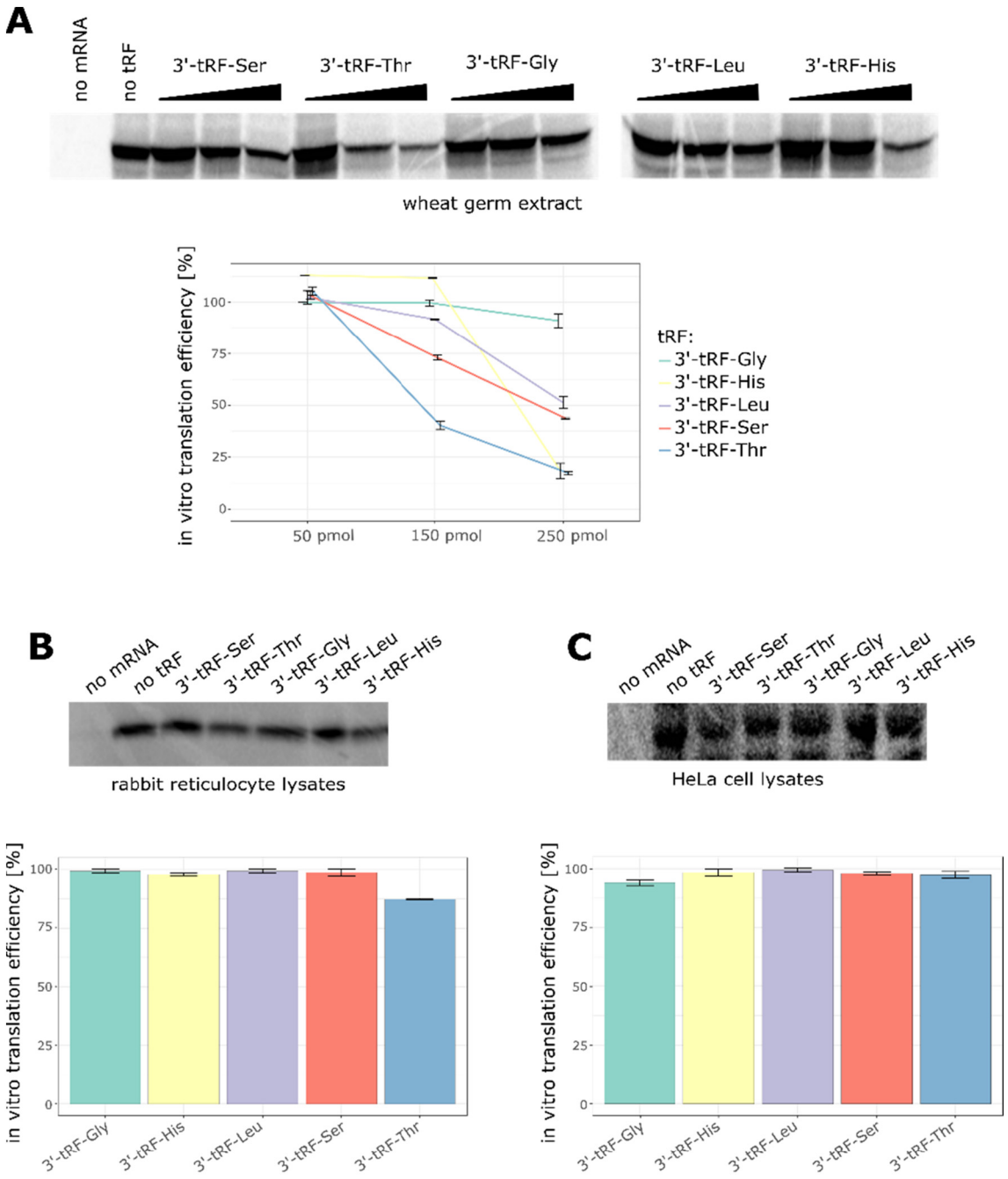

Fig. 3. *S. cerevisiae* tRNA-derived fragment inhibition of protein biosynthesis in *in vitro* eukaryotic translation systems.
(A) A representative *in vitro* translation in wheat germ extracts. The reactions were performed in the absence (no tRF) or presence of yeast tRFs (50–250 pmol). The mean and SE of three *in vitro* translation experiments are shown beneath the gel.
(B) A representative *in vitro* translation in rabbit reticulocyte lysates and (C) HeLa cell lysates. The mean and SE of three *in vitro* translation experiments are shown beneath the gel.

known functional ncRNAs are associated with RNA-binding proteins, thus forming ribonucleoprotein particles. Therefore, we aimed to verify that tRFs from *S. cerevisiae* form ribonucleoprotein particle complexes with factors required for tRNA aminoacylation.

To determine if complexes are being formed by tRFs *in vitro*, we employed EMSAs. First, we tested the ability of aminoacylation reaction components to form complexes with 3′-tRF-Thr, the tRF with the highest inhibition of tRNA charging (Supplementary Fig. 2A). We incubated *S. cerevisiae* bulk tRNAs alone, bulk tRNAs combined with the S100 protein fraction, or the S100 protein fraction alone with radioactively labeled 3′-tRF-Thr under aminoacylation reaction conditions. The resulting mixture was subjected to electrophoresis through a polyacrylamide gel under native conditions. Formation of complexes of tRF and S100 components occurred because migration of radioactively labeled 3′-tRF-Thr was slower than corresponding free tRF. Bulk tRNAs alone did not form complexes with 3′-tRF-Thr. However, complex formation was clearly observed when the S100 protein fraction was present in the reaction mix, both with and without the addition of bulk tRNAs, suggesting a protein component of the post-ribosomal supernatant fraction (S100) is capable of stably interacting with yeast tRNA-Thr 3′-derived fragments. Importantly, scr-3′-tRF-Thr, which served as a specificity control in our experiments, did not complex with S100

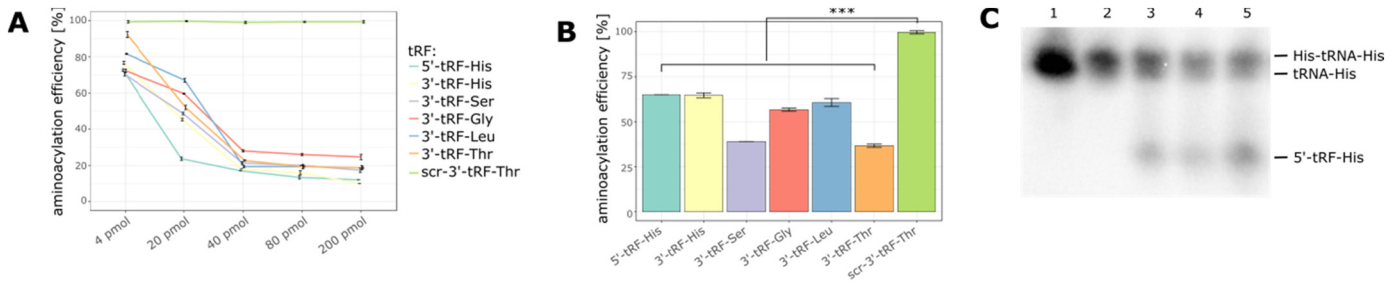

Fig. 4. Influence of *Saccharomyces cerevisiae* tRFs on efficiency of tRNA aminoacylation.
The efficiency of aminoacylation in the absence of tRFs (no tRF) was set as 100% and reactions in the presence of synthetic tRFs or a scrambled 3′-tRF-Thr (negative control) were compared to this value.
(A) Efficiency of bulk tRNA aminoacylation with His, Ser, Gly, Leu, or Thr [%]. Different amounts of corresponding tRFs (4–200 pmol/reaction) were used. The mean and SE of three aminoacylation experiments are shown.
(B) Efficiency of bulk tRNA aminoacylation with a mixture of L-amino acids (AA mix) [%]. For each reaction, 40 pmol of a particular tRF was used. The mean and SE of three aminoacylation experiments are shown. *** p-value < 0.005.
(C) Representative northern blot result presenting analysis of tRNA-His aminoacylation status under influence of increasing amounts of yeast tRFs. 1 – deacylated tRNA; 2 – aminoacylated tRNA, no tRF; 3 - aminoacylated tRNA, 50 pmol tRF; 4 - aminoacylated tRNA, 100 pmol tRF; 5 - aminoacylated tRNA, 250 pmol tRF. 5′-tRF-His signal is depicted.

components, even when increasing amounts of protein fraction were added (Supplementary Fig. 2B). Therefore, we assessed whether other yeast tRFs were also able to form complexes with protein components in the S100 fraction. Indeed, we observed clear tRF/S100 complexes in EMSAs for all tested tRFs (Supplementary Fig. 2C). The most prominent complex was observed with 5′-tRF-His, for which three shifted bands appeared on a native polyacrylamide gel. In all other cases, two bands were observed.

3.5. S. cerevisiae tRFs interact with aminoacyl-tRNA synthetases

Because we had already characterized the influence of tRFs on tRNA aminoacylation and one of the components of post-ribosomal S100 fraction are aminoacyl-tRNA synthetases, we decided to verify that tRFs interact with these enzymes.

To this end, we overexpressed in *S. cerevisiae* and purified the following GST-fusion proteins: histidyl-tRNA synthetase (His-RS), seryl-tRNA synthetase (Ser-RS), glycil-tRNA synthetase (Gly-RS), leucil-tRNA synthetase (Leu-RS), and threonyl-tRNA synthetase (Thr-RS). We verified the purity of the overexpressed proteins by SDS-PAGE. Next, we performed EMSAs on tRFs with their corresponding purified aa-RSs. First, we incubated 3′-tRF-Thr with increasing amounts of purified *S. cerevisiae* Thr-RS (50–380 μg) and then performed EMSAs. We found that yeast 3′-tRF-Thr forms a stable complex with Thr-RS, as revealed by the slower migration of radioactively labeled 3′-tRF-Thr compared to the corresponding free tRF (Fig. 5A). Importantly, scr-3′-tRF-Thr, which served as a specificity control in our experiments, did not form any complexes with Thr-RS, even when we used increasing amounts of protein (Fig. 5B). We therefore checked if other tested aa-RSs with impaired aminoacylation activity when incubated with tRFs are also targets of yeast tRFs. Our results revealed that all tested yeast tRFs form stable complexes with His-RS, Ser-RS, Gly-RS, Leu-RS, and Thr-RS (Fig. 5C). These tRF/aa-RS complexes were detected in non-denaturating gels at the same position as the tRF/S100 complex, indicating the protein components in the post-ribosomal S100 supernatant responsible for interactions with yeast tRFs are indeed aa-RSs.

Importantly, we observed not only *in vitro* and *in vivo* interactions between yeast tRFs and ribosomes, but also verified the cellular distribution of complexes formed by tRFs between the postribosomal supernatant (S100) and ribosome-containing pellet (P100). Our EMSAs revealed that tRFs predominantly co-migrated with the S100 fraction, where 67–85% of tRF complexes formed with S100 components and 15–33% with P100 components, depending on the tRF used (Fig. 6), which is in a good agreement with the polysome profiling results (Fig. 1). Moreover, tRF/P100 complexes were detected on non-denaturating gels at the same position as tRF/S100 complexes, although additional distinct complexes with slower migrations were observed for 3′-tRF-His, 3′-tRF-Gly, 3′-tRF-Leu, and 3′-tRF-Thr. This suggests there are interaction partners of *S. cerevisiae* tRFs located in the cytosol as well as within ribosomes.

3.6. S. cerevisiae aa-RSs interact with ribosomes

Aa-RSs form a variety of complexes that promote their associations with ribosomes in a number of organisms [34, 36, 37]. This together with our observations that (i) yeast tRFs interact with both ribosomes and aa-RSs, and (ii) tRF/S100 and tRF/P100 complexes migrate at similar speeds in EMSAs verify the existence of direct interactions between *S. cerevisiae* ribosomes and aa-RSs. Ribosomes purified from *S. cerevisiae* cells were incubated with aa-RSs and then ultracentrifuged (Fig. 7A). After removal of supernatants, the pellets were resuspended and samples were analyzed by SDS-PAGE followed by western blot. In ribosome-containing reaction mixtures, His-RS, Ser-RS, Leu-RS, and Thr-RS were predominantly found in the ribosomal pellet, indicating the formation of aa-RS/ribosome complexes. By contrast, when reaction mixtures lacking ribosomes were added, aa-RSs were found in the supernatant fraction. The weakest signal in the pelleting assays was observed for Gly-RS, indicating weak interactions between this enzyme and ribosomes.

The distribution of aa-RSs associated with yeast ribosomes was further investigated by measuring bulk tRNA aminoacylation activity within polysomes, monosomes, and individual small and large ribosomal subunits following fractionation over sucrose density gradients. The ribosomal particles were pelleted, resuspended, and assayed for aa-RS activity, with no addition of exogenous aa-RSs. Therefore, if the aminoacylation activity would be observed, it would derive from aa-RSs associated with particular ribosomal fractions. The resulting data are presented in Fig. 7C as percentage of total activity of the lysate associated with the ribosomal pellet. His-RS, Ser-RS, Leu-RS, and Thr-RS activities were associated with polysomes, small ribosomal subunits and, to a lesser extent, monosomes, providing further support for direct associations between yeast aa-RSs and ribosomes. Gly-RS was not significantly associated with ribosomes and this results clearly correlates with the pelleting assays (Fig. 7A). This indicates that Gly-RS may be associated with yeast ribosomes, but to a lesser extent.

4. Discussion

Protein biosynthesis is a highly choreographed process. An emerging class of regulators of ribosomal activity consists of short RNAs,

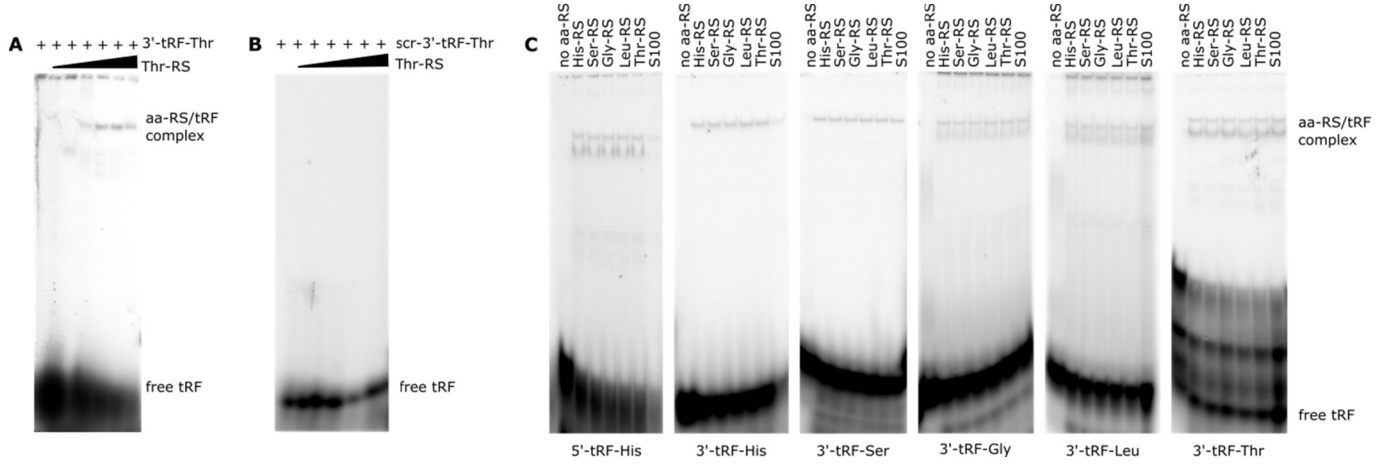

Fig. 5. *S. cerevisiae* tRFs interact with aminoacyl-tRNA synthetases.
Representative EMSA experiments are shown.
(A) Stable complexes formed of 3′-tRF-Thr with Thr-RS. Increasing concentrations of Thr-RS were used.
(B) For EMSA experiments, scr-3′-tRF-Thr served as a negative control. Increasing concentrations of Thr-RS were used.
(C) *S. cerevisiae* 5′- and 3′-part-derived tRFs form stable complexes with *S. cerevisiae* aa-RSs.

which directly interact with ribosomes both *in vitro,* as described in [38–40] and cited therein, and *in vivo*, as described in [5, 28, 41] and cited therein. These ribosome-associated small RNAs, which are being steadily discovered, are primarily processed from existing, functional RNAs, including mRNAs, rRNAs, and tRNAs, which has been reviewed in [4].

To date, the precise molecular mechanisms of action of tRNA-derived small RNAs remain mysterious. However, tRNA halves, a distinctive class of ncRNAs derived from tRNAs, have been demonstrated to regulate translation by interacting with and inhibiting initiation complexes [23]. Shorter 5′-tRFs repress global translation in a sequence-independent manner, possibly by affecting the elongation step of translation [25] or interfering with mRNA decoding *via* the small ribosomal subunit [8]. Meanwhile, 3′-tRFs, which have functions in cell proliferation [42, 43], associate with small RNA effector machinery [16] and regulate ribosome biogenesis by enhancing translation of two small ribosomal subunit protein mRNAs [44], have been shown in our recent studies to interact with yeast ribosomes [9]. In this present study, we discovered an association of five yeast 3′-tRFs and one 5′-tRF-His, previously classified as rancRNAs [28] with small ribosomal subunits (Fig. 1). These results are consistent with similar studies performed in *H. volcanii*, where 5′-tRF-Val was shown to interact with small ribosomal subunits near the mRNA decoding channel [8].

In our recent study, we revealed that the association of 3′-tRFs with ribosomes inhibits *in vitro* translation in the *S. cerevisiae* system [9]. In this present study, we evaluated the role of yeast tRFs in a more physiological context; specifically, during global *in vivo* translation and *in vitro* translation of endogenous yeast mRNAs. The results of this study indicate not only ranc-5′-tRFs (such as *H. volcanii* 5′-tRF-Val and yeast 5′-tRF-His), but also ranc-3′-tRFs, have potential regulatory roles during protein biosynthesis (Fig. 2). Moreover, not only archeal, but also eukaryotic, tRFs are capable of inhibiting protein biosynthesis through interactions with ribosomes, suggesting the mechanism of translation regulation is evolutionarily conserved. This implication is further supported by the inhibition of protein synthesis by yeast tRFs in the wheat germ system with a comparable or slightly higher IC_{50} (Fig. 3A). This suggests that the mode of action and, thus, also the ribosomal target site, is conserved in a range of eukaryotic species.

The most important finding of this work is that yeast tRFs affect aminoacylation of the corresponding parental tRNAs (Fig. 4A), as well as global aminoacylation (Fig. 4B), most probably through interactions with ribosome-associated aa-RSs. Recently, tRF and aa-RS interactions

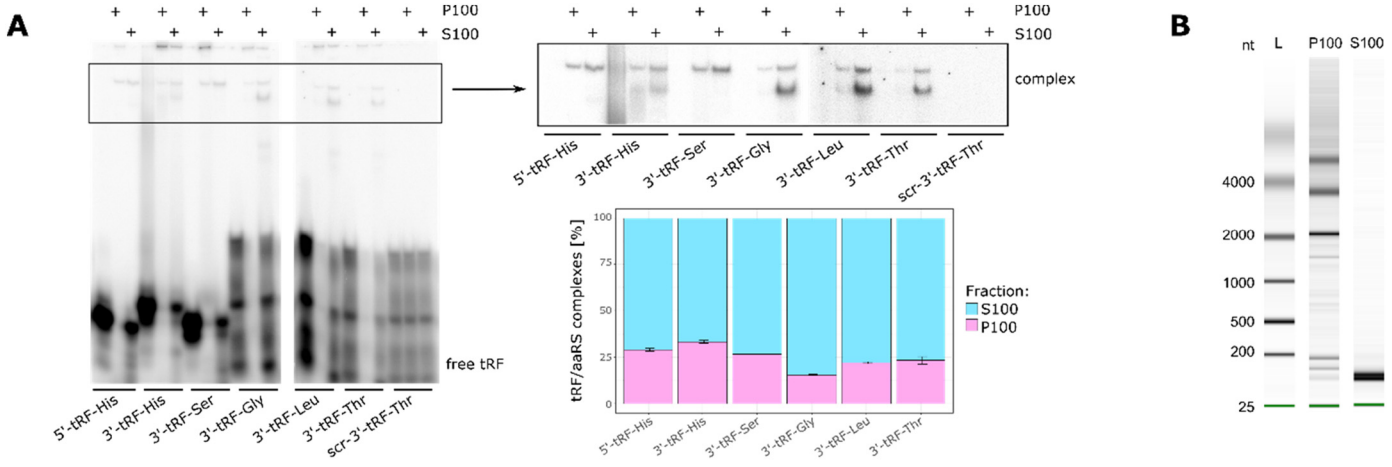

Fig. 6. Cellular distribution of tRF/aa-RS complexes based on the postribosomal supernatant (S100) and ribosome-containing pellet (P100) fractions.
(A) Representative EMSA experiments and quantifications of three independent experiments are shown. The mean and SE of three experiments are shown.
(B) Purity of P100 and S100 fractions by means of Agilent RNA 6000 Nano assay. L – ladder. The bands corresponding to ribosomal RNAs are visible in P100 fraction. Low molecular weight RNAs, up to 200 nt are mostly present in S100 fraction.

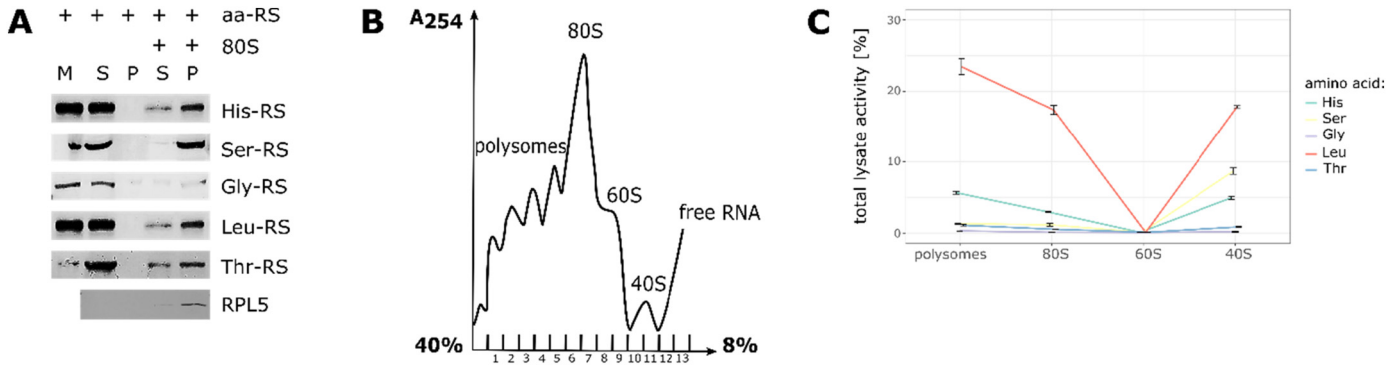

Fig. 7. Yeast aa-RSs interact with ribosomes.
(A) A representative ribosomal pelleting assay combined with western blot analysis. Complexes of purified components were formed by incubating aa-RSs with 80S ribosomes. Samples were pelleted by ultracentrifugation. Pellets (P) and supernatants (S) were analyzed by SDS-PAGE followed by western blot. Antibodies against ribosomal protein L5 (RPL5) were used to show the purity of the fractions. M - purified corresponding aa-RS used as a size marker.
(B) A representative polysome gradient of *S. cerevisiae*. There were 13 fractions per gradient, where fractions 1–5 contained polysomes, 6–7 contained 80S, 8–9 contained 60S subunits, 10–11 contained 40S subunits, and 12–13 contained free RNAs, collected and used for aminoacyl-tRNA synthetase activity.
(C) Aminoacyl-tRNA synthetase activity associated with polysomes, monosomes, and ribosomal subunits. Activity was calculated as the percentage of the total activity in the lysate for the amino acid indicated. The mean and SE of three experiments are shown.

were reported on by Keam et al. who observed an association between 5′-tRF-Gln and the human multisynthetase complex [26]. Importantly, in their previous studies, tRNA-Gln charging was unaffected by the presence of excess 5′-tRF-Gln [25] and 5′ tRF-Gln increased translation of ribosomal and poly(A)-binding proteins [26]. Therefore, yeast and human tRFs, despite having a similar cellular target (aa-RS), likely utilize different mechanisms to regulate protein biosynthesis. This implication is further supported by our observation that both 5′ and 3′ yeast tRFs do not interfere with *in vitro* translation in the human system (Fig. 3C).

Direct interactions between ribosomes and multisynthetase complexes have been reported in Archea [34, 45] and human cell cultures [37]. In *S. cerevisiae*, complexes containing GluRS, MetRS, and Arc1p have been characterized and found to enhance tRNA binding to their respective aa-RSs [46, 47]. However, direct interactions between aa-RSs and ribosomes have not been reported to date. Our data clearly indicates that four yeast aa-RSs, His-RS, Ser-RS, Leu-RS, and Thr-RS, directly interact with *S. cerevisiae* ribosomes (Fig. 7). Moreover, the presence of more than one cellular partner in yeast tRF interactions, as revealed by the multiple complexes formed by tRFs (Figs. 5 and 6), might also indicate the existence of additional unreported multisynthetase complexes in *S. cerevisiae*. Therefore, the results of this study provide a molecular basis for additional structural and genetic experiments in the yeast system and aid in future understanding of both tRF functions during protein biosynthesis and aa-RS localization to translating ribosomes.

Transparency document

The Transparency document associated with this article can be found, in online version.

Acknowledgments

This work was supported by the Foundation for Polish Science (POMOST/2011-4/1 to K.B.-Ż.), National Science Centre, Poland (2014/13/D/NZ1/00061 to K.B.-Ż.) and Institute of Bioorganic Chemistry Polish Academy of Sciences (19/GM/2017 to A.M.M). The work was also supported by the Polish Ministry of Science and Higher Education, under the KNOW program.

We thank Norbert Polacek for discussions and Agata Tyczewska for comments on the manuscript. Our thanks are extended to Marek Żywicki for bioinformatics support and Marek Tchórzewski for experimental advices with polysome profiles.

References

[1] T.C. Fleischer, C.M. Weaver, K.J. McAfee, J.L. Jennings, A.J. Link, Systematic identification and functional screens of uncharacterized proteins associated with eukaryotic ribosomal complexes, Genes Dev. 20 (2006) 1294–1307.
[2] J. Trylska, S.G. Thoduka, Z. Dąbrowska, Using sequence-specific oligonucleotides to inhibit bacterial rRNA, ACS Chem. Biol. 8 (2013) 1101–1109.
[3] T. Hermann, Drugs targeting the ribosome, Curr. Opin. Struct. Biol. 15 (2005) 355–366.
[4] A. Pircher, J. Gebetsberger, N. Polacek, Ribosome-associated ncRNAs: an emerging class of translation regulators, RNA Biol. 11 (2014) 1335–1339.
[5] A. Pircher, K. Bakowska-Zywicka, L. Schneider, M. Zywicki, N. Polacek, An mRNA-derived noncoding RNA targets and regulates the ribosome, Mol. Cell 54 (2014) 147–155.
[6] H. Luidalepp, S. Berger, O. Joss, T. Tenson, N. Polacek, Ribosome shut-down by 16S rRNA fragmentation in stationary-phase Escherichia coli, J. Mol. Biol. 428 (2016) 2237–2247.
[7] J. Gebetsberger, M. Zywicki, A. Künzi, N. Polacek, tRNA-derived fragments target the ribosome and function as regulatory non-coding RNA in Haloferax volcanii, Archaea 2012 (2012) 260909.
[8] J. Gebetsberger, L. Wyss, A.M. Mleczko, J. Reuther, N. Polacek, A tRNA-derived fragment competes with mRNA for ribosome binding and regulates translation during stress, RNA Biol. (2016), http://dx.doi.org/10.1080/15476286.2016.1257470.
[9] K. Bąkowska-Żywicka, M. Kasprzyk, T. Twardowski, tRNA-derived short RNAs bind to *Saccharomyces cerevisiae* ribosomes in a stress-dependent manner and inhibit protein synthesis *in vitro*, FEMS Yeast Res. 16 (2016) fow077.
[10] J. Gebetsberger, N. Polacek, Slicing tRNAs to boost functional ncRNA diversity, RNA Biol. 10 (2013) 1798–1806.
[11] S.P. Keam, G. Hutvagner, tRNA-derived fragments (tRFs): emerging new roles for an ancient RNA in the regulation of gene expression, Life (Basel, Switzerland) 5 (2015) 1638–1651.
[12] M. Saikia, M. Hatzoglou, The many virtues of tRNA-derived stress-induced RNAs (tiRNAs): discovering novel mechanisms of stress response and effect on human health, J. Biol. Chem. 290 (2015) 29761–29768.
[13] C. Megel, G. Morelle, S. Lalande, A.-M. Duchêne, I. Small, L. Maréchal-Drouard, Surveillance and cleavage of eukaryotic tRNAs, Int. J. Mol. Sci. 16 (2015) 1873–1893.
[14] P. Anderson, P. Ivanov, tRNA fragments in human health and disease, FEBS Lett. 588 (2014) 4297–4304.
[15] A.M. Mleczko, P. Celichowski, K. Bąkowska-Żywicka, Ex-translational function of tRNAs and their fragments in cancer, Acta Biochim. Pol. 61 (2014) 211–216.
[16] D. Haussecker, Y. Huang, A. Lau, P. Parameswaran, A.Z. Fire, M.A. Kay, Human tRNA-derived small RNAs in the global regulation of RNA silencing, RNA 16 (2010) 673–695.
[17] G. Loss-Morais, P.M. Waterhouse, R. Margis, Description of plant tRNA-derived RNA fragments (tRFs) associated with argonaute and identification of their putative targets, Biol. Direct 8 (2013) 6.
[18] Y. Kawamura, K. Saito, T. Kin, Y. Ono, K. Asai, T. Sunohara, T.N. Okada, M.C. Siomi, H. Siomi, Drosophila endogenous small RNAs bind to Argonaute 2 in somatic cells, Nature 453 (2008) 793–797.
[19] H. Goodarzi, X. Liu, H.C.B. Nguyen, S. Zhang, L. Fish, S.F. Tavazoie, Endogenous tRNA-derived fragments suppress breast cancer progression via YBX1 displacement, Cell 161 (2015) 790–802.

[20] S. Honda, P. Loher, M. Shigematsu, J.P. Palazzo, R. Suzuki, I. Imoto, I. Rigoutsos, Y. Kirino, Sex hormone-dependent tRNA halves enhance cell proliferation in breast and prostate cancers, Proc. Natl. Acad. Sci. 112 (2015) E3816–E3825.
[21] Q. Chen, M. Yan, Z. Cao, X. Li, Y. Zhang, J. Shi, G. Feng, H. Peng, X. Zhang, Y. Zhang, et al., Sperm tsRNAs contribute to intergenerational inheritance of an acquired metabolic disorder, Science 351 (2016) 397–400.
[22] U. Sharma, C.C. Conine, J.M. Shea, A. Boskovic, A.G. Derr, X.Y. Bing, C. Belleannee, A. Kucukural, R.W. Serra, F. Sun, et al., Biogenesis and function of tRNA fragments during sperm maturation and fertilization in mammals, Science 351 (2016) 391–396.
[23] P. Ivanov, M.M. Emara, J. Villen, S.P. Gygi, P. Anderson, Angiogenin-induced tRNA fragments inhibit translation initiation, Mol. Cell 43 (2011) 613–623.
[24] P. Ivanov, E. O'Day, M.M. Emara, G. Wagner, J. Lieberman, P. Anderson, G-quadruplex structures contribute to the neuroprotective effects of angiogenin-induced tRNA fragments, Proc. Natl. Acad. Sci. 111 (2014) 18201–18206.
[25] A. Sobala, G. Hutvagner, Small RNAs derived from the 5′ end of tRNA can inhibit protein translation in human cells, RNA Biol. 10 (2013) 553–563.
[26] S.P. Keam, A. Sobala, S. Ten Have, G. Hutvagner, tRNA-derived RNA fragments associate with human multisynthetase complex (MSC) and modulate ribosomal protein translation, J. Proteome Res. 16 (2017) 413–420.
[27] K. Bąkowska-Żywicka, A.M. Mleczko, M. Kasprzyk, P. Machtel, M. Żywicki, T. Twardowski, The widespread occurrence of tRNA-derived fragments in *Saccharomyces cerevisiae*, FEBS Open Bio 6 (2016) 1186–1200.
[28] M. Zywicki, K. Bakowska-Zywicka, N. Polacek, Revealing stable processing products from ribosome-associated small RNAs by deep-sequencing data analysis, Nucleic Acids Res. 40 (2012) 1–12.
[29] M. Pospísek, L. Valásek, Polysome profile analysis – yeast, Methods in Enzymology, Vol. 530 2013, pp. 173–181.
[30] I.V. Velichutina, J. Dresios, J.Y. Hong, C. Li, A. Mankin, D. Synetos, S.W. Liebman, I.V. Velichutina, J. Dresios, J.O.O.Y.U.N. Hong, et al., Mutations in Helix 27 of the Yeast *Saccharomyces cerevisiae* 18S rRNA Affect the Function of the Decoding Center of the Ribosome Mutations in Helix 27 of the Yeast *Saccharomyces cerevisiae* 18S rRNA Affect the Function of the Decoding Center of the Ribosome, (2000).
[31] M.G. Acker, S.E. Kolitz, S.F. Mitchell, J.S. Nanda, J.R. Lorsch, Reconstitution of yeast translation initiation, Methods in Enzymology, Vol. 430 2007, pp. 111–145.
[32] R. Hofbauer, F. Fessl, B. Hamilton, H. Ruis, Preparation of a mRNA-dependent cell-free translation system from whole cells of Saccharomyces cerevisiae, Eur. J. Biochem. 122 (1982) 199–203.
[33] B.D. Janssen, E.J. Diner, C.S. Hayes, Analysis of aminoacyl- and peptidyl-tRNAs by gel electrophoresis, Methods Mol. Biol. 905 (2012) 291–309.
[34] V. Godinic-Mikulcic, J. Jaric, B.J. Greber, V. Franke, V. Hodnik, G. Anderluh, N. Ban, I. Weygand-Durasevic, Archaeal aminoacyl-tRNA synthetases interact with the ribosome to recycle tRNAs, Nucleic Acids Res. 42 (2014) 5191–5201.
[35] P.J. Russell, S.J. Hambidge, K. Kirkegaard, Direct introduction and transient expression of capped and non-capped RNA in Saccharomyces cerevisiae, Nucleic Acids Res. 19 (1991) 4949–4953.
[36] M.A. Ussery, W.K. Tanaka, B. Hardesty, Subcellular distribution of aminoacyl-tRNA synthetases in various eukaryotic cells, Eur. J. Biochem. 72 (1977) 491–500.
[37] A. David, N. Netzer, M.B. Strader, S.R. Das, C.Y. Chen, J. Gibbs, P. Pierre, J.R. Bennink, J.W. Yewdell, RNA binding targets aminoacyl-tRNA synthetases to translating ribosomes, J. Biol. Chem. 286 (2011) 20688–20700.
[38] B. Dudzińska-Bajorek, K. Bąkowska, T. Twardowski, Conformational changes of L-rRNA during elongation of polypeptide, J. Plant Physiol. 163 (2006) 463–474.
[39] K. Bakowska-Zywicka, A.M. Kietrys, T. Twardowski, Antisense oligonucleotides targeting universally conserved 26S rRNA domains of plant ribosomes at different steps of polypeptide elongation, Oligonucleotides 18 (2008) 175–186.
[40] K. Bakowska-Zywicka, T. Twardowski, Correlation of the structure and conformational changes of selected fragments of plant small ribosomal RNA within the steps of polypeptide chain elongation, J. Plant Physiol. 164 (2007) 496–504.
[41] J. Gebetsberger, M. Zywicki, A. Künzi, N. Polacek, tRNA-derived fragments target the ribosome and function as regulatory non-coding RNA in *Haloferax volcanii*, Archaea 2012 (2012) 1–11.
[42] Y.S. Lee, Y. Shibata, A. Malhotra, A. Dutta, A novel class of small RNAs: tRNA-derived RNA fragments (tRFs), Genes Dev. 23 (2009) 2639–2649.
[43] R.L. Maute, C. Schneider, P. Sumazin, A. Holmes, A. Califano, K. Basso, R. Dalla-Favera, tRNA-derived microRNA modulates proliferation and the DNA damage response and is down-regulated in B cell lymphoma, Proc. Natl. Acad. Sci. 110 (2013) 1404–1409.
[44] H.K. Kim, G. Fuchs, S. Wang, W. Wei, Y. Zhang, H. Park, B. Roy-Chaudhuri, P. Li, J. Xu, K. Chu, et al., A transfer-RNA-derived small RNA regulates ribosome biogenesis, Nature 552 (2017) 57–62.
[45] M. Raina, S. Elgamal, T.J. Santangelo, M. Ibba, Association of a multi-synthetase complex with translating ribosomes in the archaeon Thermococcus kodakarensis, FEBS Lett. 586 (2012) 2232–2238.
[46] G. Simos, A. Segref, F. Fasiolo, K. Hellmuth, A. Shevchenko, M. Mann, E.C. Hurt, The yeast protein Arc1p binds to tRNA and functions as a cofactor for the methionyl- and glutamyl-tRNA synthetases, EMBO J. 15 (1996) 5437–5448.
[47] G. Simos, A. Sauer, F. Fasiolo, E.C. Hurt, A conserved domain within Arc1p delivers tRNA to aminoacyl-tRNA synthetases, Mol. Cell 1 (1998) 235–242.

Supplementary data

Transfer RNA-derived fragments target and regulate ribosome-associated aminoacyl-transfer RNA synthetases

Anna M. Mleczko, Piotr Celichowski and Kamilla Bąkowska-Żywicka*

[1]Institute of Bioorganic Chemistry Polish Academy of Sciences, Noskowskiego St. 12/14, 61-704 Poznan, Poland

*To whom correspondence should be addressed. email: bakowska@ibch.poznan.pl

Author Notes

Present address:

Piotr Celichowski, Department of Histology and Embryology, Poznan University of Medical Sciences, Poznan, Poland

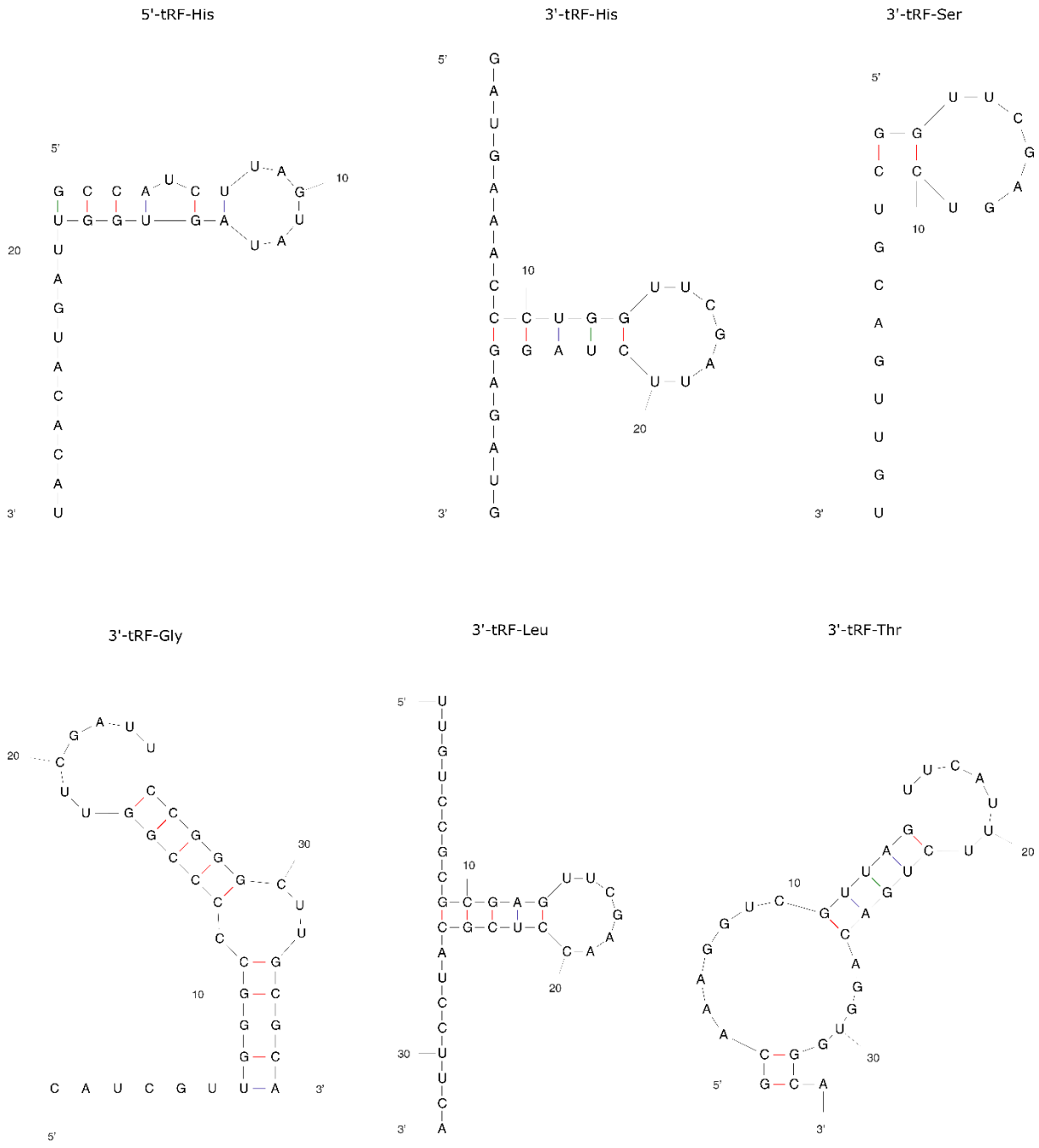

Supplementary Figure 1. Secondary structure of Saccharomyces cerevisiae tRFs predicted with mfold.

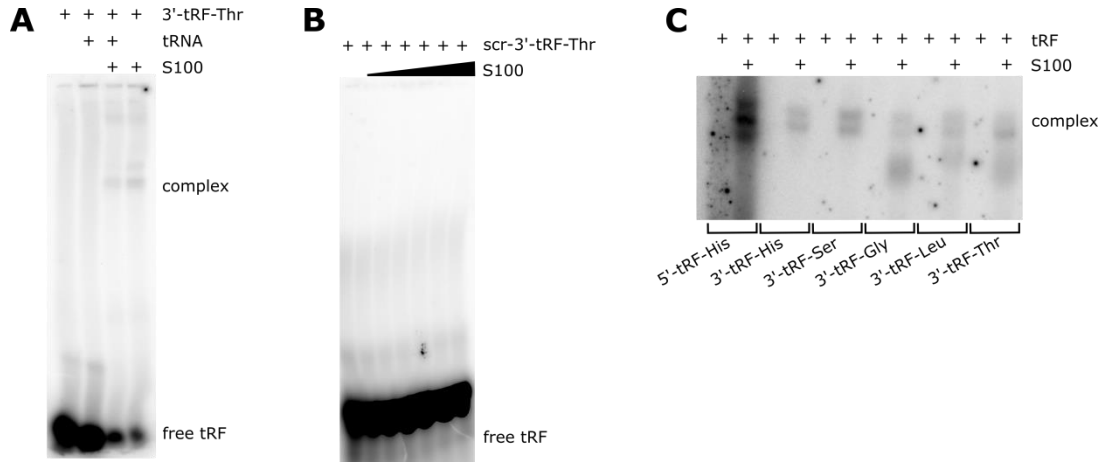

Supplementary Figure 2. Saccharomyces cerevisiae tRFs form stable complexes with components of the post-ribosomal S100 protein fraction. *Representative EMSA experiments are shown.*

(A) Complexes are formed with the components of the aminoacylation reaction by 3′-tRF-Thr.

(B) For EMSA experiments, scr-3′-tRF-Thr served as a negative control.

(C) S. cerevisiae 5′- and 3′-part-derived tRFs formed complexes with post-ribosomal S100 protein fraction components.

3

Mleczko AM, Bąkowska – Żywicka K

When small RNAs become smaller: emerging functions of snoRNAs and their derivatives

Acta Biochimica Polonica, 2016, 63(4):601-607

ACTA ABP BIOCHIMICA POLONICA

Vol. 63, No 4/2016
601–607
https://doi.org/10.18388/abp.2016_1330

Review

When small RNAs become smaller: emerging functions of snoRNAs and their derivatives

Anna M. Mleczko and Kamilla Bąkowska-Żywicka✉

Institute of Bioorganic Chemistry Polish Academy of Sciences, Poznań, Poland

Small nucleolar RNAs (snoRNAs) are molecules located in the cell nucleolus and in Cajal bodies. Many scientific reports show that snoRNAs are not only responsible for modifications of other RNAs but also fulfill multiple other functions such as metabolic stress regulation or modulation of alternative splicing. Full-length snoRNAs as well as small RNAs derived from snoRNAs have been implied in human diseases such as cancer or Prader–Willi Syndrome. In this review we describe emerging, non-canonical roles of snoRNAs and their derivatives with the emphasis on their role in human diseases.

Key words: small RNAs, snoRNAs, sdRNAs, microRNAs, regulatory RNAs

Received: 30 May, 2016; revised: 28 July, 2016; accepted: 08 August, 2016; available on-line: 26 October, 2016

INTRODUCTION

Small nucleolar RNAs (snoRNAs) are one of the most ancient and evolutionarily conserved non-protein coding RNAs. They have been identified in Eukaryotes, Archaea and one in the Epstein-Barr virus (Hutzinger *et al.,* 2009). There are two classes of snoRNAs (C/D and H/ACA box) that function as ribonucleoprotein (RNP) complexes to guide enzymatic modifications of other RNAs, mainly ribosomal RNAs (rRNAs). Posttranscriptional rRNA modifications are common for all domains of life; there are three basic types: base methylation, ribose methylation and pseudouridylation.

C/D box snoRNAs take their name from the conserved sequence elements that they contain, known as C/C' (RUGAUGA, R=purine) and D/D' (CUGA) boxes, located near the 5' and 3' ends of the snoRNA, respectively. C/D box snoRNAs form a ribonucleoprotein complex with 2'-O-methyltransferase fibrillarin and such snoRNP complex methylates the target RNAs. A conserved region of 10–21 nucleotides (nt) upstream of the D and/or D' box is complementary to the methylation site of the target RNA and enables the snoRNA to form an RNA duplex with the RNA. H/ACA box snoRNAs in turn form complexes with the pseudouridine synthase dyskerin and perform pseudouridylation. Small nucleolar RNAs from this class are built by two stems that form a pseudouridinilation pocket and two single stranded regions that enclose the H (ANANNA) and ACA elements.

Many studies have investigated snoRNA-guided modifications. As a result, some features characterizing the functional snoRNA-target site interactions have been inferred and are used in the computational prediction of snoRNA targets (e.g. sequence complementarity between putative target RNAs and the antisense elements or the recognition loops within the snoRNA) as well as biochemical identifications of snoRNA targets (e.g. based on CLASH: crosslinking, ligation, and sequencing of hybrids). However, there are numerous snoRNAs for which no target RNAs have been identified so far. They are called "orphan snoRNAs". In multiple cases, orphan snoRNAs possess the guide sequences, however, they are not complementary to other canonical RNAs targeted by snoRNAs.

Small nucleolar RNAs were initially discovered in the nucleolus and were thought to exclusively target ribosomal RNAs inside this subnuclear compartment. However, years of research on the snoRNA biology have revealed a tremendous number of unexpected discoveries that shed a new light on their functions in processes different than modifications of other RNAs. Small nucleolar RNAs may take part in the regulation of metabolic stress responses, development of some diseases or disorders, like cancer or the Prader–Willi syndrome. Moreover, there is a growing number of evidence that mature snoRNAs undergo further processing into stable shorter fragments, known as snoRNA-derived RNAs (sdRNAs) (Falaleeva & Stamm, 2013; Li *et al.,* 2012). Such fragments are present in many organisms, including mammals (Bortolin-Cavaille & Cavaille, 2012; Kishore *et al.*, 2010; Ender *et al.,* 2008; Bai *et al.,* 2014; Brameier *et al.,* 2011; Burroughs *et al.,* 2011), a primitive protozoan *Giardia lamblia* (Saraiya & Wang, 2008), budding yeast *Saccharomyces cerevisiae* (Żywicki *et al.,* 2012; Walkowiak *et al.,* 2016) and the Epstein-Barr virus (Hutzinger *et al.,* 2009). Interestingly, these fragments associate with proteins different than the full-length snoRNAs do, and therefore possibly fulfill distinct cellular functions. Moreover, such snoRNA cleavage in yeast cells is most prominent under non-optimal growth conditions, which include UV irradiation, anaerobic growth, growth in a high or low pH

✉e-mail: bakowska@ibch.poznan.pl

Abbreviations: 5-HT2CR, 5-hydroxytryptamine receptor 2; Ago, Argonaute protein; CRHR1, corticotropin-releasing hormone receptor 1; EBV, Epstein-Barr virus; DPM2, dolichol phosphate-mannose biosynthesis regulatory protein; HEK293, human embryonic kidney 293 cells; hnRNP, heterogeneous nuclear ribonucleoprotein; HNSCC, head and neck squamous cell carcinomas; MAPK/ERK, mitogen-activated protein kinases; originally called ERK, extracellular signal-regulated kinases; miRNA, microRNA; mRNA, messenger RNA; ncRNA, non-protein coding RNA; NGS, next generation sequencing, NSCLC, non-small-cell lung carcinoma; PBRM1, protein polybromo-1; PCR, polymerase chain reaction; PWS, Prader–Willi syndrome; qRT-PCR, quantitative real-time reverse transcriptase PCR; RALGPS1, Ral GEF with PH domain and SH3 binding motif 1 protein; RNP, ribonucleoprotein complex; rRNA, ribosomal RNA; sdRNA, small RNA derived from snoRNA; SL-RT-PCR, stem-loop reverse transcription combined with polymerase chain reaction; snoRNA, small nucleolar RNA; TAF1, transcription initiation factor TFIID subunit 1; TGF-β, transforming growth factor β

medium or growth in a medium with no amino acids or sugars (Żywicki *et al.,* 2012; Tyczewska *et al.,* 2016). Such response to changing environment may therefore indicate that snoRNA processing may play a crucial role in the stress-dependent metabolism regulation, similar as in case of tRNA processing (Mleczko *et al*., 2014). In this article, we highlight the current state of the art concerning non-canonical roles of snoRNAs and their derivatives, sdRNAs, with emphasis on their role in human disorders.

PROCESSING OF snoRNAs TO sdRNAs – DISCOVERING NOVEL FUNCTIONS OF KNOWN RNAs

In 2008, an unbiased sequencing study (aimed at capturing all potential human small RNAs in a range of 19–40 nt) led to the observation of specific processing and accumulation of small RNAs originating from well-characterized non-coding RNAs, including snoRNAs (Kawai *et al*., 2008). In the next year, by systematic analyses of deep-sequencing libraries from diverse eukaryotic organisms, Taft and coworkers (2009) revealed that small RNAs with evolutionarily conserved size and position, are derived from the vast majority of snoRNA loci in animals (human, mouse, chicken, fruit fly), thale cress and fission yeast. Later on, a comparison of human small RNA deep sequencing data sets revealed that box C/D sdRNA accumulation patterns are conserved across multiple cell types (Scott *et al*., 2012). Recently, in 2014, Laiho and coworkers performed deep sequencing of small RNomes in subcellular compartments of the HeLa cells (Bai *et al.,* 2014). The nucleolar small RNAs were predominantly represented by 19–20 nt and 25 nt reads and 93% of them were mapping to the box C/D snoRNAs. The most abundantly represented locus among the sdRNA reads in the nucleolar fraction was SNORD44 (RNU44) – 71.4% of all nucleolar sdRNAs. Few of the sdRNAs were detected in the cytoplasmic fraction, which could suggest their functional potential in processes different than those in which the mature precursors act (since full-length snoRNAs are localized and perform their function in the nucleolus). The list of discovered snoRNA-derived small RNAs is presented in Table 1.

Concerning the function of sdRNAs in the cells, the first and breakthrough functional study came from the Meister group. It demonstrated the miRNA-like activity of an sdRNA originating from ACA45 snoRNA (Ender *et al.,* 2008). This particular sdRNA was identified in the Ago-associated RNA library. Importantly, the sequencing reads were found to be conserved in mammals, suggesting that they are, indeed, specific processing products. In terms of both, processing and function, ACA45 sdRNA was similar to miRNAs. Firstly, this sdRNA was produced in the HEK293 cells in a Dicer-dependent manner. Secondly, an endogenous target RNA has been identified (CDC2L6 – a component of the mediator complex) and experimentally confirmed. ACA45 sdRNA was able to inhibit the activity of a CDC2L6 target in a miRNA-like pattern. Notably, the same authors identified seven additional sdRNAs with miRNA-like processing features in the follow-up experiments. Parallel NGS studies of the small transcriptome in mice revealed the presence of snoRNA-originating miRNA-like molecules in embryonic stem cells and demonstrated that sdRNAs exhibit tissue specific expression (Babiarz *et al.,* 2008; Babiarz *et al.,* 2011).

At the same time, two functional snoRNA-originating miRNA-like RNAs were described in the protozoan *Giardia lamblia*, a unicellular parasite whose genome does not encode Drosha: miRNA2 (Saraiya & Wang, 2008) and miRNA5 (Li *et al.,* 2011). These miRNA-like sdRNAs associated with the Ago proteins and were pro-

Table 1. The list of discovered snoRNA-derived RNAs.

Organism	Processed snoRNA	References
Epstein-Barr virus	v-snoRNA1	Hutzinger *et al.,* 2009
Giardia lambia	GlsR17, GlsR2	Saraiya & Wang, 2008; Li *et al.,* 2011
Saccharomyces cerevisiae	snoRNA: 78, 77, 128, 51, 76, 17a, 66, 67, 73, 18, 54, 83, 30, 8	Żywicki *et al.,* 2012 Walkowiak *et al.,* 2016
Mus musculus	MBII-52	Kishore *et al.,* 2010; Bortolin-Cavaille & Cavaille, 2012
Homo sapiens	ACA45, ACA36B, ACA56, ACA3, ACA17, ACA50, ACA47, ACA25, RNU44, SNORD48, SNORD21, SNORA48, SNORA64,SNORA73, SNORA8, SCARNA15, SCARNA15, snR39b, H/MBII-52, HBI-100, HBII-336, HBII-429, HBII-142, U27, U83a, U74, U15a. U92, U3, U78, U17a, U17b, sno-miRNA-28, hsa-miRNA-1291	Bortolin-Cavaille & Cavaille, 2012; Kishore *et al.,* 2010; Ender *et al.,* 2008; Bai *et al.,* 2014; Brameier *et al.,* 2011; Burroughs *et al.,* 2011; Yu *et al*., 2015, Pan *et al.,* 2013
Canis familiaris *Rattus norvegicus* *Mus musculus* *Canis familiaris*	ACA45	Ender *et al.*, 2008
embryonic chicken cell line	GSE10686, GSM270187, GSM270188, GSM270189	Taft *et al.,* 2009
mouse embryonic stem (ES) cells	GSE12521, GSM314552, GSM314553, GSM314552	Taft *et al.,* 2009
Drosophila melanogaster	GSE7448, GSM180328, GSM180329, GSM180330, GSM180331, GSM180332, GSM180333, GSM180334, GSM180335, GSM180336, GSM180337, GSE11086, GSM280082, GSM280083, GSM280084	Taft *et al.,* 2009
Arabidopsis thaliana	GSE12037, GSM304282, GSM304283, GSM304284, GSM304285	Taft *et al.,* 2009
Schizosaccharomyces pombe	GSE12416, GSM311595, GSM311596	Taft et *al.,* 2009

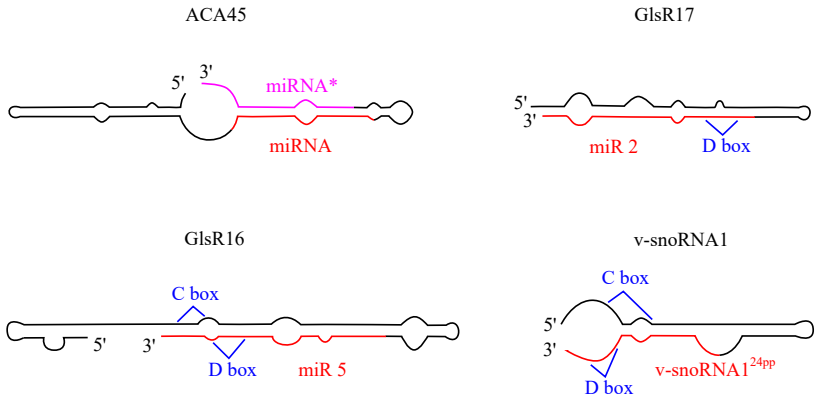

Figure 1. Examples of sdRNAs with microRNA functions.
Predicted secondary structures of the following snoRNAs are presented: human ACA45, *G. lamblia* GlsR17 and GlsR16, EBV v-snoRNA1. microRNA positions are marked in red. For C/D box snoRNAs, C boxes and D boxes are marked in blue.

duced in a Dicer-dependent but Drosha-independent manner. 26-nucleotide long miRNA2 is a processing product of GlsR17 snoRNA and is localized in the cytoplasm. miRNA5 of the same length is derived from a C/D box snoRNA, GlsR2. In this case the authors also identified a putative miRNA target sites in the 3'-UTRs of mRNAs and verified the activity of miRNA2 *in vivo*. The expression of Renilla luciferase (RL) reporter mRNA containing six identical miRNA2 target sites in the 3'-UTR was reduced by 40% when co-transfected with miRNA2 (Saraiya & Wang, 2008). Moreover, Li *et al.* took the same approach and discovered that the presence of endogenous miRNA5 in *Giardia* reduces the RL expression by 18%, whereas the presence of additional synthetic miRNA5 further decreases the expression by a total of 39% (Li *et al.,* 2011). The same pathway was described one year later in cells infected with the Epstein-Bar virus (EBV). In this system, EBV expresses a miRNA-like precursor endogenously encoded by a viral v-snoRNA1 to suppress the viral DNA polymerase upon induction of the lytic cycle (Hutzinger *et al.,* 2009). Numerous miRNAs-like molecules derived from C/D box snoRNAs which exhibit mRNA silencing features were additionally identified in human cell lines: HeLa, Jurkat (T cells) and RPMI8866 (B cell) (Brameier *et al.,* 2011). 11 RNAs derived from SNORD2 (snR39b), SNORD3@ (U3), SNORD78 (U78), SNORD93 (HBII-336), SNORD100 (HBII-429), SNORD66 (HBII-142), SNORD27 (U27), SNORD83a (U83a), SNORD74 (U74) and SNORD15a (U15a) were capable of translation regulation of reporter-gene mRNAs. Three other miRNA-like RNAs turn out to be cleaved from H/ACA box snoRNAs and they also regulated expression of the reporter gene. What is of special importance, the silencing activity differed among all investigated cell types. Representatives of the experimentally validated functional miRNA-like sdRNAs and their position within the secondary structures of snoRNA counterparts are presented in Fig. 1.

Recent research aiming at deep sequencing of small non coding RNAs from patients with prostate cancer and normal prostate at different disease stages, shed a new light on the importance of snoRNA fragments in cancer tissues (Martens-Uzunova *et al.,* 2015). Surprisingly, it turned out that at least 78 of the detected sdRNAs, including SNORD44, SNORD78, SNORD74 and SNORD81, demonstrate a strong differential expression in prostate cancer patients, which was even stronger than in the case of miRNAs. Most of sdRNAs originated from equivalent locations of their precursors and often one predominant sdRNA was observed per precursor snoRNA. High levels of SNORD78 in a patient who developed metastatic disease suggested that this sdRNA could be a novel prognostic biomarker for the prostate cancer patients with a high risk of developing metastasis. What is worth to mention, Martens-Uzunova and coworkers also discovered that the tRNA fragments could be present in high amounts in metastatic samples (Martens-Uzunova *et al.,* 2012).

The p53 protein is an tumor suppressor gene and it plays a crucial role in the prevention of oncogenic transformation. In 2015, Nielsen and his group published novel and unobvious results demonstrating a role for p53 in repression of a family of polycistronic C/D box snoRNAs, of which at least one is processed into an operative miRNA-like RNA (Yu *et al.,* 2015). This snoRNA fragment represses TAF9B-mediated stabilization of p53 and promotes cell proliferation, which in turn leads to breast cancer.

Moreover, snoRNA-derived miRNAs can also modulate cellular drug disposition (Pan *et al.,* 2013). The hsa-miRNA-1291 is a small non-coding RNA derived from H/ACA SNORA34 which modulates cellular drug disposition and chemosensitivity through binding to the 3'UTR of *ABCC1* mRNA and negative regulation of its expression. ABCC1 is a membrane transporter that is expressed ubiquitously in human tissues and contributes to cellular disposition of numerous xenobiotics. Such regulation of ABCC1 expression is responsible for a significantly increased level of intracellular drug accumulation and chemosensitivity. Furthermore, it has been found that hsa-miRNA-1291 is significantly downregulated in human pancreatic ductal adenocarcinoma, when compared to normal pancreas. Better understanding of regulation of ABC transporters might therefore help to develop a rational drug therapy for cancer patients.

Interestingly, using an alternative computational approach for non-coding RNA detection based on the properties of promoter regions of well-characterized ncRNAs, in 2015 Qu et al. were able to detect two dicistronic genes encoding precursors that are processed into mature snoRNA and miRNA molecules in *Arabidopsis thaliana* (Qu *et al.,* 2015). Both, the snoRNAs and the miRNA transcribed from the two identified dicistronic snoRNA-miRNA775 and sno-miRNA779 genes have a common precursor and they use two distinct maturation pathways that preserve the integrity of both ncRNAs.

Although the components of the machinery necessary for miRNA action are conserved in diverse eukaryotic species, including budding yeast *Saccharomyces castellii* and *Candida albicans*, they have been lost in the budding yeast *Saccharomyces cerevisiae* (Houseley *et al.,* 2008). However, the presence of snoRNA processing products was demonstrated by high throughput sequencing studies and further validated with small RNA detection techniques in *S. cerevisiae*. Although yeast sdRNAs were observed in very low abundance in small-RNA sequencing studies (Zywicki *et al.,* 2012), they could be easily detected with

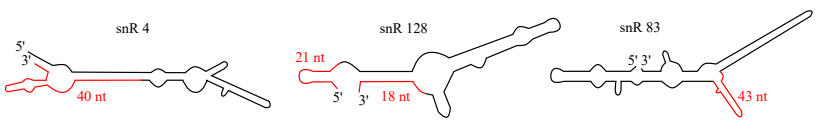

Figure 2. Atypical sdRNAs in *Saccharomyces cerevisiae*.
Predicted secondary structures of the following snoRNAs are presented: snR 4, snR 128 and snR 83. sdRNA positions as well as their length are marked in red. Different types of sdRNA locations within the secondary structure of snoRNAs: 3'-part-derived, 5'-part-derived or middle-part-derived.

stem-loop RT-PCR (SL-RT-PCR) method with as little as 50 ng of low molecular weight RNA (Walkowiak *et al.,* 2016). These results confirmed the presence of shortened version of both types of snoRNAs (C/D and H/ACA box) in baking yeast. The processing events were most prominent under non-optimal yeast growth conditions. What is interesting, yeast snoRNA fragments have different length than typical microRNA-like sdRNAs, ranging from 18 nt to 43 nt and the processing sites may be located within the 3' part of snoRNA, 5' part, both of them or snoRNA middle part (Fig. 2). What is of special importance, these sdRNAs have been co-purified with the yeast ribosomes (Zywicki *et al.,* 2012). Therefore, the sdRNA/ribosome association might implicate a novel, yet undiscovered regulatory role of sdRNAs in ribosome biosynthesis and/or function in *S. cerevisiae*, independent from the microRNA-like pathway. Considering the fact that 30% of known genes involved in human diseases have yeast orthologs, and that the oxidative stress has been linked to diseases such as cancer, or to aging processes, sdRNA interactions with ribosomes in yeast might improve our understanding of defense mechanisms ranging from microorganisms to humans. Possible functions of snoRNA-derived fragments are summarized in Table 2.

snoRNAs IN MALIGNANCY DEVELOPMENT

Cancer is one of the major causes of human death, accounting for 8.2 million deaths in 2012 worldwide (World Health Organization statistics). It is therefore of crucial importance to identify and characterize the genetic alterations causing distinct types of cancer. One of the processes that could lead to the transformation of normal cells into the tumor cells are defects in ribosome maturation and function. Ribosomal RNA biogenesis is known to be more robust in cancer cells than in normal cells (Belin *et al.,* 2009). Since snoRNAs are involved in the regulation of ribosomal RNA modification, it is therefore logical to suspect their possible roles in cancer development. It can be assumed that increase in the snoRNA levels is necessary for the acceleration of rRNA maturation, ribosome assembling and protein synthesis during tumorigenesis. Indeed, in 2002 Chang and coworkers showed for the first time that snoRNAs are involved in the development of cancer (Chang *et al.,* 2002). They found that h5sn2 snoRNA which belongs to H/ACA box family was highly expressed in normal brain but its expression was reduced in meningioma, pointing that loss of snoRNA h5sn2 is involved in brain tumorigenesis.

snoRNAs have been also found to be involved in development of the non-small-cell lung cancer (NSCLC), which is the leading cause of cancer deaths in the world (1.59 million deaths in 2012, according to the World Health Organization). Unfortunately, for most patients the available treatments are not sufficient, which clearly provides the reason for improving the NSCLC early detection. In 2010 Liao and coworkers presented the first study which globally analyzed the snoRNA expression patterns in human tumor tissues (Liao *et al.,* 2010). Interestingly, the set of snoRNAs was overexpressed in the lung tumor tissue and compared with their normal counterparts. In this study, Liao and coworkers proposed a potential diagnostic test for NSCLC by measuring plasma snoRNA expressions by real-time quantitative reverse transcriptase PCR (qRT-PCR). Later on, the function of one of the overexpressed H/ACA box snoRNAs, SNORA42 (U42) was studied in greater detail (Mei *et al.,* 2012). siRNA knockdown of SNORA42 resulted in a reduced cancer cell growth and compromised tumorigenicity in animal models by inducing p53-dependent apoptosis. On the contrary, overexpression of SNORA42 activated cancer cell growth. Moreover, the expression level of SNORA42 in lung tumor tissue specimen was found to be inversely correlated with the survival of NSCLC patients. In 2015, a significant upregulation of SNORD78 (U78) levels in NSCLC tissues was observed by Zheng and coworkers (2015). In this case, silencing of SNORD78 expression inhibited cell proliferation by inducing the phase G0/G1 arrest and cell apoptosis.

snoRNA expression profiling may be useful in the diagnosis of some subtypes of Peripheral T-cell lymphoma and the prognostication of cancer patients treated with chemotherapy. In 2012, it has been revealed that multiple snoRNAs are globally down-regulated in the T-cell lymphoma cells when compared with normal tissues; the same was also observed for miRNA (Valleron *et al.,* 2012). Particularly interesting was the prognostic value of SNORD71 (HBII-239) snoRNA, which was significantly overexpressed in the case of angio-immunoblastic T-cell lymphoma and Peripheral T-cell lymphoma that were not otherwise specified. Such overexpression predicts a good prognosis for patients. What is also worth to mention, the SNORD71 fragment (which was called miRNA-768) is also overexpressed in tissues of patients with good prognosis and can be a powerful prognostic tool.

Another example of snoRNA downregulation in tumor cells comes from the research on hepatocellular carcinoma (Xu *et al.,* 2014). Lowered expression of SNORD113-1 was correlated with cancer progression, cancer development and patient survival. Functional analyses revealed that overexpression of this snoRNA inhibited viability, tumorigenicity and cell growth of tumor cells, probably by the MAPK/ERK and TGF-β pathway-dependent mechanisms. Hence, SNORD113-1 was proposed to be not only a potential diagnostic tool for hepatocellular cancer but also a potential therapeutic target.

One of the most common mutations causing many different types of human cancers, including breast and prostate cancer, is a deletion of chromosome 6 and its q14-q22 fragment (Dong, 2001). In 2008, Dong and his group revealed that SNORD50a (U50) gene can act as a 6q tumor suppressor (Dong *et al.,* 2008). They have discovered that a 2-bp germline homozygous deletion of SNORD50a was associated with clinically significant prostate cancer. What is more, one year later the same group revealed that deletion of SNORD50a leads to de-

Table 2. Examples of diverse snoRNA and sdRNA functions with emphasis on human diseases.

sno/ sdRNA	Name	Type	Disease/function	Organism	References
full-lenght snoRNAs	SNORD116 (HBII-85)	C/D	PWS	Clinical specimens	Duker *et al.,* 2010
	SNORD115 (HBII – 52)	C/D	PWS/alternative splicing	Clinical specimens	Kishore & Stamm, 2006
	SNORD32a (U32a), SNORD32a (U33), SNORD34 (U34), SNORD35a (U35a)	C/D	lipotoxic and oxidative cellular stress response	Chinese hamster ovary cells	Michel *et al.,* 2011
	SNORD50a (U50)	C/D	prostate and breast cancer	Human prostate / breast cancer cell lines and clinical specimens	Dong *et al*., 2008; Dong *et al.,* 2009
	SNORD42 (U42)	C/D	NSCLC	Human lung cancer cell lines and clinical specimens	Mei *et al.,* 2012
	SNORD78 (U78)	C/D	NSCLC	Clinical specimens	Zheng *et al.,* 2015
	SNORD113-1	C/D	hepatocellular carcinoma	Human hepatocellular carcinoma cell lines and clinical specimens	Xu *et al.,* 2014
	SNORD35B (U35B)	C/D	HNSCC	Clinical specimens	Zou *et al.,* 2015
	SNORD71 (HBII-239)	C/D	peripheral T-cell lymphoma	Clinical specimens	Valleron *et al.*, 2012
	h5sn2	H/ACA	brain tumors	Clinical specimens	Chang *et al.,* 2002
snoRNA-derived fragments	SNORD44, SNORD78, SNORD74, SNORD81	C/D	prostate cancer	Clinical specimens	Martens-Uzunova *et al.,* 2015
	MBII-52	C/D	PWS/alternative splicing	TgPWS mouse model	Bortolin-Cavaille & Cavaille, 2012, Kischore *et al.*, 2010
	GlsR17, GlsR2	C/D	miRNA-like functions	Giardia lambia	Saraiya & Wang, 2008 Li *et al*., 2011
	SNORD2 (snR39b), SNORD78 (U78), SNORD93 (HBII-336), SNORD100 (HBII-429),SNORD66 (HBII-142), SNORD74 (U74), SNORD15a (U15a)	C/D	miRNA-like functions	HeLa, Jurkat (T cells) and RPMI8866 (B cell)	Brameier *et al*., 2011
	SNORD3@ (U3)	C/D	miRNA-like functions	HeLa and RPMI8866	Brameier *et al.,* 2011
	SNORD83a (U83a)	C/D	miRNA-like functions	Jurkat and RPMI8866	Brameier *et al.,* 2011
	SNORD27 (U27)	C/D	miRNA-like functions	Jurkat	Brameier *et al*., 2011
	Sno-miRNA-28	C/D	miRNA-like functions	Breast cancer cell lines (MDA-MB-231 MCF10A)	Yu *et al.,* 2015
	SNORA34 (ACA34), SNORA81 (HBI-61)	H/ACA	miRNA-like functions	HeLa, Jurkat, RPMI8866	Brameier *et al.,* 2011
	SNORA36b (ACA36b)	H/ACA	miRNA-like functions	HeLa, Jurkat	Brameier *et al.,* 2011
	SCARNA15 (ACA45)	H/ACA	miRNA-like functions	HEK293	Ender *et al.,* 2009
	hsa-miRNA-1291	H/ACA	miRNA-like functions	PANC-1	Pan *et al.,* 2013

velopment and/or progression of breast cancer (Dong *et al.,* 2009). Interestingly, in breast cancer, homozygosity of the deletion was rare in both, the cases and controls. This difference between prostate cancer and breast cancer could suggest that breast cells are more susceptible to SNORD50a mutation, when comparing to prostate cancer cells.

Head and neck squamous cell carcinoma (HNSCC) is one of the six most common cancers in the world (Ferlay *et al.* 2008). Recent research aiming at sequencing of a transcriptome of head and neck squamous cell carcinoma tissue revealed 33 significantly deregulated snoRNAs, ranging from about 4-fold to 3-fold for SNORD116-20 and SNORD60, respectively (Zou *et al.,* 2015). Moreover, lower expression of SNORD35B (U35B), a snoRNA downregulated in HNSCC, served as an adverse prognostic factor for patient survival.

snoRNAs IN THE PRADER–WILLI SYNDROME

The Prader–Willi syndrome (PWS) is a rare genetic disorder manifested by mental retardation, poor muscle tone, incomplete sexual development, cognitive and behavioral disabilities. The major cause of the PWS is the loss of paternal gene expression from a maternally imprinted region 15q11–q13 on chromosome 15. This locus contains numerous copies of snoRNAs and already in the year of 2000 it was reported that three human snoRNAs, expressed in brain tissue, map to the PWS region (de los Santos *et al.,* 2000). Recent discoveries have indeed pointed out that snoRNAs play a significant role in this disease. It has been observed that even a small microdeletion at 15q11.2 critical region that included the SNORD116 cluster (HBII-85), caused a Prader-Willi syndrome phenotype in an 11-year old patient (Duker *et al.,* 2010). Other studies had shown additional evidence that the same cluster of snoRNAs with unique, yet overlapping microdeletions lead to the loss of a paternal copy of the SNORD116 and PWS phenotype (Sahoo *et al.,* 2008; de Smith *et al.,* 2009).

The genetic loss of SNORD115 (HBII-52) likewise results in the PWS (Kishore & Stamm, 2006). It appeared that this missing snoRNAs is of special importance in PWS, since it changes the splice site selection. HBII-52 holds a sequence complementary to an alternatively spliced exon Vb of serotonin receptor 5-HT2CR and therefore regulates the alternative splicing of 5-HT2CR by binding to a silencing element in exon Vb. Lack of HBII-52 leads to defects in pre-mRNA processing and, as a consequence, patients with the Prader-Willi syndrome with loss of paternal HBII-52 gene have different messenger RNA isoforms. As a follow-up of these studies, the same group identified five additional pre-mRNAs (DPM2, TAF1, RALGPS1, PBRM1 and CRHR1) containing alternative exons that are regulated by MBII-52, a mouse homolog of HBII-52 (Kishore *et al.,* 2010). Notably, the analysis of a single member of the MBII-52 cluster had shown that the MBII-52 expressing unit generates shorter RNAs that originate from the full-length MBII-52 snoRNA, through an additional processing steps. These novel RNAs interact with hnRNPs and not with the proteins associated with canonical C/D box snoRNAs. These data indicated that not a traditional C/D box snoRNA MBII-52, but a processed version lacking the snoRNA stem is a predominant MBII-52 RNA missing in PWS. This processed snoRNA is a few nucleotides shorter at the 5' end than the full-length snoRNA and functions in alternative splice-site selection (Bortolin-Cavaille & Cavaille, 2012; Kischore *et al.,* 2010).

snoRNAs AS METABOLIC STRESS REGULATORS

SnoRNAs can be also regulators of metabolic stress response pathways, as observed in Chinese hamster ovary cells (Michel *et al.,* 2011). Four C/D box snoRNAs: SNORD32a (U32a), SNORD32a (U33), SNORD34 (U34) and SNORD35a (U35a) located in the ribosomal protein rpL13a locus, are highly conserved across mammalian species. In addition to their primary role in the ribosomal RNA modification, they also regulate a lipotoxic and oxidative cellular stress responses. Loss of three snoRNAs encoded in the rpL13a locus is sufficient to induce resistance to oxidative and lipotoxic stresses *in vitro* and prevents the spread of oxidative stress *in vivo*.

CONCLUSIONS

Small nucleolar RNAs are a large class of small noncoding RNAs which primarily guide chemical modifications of other RNAs. Rapid development of high-throughput and deep-sequencing technologies has significantly broadened our view of snoRNA characteristics and functionality. However, in higher eukaryotes, many orphan snoRNAs were discovered without known target and function, suggesting that they may play different roles in the cellular life. Moreover, a growing number of evidence clearly shows that many snoRNAs are processed into shorter functional forms, whose generation is still not completely understood. Small nucleolar RNAs may be processed into short miRNA-like RNAs as well as longer sdRNAs. miRNA-like molecules derived from snoRNAs can play a role in regulation of gene expression, whereas many other sdRNAs possess yet undiscovered functions. In the 1990s and at the beginning of the 21st century many investigations gave numerous information concerning the structure and function of canonical snoRNAs. Recently, many studies revealed new functions of snoRNAs and their fragments. The knowledge in the field of snoRNAs and sdRNAs is still developing and more information is being gained. Thus, in the next years we may discover a great number of novel snoRNAs and sdRNAs functions.

Acknowledgements

This work was supported by the National Science Centre, Poland [2014/13/D/NZ1/00061 to K.B.-Ż.] and by the Polish Ministry of Science and Higher Education, under the KNOW program.

REFERENCES

Babiarz JE, Hsu R, Melton C, Thomas M, Ullian EM, Blelloch R (2011) A role for noncanonical microRNAs in the mammalian brain revealed by phenotypic differences in Dgcr8 versus Dicer1 knockouts and small RNA sequencing. *RNA* **17**: 1489–1501. doi 10.1261/rna.2442211

Babiarz JE, Ruby JG, Wang Y, Bartel DP, Blelloch R (2008) Mouse ES cells express endogenous shRNAs, siRNAs, and other Microprocessor-independent, Dicer-dependent small RNAs. *Genes Dev* **22**: 2773–2785. doi 10.1101/gad.1705308

Bai B, Yegnasubramanian S, Wheelan SJ, Laiho M (2014) RNA-Seq of the nucleolus reveals abundant SNORD44-derived small RNAs. *PLoS One* **9**: e107519. doi 10.1371/journal.pone.0107519

Belin S, Beghin A, Solano-Gonzalez E, Bezin L, Brunet-Manquat S, Textoris J, Prats AC, Mertani HC, Dumontet C, Diaz JJ (2009) Dysregulation of ribosome biogenesis and translational capacity is

associated with tumor progression of human breast cancer cells. *PLoS One* **4**: e7147. doi 10.1371/journal.pone.0007147
Bortolin-Cavaille ML, Cavaille J (2012) The SNORD115 (H/MBII-52) and SNORD116 (H/MBII-85) gene clusters at the imprinted Prader-Willi locus generate canonical box C/D snoRNAs. *Nucleic Acids Res* **40**: 6800–6807. doi 10.1093/nar/gks321
Brameier M, Herwig A, Reinhardt R, Walter L, Gruber J (2011) Human box C/D snoRNAs with miRNA like functions: expanding the range of regulatory RNAs. *Nucleic Acids Res* **39**: 675–686. doi 10.1093/nar/gkq776
Burroughs AM, Ando Y, de Hoon MJ, Tomaru Y, Suzuki H, Hayashizaki Y, Daub CO (2011) Deep-sequencing of human Argonaute-associated small RNAs provides insight into miRNA sorting and reveals Argonaute association with RNA fragments of diverse origin. *RNA Biol* **8**: 158–177
Chang LS, Lin SY, Lieu AS, Wu TL (2002) Differential expression of human 5S snoRNA genes. *Biochem Biophys Res Commun* **299**: 196–200
de los Santos T, Schweizer J, Rees CA, Francke U (2000) Small evolutionarily conserved RNA, resembling C/D box small nucleolar RNA, is transcribed from PWCR1, a novel imprinted gene in the Prader-Willi deletion region, which Is highly expressed in brain. *Am J Hum Genet* **67**: 1067–1082. doi 10.1086/303106
de Smith AJ, Purmann C, Walters RG, Ellis RJ, Holder SE, Van Haelst MM, Brady AF, Fairbrother UL, Dattani M, Keogh JM, Henning E, Yeo GS, O'Rahilly S, Froguel P, Farooqi IS, Blakemore AI (2009) A deletion of the HBII-85 class of small nucleolar RNAs (snoRNAs) is associated with hyperphagia, obesity and hypogonadism. *Hum Mol Genet* **18**: 3257–3265. doi 10.1093/hmg/ddp263
Dong JT (2001) Chromosomal deletions and tumor suppressor genes in prostate cancer. *Cancer Metastasis Rev* **20**: 173–193
Dong XY, Guo P, Boyd J, Sun X, Li Q, Zhou W, Dong JT (2009) Implication of snoRNA U50 in human breast cancer. *J Genet Genomics* **36**: 447–454. doi 10.1016/S1673-8527(08)60134-4
Dong XY, Rodriguez C, Guo P, Sun X, Talbot JT, Zhou W, Petros J, Li Q, Vessella RL, Kibel AS, Stevens VL, Calle EE, Dong JT (2008) SnoRNA U50 is a candidate tumor-suppressor gene at 6q14.3 with a mutation associated with clinically significant prostate cancer. *Hum Mol Genet* **17**: 1031–1042. doi 10.1093/hmg/ddm375
Duker AL, Ballif BC, Bawle EV, Person RE, Mahadevan S, Alliman S, Thompson R, Traylor R, Bejjani BA, Shaffer LG, Rosenfeld JA, Lamb AN, Sahoo T (2010) Paternally inherited microdeletion at 15q11.2 confirms a significant role for the SNORD116 C/D box snoRNA cluster in Prader-Willi syndrome. *Eur J Hum Genet* **18**: 1196–1201. doi 10.1038/ejhg.2010.102
Ender C, Krek A, Friedlander MR, Beitzinger M, Weinmann L, Chen W, Pfeffer S, Rajewsky N, Meister G (2008) A human snoRNA with microRNA-like functions. *Mol Cell* **32**: 519–528. doi 10.1016/j.molcel.2008.10.017
Falaleeva M, Stamm S (2013) Processing of snoRNAs as a new source of regulatory non-coding RNAs: snoRNA fragments form a new class of functional RNAs. *Bioessays* **35**: 46–54. doi 10.1002/bies.201200117
Ferlay J, Shin HR, Bray F, Forman D, Mathers C, Parkin DM (2010) Estimates of worldwide burden of cancer in 2008: GLOBOCAN 2008. *Int J Cancer* **127**: 2893–2917. doi 10.1002/ijc.25516
Houseley J, Tollervey D (2008) The nuclear RNA surveillance machinery: the link between ncRNAs and genome structure in budding yeast? *Biochim Biophys Acta* **1779**: 239–246. doi 10.1016/j.bbagrm.2007.12.008
Hutzinger R, Feederle R, Mrazek J, Schiefermeier N, Balwierz PJ, Zavolan M, Polacek N, Delecluse HJ, Huttenhofer A (2009) Expression and processing of a small nucleolar RNA from the Epstein-Barr virus genome. *PLoS Pathog* **5**: e1000547. doi 10.1371/journal.ppat.1000547
Kawaji H, Nakamura M, Takahashi Y, Sandelin A, Katayama S, Fukuda S, Daub CO, Kai C, Kawai J, Yasuda J, Carninci P, Hayashizaki Y (2008) Hidden layers of human small RNAs. *BMC Genom* **9**: 157. doi 10.1186/1471-2164-9-157
Kishore S, Khanna A, Zhang Z, Hui J, Balwierz PJ, Stefan M, Beach C, Nicholls RD, Zavolan M, Stamm S (2010) The snoRNA MBII-52 (SNORD 115) is processed into smaller RNAs and regulates alternative splicing. *Hum Mol Genet* **19**: 1153–1164. doi 10.1093/hmg/ddp585
Kishore S, Stamm S (2006) The snoRNA HBII-52 regulates alternative splicing of the serotonin receptor 2C. *Science* **311**: 230–232. doi 10.1126/science.1118265
Li W, Saraiya AAWang CC (2011) Gene regulation in *Giardia lambia* involves a putative microRNA derived from a small nucleolar RNA. *PLoS Negl Trop Dis* **5**: e1338. doi 10.1371/journal.pntd.0001338
Li Z, Ender C, Meister G, Moore PS, Chang Y, John B (2012) Extensive terminal and asymmetric processing of small RNAs from rRNAs, snoRNAs, snRNAs, and tRNAs. *Nucleic Acids Res* **40**: 6787–6799. doi 10.1093/nar/gks307
Liao J, Yu L, Mei Y, Guarnera M, Shen J, Li R, Liu Z, Jiang F (2010) Small nucleolar RNA signatures as biomarkers for non-small-cell lung cancer. *Mol Cancer* **9**: 198. doi 10.1186/1476-4598-9-198
Martens-Uzunova ES, Hoogstrate Y, Kalsbeek A, Pigmans B, Vredenbregt-van den Berg M, Dits N, Nielsen SJ, Baker A, Visakorpi T, Bangma C, Jenster G (2015) C/D-box snoRNA-derived RNA production is associated with malignant transformation and metastatic progression in prostate cancer. *Oncotarget* **6**: 17430–17444. doi 10.18632/oncotarget.4172
Martens-Uzunova ES, Jalava SE, Dits NF, van Leenders GJ, Moller S, Trapman J, Bangma CH, Litman T, Visakorpi T, Jenster G (2012) Diagnostic and prognostic signatures from the small non-coding RNA transcriptome in prostate cancer. *Oncogene* **31**: 978–991. doi 10.1038/onc.2011.304
Mei YP, Liao JP, Shen J, Yu L, Liu BL, Liu L, Li RY, Ji L, Dorsey SG, Jiang ZR, Katz RL, Wang J, YJiang F (2012) Small nucleolar RNA 42 acts as an oncogene in lung tumorigenesis. *Oncogene* **31**: 2794–2804. doi 10.1038/onc.2011.449
Michel CI, Holley CL, Scruggs BS, Sidhu R, Brookheart RT, Listenberger LL, Behlke MA, Ory DS, Schaffer JE (2011) Small nucleolar RNAs U32a, U33, and U35a are critical mediators of metabolic stress. *Cell Metab* **14**: 33–44. doi 10.1016/j.cmet.2011.04.009
Mleczko AM, Celichowski P, Bąkowska-Żywicka K (2014) Ex-translational function of tRNAs and their fragments in cancer. *Acta Biochim Pol* **61**: 211–216.
Pan YZ, Zhou A, Hu Z, Yu AM (2013) Small nucleolar RNA-derived microRNA hsa-miR-1291 modulates cellular drug disposition through direct targeting of ABC transporter ABCC1. *Drug Metab Dispos* **41**: 1744–1751. doi 10.1124/dmd.113.052092
Qu G, Kruszka K, Plewka P, Yang SY, Chiou TJ, Jarmolowski A, Szweykowska-Kulinska Z, Echeverria M, Karlowski WM (2015) Promoter-based identification of novel non-coding RNAs reveals the presence of dicistronic snoRNA-miRNA genes in Arabidopsis thaliana. *BMC Genomics* **16**: 1009. doi 10.1186/s12864-015-2221-x
Sahoo T, del Gaudio D, German JR, Shinawi M, Peters SU, Person RE, Garnica A, Cheung SW, Beaudet AL (2008) Prader-Willi phenotype caused by paternal deficiency for the HBII-85 C/D box small nucleolar RNA cluster. *Nat Genet* **40**: 719–721. doi 10.1038/ng.158
Saraiya AA, Wang CC (2008) snoRNA, a novel precursor of microRNA in *Giardia lamblia*. *PLoS Pathog* **4**: e1000224. doi 10.1371/journal.ppat.1000224
Scott MS, Ono M, Yamada K, Endo A, Barton GJ, Lamond AI (2012) Human box C/D snoRNA processing conservation across multiple cell types. *Nucleic Acids Res* **40**: 3676–3688. doi 10.1093/nar/gkr1233
Taft RJ, Glazov EA, Lassmann T, Hayashizaki Y, Carninci P, Mattick JS (2009) Small RNAs derived from snoRNAs. *RNA* **15**: 1233–1240. doi 10.1261/rna.1528909
Tyczewska A, Bąkowska-Żywicka K, Gracz J, Twardowski T (2016) Stress responsive non-protein coding RNAs, Abiotic and biotic stress in plants – recent advances and future perspectives, chapter 7
Valleron W, Laprevotte E, Gautier EF, Quelen C, Demur C, Delabesse E, Agirre X, Prosper F, Kiss T, Brousset P (2012) Specific small nucleolar RNA expression profiles in acute leukemia. *Leukemia* **26**: 2052–2060. doi 10.1038/leu.2012.111
Valleron W, Ysebaert L, Berquet L, Fataccioli V, Quelen C, Martin A, Parrens M, Lamant L, de Leval L, Gisselbrecht C, Gaulard P, Brousset P (2012) Small nucleolar RNA expression profiling identifies potential prognostic markers in peripheral T-cell lymphoma. *Blood* **120**: 3997–4005. doi 10.1182/blood-2012-06-438135
Walkowiak M, Mleczko AM, Bąkowska – Żywicka K (2016) Evaluation of methods for detection of low-abundant snoRNA-derived small RNAs in *Saccharomyces cerevisiae*. *BioTechnologia* **97**: 19–26. DOI: 10.5114/bta.2016.58540
Xu G, Yang F, Ding CL, Zhao LJ, Ren H, Zhao P, Wang W, Qi ZT (2014) Small nucleolar RNA 113-1 suppresses tumorigenesis in hepatocellular carcinoma. *Mol Cancer* **13**: 216. doi 10.1186/1476-4598-13-216
Yu F, Bracken CP, Pillman KA, Lawrence DM, Goodall GJ, Callen DF, Neilsen PM (2015) p53 Represses the Oncogenic Sno-MiR-28 Derived from a SnoRNA. *PLoS One* **10**: e0129190. doi 10.1371/journal.pone.0129190
Zheng D, Zhang J, Ni J, Luo J, Wang J, Tang L, Zhang L, Wang L, Xu J, Su B, Chen G (2015) Small nucleolar RNA 78 promotes the tumorigenesis in non-small cell lung cancer. *J Exp Clin Cancer Res* **34**: 49. doi 10.1186/s13046-015-0170-
Zou AE, Ku J, Honda TK, Yu V, Kuo SZ, Zheng H, Xuan Y, Saad MA, Hinton A, Brumund KT, Lin JH, Wang-Rodriguez J, Ongkeko WM (2015) Transcriptome sequencing uncovers novel long noncoding and small nucleolar RNAs dysregulated in head and neck squamous cell carcinoma. *RNA* **21**: 1122–1134. doi 10.1261/rna.049262.114
Zywicki M, Bakowska-Zywicka K, Polacek N (2012) Revealing stable processing products from ribosome-associated small RNAs by deep-sequencing data analysis. *Nucleic Acids Res* **40**: 4013–4024. doi 10.1093/nar/gks020

4

Walkowiak M*, **Mleczko AM*,** Bąkowska – Żywicka K

Evaluation of methods for detection of low-abundant snoRNA-derived small RNAs in Saccharomyces cerevisiae

BioTechnologia, 2016, 97(1):19-26 *Autorzy mieli taki sam wkład w przygotowanie publikacji

BioTechnologia vol. 97(1) • pp. 19-26 • 2016
Journal of Biotechnology, Computational Biology and Bionanotechnology RESEARCH PAPERS
DOI: 10.5114/bta.2016.58540

Evaluation of methods for the detection of low-abundant snoRNA-derived small RNAs in *Saccharomyces cerevisiae*

MATEUSZ WALKOWIAK#, ANNA M. MLECZKO#, KAMILLA BĄKOWSKA-ŻYWICKA*

Institute of Bioorganic Chemistry, Polish Academy of Sciences, Poznań, Poland

# both authors contributed equally to this work

Abstract

In recent years, there are a growing number of studies demonstrating the existence of small RNAs derived from snoRNAs (sdRNAs) in multiple eukaryotic organisms. Such RNAs have been initially observed in high throughput sequencing studies and assumed to be processed by miRNA machinery. Recently, we have identified sdRNAs that are associated with ribosomes in yeast *Saccharomyces cerevisiae*. Although sdRNAs were detectable in sequencing data, their low abundance hampered their detection by other methods. Here, we present the results of our survey for optimized experimental method for sdRNA detection. We have compared two extraction procedures of total RNA from *S. cerevisiae*: MasterPure™ kit and Trizol with two methods resulting in enrichment in small RNA fraction and MasterPure™ with selective isopropanol precipitation and bulk tRNA isolation methods. Also the sensitivity of three methods for sdRNA detection was verified: a northern blot using standard or LNA probes and stem-loop reverse transcription followed by PCR (SL-RT-PCR). Our results reveal that Trizol isolation method combined with SL-RT-PCR is the most effective in the detection of low-abundant sdRNAs.

Key words: snoRNA, sdRNA, small RNA, ribosome-associated RNA, rancRNA, *Saccharomyces cerevisiae*

Introduction

Small nucleolar RNAs (snoRNAs) are highly evolutionarily conserved class of RNAs, which are present throughout the eukaryotes, and are classified into two groups, namely, C/D and H/ACA box that function as ribonucleoprotein (RNP) complexes to guide enzymatic modification of the target RNAs at sites determined by RNA : RNA antisense interactions. Generally, most of C/D box snoRNAs are 70-120 nucleotides (nt) long guiding methylation of the target RNAs, while H/ACA box snoRNAs are usually 100-300 nt long guiding pseudouridylation. These RNAs were initially discovered in nucleolus and thought to exclusively target ribosomal RNAs inside this sub-nuclear compartment. However, the finding that numerous snoRNAs do not possess target RNAs (Huttenhofer et al. 2001; Jady and Kiss 2000; Cavaille et al. 2000; Vitali et al. 2003) opened us (scientists) to new possibilities concerning snoRNAs' functions and targets. For example, SNORD114-1 snoRNA has been shown to promote G0/G1 to S phase transition through cell cycle and to be deregulated in cancer cells (Valleron et al. 2012). Another C/D box snoRNA, SNORD115 (HBII-52), reveals the sequence complementarity to the alternative splice site of serotonin receptor 2C pre-mRNA, and thus influences its alternative splicing (Kishore and Stamm 2006). Unexpectedly, some canonical snoRNAs with known ribosomal targets (SNORD32A (U32A), SNORD33 (U33), and SNORD35A (U35A)) have been shown to accumulate in the cytosol under cellular stress conditions in higher eukaryotes (Michel et al. 2011). Similar to other RNA species, they can be subjected to degradation and processing performed by non-nuclear RNases. Recently, several reports have identified small (18-22 nt) RNA derivatives of snoRNAs, termed as "snoRNA-derived RNAs" (sdRNAs, reviewed in Falaleeva and Stamm 2013 and Tyczewska et al. 2016). It has been shown that several sdRNAs reveal miRNA-like properties, or regulate alternative mRNA splicing (Ender et al. 2008; Brameier et al. 2011; Kishore et al. 2010). Parallel next-generation sequencing

* Corresponding author: Institute of Bioorganic Chemistry, Polish Academy of Sciences, Noskowskiego St. 12/14, 61-704 Poznań, Poland; e-mail: bakowska@ibch.poznan.pl

studies of the small transcriptome in mice revealed the presence of snoRNA-originating miRNAs in embryonic stem cells and demonstrated that such sdRNAs exhibit tissue-specific expression profiles (Babiarz et al. 2008; Babiarz et al. 2011). At the same time, snoRNA-originating miRNA-like molecules were described in the protozoan *Giardia lamblia*, a unicellular parasite whose genome does neither encode Drosha nor Dicer, suggesting the existence of an alternative processing pathway (Saraiya and Wang 2008; Li et al. 2011). One year later, the same snoRNA-processing event was described in cells infected with Epstein-Bar virus (EBV). In this system, a miRNA-like precursor endogenously encoded by a viral v-snoRNA1 is expressed upon induction of the lytic cycle to suppress viral DNA polymerase (Hutzinger et al. 2009). miRNA-independent pathway of sdRNA maturation and function could also be expected in the budding yeast *Saccharomyces cerevisiae*, which does not possess components of the machinery necessary for microRNA action (Houseley and Tollervey 2008). Indeed, in our previous study, 10 known sdRNAs from *S. cerevisiae* have been identified as ribosome-associated ncRNAs (rancRNAs) (Zywicki et al. 2012). These yeast snoRNA fragments possess different length than typical microRNA-like sdRNAs, ranging from 18 nt to 60 nt. Although sdRNAs were observed in very low abundance within our cDNA libraries, their regulatory potential cannot be excluded. Our recent studies demonstrated that even a relatively small amount of 18-mer rancRNA (~27 000 molecules/cell) is sufficient to substantially influence global ribosome activity (~200 000 ribosomes/cell) and switch translation in the cell (Pircher et al. 2014).

Emerging novel regulatory potential of sdRNAs demonstrate that reliable detection of sdRNA expression is essential for better understanding of sdRNA-mediated gene expression regulation. However, due to their low abundance, conventional techniques such as cloning, northern hybridization, and microarray analyzes may not be sensitive enough to detect the complete repertoire of sdRNAs. This has been proven for low-abundant miRNAs that routinely escape detection with cloning, northern hybridization (Lim et al. 2003), and microarray analyzes (Krichevsky et al. 2003). Using the sensitive reverse transcription-polymerase chain reaction (RT-PCR) detection method, poor sensitivity and low throughput of conventional technologies can be overcome. However, the detection of sdRNAs by PCR is technically demanding due to their small size. A number of specific RT-PCR techniques were developed and optimized for miRNA detection, including real-time methods based on reverse transcription (RT) reaction with a stem-loop primer followed by a TaqMan PCR analysis (Chen et al. 2005; Tang et al. 2006; Varkonyi-Gasic et al. 2007). The stem-loop reverse transcription primers ensure higher specificity and sensitivity than linear primers because of base stacking and spatial constraints of the stem-loop structure (Chen et al. 2005). Detection sensitivity can be further increased by a pulsed RT reaction (Tang et al. 2006). These methods were, however, optimized for the detection of miRNAs, which are supposedly more abundant than sdRNAs.

On the contrary, it has also been shown that different purification methods may significantly affect the composition of RNA species in isolated RNA fractions (Kim et al. 2012). Several studies have tackled this point, focusing on methods for miRNA extraction (Monleau et al. 2014; Li and Kowdley 2012; Podolska et al. 2011); however, similar considerations could also be true in analyzing sdRNAs.

Here, the suitability of the northern blot and stem-loop RT-PCR (SL-RT-PCR) methods in detecting small RNAs derived from snoRNAs in *S. cerevisiae* was compared. Different RNA isolation methods that could vary in recovery of small RNA fraction were also evaluated. We provide evidence that low-abundant *S. cerevisiae* sdRNAs can be easily detected with SL-RT-PCR method with as little as 50 ng of low-molecular-weight RNA (LMW RNA, 10-60 nt). Using such protocol, we were able to robustly detect the expression of three sdRNAs identified in our previous studies as ribosome-associated RNAs (Zywicki et al. 2012).

Materials and methods

Strains and growth conditions

S. cerevisiae wild-type strain BY4741 (MATα; his3Δ1; leu2Δ0; met15Δ0; ura3Δ0) was grown in YPD medium at 30 °C.

RNA isolation

Using the following two different methods, total RNA was isolated from *S. cerevisiae*: 1) MasterPure™ Yeast RNA Purification kit (Epicenter) and 2) Trizol (Ambion), according to manufacturer's protocol.

Table 1. The sdRNAs, primers, and probes used in this study

Name	Type	Sequence [5′-3′]	Length [nt]
5′-sdRNA 67	**sdRNA**	**AACAUGAUGACUAAGUUGU**	**19**
	RT primer	GTCGTATCCAGTGCAGGGTCCGAGGTATTCGCACTGGATACGACACAACT	50
	Fwd primer	GGCGCGCGCGAACATGATGACTA	23
sdRNA 83	**sdRNA**	**GGACCAAUUACCGUAGUUGCGACUACAACAAUUUUGUUCAUA**	**42**
	RT primer	GTCGTATCCAGTGCAGGGTCCGAGGTATTCGCACTGGATACGACTATGAA	50
	Fwd primer	GACCAAUUACCGUAGUUGCGAC	22
	NB LNA	TATGA*ACA*CAATTG*TTGTA*GT	21
5′-sdRNA 128	**sdRNA**	**CACGGUGAUGAAAGACUGGUU**	**21**
	RT primer	GTCGTATCCAGTGCAGGGTCCGAGGTATTCGCACTGGATACGACAACCAG	50
	Fwd primer	GCGCGGGCACGGTGATGAAAGA	22
	NB aDNA	ACCAGTCTTTCATCACCGTGA	21
3′-sdRNA 128	**sdRNA**	**UCCUAGGAUGUCUGAGUG**	**18**
	RT primer	GTCGTATCCAGTGCAGGGTCCGAGGTATTCGCACTGGATACGACCACTCA	50
	Fwd primer	CGGCGGCCTCCTAGGATGTC	20
3′-sdRNA 4	**sdRNA**	**CCUUUAUAGCGGUGCUUUAACUAUUAAUAACU**	**32**
	NB aDNA	AGTTATTAATAGTTAAAGCACCGCTATAAAGG	32
	Uni primer	CCAGTGCAGGGTCCGAGGTA	20

Abbreviations: RT primer – stem-loop primer used for reverse transcription; Fwd primer – forward PCR primer; NB LNA – LNA probe for northern blot hybridization; NB aDNA – DNA probe for northern blot hybridization; Uni primer – universal PCR primer; sdRNA sequences are presented in bold. Position of LNA modification is underlined and marked with *

The RNA enriched in small RNA fraction (up to ~120 nt) was isolated according to two different protocols. First, MasterPure™ Yeast RNA purification kit (Epicenter) was combined with the enrichment of LMW RNAs with isopropanol. Briefly, RNA fraction longer than ~120 nt in size was precipitated using one third volume of isopropanol and discarded. Next, small RNAs (up to ~120 nt) that remained in the supernatant were precipitated using one volume of isopropanol. Second, bulk (unfractionated) tRNAs from *S. cerevisiae* were prepared as previously described (Monier et al. 1960). Briefly, unbuffered phenol 90% (equilibrated with water, Sigma) was added to cell lysates and mildly shaken at room temperature. Under such mild phenol treatment, preferentially the "soluble" RNAs (essentially tRNA, 5S-RNA, and small cellular RNAs) are released from the unbroken cells (Monier et al. 1960). The possible contamination of large ribosomal RNA was removed with 2 M LiCl.

For SL-RT-PCR method, Trizol-isolated total RNA was loaded on 10% denaturing polyacrylamide gel and LMW RNAs (LMW, 10-60 nt) were eluted from gel. Briefly, the bands of interest were excised from the gel with a razor blade. The gel slice was crushed, soaked in the elution buffer (300 mM NaOAc, 1 mM EDTA), and incubated with shaking for at least 16 h at 4°C. LMW RNAs were recovered from the eluate by ethanol precipitation. The concentration of RNA was determined using NanoDrop ND-1000 Spectrophotometer (NanoDrop Technologies).

Northern blot analysis

Of about 50-100 μg of RNAs were separated on 12% denaturing polyacrylamide gels and electrotransferred (45 min, 0.8 mA/cm^2 of a membrane) to positively charged Amersham Hybond N$^+$ membrane using a semi-dry blotter (BioRad). Nucleic acids were UV-cross-linked to membranes, which were then used immediately for northern blot hybridization or stored at room temperature. DNA oligonucleotide probes were synthesized by Genomed, LNA probe by Future Synthesis (Table 1). Hybridization was carried out overnight in 30 ml of a buffer (178 mM Na_2HPO_4, 882 mM NaH_2PO_4, 7% SDS). Two-

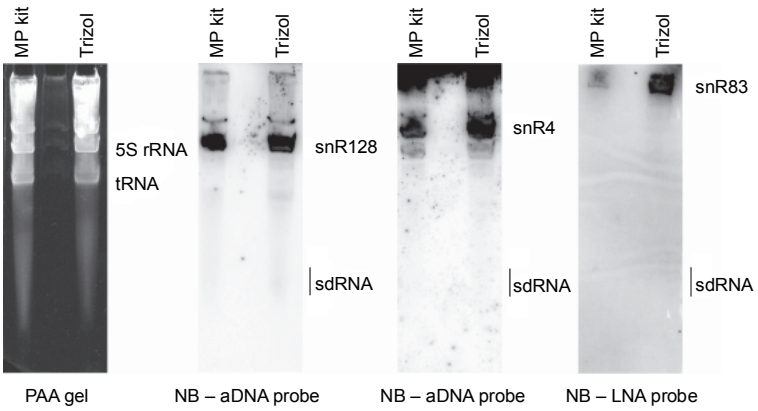

Fig. 1. Northern blot hybridization membranes with the total RNA. Denaturing polyacrylamide gel electrophoresis (left) and northern blot hybridization results (right) with 100 μg of total RNA isolated with MasterPure™ kit (MP kit, lane 1) and Trizol (lane 2). Position of tRNAs and 5S rRNA are marked on gel. Positions of full-length snoRNAs and estimated position of sdRNAs are marked on hybridization membranes

step washing was performed after hybridization: for 2 min in a washing solution I (2 × SSC, 0.1% SDS) and for 1 min in a washing solution II (0.1 × SSC, 0.1% SDS). Membranes were exposed overnight on the phosphor – storage intensity screen (Fujifilm). Screens were scanned with Fujifilm Fluorescent Image Analyzer FLA-5100. Size estimates for detected RNAs were determined using RNA markers (Promega or Invitrogen).

Stem-loop pulsed reverse transcription combined with PCR (SL-RT-PCR)

Reverse transcription reactions contained 10–200 ng of RNA samples, 50 nM stem-loop RT primer, 1 × RT buffer, 0.25 mM of each dNTPs, 50 U SuperScript SSIII reverse transcriptase (Invitrogen), 5 U RiboLock RNase Inhibitor (Thermo Scientific), and 10 mM of DTT. About 20 μl reactions were incubated in a Bio-Rad T100™ Thermocycler for 30 min at 16 °C, followed by pulsed RT of 60 cycles at 30 °C for 30 s, 42 °C for 30 s, and 50 °C for 1 s. To inactivate the reverse transcriptase, samples were incubated at 85 °C for 5 min and then held at 4 °C. All reverse transcriptase reactions, including no template controls, were run in triplicate. About 50 μl PCR reaction included 2 μl RT product, 25 μl of 2 × DreamTaq MasterMix, and 0.2 μM primers. The reactions were incubated at 95 °C for 3 min, followed by 25-31 cycles of 94 °C for 30 s, and 60 °C for 30 s, followed by 72 °C for 30 s. All reactions were run in triplicate.

The stem-loop RT primers were designed according to Chen et al. (2005). The specificity of SL-RT primers to individual sdRNA was conferred by a six nucleotide extension at the 3′ end; this extension was a reverse complement of the last six nucleotides at the 3′ end of the sdRNA (Table 1). Forward primers were specific to sdRNA sequence but excluded the last six nucleotides at the 3′ end of sdRNA. A 5′ extension of 5-7 nucleotides was added to each forward primer to increase melting temperature of the primers; these sequences were chosen randomly and are relatively GC-rich. We used Primer3Plus design software to assess the quality of forward primers.

Results

Hybridization-based technologies fail to detect sdRNAs

At the very first step, we decided to compare the efficiency of recovery of snoRNA fragments between two different methods of total RNA isolation: MasterPure™ Yeast RNA Purification kit and Trizol. After loading 100 μg of total RNA on 12% polyacrylamide gels and SYBR® Safe staining, we clearly observed good separation of distinct RNAs, including bulk tRNAs, 5S rRNA, and a portion of small RNAs (Fig. 1, left panel). Northern blot experiments were performed using antisense DNA (aDNA) probes specific for sdRNAs derived from snR128 and snR4 and LNA probe specific for sdRNA derived from snR83 (Table 1). In all tested cases, clear signals derived from full-length snoRNAs were observed (Fig. 1). However, both of the total RNA isolation methods failed to provide amounts of sdRNA fragments

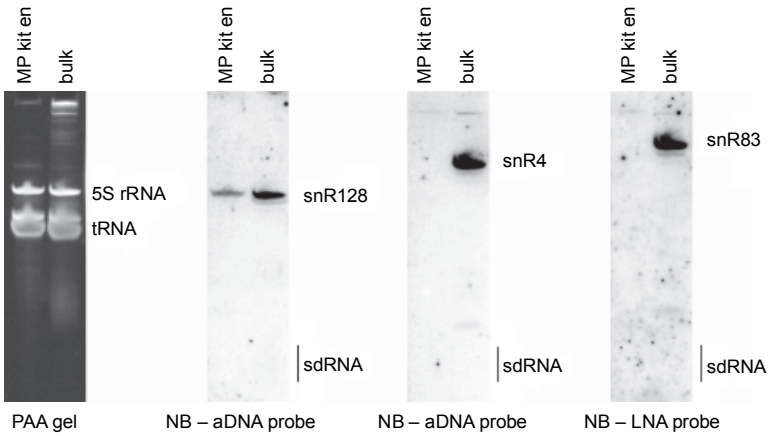

Fig. 2. Northern blot hybridization membranes with the total RNA enriched in small RNA fraction. Denaturing polyacrylamide gel electrophoresis (left) and northern blot hybridization results (right) with 25 μg of small RNAs (up to ~120 nt) isolated with MasterPure™ kit followed by selective small RNA precipitation (MP kit en, lane 1) and the bulk RNA isolation method (lane 2). Position of tRNAs and 5S rRNA are marked on the gel. Positions of full-length snoRNAs and the estimated position of sdRNAs are marked on hybridization membranes

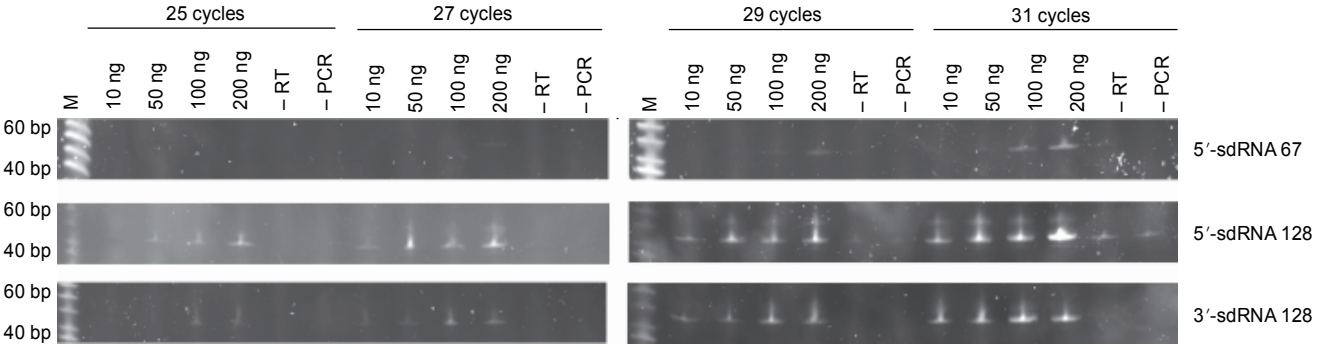

Fig. 3. Stem-loop RT-PCR assay for sdRNAs. Stem-loop RT-PCR analyses of the expression of sdRNAs: 5′-sdRNA 67, 5′-sdRNA 128 and 3′-sdRNA 128. About 10-200 ng of low molecular weight RNA (10-60 nt) was used for reverse transcription reactions. The number of PCR cycles is indicated at the top of lanes

above the clear detection threshold with either aDNA or LNA probe (Fig. 1).

Therefore, in order to maximize and concentrate the sdRNAs' amount within the tested RNA pools, total RNA fractions were enriched with small RNA fractions, up to ~120 nt in size. We have 1) combined MasterPure™ Yeast Purification kit with the selective isopropanol precipitation of small RNAs and 2) used bulk tRNA isolation method that results in isolation of soluble RNAs, including 5S rRNA, tRNAs, and small RNAs (Monier et al. 1960). After loading 25 μg of small RNAs on 12% denaturing polyacrylamide gels and SYBR® Safe staining, we observed a good separation of distinct RNAs, including bulk tRNAs, 5S rRNA, and a portion of small RNAs (Fig. 2, left panel). Northern blot experiments were performed using antisense DNA (aDNA) probes specific for sdRNAs derived from snR128 and snR4 and LNA probe specific for sdRNA derived from snR83 (Table 1). We have observed clear signals derived from full-length snoRNAs within the small RNAs isolated with the bulk method (Fig. 2). We have observed that MasterPure™ Yeast Purification kit with the selective isopropanol precipitation of small RNAs' method resulted in purification of RNAs of ~120 nt and less. In this case, northern blot signals were observed from full-length snR128 (126 nt in length) but longer snoRNAs: snr4 (186 nt) and snR83 (306 nt) were not detected. Moreover, we did not observe any significant improvement in terms of

sdRNA detection since both of the small RNA-enrichment methods failed to provide amounts of sdRNA fragments above the clear detection threshold either with aDNA or LNA probe (Fig. 2).

Stem-loop RT-PCR assays confer sensitivity required to detect sdRNAs

Traditional RT-PCR amplification methods can lack specificity for sdRNAs that are processed from snoRNA and carry exactly the same sequence as their precursor snoRNAs. As revealed in our northern blot hybridization assays, total RNA pool contains high amounts of full-length snoRNAs but none of tested sdRNAs were detected with this technique (Fig. 1). To investigate the ability of stem-loop RT-PCR assays to detect only short sdRNAs but not the full-length snoRNAs, the reactions were performed with LMW RNA (LMW, 10-60 nt) purified from total RNA. Based on polyacrylamide gel electrophoresis results (Fig. 1, left panel), we decided to use Trizol-isolated RNAs for size separation since this RNA pool was visibly enriched in small RNA fraction.

To establish the sensitivity of stem-loop RT-PCR, a step-wise dilution of LMW RNA obtained from *S. cerevisiae* were prepared. This amplification was performed in a semi-quantitative manner, using 25-31 cycles (Fig. 3). After gel separation of the reaction products, we were able to observe clear detection signals for *S. cerevisiae* 5′-sdRNA 128 from as little as 50 ng RNA after 25 cycles of PCR, 3′-sdRNA 128 from 100 ng of RNA after 25 PCR cycles, and 5′-sdRNA 67 from 100 ng of RNA after 29 PCR cycles. At this number of cycles, no amplification was obtained in RT nor PCR water controls (-RT and -PCR lanes in Fig. 3, respectively). However, 31 or more cycles of PCR gave rise to some non-specific amplification in control reactions in case of 5′-sdRNA 128 primers. These results suggest that the stem-loop RT-PCR assay provides sensitivity sufficient for detection of sdRNAs in small RNA fractions.

Discussion

Since the discoveries of the functional potential of small RNAs, there are growing number of efforts for the development of techniques characterized by improved sensitivity and specificity of small RNA detection. Current methods for the detection and quantification of small RNAs are largely based on cloning, northern blotting, primer extension, or microarrays. All of these techniques are widely used and tested, especially for microRNA profiling. For the quantification of small RNA, low sensitivity becomes a problem because it is difficult to amplify short RNA molecules. Furthermore, low specificity may lead to false positive signals from closely related RNAs, precursors, or genomic sequences. Concerning northern blot hybridization assays, which is a gold standard for RNA detection and quantification, many efforts were focused on probing techniques and RNA/membrane attachment. It has been shown that using LNAs instead of standard antisense DNA probes increases sensitivity in detecting short RNA at least 10-fold, with the same specificity to the target molecule (Válóczi et al. 2004). LNA probes allowed, for instance, to detect small amounts (~27 000 molecules/cell) of 18-mer RNA, a regulatory ribosome-associated molecule needed for stress-adaptation in *S. cerevisiae* (Pircher et al. 2014). Alternatively, instead of conventional UV-cross-linking of total RNAs on nylon detection membranes, the use of 1-ethyl-3-(3-dimethylaminopropyl) carbodiimide (EDC)-mediated chemical cross-linking enhanced detection of small RNAs by up to 50-fold (Pal and Hamilton 2008). However, when it comes to less-abundant snoRNA-derived small RNAs, none of techniques mentioned above possess sensitivity sufficient enough for their reliable detection in *S. cerevisiae* (Fig. 1 and Fig. 2).

We have therefore decided to use a RT-PCR-based method. Because of the small size of sdRNAs, the reverse transcription reaction is initiated with a stem-loop primer that provides higher specificity and sensitivity than linear ones (Chen et al. 2005). Detection sensitivity was further increased by a pulsed RT reaction (Tang et al. 2006). Varkonyi-Gasic et al. (2007) have demonstrated a successful detection of several microRNAs from 20 pg of plant tissue total RNA. We have also successfully implemented this method and were able to detect three sdRNAs of different origin with as little as 50 ng of LMW RNAs (10-60 nt) from *S. cerevisiae*.

It has been shown that small RNA expression levels vary significantly among different species and tissues. Therefore, the reliable and sensitive quantification of small RNA expression levels in specific cellular compartments is of special importance. A number of specific quantitative RT-PCR (qRT-PCR) techniques were developed and optimized for miRNA detection, including real-time methods based upon reverse transcription (RT) reaction with a stem-loop primer followed by a TaqMan PCR ana-

lysis (Chen et al. 2005). Quantification of sdRNAs in *S. cerevisiae* with the means of qRT-PCR cannot be done because of two major reasons: 1) the processing events take place on stable, functional, and essential RNA and 2) in real-time PCR assays, there is a need for a reporter gene expression-level estimation. Concerning the processing events of the precursor snoRNA, the full-length snoRNA and its derivative sdRNA are of the same sequence. Therefore, stem-loop primer for RT reaction cannot distinguish between sdRNA and its precursor molecule. This was clearly visible in our experimental data, when we observed amplification products in both LMW and high-molecular-weight (HMW) RNA fractions (data not showed). The amplification product was derived from small sdRNA (within LMW RNA) and full-length precursor snoRNA (within HMW RNA). Similar situation takes place with the second consideration – the need for estimation of sdRNA expression levels in relation to the reporter RNA expression levels. Choosing a proper RNA with constitutive expression pattern is not a problem within the total RNA pool. However, within the total RNA, it would not be possible to distinguish between the sdRNA and their precursors. This problem could be overcome by using LMW RNA fraction instead of total RNA. Unfortunately, in *S. cerevisiae,* there is no known small RNA that could be considered as a reporter RNA for the estimation of relative gene expression levels. Considering all of the above, a stem-loop pulsed reverse transcription followed by PCR used in this study is a suitable method for sensitive detection and semi-quantification of low-abundant sdRNA expression in *S. cerevisiae*.

Acknowledgments

This work was supported by the National Science Center, Poland [2014/13/D/NZ1/00061 to K.B.-Ż.], and by the Polish Ministry of Science and Higher Education, under the KNOW program.

References

Brameier M., Herwig A., Reinhardt R., Walter L., Gruber J. (2011) *Human box C/D snoRNAs with miRNA like functions: expanding the range of regulatory RNAs*. Nucl. Acids Res. 39: 675-686.

Cavaille J., Buiting K., Kiefmann M., Lalande M., Brannan C.I., Horsthemke B., Bachellerie J.P., Brosius J., Hüttenhofer A. (2000) *Identification of brain-specific and imprinted small nucleolar RNA genes exhibiting an unusual genomic organization*. Proc. Natl. Acad. Sci. USA 97: 14311-14316.

Chen C., Ridzon D.A., Broomer A.J., Zhou Z., Lee D.H., Nguyen J.T., Barbisin M., Xu N.L., Mahuvakar V.R., Andersen M.R., Lao K.Q., Livak K.J., Guegler K.J. (2005) *Real-time quantification of microRNAs by stem-loop RT-PCR*. Nucl. Acids Res. 33: e179.

Ender C., Krek A., Friedländer M.R., Beitzinger M., Weinmann L., Chen W., Pfeffer S., Rajewsky N., Meister G. (2008) *A human snoRNA with microRNA-like functions*. Mol. Cell. 32: 519-528.

Falaleeva M., Stamm S. (2013) *Processing of snoRNAs as a new source of regulatory non-coding RNAs: snoRNA fragments form a new class of functional RNAs*. Bioessays 35: 46-54.

Hüttenhofer A., Kiefmann M., Meier-Ewert S., O'Brien J., Lehrach H., Bachellerie J.P., Brosius J. (2001) *RNomics: an experimental approach that identifies 201 candidates for novel, small, non-messenger RNAs in mouse*. EMBO J. 20: 2943-2953.

Hutzinger R., Feederle R., Mrazek J., Schiefermeier N., Balwierz P.J., Zavolan M., Polacek N., Delecluse H.J., Hüttenhofer A. (2009) *Expression and processing of a small nucleolar RNA from the Epstein-Barr virus genome*. PLoS Pathog. 5: e1000547.

Houseley J., Tollervey D. (2008) *The nuclear RNA surveillance machinery: the link between ncRNAs and genome structure in budding yeast?* Biochim. Biophys. Acta 1779: 239-246.

Jady B.E., Kiss T. (2000) *Characterisation of the U83 and U84 small nucleolar RNAs: two novel 2′-O-ribose methylation guide RNAs that lack complementarities to ribosomal RNAs*. Nucl. Acids Res. 28: 1348-1354.

Kim Y.K., Yeo J., Kim B., Ha M., Kim V.N. (2012) *Short structured RNAs with low GC content are selectively lost during extraction from a small number of cells*. Mol. Cell. 46: 893-895.

Kishore S., Khanna A., Zhang Z., Hui J., Balwierz P.J., Stefan M., Beach C., Nicholls R.D., Zavolan M., Stamm S. (2010) *The snoRNA MBII-52 (SNORD 115) is processed into smaller RNAs and regulates alternative splicing.* Hum. Mol. Genet. 19: 1153-1164.

Kishore S., Stamm S. (2006) *The snoRNA HBII-52 regulates alternative splicing of the serotonin receptor 2C*. Science 311: 230-232.

Krichevsky A.M., King K.S., Donahue C.P., Khrapko K., Kosik K.S. (2003) *A microRNA array reveals extensive regulation of microRNAs during brain development*. RNA 9: 1274-1281.

Li W., Saraiya A.A., Wang C.C. (2011) *Gene regulation in Giardia lambia involves a putative microRNA derived from a small nucleolar RNA*. PLoS Negl. Trop. Dis. 5: e1338.

Li Y., Kowdley K.V. (2012) *Method for microRNA isolation from clinical serum samples*. Anal. Biochem. 431: 69-75.

Lim L.P., Glasner M.E., Yekta S., Burge C.B., Bartel D.P. (2003) *Vertebrate microRNA genes*. Science 299: 1540.

Michel C.I., Holley C.L., Scruggs B.S., Sidhu R., Brookheart R.T., Listenberger L.L., Behlke M.A., Ory D.S., Schaffer J.E. (2011) *Small nucleolar RNAs U32a, U33, and U35a*

are critical mediators of metabolic stress. Cell. Metab. 14: 33-44.

Monier R., Stephenson M.L., Zamenick P.C. (1960) *The preparation and some properties of a low molecular weight ribonucleic acid from baker's yeast*. Biochim. Biophys. Acta 9: 1-8.

Monleau M., Bonnel S., Gostan T., Blanchard D., Courgnaud V., Lecellier C.H. (2014) *Comparison of different extraction techniques to profile microRNAs from human sera and peripheral blood mononuclear cells*. BMC Genomics 15: 395.

Pall G.S., Hamilton A.J. (2008) *Improved northern blot method for enhanced detection of small RNA*. Nat. Protoc. 3: 1077-1084.

Pircher A., Bakowska-Zywicka K., Schneider L., Zywicki M., Polacek N. (2014) *An mRNA-derived noncoding RNA targets and regulates the ribosome*. Mol. Cell. 54: 147-155.

Podolska A., Kaczkowski B., Litman T., Fredholm M., Cirera S. (2011) *How the RNA isolation method can affect microRNA microarray results*. Acta Biochim. Pol. 58: 535-540.

Saraiya A.A., Wang C.C. (2008) *snoRNA, a novel precursor of microRNA in Giardia lamblia*. PLoS Pathog. 4: e1000224.

Tang F., Hajkova P., Barton S.C., Lao K., Surani M.A. (2006) *MicroRNA expression profiling of single whole embryonic stem cells*. Nucl. Acids Res. 34: e9.

Tyczewska A., Bąkowska-Żywicka K., Gracz J., Twardowski T. (2016) *Stress responsive non-protein coding RNAs*. [In:] *Abiotic and biotic stress in plants – recent advances and future perspectives*. Ed. Shanker A., InTech: 153-181.

Valleron W., Laprevotte E., Gautier E.F., Quelen C., Demur C., Delabesse E., Agi rre X., Prósper F., Kiss T., Brousset P. (2012) *Specific small nucleolar RNA expression profiles in acute leukemia*. Leukemia 26: 2052-2060.

Válóczi A., Hornyik C., Varga N., Burgyán J., Kauppinen S., Havelda Z. (2004) *Sensitive and specific detection of microRNAs by northern blot analysis using LNA-modified oligonucleotide probes*. Nucl. Acids Res. 32: e175.

Varkonyi-Gasic E., Wu R., Wood M., Walton E.F., Hellens R.P. (2007) *Protocol: a highly sensitive RT-PCR method for detection and quantification of microRNAs*. Plant Meth. 3: 12.

Vitali P., Royo H., Seitz H., Bachellerie J..P, Huttenhofer A., Cavaillé J. (2003) *Identification of 13 novel human modification guide RNAs*. Nucl. Acids Res. 31: 6543-6551.

Zywicki M., Bakowska-Zywicka K., Polacek N. (2012) *Revealing stable processing products from ribosome-associated small RNAs by deep-sequencing data analysis*. Nucl. Acids Res. 40: 4013-4024.

5

Mleczko AM*, Machtel P*, Walkowiak M, Wasilewska A,
Pietras PJ, Bąkowska-Żywicka K

Levels of sdRNAs in cytoplasm and their association with ribosomes are dependent upon stress conditions but independent from snoRNA expression

Scientific Reports, 2019, 9 (1) *Autorzy mieli taki sam wkład w przygotowanie publikacji

SCIENTIFIC REPORTS
nature research

OPEN

Levels of sdRNAs in cytoplasm and their association with ribosomes are dependent upon stress conditions but independent from snoRNA expression

Anna M. Mleczko[1,3], Piotr Machtel[1,3], Mateusz Walkowiak[1], Anna Wasilewska[1], Piotr J. Pietras[1] & Kamilla Bąkowska-Żywicka[1,2*]

In recent years, a number of small RNA molecules derived from snoRNAs have been observed. Findings concerning the functions of snoRNA-derived small RNAs (sdRNAs) in cells are limited primarily to their involvement in microRNA pathways. However, similar molecules have been observed in *Saccharomyces cerevisiae*, which is an organism lacking miRNA machinery. Here we examined the subcellular localization of sdRNAs in yeast. Our findings reveal that both sdRNAs and their precursors, snoRNAs, are present in the cytoplasm at levels dependent upon stress conditions. Moreover, both sdRNAs and snoRNAs may interact with translating ribosomes in a stress-dependent manner. Likely consequential to their ribosome association and protein synthesis suppression features, yeast sdRNAs may exert inhibitory activity on translation. Observed levels of sdRNAs and snoRNAs in the cytoplasm and their apparent presence in the ribosomal fractions suggest independent regulation of these molecules by yet unknown factors.

snoRNAs are noncoding RNAs that contribute to ribosome biogenesis and RNA splicing by modifying ribosomal RNA and spliceosomal RNAs, respectively. However, recently emerging evidence suggests that some snoRNAs have non-canonical functions in RNA editing, alternative splicing or maintenance of chromatin structure[1–3]. The mechanistic details of these non-canonical functions are largely unknown. Moreover, it has recently become evident that mature, functional snoRNAs undergo processing to form stable short fragments, termed psnoRNAs, for processed snoRNAs[4] or sdRNAs for snoRNA-derived RNAs[5]. The presence of processed forms of snoRNAs has been demonstrated in several organisms, including the primitive protozoan *Giardia lamblia*[6], Epstein-Barr virus[7], the budding yeast *Saccharomyces cerevisiae*[8], and mammals[4,9–13].

Concerning possible functions of small RNAs derived from snoRNAs, their potential to regulate alternative splicing events[4] as well as their microRNA–like abilities, have been described in several organisms[10,14,15]. Recently, it has been postulated that FUS-dependent sdRNAs in human cell lines might regulate gene expression, affecting transcript stability and translation[16]. As the majority of miRNA-targeted, and thus translationally repressed, mRNAs are distributed in the cytoplasm, miRNA-like sdRNAs are expected to co-localize within the cytoplasm. Indeed, a subset of small RNAs derived from snoRNAs have been detected in the cytoplasm in *G. lamblia*[14] and humans[10]; however, their nucleolar localization has been reported as well[11]. Our recent work presented another possibility of sdRNA localization within the cytoplasm by association with ribosomes[8]. These studies were performed in *S. cerevisiae*, an organism lacking miRNA machinery; hence, one might suspect a distinct role for non-miRNA sdRNAs in yeast.

It is now commonly accepted that full-length snoRNAs are not exclusively localized within the nucleus but are also present in the cytoplasm. Moreover, their cytoplasmic abundance is dynamically regulated in various stress conditions, such as oxidative stress[17], lipotoxic conditions[18] or heat shock[19]. Knowledge concerning snoRNA

[1]Institute of Bioorganic Chemistry Polish Academy of Sciences, Noskowskiego 12/14, 61-704, Poznań, Poland. [2]Centre for Advanced Technologies, Poznań, Poland. [3]These authors contributed equally: Anna M. Mleczko and Piotr Machtel. *email: bakowska@ibch.poznan.pl

Name	Type	Sequence [5′-3′]	Length [nt]
snR67	Fwd primer	TAACATGATGACTAAGTTGTCGCC	24
	RT primer	TTTCAGAATTTTCAGTGTTTGTTGTTTG	28
sdR67	**RNA**	**AACAUGAUGACUAAGUUGU**	**19**
	RT primer	GTCGTATCCAGTGCAGGGTCCGAGGTATTCGCACTGGATACGACACAACT	50
	Fwd primer	GGCGCGCGCGAACATGATGACTA	23
snR83	Fwd primer	CCCAAAAACATCAAGAAAAGCCTTT	25
	RT primer	AACTGTCGCCCTTAATATTAGTCCC	25
sdR83	**RNA**	**GGACCAAUUACCGUAGUUGCGACUACAACAAUUUUGUUCAUA**	**42**
	RT primer	GTCGTATCCAGTGCAGGGTCCGAGGTATTCGCACTGGATACGACTATGAA	50
	Fwd primer	GACCAAUUACCGUAGUUGCGAC	22
snR128	Fwd primer	TCACGGTGATGAAAGACTGGT	21
	RT primer	TCACTCAGACATCCTAGGAAGGT	23
sdR128	**RNA**	**CACGGUGAUGAAAGACUGGUU**	**21**
	RT primer	GTCGTATCCAGTGCAGGGTCCGAGGTATTCGCACTGGATACGACAACCAG	50
Spike-in	**RNA**	**AUAGGCCAUAAGGAGUCUCGGUACGUCUUGUAUG**	**44**
	RT primer	GTCGTATCCAGTGCAGGGTCCGAGGTATTCGCACTGGATACGACCATACA	50
	Uni primer	CCAGTGCAGGGTCCGAGGTA	20

Table 1. Oligonucleotide sequences used in this study. sdRNA sequences are presented in bold. RT primer – primer used for reverse transcription; Fwd primer – forward ddPCR primer; Uni primer – universal reverse ddPCR primer.

expression regulation, however, is sparse. In 2002, it was shown for the first time that snoRNAs are involved in cancer development[20]. Since that time, a growing body of evidence has emerged linking both full-length snoRNAs and their derivatives to oncogenesis (reviewed in[21]). Considering both localization and the potential functions of full-length snoRNAs and sdRNAs, one might suspect that snoRNAs and their derivatives orchestrate responses to environmental stress outside of the nucleus. Surprisingly, studies aimed at revealing the abundance and subcellular localization of sdRNAs in stress have yet to be reported.

Yeast sdRNAs are observed in limited numbers during the sequencing of ribosome-associated small RNAs, with a maximum of 15 copies in the rancRNA library[8]. However, their regulatory potential cannot be excluded, as recent studies demonstrated that even relatively small levels (when compared to ~200,000 ribosomes/cell) of ribosome-associated noncoding RNA (ranc_18mer, ~27,000 molecules/cell) are sufficient to substantially influence global ribosome activity and regulate translation[22]. We recently demonstrated that due to sdRNA low abundance, conventional techniques, such as northern hybridization, are not sensitive enough to detect the full repertoire of cellular sdRNAs[23]. Poor sensitivity and low throughput of hybridization-based technologies can be overcome by sensitive, amplification-based detection methods, such as stem–loop reverse transcription PCR (SL-RT-PCR), originally described by Chen *et al.*[24] and successfully implemented by our group for detection of yeast sdRNAs from as little as 50 ng of low molecular weight cellular RNA[23].

Therefore, to investigate the subcellular localization of both full-length snoRNAs and snoRNA-derived small RNAs in *S. cerevisiae*, we used this amplification-based method. To enable absolute quantification of RNAs, we implemented digital droplet PCR (ddPCR) technology. Our comprehensive analysis of sdRNA and snoRNA abundance and localization was performed under 12 different yeast growth conditions. Herein, we present the first evidence that snoRNA levels and the localization of sdRNAs within the cell, including association with ribosomes, are dependent upon stress conditions. As a consequence of sdRNA binding to ribosomes, an inhibition of *in vitro* and *in vivo* translation occurs. Moreover, for the first time, we present experimental data suggesting that both the expression and ribosome association of two types of related RNAs, namely, snoRNA-derived small RNAs and full-length snoRNAs, are independent from each other during multiple growth conditions.

Materials and Methods

snoRNA-derived small RNAs. Three snoRNAs (snR67, snR83 and snR128) and 3 corresponding sdRNAs (sdR67, sdR83 and sdR128) were chosen for analysis based on the highest read coverage observed in ribosome-associated small RNA sequencing in *S. cerevisiae*[8]. Sequences of sdRNAs are shown in Table 1. Localization of sdRNAs within predicted snoRNA secondary structure is shown in Fig. 1.

Strain and growth conditions. *Saccharomyces cerevisiae* strain BY4741 was grown in YPD medium with 2% glucose at 30 °C. Environmental stress was induced as previously described[25] in two biological replicates. Briefly, cells were grown to mid-log phase, and stress conditions were applied for 15 min. Next, cells were pelleted and stored at −20 °C. Stress conditions were as follows: heat shock (37 °C), cold shock (15 °C), high salt conditions (1 M NaCl), high pH conditions (pH 7.9), low pH conditions (pH 4.0), UV exposure (120 J/m^2 UV), hyperosmotic shock (1 M sorbitol), hypoosmotic shock (cells grown to mid-log phase in YPD supplemented with 1 M sorbitol were transferred to YPD without sorbitol), amino acid starvation, sugar starvation, and anaerobic and normal growth.

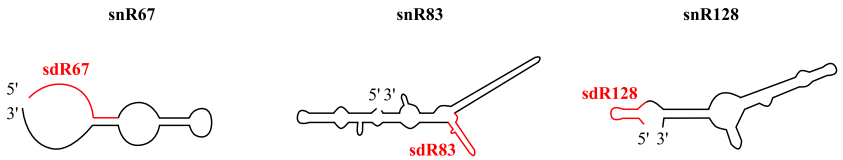

	snR67	snR83	snR128
snoRNA size:	82 nt	306 nt	126 nt
snoRNA family:	C/D box	H/ACA box	C/D box
snoRNA target:	25S rRNA	18S rRNA	18S rRNA
process affected by snoRNA:	2'-O-methylation	formation of pseudouridine	2'-O-methylation

Figure 1. snoRNAs and sdRNAs used in this study. Localization of sdRNAs within predicted snoRNAs secondary structures and functional details of snoRNAs is shown.

Yeast lysates and ribosome preparation. Yeast ribosomes were prepared as previously described[26,27]. Briefly, cell pellets were washed with ice-cold water and resuspended in buffer (10 mM $MgCl_2$, 100 mM KCl, 50 mM Tris/HCl, pH 7.5, 0.4 mM PMSF) at 4 °C. Equal volumes of glass beads (400 μm in diameter) were added, and cells were broken using 8 pulses of vortexing (30 sec each) punctuated by cooling on ice. Cell debris was precipitated at 11,300 × g for 2 min at 4 °C in F-34-6-38 Eppendorf rotor. Lysate was further clarified by centrifugation at 11.300 × g for 10 min at 4 °C in F-34-6-38 Eppendorf rotor. After clarification, 1/10 of the total lysate volume was used to isolate total cellular RNA (S30). Subsequently, ribosomes were pelleted (P100) from lysates by centrifugation at 160,000 × g for 90 min at 4 °C in Beckman 70.1 Ti rotor and suspended in the storage buffer (2 mM $Mg(OAc)_2$, 100 mM KOAc, 20 mM HEPES, pH 7.4, 0.1 mM PMSF, 1 mM DTT, 20% glycerol). The top two-thirds of the post-ribosomal supernatant were collected and frozen, and designated as the S100 fraction. P100, S100 and S30 fractions were mixed with TRI Reagent (MRC), flash frozen in liquid nitrogen and subjected to RNA isolation following the manufacturer's instructions. The purity of P100 and S100 fraction was verified with Agilent Bioanalyzer 2100 with the use of RNA Nano 6000 kit.

Reverse transcription. Stem-loop RT primers for sdRNA amplification (Table 1) were designed as previously described[23]. Standard RT primers for snoRNA amplification were designed using the Primer3Plus tool. All reverse transcription reactions were performed in a multiplex manner. Reverse transcription reactions contained 10 or 100 ng RNA from P100, S100 or S30 fractions, 50 nM of each stem-loop RT primer for sdRNAs and spike-in RNA, 50 nM of each standard RT primer for snoRNAs, 1 × RT buffer, 0.25 mM of each dNTPs, 50 U SuperScript SSIII reverse transcriptase (Invitrogen), 5 U RiboLock RNase Inhibitor (Thermo Scientific), 10 mM DTT and 500 fM spike-in RNA (Table 1) as a normalizer. Twenty-microlitre reactions were incubated in a Bio-Rad T100TM Thermocycler for 30 min at 16 °C, followed by pulsed RT of 60 cycles at 30 °C for 30 sec, 42 °C for 30 sec, and 50 °C for 1 sec.

Digital droplet PCR (ddPCR). Copy numbers of sdRNAs and snoRNAs were determined using the QX100™ Droplet Digital™ PCR system (Bio-Rad, Pleasanton, CA). The reaction mixture was composed of 10 μl of 2x QX200™ ddPCR™ EvaGreen Supermix, 200 nM specific forward and universal reverse primers (Table 1), and 1 μl cDNA.

Translation of poly(U) templates *in vitro*. Translation of poly(U) templates was performed as described[28] using 5 A260 units of ribosomes isolated from yeast grown under optimal and stress conditions, 25 mg poly(U), 100 mg soluble protein factors isolated from yeast grown under optimal and stress conditions, 25 mg deacylated yeast tRNA and 0.3 nmol [^{3}H]-phenylalanine. The reaction was performed at 30 °C for 30 min. Products were precipitated in TCA, recovered on Whatman glass fibre GF/C filters and subjected to scintillation counting. *In vitro* translation assays were performed in triplicate. Reported values are corrected for control samples lacking ribosomes, which were typically 0.5% to 1% of the total probe counts applied.

***In vitro* translation.** *S. cerevisiae* cell-free extracts were prepared in the cold-room, as previously described in[29] with modifications. To prepare *S. cerevisiae* S30 extract, yeast culture was grown to a final OD600 of 1.2 at 30 °C in YPD medium. Cells were chilled on ice, harvested by centrifugation at 1,500 × g for 5 min at 4 °C in F-34-6-38 Eppendorf rotor and washed five times with 30 ml of ice-cold buffer A (30 mM HEPES/KOH, pH 7.6, 100 mM KOAc, 3 mM $Mg(OAc)_2$, 2 mM DDT, 0.5 mM PMSF) supplemented with 8.5% (w/v) mannitol. Subsequently, cell pellet was resuspended in 1.5 ml of buffer A (supplemented with 8.5% mannitol and 0.5 mM PMSF) per 1 g of the cell pellet and six-time weight of cold glass beads (400 μm in diameter) was added.

Cells were broken by performing eigh-1 min cycles of vortexing (30 sec) and handshaking (30 sec, approximately 2 Hz over 50 cm hand patch). To remove the glass beads, the lysates were centrifuged at 120 × g for 2 min at 4 °C in F-34-6-38 Eppendorf rotor, transferred to a fresh tube, and centrifuged at 30,000 × g for 7 min at 4 °C in Hettich ROTINA 380 R rotor. The resulting S30 supernatant was purified on a G-25 Sephadex column. A portion of purified S30 extract was supplemented with 1 mM $CaCl_2$ and treated with 50 U/ml micrococcal nuclease at 26 °C for 10 min in order to eliminate endogenous mRNAs. The reaction was stopped by adding 2.5 mM EGTA. Both types of S30 extracts were aliquoted, snap-frozen in liquid nitrogen and stored at −80 °C.

For *in vitro* translation assays, 4 μl master mix (50 mM HEPES/KOH, pH 7.6, 2.5 mM ATP, 250 μM GTP, 50 mM creatine phosphate, 5 mM DTT, 0.6 U creatine phosphokinase, 125 mM KOAc, 5 mM MgOAc, 25 μM

amino acid mix (-Met), 4 U Ribonuclease Inhibitor, 500 nCi ^{35}S-methionine (1,000 Ci/mmol, 10 mCi/ml)) was mixed with 5 µl cell-free extract. Synthetic sdRNA or control RNA oligomers (10–500 pmol) or cycloheximide (7.5 µg/µl) was added to reach a final volume of 14 µl and mixtures were incubated at 26 °C for 40 min. The labeled proteins were precipitated by adding four volumes of ice-cold acetone and incubating at −20 °C for 30 min. Then, samples were centrifuged at 16 300 × g for 15 min at 4 °C in Eppendorf FA-45-24-11 rotor. The precipitate was dissolved in 15 µl 1x loading buffer (50 mM Tris-Cl, pH 6.8, 2% (w/v) SDS, 0.1% (w/v) bromophenol blue, 10% (v/v) glycerol, 100 mM DTT). Proteins were resolved on 10% SDS-polyacrylamide gels using 1xTGB running buffer and visualized on phosphor – storage intensity screen (Fujifilm) overnight. Screens were scanned using Fujifilm Fluorescent Image Analyzer FLA – 5100. We have measured the intensity of labelled proteins within the gel and subtracted background screen intensity. All measurements were performed at least in triplicate and standard error (SE) has been calculated. p-value has been calculated using t-test.

In vitro translation reactions were performed in wheat germ (Promega), rabbit reticulocyte (Promega), and human (Pierce Human *In Vitro* Protein Expression Kit, Fisher Scientific) systems according to the manufacturers' instructions. The reactions were incubated for 90 min. at 25 °C (wheat germ extract) or at 30 °C (rabbit reticulocyte and human systems). In all cases, an uncapped *in vitro*-transcribed luciferase mRNA containing a 30-base poly(A) tail was used as a template. ^{35}S-labeled proteins were resolved using SDS-PAGE and visualized on a storage phosphor intensity screen (Fujifilm) overnight. Screens were scanned using a Fujifilm Fluorescent Image Analyzer FLA-5100. All reactions were performed in triplicate and standard error (SE) has been calculated.

Metabolic labeling. Yeast spheroplasts were prepared from a 50-ml culture grown to an OD600 of 0.8 by adding 350 U of zymolyase (Zymo Research) and incubating at 30 °C for 25–30 min as previously described[22]. Spheroplasts were combined with synthetic sdRNA (10–100 pmol) or 100 pmol control RNA oligomers (scr-sdR128 5′-CUUGAGAUGAUUGCUAUGAUAC-3′, scr-ranc18 5′-AAGUGAAGAAGGAAGAAA-3′ or spike-in RNA 5′-AUAGGCCAUAAGGAGUCUCGGUACGUCUUGUAUG-3′) and electroporated. For controls, translation was inhibited by adding 7.5 µg/µl cycloheximide to the spheroplasts. Electroporated spheroplasts were incubated at 30°C with 1 µl ^{35}S-methionine (1 000 Ci/mmol, 10 mCi/ml) for 1 h. Labelled proteins were precipitated in TCA, recovered on Whatman glass fibre GF/C filters and subjected to scintillation counting. Metabolic labelling measurements were performed at least in triplicate, and standard error (SE) was calculated. Statistical significance was determined using t-test.

Results

SL-RT-ddPCR method enables for detection of small RNA input amounts. Quantitative determination of low levels of small RNAs remains challenging. Because low abundant sdRNAs are not detectable using standard methods, such as northern blot hybridization[23], we decided to employ an optimized stem-loop reverse transcription (SL-RT) followed by ddPCR. The ddPCR system measures fluorescence intensities of droplets after completion of all thermal cycling. The copy number of target genes is determined based on the number of fluorescent-positive and -negative droplets in a sample well. ddPCR provides an absolute number of RNA copies present in the sample. To define the minimum number of sdRNA copies that can be detected using the pulsed SL-RT-ddPCR method, we spiked 0.5 pg of an exogenous synthetic RNA (37nt in length, no sequence similarity to *S. cerevisiae* snoRNAs) to total RNA isolated from *S. cerevisiae*. Total RNA was subjected to the SL-RT method. Various dilutions of cDNA were amplified using ddPCR technology. These analyses demonstrated the ability of ddPCR to detect small RNA input levels, as low as 0.005 pg (Suppl. Fig. 1).

snoRNA and sdRNA levels are dependent upon stress conditions but are independent from each other. Using ddPCR, we investigated the accumulation of individual snoRNAs and sdRNAs across different *S. cerevisiae* growth conditions. In the first steps, we have verified the lengths of amplicons with means of standard agarose electrophoresis (Suppl. Fig. 2). Spiked-in synthetic RNA was used as a reference for ddPCR experiments. Absolute concentrations of spike-in reference RNA in different cDNA samples were uniformly distributed, with a mean value of 19,064 (±114) copies/µl. Therefore, we concluded that possible differences in snoRNA or sdRNA concentrations under particular stress conditions would be derived from their abundance and not from biases in experimental design.

All full-length snoRNAs were least abundant under low pH stress, and absolute concentrations were as follows: 10,360 copies/µl for snR67, 717 copies/µl for snR83 and 13,200 copies/µl for snR128 (Fig. 2A and Suppl. Fig. 3A). Except for this stress, where the observed snoRNA concentrations were markedly lower, absolute concentrations under the remaining stress conditions were in a range of 169,000–578,200 copies/µl for snR67, 182,400–463,200 copies/µl for snR83 and 333,900–1,072,000 copies/µl for snR128. Under optimal yeast growth conditions, snR128 was significantly more abundant (698,000 copies/µl) than snR67 and snR83 (422,700 copies/µl and 440,700 copies/µl, respectively).

For sdRNAs, we clearly observed that sdR67 was present in the smallest levels compared to other sdRNAs, just above ddPCR detection level (Fig. 2B and Suppl. Fig. 3B). Its maximum concentration was noted under low pH conditions, at 74 copies/µl. sdR83 was moderately abundant compared to other two sdRNAs. The highest concentration of sdR83 was observed under high salinity conditions, and it reached 953 copies/µl. The most abundant of tested sdRNAs, sdR128, was equally distributed, with the most prominent concentrations under heat stress (19,470 copies/µl), UV shock (21,900 copies/µl) and hypoosmotic stress (17,220 copies/µl).

Since we observed clear differences in both snoRNA and sdRNA levels across different stress conditions, we next performed analysis of possible correlations between accumulation of these two molecules under particular types of stress (Fig. 3). We observed antagonistic changes under three stress conditions, namely, in low pH stress for snR67, high salinity for snR83 and heat stress for snR128. Under these three conditions, snoRNAs were significantly less abundant and sdRNAs were significantly more abundant. Apart from these observations, in most

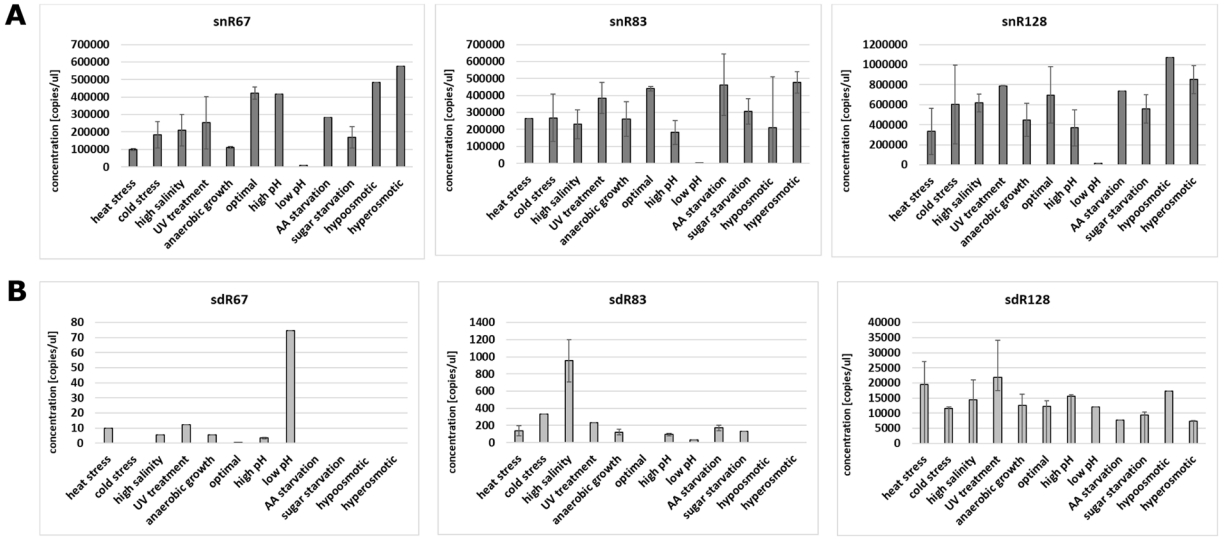

Figure 2. Quantitation of snoRNAs and sdRNAs within the total cellular RNA pool (S30). Concentration (copies/microlitre) of snoRNAs (**A**) and sdRNAs. (**B**) The mean and SE of two experiments are shown. Environmental stress was induced as described in Materials and methods.

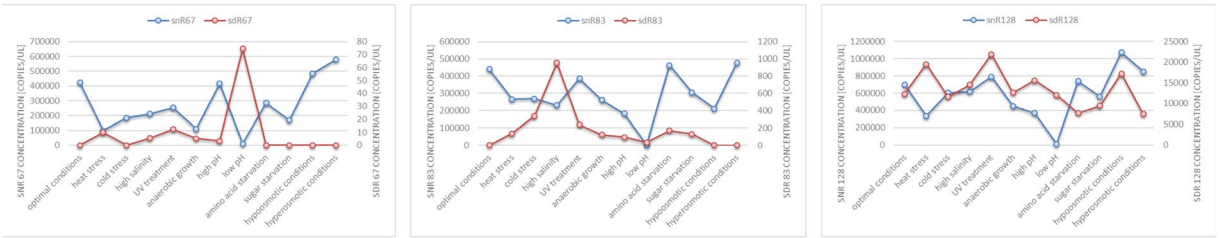

Figure 3. Differential accumulation of snoRNAs and sdRNAs in the cytoplasm. Values are means of replicates that are fully presented in Fig. 2.

of the stress conditions, snoRNA levels did not correlate with sdRNA abundance. This observation suggests that differential accumulation of sdRNAs is not directly dependent upon the levels of individual snoRNAs under particular yeast growth conditions. This suggests possible stress-dependent regulation of sdRNA excision.

snoRNAs and sdRNAs associate with ribosomes *in vivo* in a stress-dependent manner. Ultracentrifugation of yeast lysates allowed us to separate ribosome-containing pellet (P100) from post-ribosomal supernatant (S100) and to verify the cellular distribution of sdRNAs between these two fractions. The purity of P100 and S100 fraction was verified with Agilent Bioanalyzer 2100 with the use of RNA Nano 6000 kit (Fig. 4). The activity of the ribosomes within P100 pellet was verified using translation of poly(U) template *in vitro* (Suppl. Fig. 4).

For accurate quantification of snoRNAs and sdRNAs within P100 and S100 fractions, we employed ddPCR technology. Spiked-in synthetic RNA was used as a control for experiments, as previously described for total cellular RNA pools. Absolute concentrations of spike-in reference RNA in different cDNA samples derived from ribosome-associated RNA pools were uniformly distributed, with a mean value of 7,573 (±11) copies/µl in P100 and 20,125 (±122) copies/µl in S100 fraction. Therefore, we concluded that possible differences in snoRNA or sdRNA concentrations in different pools derive from their differential association with ribosomes and not from biases due to experimental design.

The first observation was that both full-length snoRNAs and sdRNAs are present in ribosome-containing fractions (Fig. 5 and Suppl. Fig. 5). Moreover, analysis of snoRNA sdRNA concentrations in P100 fraction obtained from yeast cultured under 12 different growth conditions illustrate that this association is strongly stress-dependent. snoRNAs are present on considerable quantities in ribosome-containing fractions (Fig. 5A), exceeding the concentration of sdRNAs over 800 times on average (Fig. 5B). In case of snR67, its highest concentration in ribosomal fractions was observed when ribosomes were isolated from yeast subjected to high pH conditions (292,400 copies/µl). The lowest snR67 concentration was noted in optimal conditions, as well as cold stress, and it oscillated approximately 2,800 copies/µl. snR83 was characterized by the lowest concentration among all three examined snoRNAs, with the maximum of 157,200 copies/µl in high pH conditions. Similarly, to snR67, cold stress caused the lowest accumulation of snR83 in the ribosomal fraction (22,100 copies/µl). The highest concentration in ribosomal fraction was observed for snR128, ranging from 57,300 copies/µl

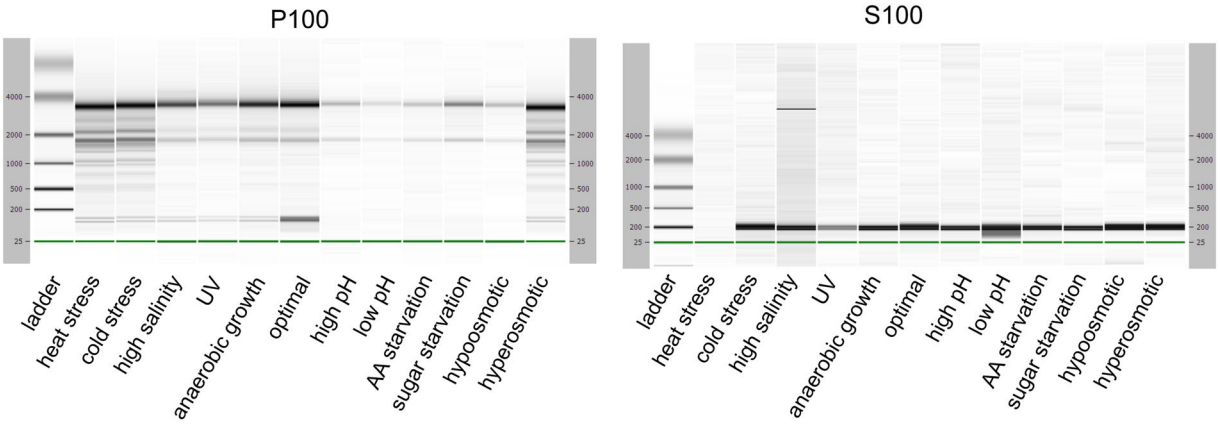

Figure 4. RNA length composition of the P100 (ribosome-enriched pellet) and S100 (ribosome-depleted supernatant) fractions derived from the lysates of native and stressed cells. RNA was isolated with TRI Reagent and subjected to Agilent RNA 6000 Nano assay. The bands corresponding to ribosomal RNAs (18 S rRNA of ~2000 bp and 26 S rRNA of ~3,800 bp) are visible in P100 fraction. Low molecular weight RNAs, up to 200 bp are mostly present in S100 fraction.

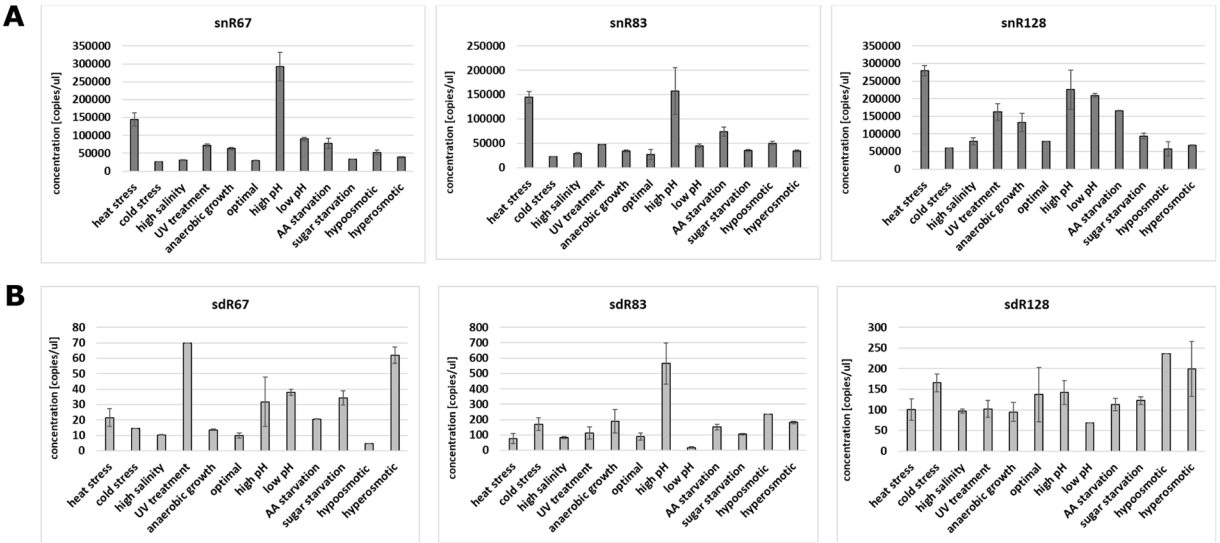

Figure 5. Quantitation of snoRNAs and sdRNAs within ribosome-associated RNAs (P100). Concentration (copies/microlitre) of snoRNAs (**A**) and sdRNAs (**B**) is presented. The mean and SE of two experiments are shown. Environmental stress was induced as described in Materials and methods.

(hypoosmotic growth conditions) to 279,400 copies/µl (heat shock). In general, heat stress and high pH stress induced significant increases in ribosome-associated snoRNAs.

Among investigated sdRNAs (Fig. 5B), sdR67 was the least abundant, reaching a maximum of 70 and 62 copies/µl after UV treatment and hyperosmotic stress conditions, respectively. The lowest accumulation of sdR67 in the ribosomal fraction was detected during hypoosmotic stress with 4.5 copies/µl. Generally, the amount of sdR83 was significantly higher in most stress conditions compared to sdR67. The highest concentration was observed during high pH conditions (565.5 copies/µl). In contrast, in low pH conditions, only 18.5 copies/µl of sdR83 were detected. For sdR128, a variety of growth conditions did not strongly affect its presence in the ribosome-associated RNA pool. Highest sdR28 accumulation was observed in hypo- and hyperosmotic conditions, reaching 236 and 199 copies/µl, respectively.

To elaborate on possible *in vivo* interactions with ribosomes, we compared the differential accumulation of both snoRNAs and sdRNAs in ribosome-associated RNA fractions (Fig. 6). In cases of high pH stress, both snR83 and its derivative, sdR83, were highly abundant. Except for this case, in the remaining stress conditions, snoRNA and sdRNA levels within ribosome-associated RNA pools were not well correlated. Such observation suggests that stress-dependent association of full-length snoRNAs and small sdRNAs with yeast ribosomes is independent.

Both full-length snoRNAs and sdRNAs are present in post-ribosomal supernatant fractions (Fig. 7A and Suppl. Fig. 6A) and their concentration differs in yeast cultivated under different conditions. snoRNA

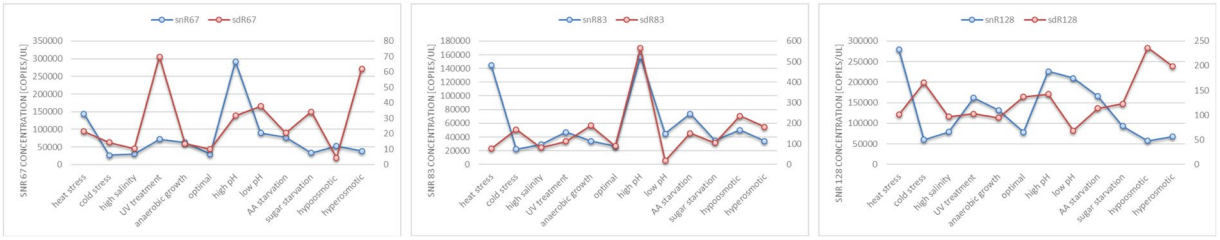

Figure 6. Differential accumulation of snoRNAs and sdRNAs in ribosomes. Values are means of replicates that are fully presented in Fig. 5.

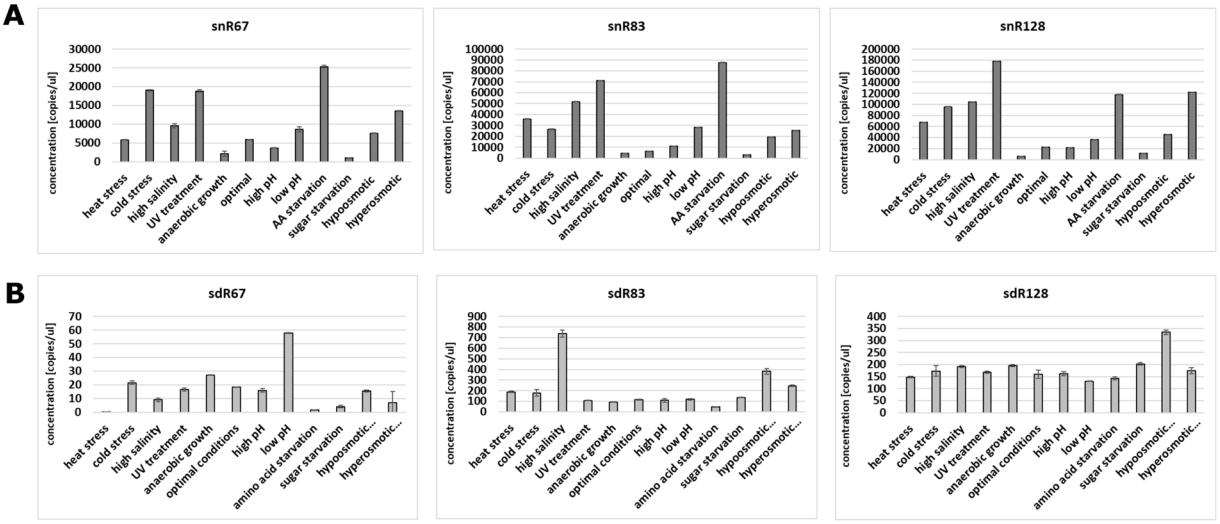

Figure 7. Quantitation of snoRNAs and sdRNAs within post-ribosomal supernatant. Concentration (copies/microlitre) of snoRNAs (**A**) and sdRNAs. (**B**) The mean and SE of two experiments are shown. Environmental stress was induced as described in Materials and methods.

concentrations are much more higher than sdRNA concentrations, similarly like in S30 and P100 fractions. In contrast to the situation observed in S30 fractions, snoRNAs were not least abundant under low pH stress but under sugar starvation (1,018 copies/µl for snR67, 4,510 copies/µl for snR83 and 6,070 copies/µl for snR128) and anaerobic growth (2,060 copies/µl for snR67, 3,115 copies/µl for snR83 and 11,650 copies/µl for snR128). Except of these conditions, absolute concentrations of snoRNAs in S100 fraction were in a range of 5,880–25,350 copies/µl for snR67, 11,020–87,700 copies/µl for snR83 and 22,200–121,850 copies/µl for snR128.

For sdRNAs, we clearly observed that sdR67 was present in the smallest levels compared to other sdRNAs, just above ddPCR detection level (Fig. 7B and Suppl. Fig. 6B). Its maximum concentration was noted under low pH conditions, at 57 copies/µl. The highest concentration of sdR83 was observed under high salinity conditions, and it reached 738 copies/µl. sdR128, was equally distributed (147–202 copies/µl), with the exception of hypoosmotic stress (334 copies/µl).

We next performed analysis of possible correlations between accumulation of snoRNAs and sdRNAs under particular types of stress in all cellular fractions analyzed (Fig. 8). We observed that in all cases an absolute concentration of both, snoRNAs and sdRNAs was higher in S30 than in P100 and S100 fractions, as expected. Patterns of snR and sdR accumulation in ribosome-containing fractions resembles those in post-ribosomal supernatant rather than total cellular RNA pool. This suggest that stress-related differential accumulation of snoRNAs and sdRNAs in ribosome fractions is related to their possible functional interactions with the ribosomes. Concentrations of snR and sdR in S100 fractions were lower than in P100 and S30, which implicates that a prominent portion of snoRNAs and sdRNAs present in the cell associate with the ribosomes. This suggests possible stress-dependent regulation of ribosome function by snoRNAs and/or sdRNAs.

Yeast sdRNAs inhibit translation *in vitro* and *in vivo*. The observation that sdRNAs accumulate in ribosomal fractions in a stress-dependent manner led to speculation of their potential function as regulatory ncRNAs during protein biosynthesis. To clarify this, we set up an *in vitro* translation system for *S. cerevisiae* grown under optimal conditions using the total endogenous mRNA pool as template and ^{35}S-methionine incorporation into proteins as readout (Fig. 9A). In the presence of the ribosome-targeting antibiotic cycloheximide, all radiolabeled bands were drastically reduced, demonstrating that the ^{35}S-methionine labeling of proteins was translation-dependent. When the assay was performed in the presence of synthetic sdR67, sdR83 or sdR128 we

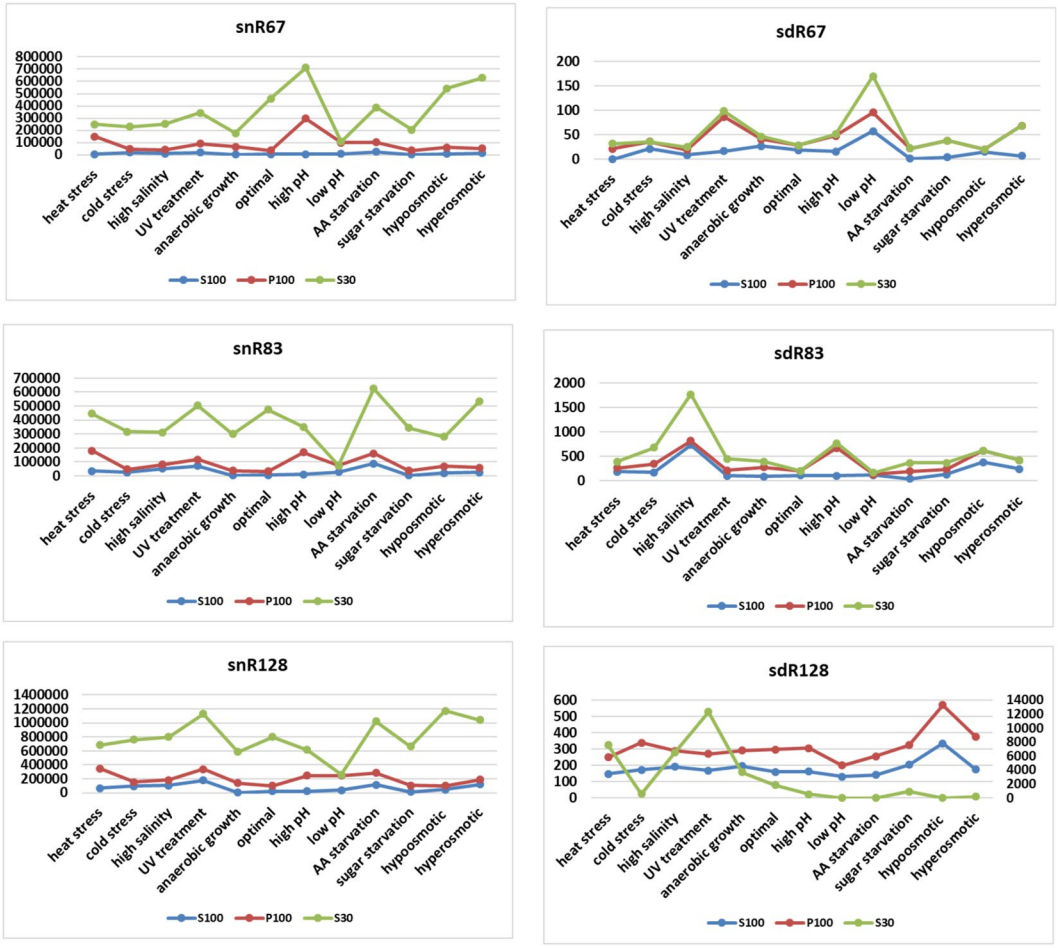

Figure 8. Differential accumulation of snoRNAs and sdRNAs in S30, S100 and P100 fractions. Values are means of replicates that are fully presented in Figs. 2, 5 and 7.

observed a reproducible inhibitory effect on translation. Introduction of 35.7 µM sdR67 or sdR83 (equivalent to 500 pmol per reaction) reduced *in vitro* translation to 40% and 75%, respectively. The highest inhibitory effect was observed for sdR128. Even small concentrations of sdR128, such as 0.7 µM (equivalent to 10 pmol per reaction), observably reduced *in vitro* protein synthesis. Conversely, the addition of the highest tested dose of the scrambled sdRNA128 (scr-sdR128) or 18nt-long control RNA oligomer (scr-ranc18), 35.7 µM, did not have any influence on translation efficiency.

To investigate whether *in vitro* effects have a physiological significance in yeast we used electroporation to introduce synthetic sdRNAs into *S. cerevisiae* cells. Conditions for small RNA electroporation were optimized in our previous studies, where quantification of the uptake efficiency of the synthetic 18-mer into spheroplasts indicated the presence of about 200,000 molecules per cell, thus roughly equaling the ribosome concentration[22]. We measured ^{35}S-Met incorporation into newly synthetized proteins in the presence and absence of sdR128, sdR83 and sdR67. As controls, we have used RNA oligomers with similar length to tested sdRNAs: scr-sdR128 (22 nt) as a control for sdR128, scr-ranc18 (18 nt) for sdR67 and spike-in RNA (44 nt) for sdR83. Control oligomers did not affect *in vivo* translation (Fig. 9B). Yeast sdRNAs decreased translational efficiency *in vivo*. Inhibition efficiency was in a range similar to the well-known ribosome-targeting antibiotic cycloheximide. Similarly to *in vitro* translation, sdR128 had the highest inhibitory effect on *in vivo* translation.

Because both snoRNAs and ribosomes are universally conserved, we tested if sdRNA-mediated repression of translation is functionally conserved in other eukaryotic species as well. To test this possibility, we examined three cell-free *in vitro* translation systems using wheat germ extracts, rabbit reticulocyte lysates, and HeLa cell lysates (Fig. 10). *In vitro* translation reactions were performed either in the absence (mock) or in the presence of synthetic sdRNAs. The addition of *S. cerevisiae* sdRNAs reproducibly inhibited *in vitro* protein biosynthesis in the wheat germ system (Fig. 10). *In vitro* translation was very mildly inhibited by yeast sdR67 in the rabbit reticulocyte but not by sdR83 nor sdR128. No inhibition was observed in human systems. These data suggest that *S. cerevisiae* sdRNAs might potentially inhibit some translation systems in selected eukaryotes.

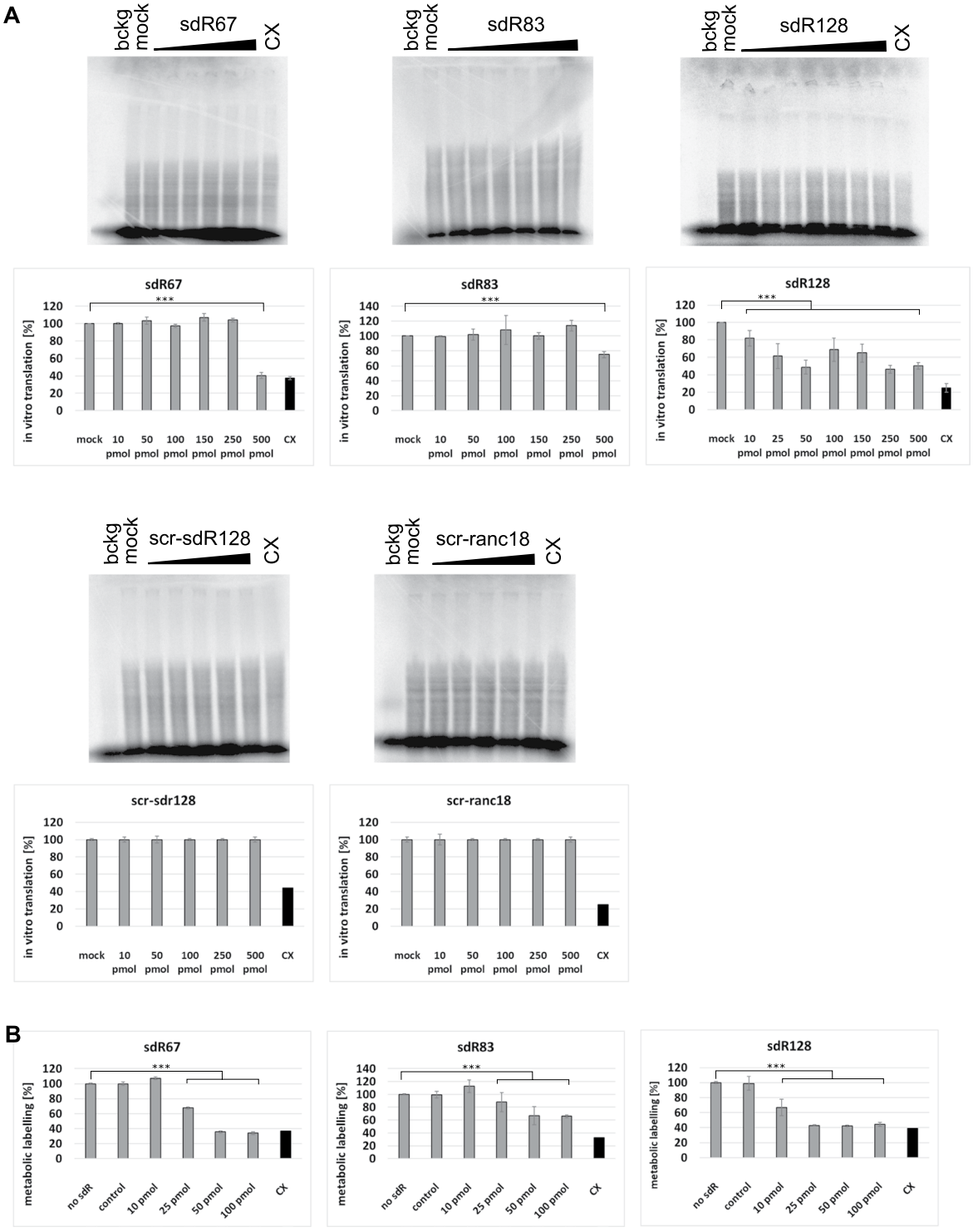

Figure 9. S. cerevisiae snoRNA-derived RNAs inhibit protein biosynthesis. Cycloheximide (CX) served as a control translational inhibitor. The mean and SE of three to six experiments are shown. ***p-value < 0.005. (**A**) Dose-dependent effects of sdRNAs on *in vitro* translation system. The autoradiographs of representative SDS polyacrylamide gels of *in vitro* translation assays performed in the absence (mock) or in the presence of synthetic sdRNAs, are shown. Translational efficiency of endogenous yeast mRNA is shown on graphs, as a percentage [%] of activity of the control experiment without sdRNA. (**B**) Incorporation of ^{35}S-methionine into the translatome of yeast spheroplasts is presented as translation *in vivo* efficiency [%]. The efficiency of metabolic labelling in the absence of sdRNA was set at 100%, and spheroplasts harbouring synthetic sdRNAs were compared to this value.

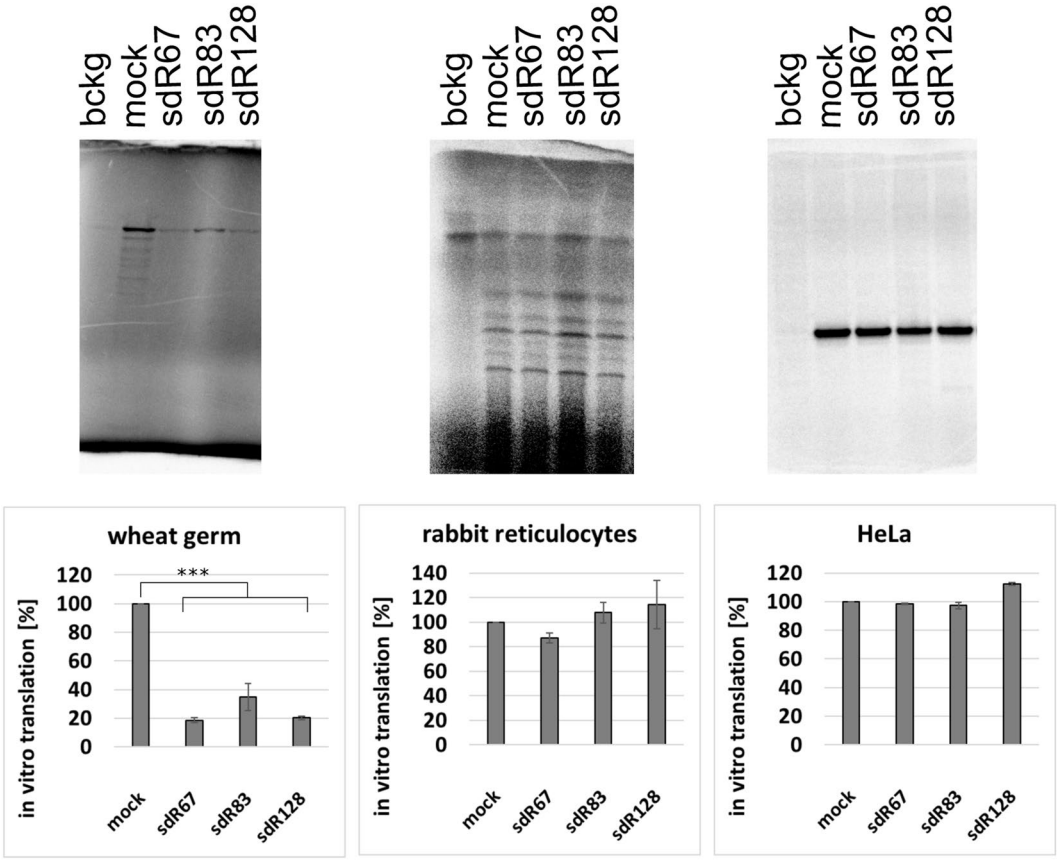

Figure 10. S. cerevisiae sdRNAs inhibition of protein biosynthesis in *in vitro* eukaryotic translation systems. A representative *in vitro* translation of synthetic non-capped poly(A)-tailed luciferase mRNA in wheat germ extracts, rabbit reticulocyte lysates and HeLa cell lysates. The reactions were performed in the absence (mock) or presence of yeast sdRNAs (500 pmol). The mean and SE of three *in vitro* translation experiments are shown beneath the gels. Cropped gels are displayed, full-length gels are included on Suppl. Fig. 7. ***p-value < 0.005

Discussion

In a recent study, we revealed that snoRNAs and sdRNAs in *Saccharomyces cerevisiae* are present in the cytoplasm, where they associate with ribosomes[30]. Herein, we show that the presence of *S. cerevisiae* sdRNA in the ribosomal fractions influences protein biosynthesis *in vivo* and *in vitro*. Moreover, accumulation of snoRNAs and sdRNAs in the cytoplasmatic and ribosomal fractions is strongly dependent upon stress conditions. For the first time, we have shown that snoRNA and sdRNA levels in the cytoplasm and their possible association with ribosomes are independent from each other.

It has been already shown that snoRNAs play crucial roles in adaptation to stress conditions[21]. In yeast, U3 snoRNA (snR17) is upregulated during heat shock, amino acid starvation and sugar starvation and downregulated under high salinity and hyperosmotic conditions[31]. Interestingly, the expression pattern of snoRNAs studied herein do not resemble those of snR17. In Chinese hamster ovary (CHO) cells U14 snoRNA, which corresponds to yeast snR128, is strongly upregulated during heat shock[19]. In yeast, however, we observed almost 2-fold downregulation of snR128 during heat stress. Such observations suggest that different snoRNAs possess distinct expression patterns during stress responses, which might be related to their functions.

Despite the fact that dysregulation of snoRNAs is involved in adaptation to stress conditions, only a few publications have reported the roles of sdRNAs in tumour development, which may be considered a stress for human cells[21,32,33]. Expression analysis of sdRNAs has been performed in several types of cancer with the conclusion that accumulation of sdRNAs is associated with malignant transformation and that increased global production or accumulation of sdRNAs is already occurring in the early stages of cancer. Surprisingly, there is no data reporting sdRNA levels in canonical stress conditions. To our knowledge, differential expression of sdRNAs has not previously been reported. Here, we report for the first time that sdRNAs in *S. cerevisiae* are present under a wide repertoire of growth conditions, though in some cases in limited amounts. So far, sdRNAs have been reported to localize in the cytoplasm in organisms where they act within microRNA pathways[6,10,12–14]. Here, we present new data demonstrating cytoplasmatic localization of sdRNAs in an organism that lacks miRNA pathways.

Moreover, for the first time, we present data showing that snoRNAs and sdRNAs are differentially abundant in both the cytoplasmatic and in ribosomal fractions. Such observations indicate that sdRNAs and snoRNAs might perform distinct cellular functions in response to stress conditions, probably during translation regulation.

These observations strongly support the hypothesis for separate roles of both snoRNAs and sdRNAs during stress conditions.

The presence of both sdRNAs and snoRNAs in ribosome-associated RNAs indicates the possible existence of a novel, yet to be discovered stress-dependent translation regulation mechanism. The data presented herein strongly suggest that possible interactions between yeast ribosomes and sdRNAs downregulate translational activity during optimal growth conditions. Moreover, the observation of the inhibition of protein synthesis by yeast sdRNAs in the wheat germ system suggests the mechanism of translation regulation by sdRNAs is evolutionarily conserved. This suggests that the mode of action and, thus, also the ribosomal target site, is conserved in a range of eukaryotic species. In this aspect, sdRNAs could be classified as an example of ribosome-associated noncoding RNAs (rancRNAs), next to an mRNA exon-derived 18-residue-long ncRNA[22] and tRNA-derived fragments[26] previously described by our lab.

Received: 12 February 2019; Accepted: 18 November 2019;
Published online: 05 December 2019

References

1. Vitali, P. *et al*. ADAR2-mediated editing of RNA substrates in the nucleolus is inhibited by C/D small nucleolar RNAs. *J. Cell Biol.* **169**, 745–53 (2005).
2. Kishore, S. & Stamm, S. The snoRNA HBII-52 regulates alternative splicing of the serotonin receptor 2C. *Science* **311**, 230–2 (2006).
3. Schubert, T. *et al*. Df31 Protein and snoRNAs Maintain Accessible Higher-Order Structures of Chromatin. *Mol. Cell* **48**, 434–444 (2012).
4. Kishore, S. *et al*. The snoRNA MBII-52 (SNORD 115) is processed into smaller RNAs and regulates alternative splicing. *Hum. Mol. Genet.* **19**, 1153–1164 (2010).
5. Taft, R. J. *et al*. Small RNAs derived from snoRNAs. *RNA* **15**, 1233–1240 (2009).
6. Saraiya, A. A. & Wang, C. C. snoRNA, a novel precursor of microRNA in Giardia lamblia. *PLoS Pathog.* **4**, e1000224 (2008).
7. Hutzinger, R. *et al*. Expression and Processing of a Small Nucleolar RNA from the Epstein-Barr Virus Genome. *PLoS Pathog.* **5**, e1000547 (2009).
8. Zywicki, M., Bakowska-Zywicka, K. & Polacek, N. Revealing stable processing products from ribosome-associated small RNAs by deep-sequencing data analysis. *Nucleic Acids Res.* **40**, 4013–4024 (2012).
9. Bortolin-Cavaille, M.-L. & Cavaille, J. The SNORD115 (H/MBII-52) and SNORD116 (H/MBII-85) gene clusters at the imprinted Prader-Willi locus generate canonical box C/D snoRNAs. *Nucleic Acids Res.* **40**, 6800–6807 (2012).
10. Ender, C. *et al*. A Human snoRNA with MicroRNA-Like Functions. *Mol. Cell* **32**, 519–528 (2008).
11. Bai, B., Yegnasubramanian, S., Wheelan, S. J. & Laiho, M. RNA-Seq of the Nucleolus Reveals Abundant SNORD44-Derived Small RNAs. *PLoS One* **9**, e107519 (2014).
12. Brameier, M., Herwig, A., Reinhardt, R., Walter, L. & Gruber, J. Human box C/D snoRNAs with miRNA like functions: expanding the range of regulatory RNAs. *Nucleic Acids Res.* **39**, 675–686 (2011).
13. Burroughs, A. M. *et al*. Deep-sequencing of human Argonaute-associated small RNAs provides insight into miRNA sorting and reveals Argonaute association with RNA fragments of diverse origin. *RNA Biol.* **8**, 158–77.
14. Li, W., Saraiya, A. A. & Wang, C. C. Gene regulation in Giardia lambia involves a putative microRNA derived from a small nucleolar. *RNA. PLoS Negl. Trop. Dis.* **5**, e1338 (2011).
15. Ono, M. *et al*. Identification of human miRNA precursors that resemble box C/D snoRNAs. *Nucleic Acids Res.* **39**, 3879–3891 (2011).
16. Plewka, P. *et al*. FUS controls the processing of snoRNAs into smaller RNA fragments that can regulate gene expression, https://doi.org/10.1101/409250.
17. Holley, C. L. *et al*. Cytosolic Accumulation of Small Nucleolar RNAs (snoRNAs) Is Dynamically Regulated by NADPH Oxidase. *J. Biol. Chem.* **290**, 11741–11748 (2015).
18. Michel, C. I. *et al*. Small Nucleolar RNAs U32a, U33, and U35a Are Critical Mediators of Metabolic Stress. *Cell Metab.* **14**, 33–44 (2011).
19. Chen, M.-S., Goswami, P. C. & Laszlo, A. Differential accumulation of U14 snoRNA and hsc70 mRNA in Chinese hamster cells after exposure to various stress conditions. *Cell Stress Chaperones* **7**, 65–72 (2002).
20. Chang, L. S., Lin, S. Y., Lieu, A. S. & Wu, T. L. Differential expression of human 5S snoRNA genes. *Biochem. Biophys. Res. Commun.* **299**, 196–200 (2002).
21. Mleczko, A. M. & Bakowska-Zywicka, K. When small RNAs become smaller: Emerging functions of snoRNAs and their derivatives. *Acta Biochim. Pol.* **63** (2016).
22. Pircher, A., Bakowska-Zywicka, K., Schneider, L., Zywicki, M. & Polacek, N. An mRNA-Derived Noncoding RNA Targets and Regulates the Ribosome. *Mol. Cell* **54**, 147–155 (2014).
23. Walkowiak, M., Mleczko, A. M. & Bąkowska-Żywicka, K. Evaluation of methods for the detection of low-abundant snoRNA-derived small RNAs in Saccharomyces cerevisiae. *Biotechnologia* **97** (2016).
24. Chen, C. *et al*. Real-time quantification of microRNAs by stem-loop RT-PCR. *Nucleic Acids Res.* **33**, e179–e179 (2005).
25. Bąkowska-Żywicka, K. *et al*. The widespread occurrence of tRNA-derived fragments in *Saccharomyces cerevisiae*. *FEBS Open Bio* **6**, 1186–1200 (2016).
26. Velichutina, I. V *et al*. Mutations in helix 27 of the yeast Saccharomyces cerevisiae 18S rRNA affect the function of the decoding center of the ribosome Mutations in helix 27 of the yeast Saccharomyces cerevisiae 18S rRNA affect the function of the decoding center of the ribosome. 1174–1184 (2000).
27. Mleczko, A. M., Celichowski, P. & Bąkowska-Żywicka, K. Transfer RNA-derived fragments target and regulate ribosome-associated aminoacyl-transfer RNA synthetases. *Biochim. Biophys. Acta - Gene Regul. Mech.* **1861**, 647–656 (2018).
28. Bąkowska-Żywicka, K., Kasprzyk, M. & Twardowski, T. tRNA-derived short RNAs bind to *Saccharomyces cerevisiae* ribosomes in a stress-dependent manner and inhibit protein synthesis *in vitro*. *FEMS Yeast Res.* **16**, fow077 (2016).
29. Wu, C. & Sachs, M. S. Preparation of a Saccharomyces cerevisiae Cell-Free Extract for *In Vitro* Translation. in. *Methods in enzymology* **539**, 17–28 (2014).
30. Zywicki, M., Bakowska-Zywicka, K. & Polacek, N. Revealing stable processing products from ribosome-associated small RNAs by deep-sequencing data analysis. *Nucleic Acids Res.* **40**, 1–12 (2012).
31. Bergkessel, M., Whitworth, G. B. & Guthrie, C. Diverse environmental stresses elicit distinct responses at the level of pre-mRNA processing in yeast. *RNA* **17**, 1461–78 (2011).
32. Patterson, D. G. *et al*. Human snoRNA-93 is processed into a microRNA-like RNA that promotes breast cancer cell invasion. *npj Breast Cancer* **3**, 25 (2017).
33. Martens-Uzunova, E. S. *et al*. C/D-box snoRNA-derived RNA production is associated with malignant transformation and metastatic progression in prostate cancer. *Oncotarget* **6**, 17430–44 (2015).

Acknowledgements
This work was supported by the National Science Centre, Poland [UMO-2014/13/D/NZ1/00061 to K.B.Ż.] and [UMO-2017/27/B/NZ1/01416 to K.B.Ż.]. The work was also supported by the Polish Ministry of Science and Higher Education, under the KNOW programme.

Author contributions
K.B.Ż. planned experiments. A.M.M., P.M., A.W., M.W. and P.J.P. performed experiments. K.B.Ż., A.M.M. and P.M. analysed the data and wrote the paper.

Competing interests
The authors declare no competing interests.

Additional information
Supplementary information is available for this paper at https://doi.org/10.1038/s41598-019-54924-2.

Correspondence and requests for materials should be addressed to K.B.-Ż.

Reprints and permissions information is available at www.nature.com/reprints.

Publisher's note Springer Nature remains neutral with regard to jurisdictional claims in published maps and institutional affiliations.

Supplementary material

Levels of sdRNAs in cytoplasm and their association with ribosomes are dependent upon stress conditions but independent from snoRNA expression

Anna M. Mleczko[#], Piotr Machtel[#], Mateusz Walkowiak, Anna Wasilewska, Piotr J. Pietras, Kamilla Bąkowska-Żywicka*

Institute of Bioorganic Chemistry Polish Academy of Sciences, Noskowskiego 12/14, 61-704 Poznań, Poland

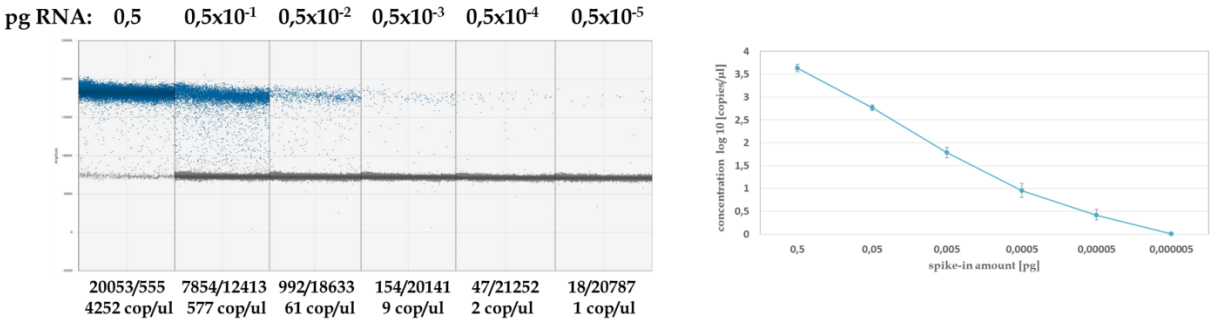

Supplementary Figure 1. Detection and quantitation of synthetic spike-in RNA.
A) Fluorescence amplitude of different concentrations of spike-in RNA. Levels of input RNA are reported at the top, whereas the number of positive/negative droplets and the concentration (copies/microlitre) are reported on the bottom of each panel.
B) The relationship between calculated copies/microlitre and input RNA.

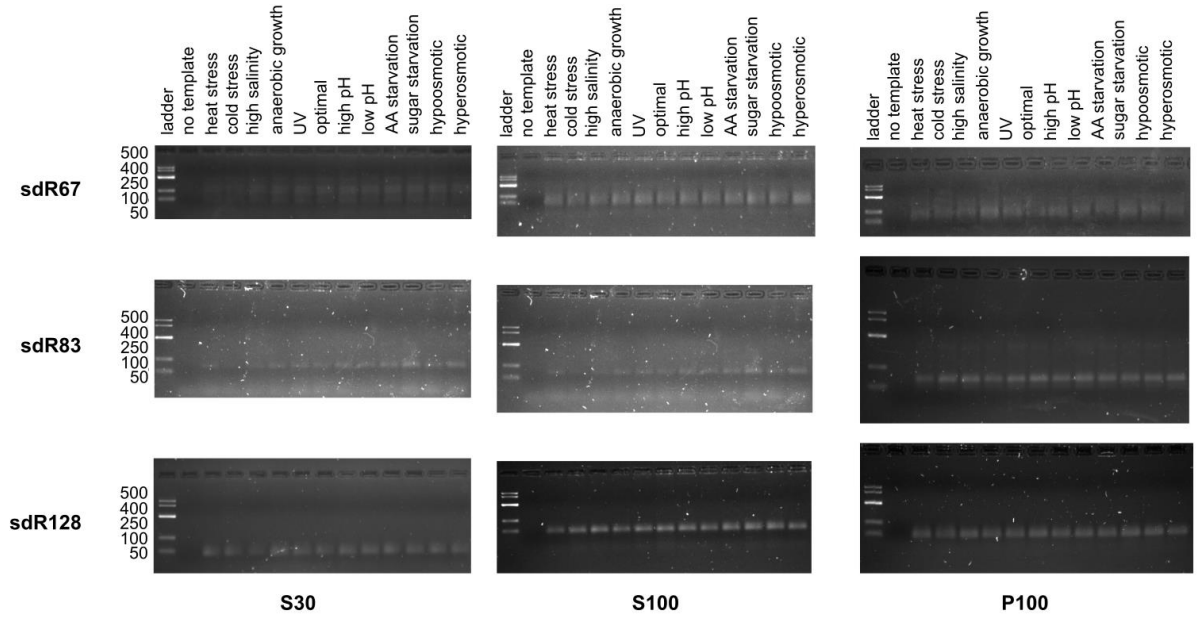

Supplementary Figure 2. Detection of sdRNAs within total cellular RNA (S30), postribosomal supernatant (S100) and ribosomal pellet (P100) pools.
Stem-loop RT-PCR analyses of expression of sdRNAs. 100 ng of S30, P100 or S100 RNA was used for reverse transcription reactions. 40 PCR cycles were performed. The band corresponds to the amplification product of sdRNAs.

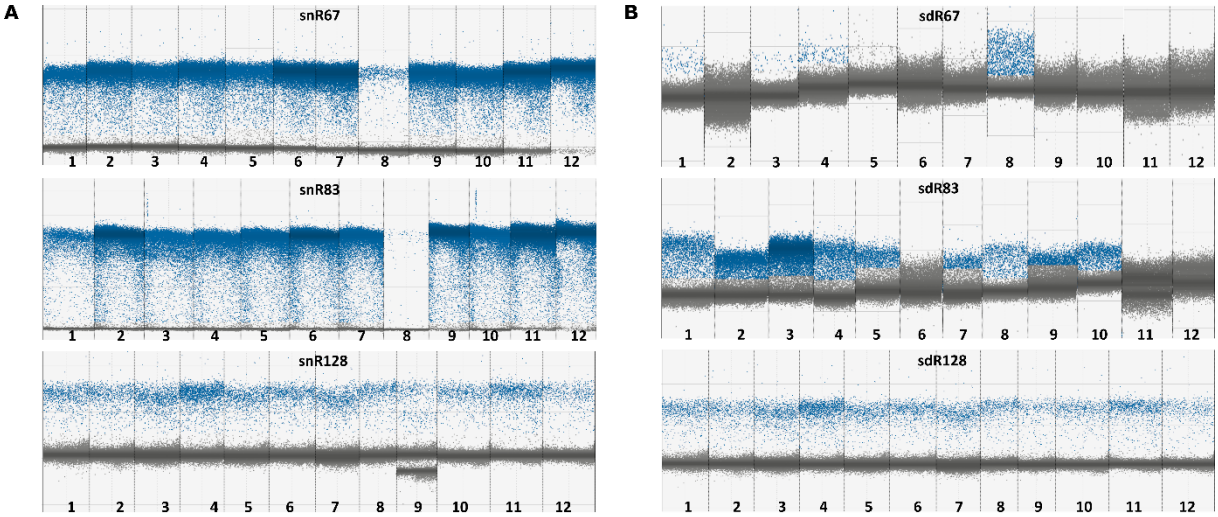

Supplementary Figure 3. Detection of snoRNAs and sdRNAs within total cellular RNA pools.
Representative fluorescence amplitude of snoRNAs (A) and sdRNAs (B). Positive droplets are in shown in blue, negative droplets in grey. Slot numbers correspond to stress conditions as follows: 1 – heat stress, 2 – cold stress, 3 – high salinity, 4 – UV treatment, 5 – anaerobic growth, 6 – optimal conditions, 7 – high pH, 8 – low pH, 9 – AA starvation, 10 – sugar starvation, 11 – hypoosmotic conditions, and 12 – hyperosmotic conditions.

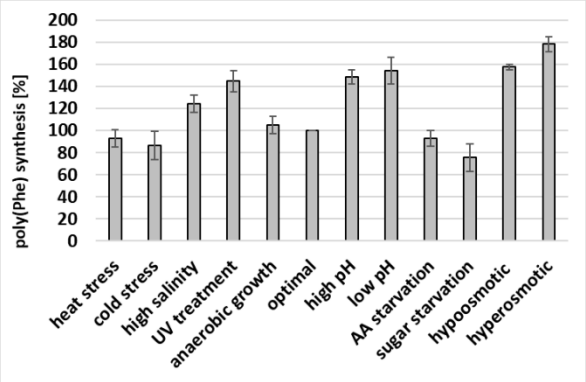

Supplementary Figure 4. Activity of ribosomes isolated from yeast cultured under different conditions.
Activity of the ribosomes was measured as translation of poly(U) templates in vitro. Activity of the ribosomes isolated from yeast grown under optimal conditions was set to 100%.

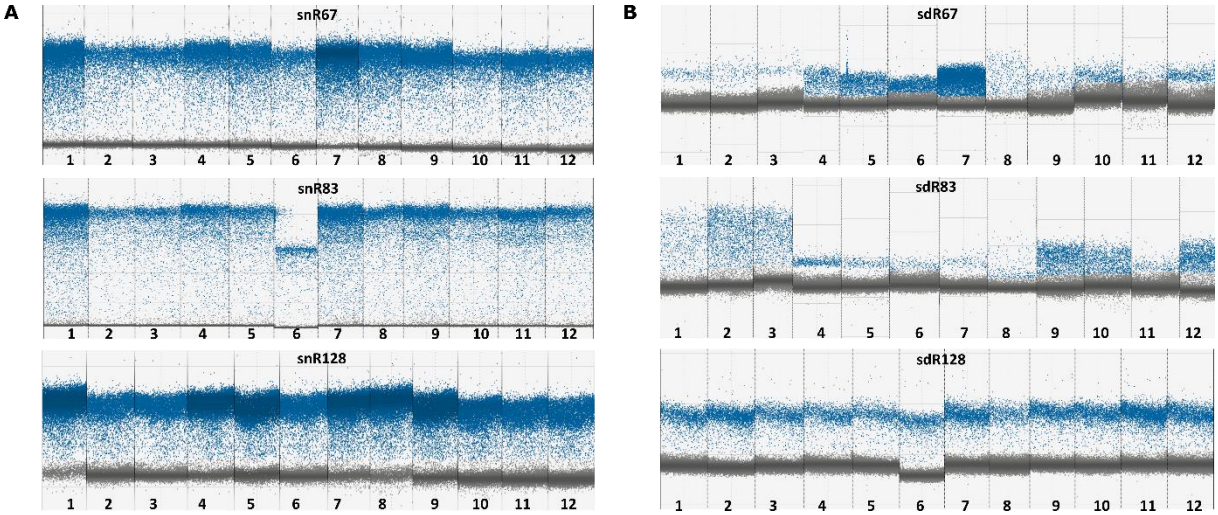

Supplementary Figure 5. Detection of snoRNAs and sdRNAs within ribosome-associated RNAs.

Representative fluorescence amplitude of snoRNAs (A) and sdRNAs (B). Positive droplets are in shown blue, negative droplets in grey. Slot numbers correspond to stress conditions as follows: 1 – heat stress, 2 – cold stress, 3 – high salinity, 4 – UV treatment, 5 – anaerobic growth, 6 – optimal conditions, 7 – high pH, 8 – low pH, 9 – AA starvation, 10 – sugar starvation, 11 – hypoosmotic conditions, and 12 – hyperosmotic conditions.

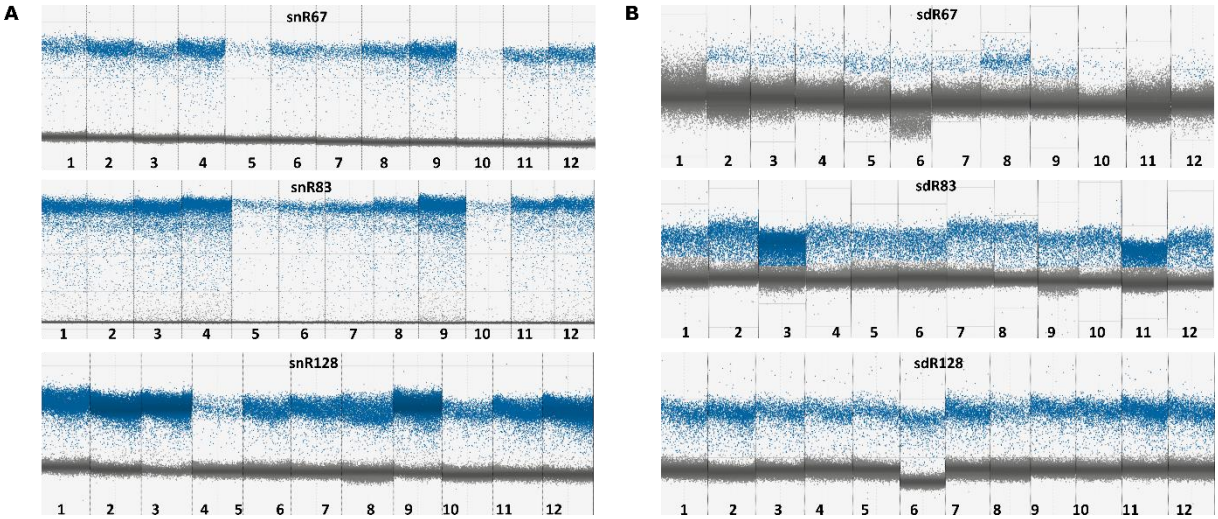

Supplementary Figure 6. Detection of snoRNAs and sdRNAs within the post-ribosomal supernatant fraction (S100).

Representative fluorescence amplitude of snoRNAs (A) and sdRNAs (B) is presented. Positive droplets are in blue, negative droplets – in grey. Numbers correspond to stress conditions: 1 – heat stress, 2 – cold stress, 3 – high salinity, 4 – UV treatment, 5 – anaerobic growth, 6 – optimal conditions, 7 – high pH, 8 – low pH, 9 – AA starvation, 10 – sugar starvation, 11 – hypoosmotic conditions, 12 – hyperosmotic conditions.

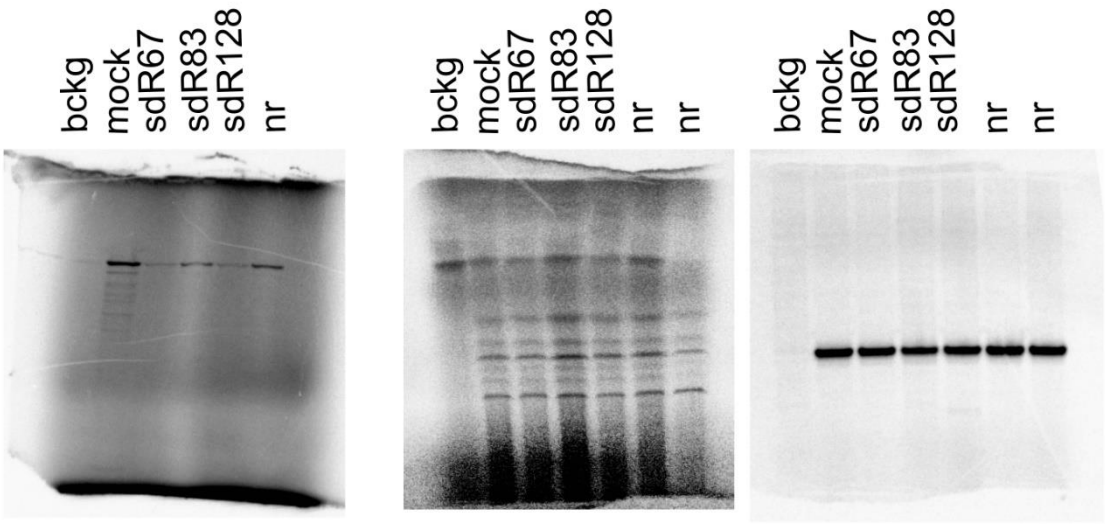

Supplementary Figure 7. *S. cerevisiae* sdRNAs inhibition of protein biosynthesis in *in vitro* eukaryotic translation systems.

A representative of full-length gels displaying in vitro translation in wheat germ extracts, rabbit reticulocyte lysates and HeLa cell lysates. The reactions were performed in the absence (mock) or presence of yeast sdRNAs (500 pmol). nr - RNA oligomer not relevant to the present study. Cropped gels and full description are presented on Fig. 10.

OŚWIADCZENIA WSPÓŁAUTORÓW

INSTYTUT CHEMII BIOORGANICZNEJ
Polskiej Akademii Nauk

ul. Noskowskiego 12/14, 61-704 Poznań
tel.: centrala 61 852 85 03, sekretariat 61 852 89 19
faks: 61 852 05 32, e-mail: ibch@ibch.poznan.pl
REGON 000849327 NIP 777-00-02-062
http://www.ibch.poznan.pl

dr hab. Kamilla Bąkowska –Żywicka,
Prof. ICHB PAN

Poznań, 17.12.19

OŚWIADCZENIA

Dotyczy rozprawy doktorskiej mgr Anny M. Mleczko

Mgr Anna M. Mleczko wykonywała pracę doktorską w Instytucie Chemii Bioorganicznej PAN. Poniżej przedstawiam zakres prac wykonanych przez mgr Annę Mleczko, oraz mój udział w poszczególnych publikacjach:

Oświadczam, że w pracach:

- Bąkowska-Żywicka K, **Mleczko AM**, Kasprzyk M, Machtel P, Żywicki M, Twardowski T

The widespread occurrence of tRNA-derived fragments in Saccharomyces cerevisiae
FEBS Open Bio, 2016, 6(12):1186-1200

Wkład w niniejszą pracę mgr Anny Mleczko to izolacja RNA przy użyciu optymalnej metody z drożdży poddanym różnym stresom środowiskowym, wykonanie eksperymentów hybrydyzacji typu northern, analiza statystyczna wyników.
Mój wkład polegał na: przygotowaniu koncepcji, zaplanowaniu doświadczeń, wykonaniu części eksperymentów, analizie i interpretacji wyników badań, przygotowaniu manuskryptu do publikacji i kierowaniu projektem naukowym obejmującym badania opisane w tej pracy.

- **Mleczko AM**, Celichowski P, Bąkowska-Żywicka K

Transfer RNA-derived fragments target and regulate ribosome-associated aminoacyl-transfer RNA synthetases,
Biochimica et Biophysica Acta – Gene Regulatory Mechanisms, 2018, 1861(7): 647-656

W niniejszej pracy mgr Anna Mleczko wykonała eksperymenty profilowania polisomowego i northern blot oraz wpływ tRF na *in vivo* aminoacylację tRNA.
Mój wkład w niniejszą pracę polegał na przygotowaniu koncepcji, zaplanowaniu doświadczeń, wykonaniu części eksperymentów, analizie i interpretacji wyników badań, przygotowaniu manuskryptu do publikacji i kierowaniu projektem naukowym obejmującym badania opisane w tej pracy.

- **Mleczko AM**, Bąkowska – Żywicka K

When small RNAs become smaller: emerging functions of snoRNAs and their derivatives
Acta Biochimica Polonica, 2016, 63(4):601-607

Mgr Anna Mleczko zgromadziła i przeanalizowała stosowną literaturę oraz przygotowała pierwszą wersję manuskryptu.
Mój wkład polegał na zaplanowaniu jej koncepcji, zgromadzeniu i analizie stosownej literatury, współtworzeniu manuskryptu jak i opracowaniu jego końcowej wersji.

- Walkowiak M*, **Mleczko AM***, Bąkowska – Żywicka K

Evaluation of methods for detection of low-abundant snoRNA-derived small RNAs in Saccharomyces cerevisiae, BioTechnologia, 2016, 1(97):19-26

Anna Mleczko wykonała doświadczenia hybrydyzacji typu northern oraz współuczestniczyła w wykonywaniu doświadczeń metodą pulsacyjnej odwrotnej transkrypcji połączonej z amplifikacją z użyciem starterów o strukturze pnia i pętli.
Mój wkład polegał na przygotowaniu koncepcji, zaplanowaniu doświadczeń, analizie i interpretacji wyników badań, przygotowaniu manuskryptu do publikacji i kierowaniu projektem naukowym obejmującym badania opisane w tej pracy.

- **Mleczko AM***, Machtel P*, Walkowiak M, Wasilewska A, Pietras PJ, Bąkowska-Żywicka K

Levels of sdRNAs in cytoplasm and their association with ribosomes are dependent upon stress conditions but independent from snoRNA expression Scientific Reports, 2019, *Autorzy mieli taki sam wkład w przygotowanie publikacji

W niniejszej pracy mgr Anna Mleczko hodowała drożdże w różnych warunkach środowiskowych, izolowała rybosomy oraz RNA z poszczególnych frakcji. Ponadto wykonała eksperymenty znakowania metabolicznego i translacji *in vitro* w systemach ludzkim, króliczym i pszenicznym. Brała także udział w analizie wyników oraz przygotowaniu manuskryptu do publikacji.
Mój udział w publikacji polegał na przygotowaniu koncepcji, zaplanowaniu doświadczeń, analizie i interpretacji wyników badań, przygotowaniu manuskryptu do publikacji i kierowaniu projektem naukowym obejmującym badania opisane w tej pracy.

Żywicka

Mgr Marta Kasprzyk

01.12.19

OŚWIADCZENIE

Oświadczam, że w pracy:

Bąkowska-Żywicka K, Mleczko AM, Kasprzyk M, Machtel P, Żywicki M, Twardowski T

The widespread occurrence of tRNA-derived fragments in Saccharomyces cerevisiae

FEBS Open Bio, 2016, 6(12):1186-1200

Mój udział polegał na wykonaniu izolacji RNA przy użyciu optymalnej metody z drożdży poddanym różnym stresom środowiskowym, wykonanie eksperymentów hybrydyzacji typu northern, analiza statystyczna wyników.

Kasprzyk Marta

INSTYTUT CHEMII BIOORGANICZNEJ
Polskiej Akademii Nauk

ul. Noskowskiego 12/14, 61-704 Poznań
tel.: centrala 61 852 85 03, sekretariat 61 852 89 19
faks: 61 852 05 32, e-mail: ibch@ibch.poznan.pl
REGON 000849327 NIP 777-00-02-062
http://www.ibch.poznan.pl

Dr Piotr Machtel

04.12.19

OŚWIADCZENIA

Oświadczam, że w pracy:

Bąkowska-Żywicka K, Mleczko AM, Kasprzyk M, Machtel P, Żywicki M, Twardowski T
The widespread occurrence of tRNA-derived fragments in Saccharomyces cerevisiae
FEBS Open Bio, 2016, 6(12):1186-1200

mój udział polegał na wykonaniu doświadczeń techniką ilościowego PCR (qRT-PCR) w czasie rzeczywistym oraz analizie statystycznej eksperymentów.

W pracy:

Mleczko AM*, Machtel P*, Walkowiak M, Wasilewska A, Pietras PJ, Bąkowska-Żywicka K
Levels of sdRNAs in cytoplasm and their association with ribosomes are dependent upon stress conditions but independent from snoRNA expression
Scientific Reports, 2019 (IF2018=4.011) *Autorzy mieli taki sam wkład w przygotowanie publikacji

mój udział polegał na wykonaniu eksperymentów techniką PCR emulsyjnego (ddPCR), analizie i interpretacji wyników oraz przygotowaniu manuskryptu do publikacji.

P. Machtel

UNIWERSYTET IM. ADAMA MICKIEWICZA W POZNANIU
Wydział Biologii
Instytut Biologii Molekularnej i Biotechnologii

Poznań,01.12.2019

Dr Marek Żywicki
Zakład Biologii Obliczeniowej
Wydział Biologii UAM

OŚWIADCZENIE

Oświadczam, że w pracy: *Bąkowska-Żywicka K, Mleczko AM, Kasprzyk M, Machtel P, Żywicki M, Twardowski T, The widespread occurrence of tRNA-derived fragments in Saccharomyces cerevisiae, FEBS Open Bio, 2016, 6(12):1186-1200,* mój udział polegał na wykonaniu analizy statystycznej wyników oraz udziale w ich interpretacji i pisaniu manuskryptu.

ul. Uniwersytetu Poznańskiego 6, Collegium Biologicum, 61-614 Poznań
NIP 777 00 06 350, REGON 000001293
tel. +48 61 829 58 42
Marek.Zywicki@amu.edu.pl

www.combio.pl

INSTYTUT CHEMII BIOORGANICZNEJ
Polskiej Akademii Nauk

ul. Noskowskiego 12/14, 61-704 Poznań
tel.: centrala 61 852 85 03, sekretariat 61 852 89 19
faks: 61 852 05 32, e-mail: ibch@ibch.poznan.pl
REGON 000849327 NIP 777-00-02-062
http://www.ibch.poznan.pl

Prof. dr hab. Tomasz Twardowski

16.12.19r

OŚWIADCZENIE

Oświadczam, że w pracy:

Bąkowska-Żywicka K, Mleczko AM, Kasprzyk M, Machtel P, Żywicki M, Twardowski T
The widespread occurrence of tRNA-derived fragments in Saccharomyces cerevisiae
FEBS Open Bio, 2016, 6(12):1186-1200

mój udział polegał na współudziale w dyskusji i analizie wyników wchodzących w skład manuskryptu.

UNIWERSYTET MEDYCZNY IM. KAROLA MARCINKOWSKIEGO W POZNANIU

KATEDRA I ZAKŁAD HISTOLOGII I EMBRIOLOGII

dr n.med Piotr Celichowski

Collegium Anatomicum, ul. H. Święcickiego 6, 60-781 Poznań

tel.: 061 8546443, e-mail: pcelichowski@ump.edu.pl

OŚWIADCZENIE

Oświadczam, że w pracy:

Mleczko AM, Celichowski P, Bąkowska-Żywicka K

Transfer RNA-derived fragments target and regulate ribosome-associated aminoacyl-transfer RNA synthetases, Biochimica et Biophysica Acta – Gene Regulatory Mechanisms, 2018, 1861(7): 647-656

Mój udział polegał na optymalizacji reakcji bezkomórkowej translacji *in vitro* oraz zbadaniu wpływu krótkich RNA pochodzących z tRNA na proces translacji w innych niż drożdżowe systemach eukariotycznych.

Mgr Mateusz Walkowiak
01.12.19r

OŚWIADCZENIA

Oświadczam, że w pracy:

Walkowiak M*, Mleczko AM*, Bąkowska – Żywicka K

Evaluation of methods for detection of low-abundant snoRNA-derived small RNAs in Saccharomyces cerevisiae

BioTechnologia, 2016, 1(97):19-26 *Autorzy mieli taki sam wkład w przygotowanie publikacji

mój współudział polegał na wykonywaniu doświadczeń metodą pulsacyjnej odwrotnej transkrypcji połączonej z amplifikacją z użyciem starterów o strukturze pnia i pętli.

W pracy:

Mleczko AM*, Machtel P*, Walkowiak M, Wasilewska A, Pietras PJ, Bąkowska-Żywicka K

Levels of sdRNAs in cytoplasm and their association with ribosomes are dependent upon stress conditions but independent from snoRNA expression

Scientific Reports, 2019

mój współudział w pracy polegał na hodowli drożdży w 12 warunkach środowiskowych, izolacji RNA oraz na optymalizacji metody ddPCR.

Walkowiak Mateusz 4.12.2019

INSTYTUT CHEMII BIOORGANICZNEJ
Polskiej Akademii Nauk

ul. Noskowskiego 12/14, 61-704 Poznań
tel.: centrala 61 852 85 03, sekretariat 61 852 89 19
faks: 61 852 05 32, e-mail: ibch@ibch.poznan.pl
REGON 000849327 NIP 777-00-02-062
http://www.ibch.poznan.pl

Mgr Anna Wasilewska

01.12.19r

OŚWIADCZENIA

Oświadczam, że w pracy:

Mleczko AM*, Machtel P*, Walkowiak M, Wasilewska A, Pietras PJ, Bąkowska-Żywicka K

Levels of sdRNAs in cytoplasm and their association with ribosomes are dependent upon stress conditions but independent from snoRNA expression

Scientific Reports, 2019

mój współudział w pracy polegał na optymalizacji metody ddPCR.

Wasilewska Anna

INSTYTUT CHEMII BIOORGANICZNEJ
Polskiej Akademii Nauk

ul. Noskowskiego 12/14, 61-704 Poznań
tel.: centrala 61 852 85 03, sekretariat 61 852 89 19
faks: 61 852 05 32, e-mail: ibch@ibch.poznan.pl
REGON 000849327 NIP 777-00-02-062
http://www.ibch.poznan.pl

Mgr Piotr Pietras

01.12.19r

OŚWIADCZENIA

Oświadczam, że w pracy:

Mleczko AM*, Machtel P*, Walkowiak M, Wasilewska A, Pietras PJ, Bąkowska-Żywicka K

Levels of sdRNAs in cytoplasm and their association with ribosomes are dependent upon stress conditions but independent from snoRNA expression

Scientific Reports, 2019

mój współudział w pracy polegał na wykonaniu eksperymentów translacji *in vitro* w systemie drożdżowym oraz analizie wyników.

Piot Pietras